

## Databases of L-shell X-ray intensity ratios for various elements after photon excitation

A. Zidi <sup>a,b</sup>, A. Kahoul <sup>a,b,\*</sup>, J.P. Marques <sup>c,d</sup>, S. Daoudi <sup>a,b</sup>, J.M. Sampaio <sup>c,d</sup>, F. Parente <sup>e</sup>,  
A. Hamidani <sup>a,b</sup>, S. Croft <sup>f</sup>, A. Favalli <sup>g,h</sup>, Y. Kasri <sup>i,j</sup>, K. Amari <sup>a,b</sup>, B. Berkani <sup>a,b</sup>

<sup>a</sup> Department of Matter Sciences, Faculty of Sciences and Technology, Mohamed El Bachir El Ibrahim University, Bordj-Bou-Arreidj 34030, Algeria

<sup>b</sup> Laboratory of Materials Physics, Radiation and Nanostructures (LPMRN), Faculty of Sciences and Technology, Mohamed El Bachir El Ibrahim University, Bordj-Bou-Arreidj 34030, Algeria

<sup>c</sup> LIP – Laboratório de Instrumentação e Física Experimental de Partículas, Av. Prof. Gama Pinto 2, 1649-003 Lisboa, Portugal

<sup>d</sup> Faculdade de Ciências da Universidade de Lisboa, Campo Grande, C8, 1749-016 Lisboa, Portugal

<sup>e</sup> Laboratory of Instrumentation, Biomedical Engineering and Radiation Physics (LIBPhys-UNL), Department of Physics, NOVA School of Science and Technology, NOVA University Lisbon, 2829-516 Caparica, Portugal

<sup>f</sup> School of Engineering, Faculty of Science of Technology, Nuclear Science & Engineering Research Group, Lancaster University, Bailrigg, Lancaster, LA1 4YW, United Kingdom

<sup>g</sup> European Commission, Joint Research Centre, Ispra, I-21027, Italy

<sup>h</sup> Los Alamos National Laboratory, P.O. Box 1663, Los Alamos, NM 87545, USA

<sup>i</sup> Physics Department, Faculty of Sciences, University of Mohamed Boudiaf, 28000 M'sila, Algeria

<sup>j</sup> Theoretical Physics Laboratory, Physics Department, University of Bejaia, 06000 Bejaia, Algeria

### ARTICLE INFO

#### Keywords:

X-rays  
Atomic parameters  
Intensity ratios  
Weighted average values

### ABSTRACT

In this study, a comprehensive dataset of X-ray emission intensity ratios has been compiled, including  $I_{L\beta}/I_{L\alpha}$ ,  $I_{L\gamma}/I_{L\alpha}$ ,  $I_{L1}/I_{L\alpha}$ ,  $I_{L\gamma}/I_{L\beta}$ ,  $I_{L1}/I_{L\gamma}$ ,  $I_{L1}/I_{L\beta}$ ,  $I_{L\gamma5}/I_{L\alpha}$ ,  $I_{L\gamma44}/I_{L\alpha}$ ,  $I_{L\eta}/I_{L\alpha}$ , and  $I_{L\gamma1}/I_{L\alpha}$ , extracted from literature spanning the years 1971 to 2023, and encompassing 83 research papers. Over this timeframe, a total of 2600 values were collected, comprising some 678 values for  $I_{L\beta}/I_{L\alpha}$ , 696 values for  $I_{L\gamma}/I_{L\alpha}$ , 617 values for  $I_{L1}/I_{L\alpha}$ , along with 132, 132, 89, 60, 70, 71, and 55 data points for  $I_{L\gamma}/I_{L\beta}$ ,  $I_{L1}/I_{L\gamma}$ ,  $I_{L1}/I_{L\beta}$ ,  $I_{L\gamma5}/I_{L\alpha}$ ,  $I_{L\gamma44}/I_{L\alpha}$ ,  $I_{L\eta}/I_{L\alpha}$ , and  $I_{L\gamma1}/I_{L\alpha}$ , respectively. The reported values are presented with precision up to three to four decimal places, accompanied by their associated uncertainties. Additionally, the tables include calculated weighted averages  $(I_{Li}/I_{Lj})_W$ , uncertainty values ( $\epsilon_{ISD}$ ,  $\epsilon_{ESD}$ ), combined standard deviations ( $z_{ISD}$ ,  $z_{ESD}$ ), and average z-scores ( $\bar{z}_{ISD}$ ,  $\bar{z}_{ESD}$ ) for these intensity ratios. The data encompasses elements ranging from  ${}_{39}\text{Y}$  to  ${}_{94}\text{Pu}$  when excited by photon bombardment. The assessment of how these experimental data values are distributed according to atomic number indicates extensive coverage across most elements. However, a few isolated instances were identified where either no data or fewer than two data values were available.

### 1. Introduction

Data on the L sub-shell X-ray production cross sections, fluorescence yields and intensity ratios are needed for many scientific, medical and engineering applications [1]. Intensity ratios play a significant role in nuclear spectroscopy and atomic physics. Extensive research across different disciplines has been dedicated to these quantities, resulting in their summarization in several comprehensive review articles. Investigating these parameters for elements on the periodic table has been a primary focus of various experiments, along with growing theoretical

interest, in recent years. This interest stems from their potential applications in non-destructive elemental analysis in fields such as medical physics, surface chemistry, environmental sciences, nuclear safeguards, materials accountancy, and industry. Radiative transitions within the l-shell are designated in accordance with the Siegbahn or the International Union of Pure and Applied Chemistry (IUPAC) notations [2]. In the Siegbahn notation,  $L_{\alpha}$  denotes IUPAC l-m transitions,  $L_{\beta}$  signifies IUPAC l-m, l-n, and l-o transitions, while  $L_{\gamma}$  correspond to IUPAC l-n and l-o transitions. Table A illustrates the correspondence between Siegbahn, IUPAC notation diagram lines and the Z atomic numbers

\* Corresponding author.

E-mail address: [a.kahoul@univ-bba.dz](mailto:a.kahoul@univ-bba.dz) (A. Kahoul).

<https://doi.org/10.1016/j.adt.2024.101645>

Received 21 December 2023; Received in revised form 2 February 2024; Accepted 2 February 2024

Available online 26 March 2024

0092-640X/© 2024 Elsevier Inc. All rights reserved.

associated with the appearance of these lines. Numerous efforts have been made to determine l-shell intensity ratios across a diverse set of elements, either through the application of theoretical models or by fitting experimental data using empirical and semi-empirical formulas.

Scofield [3] performed a Hartree-Slater calculation, including relativistic effects, to determine L X-ray emission rates for elements ranging from  $Z = 5$  to  $Z = 104$ . Subsequently, Campbell and Wang [4] presented a comprehensive collection of  $L_i$  ( $i = 1-3$ ) subshell X-ray emission rates for all elements with  $Z = 18-94$ , obtaining these values through interpolation from the tabulated Dirac-Fock (DF) model based data originally provided by Scofield [3]. Theoretical l-shell intensity ratios for elements with atomic number  $36 \leq Z \leq 92$  were calculated by [5] using the Dirac-Hartree-Slater model for incident photon energies in the range  $E_{L1} < E_{inc} \leq 200$  keV.

In 2014, Puri [6] compiled intensity ratios, specifically  $I_{Lk}/I_{La1}$  ( $k = l, \eta, \alpha_2, \beta_1, \beta_{2.15}, \beta_3, \beta_4, \beta_{5.7}, \beta_6, \beta_{9.10}, \gamma_{1.5}, \gamma_{6.8}, \gamma_{2.3}, \gamma_4$ ), and  $I_{Lj}/I_{La}$  ( $j = \beta, \gamma$ ), for all elements with atomic numbers ranging from 35 to 92. These ratios were evaluated for incident photon energies starting from the  $L_i$  sub-shell ( $i = 1-3$ ) binding energy, with the calculations based on the Dirac-Fock model. The aim of that work was to provide a comprehensive dataset of intensity ratios for various elements and photon energies, which is valuable for understanding the behavior of X-rays in different materials.

Several researchers and research groups have determined experimentally the values of the l-shell X-ray intensity ratios. The photon-induced relative intensities of l-shell X-rays, including  $I_{Ll}/I_{La}$ ,  $I_{L\beta}/I_{La}$  and  $I_{L\gamma}/I_{La}$  for  $^{79}\text{Au}$  [7], and for  $^{79}\text{Au}$ ,  $^{82}\text{Pb}$ ,  $^{90}\text{Th}$ , and  $^{92}\text{U}$  [8], were measured in the energy range  $17 \leq E \leq 60$  keV. Yalçin et al., [46] determined  $I_{La}/I_{L\beta}$ ,  $I_{La}/I_{L\gamma}$ ,  $I_{La}/I_{Ll}$ ,  $I_{L\beta}/I_{L\gamma}$ , and  $I_{Ll}/I_{L\gamma}$  intensity ratios for elements  $^{66}\text{Dy}$ ,  $^{67}\text{Ho}$ ,  $^{70}\text{Yb}$ ,  $^{74}\text{W}$ ,  $^{80}\text{Hg}$ ,  $^{81}\text{Tl}$ , and  $^{82}\text{Pb}$  by radioactive decay and photo-ionization. Demir and Sahin, [9] calculated  $I_{Ll}/I_{La}$  intensity ratios for some elements spanning  $73 \leq Z \leq 92$  using 59.54 keV excitation photons in an external magnetic field with intensities  $\pm 0.75$  T. In the study of Aylikci et al., [10], new interpolations (empirical and semi-empirical) of L X-ray intensity ratios of elements have been performed in the range  $50 \leq Z \leq 92$ .

Researchers have employed a multitude of experimental techniques and diverse conditions to investigate intensity ratios. There are over a thousand measured data points in the technical literature. Extracting valuable and crucial insights from this vast dataset necessitates a comprehensive analysis. In the present paper, new databases containing l-line intensity ratios  $I_{L\beta}/I_{La}$ ,  $I_{L\gamma}/I_{La}$ ,  $I_{Ll}/I_{La}$ ,  $I_{L\gamma}/I_{L\beta}$ ,  $I_{Ll}/I_{L\gamma}$ ,  $I_{Ll}/I_{L\beta}$ ,  $I_{L\gamma5}/I_{La}$ ,  $I_{L\gamma44}/I_{La}$ ,  $I_{L\eta}/I_{La}$ , and  $I_{L\gamma1}/I_{La}$  were obtained directly from various sources. These databases comprise a total of 2600 published values from 1971 to April 2023 and cover elements with atomic numbers in the range  $39 \leq Z \leq 94$ . The weighted mean values, average z-scores, and combined standard deviations have been calculated for each element and ratio and are also presented in the databases.

### 1.1. Review of calculation errors (standard deviation)

In the current research, we carried out an in-depth analysis of ten databases and their calculation methodologies. It is worth noting that the data consolidated in this study can be categorized into five different groups [11]:

- 1)  $I_{Li}/I_{Lj}$  X-ray intensity ratios are given and their related uncertainties (standard deviation  $\Delta(I_{Li}/I_{Lj})$ ) are indicated as a percentage ( $p\%$ ) in the texts by [12–18]; and [19]. In this context, the (absolute) standard deviation  $\Delta(I_{Li}/I_{Lj})$  is computed as follows:

$$\Delta(I_{Li}/I_{Lj}) = 0.01 \times (p\%) \times I_{Li}/I_{Lj} \quad (1)$$

where  $i = \beta, \gamma, \eta, l, \gamma_5, \gamma_{44}$ , and  $\gamma_1$ ;  $j = \alpha, \beta$ , and  $\gamma$ .

- 1) Intensities and their corresponding uncertainties are provided for  $I_{Li} \pm \Delta(I_{Li})$  and  $I_{Lj} \pm \Delta(I_{Lj})$ , as reported in the works of [20–27]. In these instances, the target ratio is computed directly by dividing  $I_{Li}$  by  $I_{Lj}$ .

The standard deviation of the ratio is determined by applying the following expression:

$$\Delta(I_{Li}/I_{Lj}) = I_{Li}/I_{Lj} \times \sqrt{\left(\frac{\Delta(I_{Li})}{I_{Li}}\right)^2 + \left(\frac{\Delta(I_{Lj})}{I_{Lj}}\right)^2} \quad (2)$$

here  $i = \beta, \gamma, \eta, l, \gamma_5, \gamma_{44}$ , and  $\gamma_1$ ;  $j = \alpha, \beta$ , and  $\gamma$ .

The text of the research paper provides information on the  $I_{Lj}/I_{Li}$  X-ray intensity ratios and their associated uncertainties  $\Delta(I_{Lj}/I_{Li})$ . These data are sourced from multiple references, including works by [8,28,55,84,89]; and [91]. In these cases, the calculation of the  $I_{Li}/I_{Lj}$  ratio is performed as follows:

$$I_{Li}/I_{Lj} = \left(\frac{1}{I_{Lj}/I_{Li}}\right) \quad (3)$$

Furthermore, the standard deviation linked to the ratio  $\Delta(I_{Li}/I_{Lj})$  is determined through the following formula:

$$\Delta(I_{Li}/I_{Lj}) = \Delta\left(\frac{1}{I_{Lj}/I_{Li}}\right) = \frac{\Delta(I_{Lj}/I_{Li})}{(I_{Lj}/I_{Li})^2} \quad (4)$$

for  $i = \beta, \gamma, \eta, l, \gamma_5, \gamma_{44}$ , and  $\gamma_1$ ;  $j = \alpha, \beta$ , and  $\gamma$ .

- 1) The reporting authors provide the  $I_{Lj}/I_{Li}$  X-ray intensity ratios, and they express in their text the associated uncertainties as a percentage ( $p\%$ ), as observed in [56]. Consequently, the standard deviation for the ratio  $\Delta(I_{Li}/I_{Lj})$  is determined using equation:

$$\Delta(I_{Li}/I_{Lj}) = \frac{0.01 \times (p\%) \times I_{Lj}/I_{Li}}{(I_{Lj}/I_{Li})^2} = \frac{0.01 \times (p\%)}{(I_{Lj}/I_{Li})} \quad (5)$$

In this context, the calculation of  $\Delta(I_{Lj}/I_{Li})$  is performed according to:

$$\Delta(I_{Lj}/I_{Li}) = 0.01 \times (p\%) \times I_{Lj}/I_{Li} \quad (6)$$

for  $i = \beta, \gamma, \eta, l, \gamma_5, \gamma_{44}$ , and  $\gamma_1$ ;  $j = \alpha, \beta$ , and  $\gamma$ .

Regarding the other reviewed articles, the uncertainties (expressed as standard deviations)  $\Delta(I_{Li}/I_{Lj})$  for the  $I_{Li}/I_{Lj}$  X-ray intensity ratios are explicitly stated in the text of [7,9,10,18,33,57–81,86,87,90]; and [92], making them immediately applicable without further calculation.

### 1.2. Survey of the experimental works

Table 1 gives an extensive overview of  $I_{Li}/I_{Lj}$  ( $i = \beta, \gamma, \eta, l, \gamma_5, \gamma_{44}$ , and  $\gamma_1$ ;  $j = \alpha, \beta$  and  $\gamma$ ) intensity ratio measurements collected between 1971 and 2023. These measurements were carried out using a variety of experimental techniques and under various experimental conditions. The table includes atomic parameters for elements spanning from  $^{39}\text{Y}$  to  $^{94}\text{Pu}$ , along with the corresponding references, excitation sources employed, target sample types, and X-ray spectrometers used. Regarding excitation sources, they encompass photons. Photon sources commonly involve the use of 59.5 keV  $\gamma$ -rays emitted from a  $^{241}\text{Am}$  radioactive source whenever feasible, although 122 keV  $\gamma$ -rays  $^{57}\text{Co}$  and 22.69 keV x-rays from  $^{109}\text{Cd}$  are also frequently employed. Numerous other radioactive sources are also used. As for target samples, they come in the form of pure elements, alloys, or compounds, and can be found as powder samples, foils, pellets, or circular discs. Various detectors types are employed to measure the X-ray emissions, with the most prevalent ones being single crystal semiconductors such as Si(Li) and germanium

**Table 1**

Summary of the atomic parameters for elements ranging from  ${}_{39}\text{Y}$  to  ${}_{94}\text{Pu}$ , the excitation sources, the target samples and the detectors. The references from which these data are obtained is also included.

References	Atomic parameters	Excitation sources	Target samples	Detectors
[28]	$I_{L\alpha}/I_{L\beta}$	Decays of ${}^{159}\text{Dy}$ , ${}^{171}\text{Tm}$ , ${}^{181}\text{W}$ , ${}^{191}\text{Os}$ , ${}^{186}\text{Re}$ , ${}^{207}\text{Bi}$ , ${}^{210}\text{Pb}$ , ${}^{238}\text{Pu}$ , ${}^{241}\text{Am}$ , and ${}^{244}\text{Cm}$ (with the majority of them being free of carrier substances).	${}^{65}\text{Tb}$ , ${}^{70}\text{Yb}$ , ${}^{73}\text{Ta}$ , ${}^{77}\text{Ir}$ , ${}^{78}\text{Pt}$ , ${}^{81}\text{Tl}$ , ${}^{82}\text{Pb}$ , ${}^{83}\text{Bi}$ , ${}^{92}\text{U}$ , ${}^{93}\text{Np}$ , and ${}^{94}\text{Pu}$ .	Three distinct Si(Li) detectors with varying resolutions: one having a resolution of 260 eV FWHM at 6.4 keV, another with a resolution of 220 eV FWHM at 6.4 keV, and the third exhibiting a resolution of 155 eV FWHM at 6.4 keV.
[57]	$I_{L\gamma1}/I_{L\beta1}$ , $I_{L\eta}/I_{L\beta1}$ , $I_{L\beta1}/I_{L\alpha}$ & $I_{L\beta2,15}/I_{L\alpha}$	Commercial ${}_{24}\text{Cr}$ X-ray tube with $Z \leq 48$ and commercial ${}_{74}\text{W}$ X-ray tube for samples with $Z \geq 49$ .	${}^{44}\text{Ru}$ , ${}^{45}\text{Rh}$ , ${}^{46}\text{Pd}$ , ${}^{47}\text{Ag}$ , ${}^{48}\text{Cd}$ , ${}^{49}\text{In}$ , ${}^{50}\text{Sn}$ , ${}^{51}\text{Sb}$ , ${}^{52}\text{Te}$ , ${}^{53}\text{I}$ , ${}^{55}\text{Cs}$ , ${}^{56}\text{Ba}$ , ${}^{57}\text{La}$ , ${}^{58}\text{Ce}$ , ${}^{59}\text{Pr}$ , ${}^{60}\text{Nd}$ , and ${}^{62}\text{Sm}$ . (with the exception of ${}^{56}\text{Ba}$ , ${}^{59}\text{Pr}$ , and ${}^{60}\text{Nd}$ , which were utilized in their oxide forms, all the samples consisted of pure metals in an amorphous state.	Single-crystal spectrometer in conjunction with a flow proportional counter.
[7]	$I_{L\beta}/I_{L\alpha}$ , $I_{L\beta1}/I_{L\alpha}$ , & $I_{L\gamma}/I_{L\alpha}$	From an ${}^{241}\text{Am}$ annular source of 1000mCi and using an A NEN X-ray exciter, photons with energy levels of 17.8 keV, 25.8 keV, 46.9 keV, and 59.5 keV were emitted.	${}^{79}\text{Au}$ . (Thin gold foil).	Si(Li) detector.
[89]	$I_{L\alpha}/I_{L\beta}$ , $I_{L\alpha}/I_{L\beta1}$ , $I_{L\alpha}/I_{L\beta2}$ , $I_{L\alpha}/I_{L\gamma}$ , $I_{L\alpha}/I_{L\gamma1}$ , $I_{L\alpha}/I_{L\gamma2}$ & $I_{L\alpha}/I_{L\gamma3}$	59.57 keV gamma rays from ${}^{241}\text{Am}$ radioactive source with a strength of about 100 mCi.	${}^{92}\text{U}$ , ${}^{90}\text{Th}$ , and ${}^{82}\text{Pb}$ . (The targets presented as discs with a circular shape).	ORTEC Si(Li) detector having 240 eV resolution at 5.9 keV.
[8]	$I_{L\alpha}/I_{L\beta}$ , $I_{L\alpha}/I_{L\beta1}$ , & $I_{L\alpha}/I_{L\gamma}$	59.57 keV gamma rays emitted from an ${}^{241}\text{Am}$ radioactive source.	${}^{39}\text{Y}$ , ${}^{40}\text{Zr}$ , ${}^{41}\text{Nb}$ , ${}^{42}\text{Mo}$ , ${}^{47}\text{Ag}$ , ${}^{49}\text{In}$ , ${}^{50}\text{Sn}$ , ${}^{53}\text{I}$ , ${}^{56}\text{Ba}$ , ${}^{57}\text{La}$ , ${}^{58}\text{Ce}$ , ${}^{62}\text{Sm}$ , and ${}^{64}\text{Gd}$ .	EG&G Ortec Si(Li) detector having 240 eV resolution at 5.9 keV.
[58]	$I_{L\beta}/I_{L\alpha}$ , $I_{L\beta1}/I_{L\alpha}$ , & $I_{L\gamma}/I_{L\alpha}$	NEN consisting of an annular source of ${}^{241}\text{Am}$ , tungsten spacer and shield and the secondary x-ray exciter have been used.	${}^{73}\text{Ta}$ , ${}^{79}\text{Au}$ , ${}^{82}\text{Pb}$ , and ${}^{83}\text{Bi}$ ( ${}^{73}\text{Ta}$ existed as a self-supporting thin foil, while ${}^{79}\text{Au}$ , ${}^{82}\text{Pb}$ , and ${}^{83}\text{Bi}$ were also employed as thin foils).	Si(Li) detector with a resolution of 170 eV at 5.9 keV coupled to an ND-100 multi-channel analyser.
[20]	$I_{L\beta}/I_{L\alpha}$ , $I_{L\beta1}/I_{L\alpha}$ , $I_{L\beta2}/I_{L\alpha}$ , $I_{L\beta3}/I_{L\alpha}$ , & $I_{L\gamma1,2,3}/I_{L\alpha}$	Decays of ${}^{141}\text{Ce}$ and ${}^{170}\text{Tm}$ sources.	${}^{59}\text{Pr}$ and ${}^{70}\text{Yb}$ .	a vertical planar HPGe detector having 459 eV FWHM resolution at 122 keV and a vertical Si(Li) detector with 165 eV resolution at 5.9 keV.
[59]	$I_{L\beta}/I_{L\alpha}$ , $I_{L\beta1}/I_{L\alpha}$ , $I_{L\beta2}/I_{L\alpha}$ & $I_{L\gamma}/I_{L\alpha}$	26 keV gamma rays emitted from the ${}^{241}\text{Am}$ source.	${}^{74}\text{W}$ and ${}^{80}\text{Hg}$ . (The targets consisted of a self-supporting tungsten foil and circular discs of mercuric chloride compressed into pellets).	EG&G Ortec Si(Li) detector having 162 eV resolution at 5.9 keV.
[60]	$I_{L\beta}/I_{L\alpha}$ & $I_{L\gamma}/I_{L\alpha}$	Photons of 22.6 keV from ${}^{109}\text{Cd}$ have been used for direct excitation of the target x-rays.	${}^{67}\text{Ho}$ , ${}^{68}\text{Er}$ , and ${}^{70}\text{Yb}$ . (thin foils were evaporated on Mylar backing).	Si(Li) detector with 170 eV resolution at 5.9 keV.
[21]	$I_{L\beta}/I_{L\alpha}$ , $I_{L\beta1}/I_{L\alpha}$ , $I_{L\beta2}/I_{L\alpha}$ , $I_{L\gamma}/I_{L\alpha}$ , $I_{L\gamma1,2,3}/I_{L\alpha}$ , $I_{L\gamma4}/I_{L\alpha}$ & $I_{L\gamma5}/I_{L\alpha}$	Decays of ${}^{192}\text{Ir}$ , ${}^{160}\text{Tb}$ , ${}^{169}\text{Yb}$ , and ${}^{152}\text{Eu}$ .	${}^{64}\text{Gd}$ , ${}^{66}\text{Dy}$ , ${}^{69}\text{Tm}$ , ${}^{76}\text{Os}$ , and ${}^{78}\text{Pt}$ .	Coaxial HPGe detector having 1.7 K eV FWHM resolution at 1332 keV, vertical planar HPGe detector with 459 eV resolution at 122 keV and vertical Si(Li) detector with 165 eV resolution at 5.9 keV.
[29]	$I_{L\beta}/I_{L\alpha}$	Decays of a 5 mCi ${}^{109}\text{Cd}$ and a 10 mCi ${}^{125}\text{I}$ sources.	${}^{67}\text{Ho}$ , ${}^{73}\text{Ta}$ , ${}^{79}\text{Au}$ , ${}^{82}\text{Pb}$ , ${}^{83}\text{Bi}$ , ${}^{90}\text{Th}$ , and ${}^{92}\text{U}$ . (The samples were deposited in thick Mylar backing).	KeveX Si(Li) detector with a resolution better than 230 eV at 6.4 keV.
[22]	$I_{L\beta}/I_{L\alpha}$ , $I_{L\beta1}/I_{L\alpha}$ , & $I_{L\gamma}/I_{L\alpha}$	Decays of ${}^{137}\text{Cs}$ and ${}^{203}\text{Hg}$ sources.	${}^{56}\text{Ba}$ and ${}^{81}\text{Tl}$ .	a vertical planar HPGe detector having 459 eV FWHM resolution at 122 keV and a vertical Si(Li) detector with 165 eV resolution at 5.9 keV.
[23]	$I_{L\beta}/I_{L\alpha}$ , $I_{L\beta1}/I_{L\alpha}$ , $I_{L\beta2}/I_{L\alpha}$ , $I_{L\gamma}/I_{L\alpha}$ , $I_{L\gamma1,2,3}/I_{L\alpha}$ , $I_{L\gamma4}/I_{L\alpha}$ & $I_{L\gamma5}/I_{L\alpha}$	Decays of ${}^{210}\text{Pb}$ , ${}^{177}\text{Lu}$ , ${}^{170}\text{Tm}$ and ${}^{141}\text{Ce}$ sources.	${}^{59}\text{Pr}$ , ${}^{72}\text{Hf}$ , and ${}^{83}\text{Bi}$ .	a vertical planar HPGe detector having 459 eV FWHM resolution at 122 keV and a vertical Si(Li) detector with 165 eV resolution at 5.9 keV.
[30]	$I_{L\alpha}/I_{L\beta}$	14–17 keV x-rays emitted by a 30 mCi ${}^{238}\text{Pu}$ source.	${}^{55}\text{Cs}$ , ${}^{56}\text{Ba}$ , ${}^{58}\text{Ce}$ , ${}^{59}\text{Pr}$ , ${}^{60}\text{Nd}$ , ${}^{61}\text{Pm}$ , ${}^{62}\text{Sm}$ , ${}^{63}\text{Eu}$ , ${}^{64}\text{Gd}$ , ${}^{65}\text{Tb}$ , ${}^{66}\text{Dy}$ , ${}^{67}\text{Ho}$ , ${}^{68}\text{Er}$ , ${}^{71}\text{Lu}$ , ${}^{73}\text{Ta}$ , ${}^{74}\text{W}$ , ${}^{78}\text{Pt}$ , ${}^{79}\text{Au}$ , and ${}^{80}\text{Hg}$ . (Every element was utilized in its oxide state, and the powdered sample was uniformly compressed between two x-ray mylar films).	Si(Li) detector with 160 eV resolution at 5.9 keV.
[12]	$I_{L\beta}/I_{L\alpha}$ & $I_{L\gamma}/I_{L\alpha}$	Photons in the 11–41 keV energy range, derived from ${}^{109}\text{Cd}$ (25mCi), were utilized to directly induce excitation, while ${}^{241}\text{Am}$ (300mCi) was employed as a secondary excitation source.	${}^{57}\text{La}$ , ${}^{59}\text{Pr}$ , ${}^{62}\text{Sm}$ , ${}^{63}\text{Eu}$ , ${}^{64}\text{Gd}$ , ${}^{65}\text{Tb}$ , and ${}^{66}\text{Dy}$ . (spectroscopically pure thin foils were evaporated on mylar backing).	Si(Li) detector having 170 eV FWHM resolution at 5.9 keV.

(continued on next page)

Table 1 (continued)

References	Atomic parameters	Excitation sources	Target samples	Detectors
[13]	$I_{L\beta}/I_{L\alpha}$ & $I_{L\gamma}/I_{L\alpha}$	Photons with an energy of 22.6 keV originating from $^{109}\text{Cd}$ (50mCi) were employed to directly induce excitation, while photons with energies of 15.2, 17.8, and 25.8 from $^{241}\text{Am}$ (300mCi) were utilized as secondary exciters.	$^{56}\text{Ba}$ , $^{58}\text{Ce}$ , and $^{60}\text{Nd}$ . (pure thin foils were evaporated on mylar backing)	Si(Li) detector having 170 eV FWHM resolution at 5.9 keV
[14]	$I_{L\alpha}/I_{L\alpha}$ , $I_{L\beta}/I_{L\alpha}$ & $I_{L\gamma}/I_{L\alpha}$	22.6 and 59.54 keV photons emitted by a $^{241}\text{Am}$ and $^{57}\text{Co}$ annular source, respectively.	$^{69}\text{Tm}$ , $^{71}\text{Lu}$ , $^{90}\text{Th}$ , and $^{92}\text{U}$ . (Spectroscopically pure samples were evaporated onto thick mylar backing using thin foils).	Si(Li) detector having 170 eV FWHM resolution at 5.9 keV.
[61]	$I_{L\beta}/I_{L\alpha}$ & $I_{L\gamma}/I_{L\alpha}$	Photons with energy values of 17.8 keV, 25.8 keV, and 46.9 keV were emitted from a $^{241}\text{Am}$ annular source and with secondary excitation excitor.	$^{73}\text{Ta}$ , $^{74}\text{W}$ , $^{75}\text{Re}$ , $^{78}\text{Pt}$ , $^{79}\text{Au}$ , $^{80}\text{Hg}$ , $^{81}\text{Tl}$ , $^{82}\text{Pb}$ , and $^{83}\text{Bi}$ . (The targets employed included self-supporting $^{73}\text{Ta}$ foils, while thin foils were used for $^{74}\text{W}$ , $^{78}\text{Pt}$ , $^{79}\text{Au}$ , $^{82}\text{Pb}$ , $^{81}\text{Tl}$ , and $^{83}\text{Bi}$ targets, and $^{75}\text{Re}$ pellets and mercuric chloride were shaped into disks).	Si(Li) detector having 170 eV FWHM resolution at 5.9 keV.
[24]	$I_{L\alpha}$ , $I_{L\beta}$ , $I_{L\gamma}$ & $I_{L\eta}$	Decays of $^{131}\text{I}$ , $^{166}\text{Ho}$ , $^{198}\text{Au}$ and $^{199}\text{Au}$ .	$^{54}\text{Xe}$ , $^{68}\text{Er}$ , and $^{80}\text{Hg}$ .	Two coaxial HPGe detectors, a vertical planar HPGe detector and two Si(Li) detectors.
[15]	$I_{L\alpha}/I_{L\alpha}$	Photons with energy values of 22.6 keV and 59.54 keV were discharged from an annular source containing $^{109}\text{Cd}$ (25mCi) and $^{241}\text{Am}$ (300mCi) respectively.	$^{72}\text{Hf}$ , $^{75}\text{Re}$ , $^{77}\text{Ir}$ , $^{78}\text{Pt}$ , and $^{82}\text{Pb}$ . (spectroscopically pure thin foils).	Si(Li) detector having 170 eV FWHM resolution at 5.9 keV
[56]	$I_{L\alpha}/I_{L\beta}$ & $I_{L\alpha}/I_{L\gamma}$	30mCi $^{238}\text{Pu}$ source.	$^{55}\text{Cs}$ , $^{56}\text{Ba}$ , $^{57}\text{La}$ , $^{58}\text{Ce}$ , $^{59}\text{Pr}$ , $^{60}\text{Nd}$ , $^{61}\text{Pm}$ , $^{62}\text{Sm}$ , $^{63}\text{Eu}$ , $^{64}\text{Gd}$ , $^{65}\text{Tb}$ , $^{66}\text{Dy}$ , $^{67}\text{Ho}$ , $^{68}\text{Er}$ , $^{69}\text{Tm}$ , $^{70}\text{Yb}$ , $^{71}\text{Lu}$ , $^{73}\text{Ta}$ , $^{74}\text{W}$ , $^{77}\text{Ir}$ , $^{78}\text{Pt}$ , $^{79}\text{Au}$ , and $^{80}\text{Hg}$ . (each element was employed in the form of its oxide, and then compressed between two x-ray mylar films).	Si(Li) detector with high-resolution.
[31]	$I_{L\alpha}/I_{L\alpha}$ , $I_{L\alpha}/I_{L\beta}$ & $I_{L\alpha}/I_{L\beta,2,15}$	Secondary excitation technique employed to generate gamma rays from a radioactive source of $^{241}\text{Am}$ with an activity of approximately 3.7 GBq.	$^{82}\text{Pb}$ , $^{90}\text{Th}$ , and $^{92}\text{U}$ . (pure samples with various thickness).	Ge(Li) detector.
[25]	$I_{L\alpha}$ , $I_{L\beta}$ & $I_{L\gamma}$	Decays of $^{182}\text{Ta}$ .	$^{72}\text{Hf}$ .	A horizontal planar Si(Li) detector (FWHM=165 eV at 5.9 keV), a vertical planar HPGe detector (FWHM=459 eV at 122 keV) and two coaxial HPGe detectors (FWHM=1.7 keV at 1332 keV).
[26]	$I_{L\alpha}$ , $I_{L\beta}$	Decays of $^{153}\text{Sm}$ and $^{153}\text{Gd}$ .	$^{63}\text{Eu}$ .	Two coaxial HPGe detectors (FWHM=1.7 keV at 1332 keV), a vertical planar HPGe detector (FWHM=459 eV at 122 keV) and two Si(Li) detector (FWHM=165 eV at 5.9 keV).
[32]	$I_{L\alpha}/I_{L\alpha}$ , $I_{L\alpha}/I_{L\beta}$ , $I_{L\alpha}/I_{L\gamma}$ & $I_{L\alpha}/I_{L\eta}$	Annular $^{109}\text{Cd}$ source which emits Ag x-rays energy 22.6 keV.	$^{62}\text{Sm}$ , $^{74}\text{W}$ , $^{77}\text{Ir}$ , $^{79}\text{Au}$ , $^{80}\text{Hg}$ , $^{82}\text{Pb}$ , and $^{92}\text{U}$ . (with intermediate thickness).	Si(Li) detector with 154 eV resolution at 5.9 keV.
[88]	$I_{L\alpha}/I_{L\alpha}$ , $I_{L\beta}/I_{L\alpha}$ & $I_{L\gamma}/I_{L\alpha}$	X-ray tube with a secondary exciter.	$^{79}\text{Au}$ and $^{82}\text{Pb}$ .	The collimated HP Ge(Li) detector having a thickness of 5 mm and 160 eV resolution at 5.9 keV.
[62]	$I_{L\alpha}/I_{L\alpha}$ , $I_{L\beta}/I_{L\alpha}$ & $I_{L\gamma}/I_{L\alpha}$	An x-ray tube containing a tungsten anode, with a maximum high voltage of 80 kV and a maximum current of 5 mA.	$^{59}\text{Pr}$ , $^{67}\text{Ho}$ , $^{70}\text{Yb}$ , $^{79}\text{Au}$ , and $^{82}\text{Pb}$ .	Ge(Li) detector with a 5 mm thickness and an energy resolution of 160 eV at 5.9keV
[63]	$I_{L\alpha}/I_{L\alpha}$ , $I_{L\beta}/I_{L\alpha}$ & $I_{L\gamma}/I_{L\alpha}$	$\gamma$ -rays with an energy of 59.54 keV emitted from a point source of $^{241}\text{Am}$ .	$^{78}\text{Pt}$ , $^{82}\text{Pb}$ , and $^{83}\text{Bi}$ . (High-purity samples in the form of foils were utilized).	Si(Li) detector.
[64]	$I_{L\alpha}/I_{L\alpha}$ , $I_{L\beta}/I_{L\alpha}$ & $I_{L\gamma}/I_{L\alpha}$	X-ray tube with a secondary exciter.	$^{79}\text{Au}$ and $^{82}\text{Pb}$ . (Circular discs of approximately 0.01 mm thickness were used for both).	Si(Li) detector.
[33]	$I_{L\alpha}/I_{L\alpha}$ , $I_{L\alpha}/I_{L\beta}$ , $I_{L\alpha}/I_{L\gamma}$ & $I_{L\beta}/I_{L\gamma}$	Gamma rays with an energy of 59.5 keV generated by a $^{241}\text{Am}$ radioactive point-source with an activity of 100 mCi.	$^{57}\text{La}$ , $^{58}\text{Ce}$ , $^{59}\text{Pr}$ , $^{60}\text{Nd}$ , $^{62}\text{Sm}$ , $^{63}\text{Eu}$ , $^{64}\text{Gd}$ , $^{65}\text{Tb}$ , $^{66}\text{Dy}$ , $^{67}\text{Ho}$ , $^{68}\text{Er}$ , $^{69}\text{Tm}$ , $^{70}\text{Yb}$ , $^{71}\text{Lu}$ , $^{73}\text{Ta}$ , $^{74}\text{W}$ , $^{75}\text{Re}$ , $^{79}\text{Au}$ , $^{80}\text{Hg}$ , $^{81}\text{Tl}$ , $^{82}\text{Pb}$ , $^{83}\text{Bi}$ , $^{90}\text{Th}$ , and $^{92}\text{U}$ .	Si(Li) detector achieving a resolution of 160 eV at 5.9 keV.
[65]	$I_{L\alpha}/I_{L\alpha}$	$\gamma$ - rays with an energy of 59.54 keV emitted by a $^{241}\text{Am}$ point-source with an activity of 200 mCi.	$^{57}\text{La}$ , $^{58}\text{Ce}$ , $^{59}\text{Pr}$ , $^{60}\text{Nd}$ , $^{62}\text{Sm}$ , $^{63}\text{Eu}$ , $^{64}\text{Gd}$ , $^{65}\text{Tb}$ , $^{66}\text{Dy}$ , $^{67}\text{Ho}$ , $^{68}\text{Er}$ , and $^{69}\text{Tm}$ . (Targets of high purity and thinness).	Si(Li) detector with 160 eV resolution at 5.9 keV.

(continued on next page)

Table 1 (continued)

References	Atomic parameters	Excitation sources	Target samples	Detectors
[34]	$I_{L\alpha}/I_{\text{II}}, I_{L\alpha}/I_{L\beta}, I_{L\alpha}/I_{L\gamma} \& I_{L\beta}/I_{L\gamma}$	Gamma rays of 59.54 keV energy generated by a $^{241}\text{Am}$ radioactive source with an activity of 100 mCi.	Uranium ( $^{92}\text{U}$ ) and Thorium ( $^{90}\text{Th}$ ).	Si(Li) detector with 160 eV resolution at 5.9 keV.
[90]	$I_{L\beta}/I_{L\alpha} \& I_{L\gamma}/I_{L\alpha}$	$\gamma$ - rays with an energy of 59.54 keV originating from a radioactive $^{241}\text{Am}$ source.	$^{80}\text{Hg}$ , $^{83}\text{Bi}$ , and $^{82}\text{Pb}$ . (Powdered specimens of elemental metals and their corresponding compounds).	Si(Li) detector achieving a resolution of 160 eV when measuring 5.9 keV.
[35]	$I_{L\alpha}/I_{\text{II}}, I_{L\alpha}/I_{L\beta} \& I_{L\alpha}/I_{L\gamma}$	Gamma-rays with energies of 59.5 and 122 keV emitted from a $^{241}\text{Am}$ and $^{57}\text{Co}$ annular source, each having an activity of 100 mCi, respectively.	$^{73}\text{Ta}$ , $^{74}\text{W}$ , $^{75}\text{Re}$ , $^{79}\text{Au}$ , $^{80}\text{Hg}$ , $^{81}\text{Tl}$ , $^{82}\text{Pb}$ , $^{83}\text{Bi}$ , $^{90}\text{Th}$ , and $^{92}\text{U}$ . (Pure targets were evaporated on thick Mylar).	Si(Li) detector with a resolution of 160 eV FWHM at 5.96 keV.
[16]	$I_{L\beta}/I_{L\alpha} \& I_{L\gamma}/I_{L\alpha}$	An x-ray tube featuring a Mo anode, having a maximum high voltage of 55 kV and a maximum current of 60 mA.	$^{65}\text{Tb}$ , $^{66}\text{Dy}$ , $^{67}\text{Ho}$ , $^{69}\text{Tm}$ , $^{70}\text{Yb}$ , $^{71}\text{Lu}$ , $^{74}\text{W}$ , $^{78}\text{Pt}$ , and $^{79}\text{Au}$ . (Pure metals).	A Si(Li) detector with a 5 mm thickness, exhibiting an energy resolution of 185 eV at 5.9 keV.
[36]	$I_{L\alpha}/I_{\text{II}}, I_{L\alpha}/I_{L\beta} \& I_{L\alpha}/I_{L\gamma}$	20.48 keV Rh-ray tube.	$^{62}\text{Sm}$ , $^{63}\text{Eu}$ , $^{71}\text{Lu}$ , $^{72}\text{Hf}$ , $^{76}\text{Os}$ , $^{78}\text{Pt}$ , $^{81}\text{Tl}$ , $^{82}\text{Pb}$ , and $^{83}\text{Bi}$ . (Powdered specimens composed of elemental purity).	Si(Li) detector with 170 eV resolution at 5.9 keV.
[37]	$I_{L\alpha}/I_{\text{II}}, I_{L\alpha}/I_{L\beta 2,15}, I_{L\alpha}/I_{L\beta 5} \& I_{L\alpha}/I_{L\beta 6}$	Gamma rays with an energy of 59.54 keV were generated using a 100-mCi annular radioactive source containing $^{241}\text{Am}$ .	$^{80}\text{Hg}$ , $^{83}\text{Bi}$ , $^{90}\text{Th}$ , and $^{92}\text{U}$ . (Circular disk-shaped targets made of pure material).	Si(Li) detector.
[84]	$I_{L\alpha}/I_{L\beta} \& I_{L\alpha}/I_{L\gamma}$	59.5 keV gamma rays produced from a $^{241}\text{Am}$ radioactive source.	$^{56}\text{Ba}$ , $^{57}\text{La}$ , $^{58}\text{Ce}$ , $^{64}\text{Gd}$ , $^{68}\text{Er}$ , $^{70}\text{Yb}$ , $^{73}\text{Ta}$ , $^{79}\text{Au}$ , $^{80}\text{Hg}$ , $^{82}\text{Pb}$ , and $^{83}\text{Bi}$ . (Samples of pure elements in powdered form were readied by being placed onto a mylar film support).	Si(Li) detector having 160 eV resolution at 5.9 keV.
[38]	$I_{L\alpha}/I_{\text{II}}, I_{L\alpha}/I_{L\beta} \& I_{L\alpha}/I_{L\gamma}$	Photons with an energy of 59.5 keV, emitted by a 100 mCi $^{241}\text{Am}$ point source, were employed of excitation.	$^{57}\text{La}$ , $^{58}\text{Ce}$ , $^{59}\text{Pr}$ , $^{60}\text{Nd}$ , $^{62}\text{Sm}$ , $^{65}\text{Tb}$ , $^{66}\text{Dy}$ , $^{67}\text{Ho}$ , $^{68}\text{Er}$ , $^{70}\text{Yb}$ , $^{72}\text{Hf}$ , $^{74}\text{W}$ , $^{76}\text{Os}$ , $^{80}\text{Hg}$ , $^{81}\text{Tl}$ , $^{82}\text{Pb}$ , $^{90}\text{Th}$ , and $^{92}\text{U}$ . (Thin targets).	Detector Si(Li) capable of achieving a resolution of 188 eV at 5.9 keV.
[66]	$I_{\text{II}}/I_{L\alpha}, I_{L\beta}/I_{L\alpha} \& I_{L\gamma}/I_{L\alpha}$	Thoroughly filtered gamma rays with an energy of 59.6 keV, originating from a 75 mCi activity $^{241}\text{Am}$ annular point source.	$^{90}\text{Th}$ and $^{92}\text{U}$ (Samples of powdered pure elements and their corresponding compounds: $\text{ThO}_2$ , $\text{Th}(\text{NO}_3)_4 \cdot 5\text{H}_2\text{O}$ , $\text{UCl}_3$ , $\text{U}(\text{NO}_3)_3$ , $\text{U}_3\text{O}_8$ , $[(\text{CH}_3\text{COO})_2\text{UO}_2] \cdot 2\text{H}_2\text{O}$ ).	Si(Li) detector (FWHM=155 eV at 5.9 keV).
[17]	$I_{L\beta}/I_{L\alpha}$	X-ray tube with a (Mo) anode .	$^{57}\text{La}$ , $^{59}\text{Pr}$ , $^{60}\text{Nd}$ , $^{62}\text{Sm}$ , $^{63}\text{Eu}$ , $^{64}\text{Gd}$ , $^{65}\text{Tb}$ , $^{66}\text{Dy}$ , $^{67}\text{Ho}$ , $^{69}\text{Tm}$ , $^{70}\text{Yb}$ , and $^{71}\text{Lu}$ . (Pure metals).	Si(Li) detector having a thickness of 5 mm and 185 eV resolution at 5.9 keV.
[39]	$I_{L\alpha}/I_{\text{II}}, I_{L\alpha}/I_{L\beta}, I_{L\alpha}/I_{L\gamma} \& I_{L\beta}/I_{L\alpha}$	Gamma photons with an energy of 59.54 keV released from a 50 mCi annular source of radioactive $^{241}\text{Am}$ .	$^{80}\text{Hg}$ , $^{82}\text{Pb}$ , and $^{83}\text{Bi}$ . (Powder samples of pure elements and its compounds).	A Si(Li) detector with a thickness of 3 mm and a resolution of 147 eV at 5.96 keV.
[40]	$I_{L\alpha}/I_{\text{II}}, I_{L\alpha}/I_{L\beta} \& I_{L\alpha}/I_{L\gamma}$	59.5 keV gamma-photons emitted from a 75 mCi $^{241}\text{Am}$ source.	$^{70}\text{Yb}$ , $^{72}\text{Hf}$ , $^{73}\text{Ta}$ , $^{74}\text{W}$ , $^{75}\text{Re}$ , $^{76}\text{Pt}$ , $^{79}\text{Au}$ , $^{80}\text{Hg}$ , $^{81}\text{Tl}$ , $^{82}\text{Pb}$ , $^{83}\text{Bi}$ , $^{90}\text{Th}$ , and $^{92}\text{U}$ . (Powdered samples of pure targets with varying thicknesses, supported on a mylar film, for spectroscopic analysis).	Si(Li) detector (FWHM=155 eV at 5.9 keV).
[41]	$I_{L\alpha}/I_{\text{II}}, I_{L\alpha}/I_{L\beta}, I_{L\alpha}/I_{L\gamma}, I_{\text{II}}/I_{L\beta}, I_{\text{II}}/I_{L\gamma} \& I_{L\beta}/I_{L\gamma}$	Gamma rays with an energy of 59.5 keV emitted from a $^{241}\text{Am}$ point source with an activity of $3.7 \times 10^9$ Bq.	$^{66}\text{Dy}$ , $^{67}\text{Ho}$ , $^{68}\text{Er}$ , $^{72}\text{Hf}$ , $^{74}\text{W}$ , $^{81}\text{Tl}$ , $^{83}\text{Bi}$ , and $^{90}\text{Th}$ . (eight distinct elements with diverse excitation energies ranging from 8.265 to 21.705 keV).	Si(Li) detector with 160 eV resolution at 5.9 keV.
[67]	$I_{L\beta}/I_{L\alpha} \& I_{L\gamma}/I_{L\alpha}$	Generating a photon energy of 17 keV by emitting the K x-ray of Mo using an annular source of $^{241}\text{Am}$ .	$^{57}\text{La}$ , $^{59}\text{Pr}$ , $^{60}\text{Nd}$ , $^{62}\text{Sm}$ , $^{63}\text{Eu}$ , $^{64}\text{Gd}$ , $^{65}\text{Tb}$ , $^{66}\text{Dy}$ , $^{67}\text{Ho}$ , $^{69}\text{Tm}$ , $^{70}\text{Yb}$ , and $^{71}\text{Lu}$ . (Self-supporting targets of high spectroscopic purity, having thicknesses ranging between 35.58 and 37.36 $\mu\text{g cm}^{-2}$ ).	Si(Li) detector having 185 eV resolution at 5.9 keV.
[68]	$I_{\text{II}}/I_{L\alpha}, I_{L\beta}/I_{L\alpha} \& I_{L\gamma}/I_{L\alpha}$	Photon energy of 31.635 keV generated by a $3.7 \times 10^8$ Bq activity annular source containing $^{133}\text{Ba}$ .	$^{74}\text{W}$ , $^{79}\text{Au}$ , $^{80}\text{Hg}$ , $^{81}\text{Tl}$ , $^{82}\text{Pb}$ , $^{83}\text{Bi}$ , $^{90}\text{Th}$ , and $^{92}\text{U}$ . (Thick Mylar substrates were used for evaporating spectroscopically pure targets).	Si(Li) detector having 160 eV resolution at 5.9 keV.
[69]	$I_{L\beta}/I_{L\alpha} \& I_{L\gamma}/I_{L\alpha}$	15.2 keV gamma rays produced from a $^{241}\text{Am}$ annular radioactive source.	$^{57}\text{La}$ , $^{59}\text{Pr}$ , $^{60}\text{Nd}$ , $^{62}\text{Sm}$ , $^{63}\text{Eu}$ , $^{64}\text{Gd}$ , $^{65}\text{Tb}$ , $^{66}\text{Dy}$ , $^{67}\text{Ho}$ , $^{69}\text{Tm}$ , $^{70}\text{Yb}$ , and $^{71}\text{Lu}$ . (Self-supporting and pure samples).	Si(Li) detector achieving a resolution of 185 eV at 5.9 keV.
[42]	$I_{L\alpha}/I_{\text{II}}$	Thoroughly filtered gamma rays with an energy of 59.6 keV, produced from a 75 mCi activity $^{241}\text{Am}$ annular source.	$^{62}\text{Sm}$ , $^{63}\text{Eu}$ , $^{67}\text{Ho}$ , $^{68}\text{Er}$ , $^{72}\text{Hf}$ , $^{73}\text{Ta}$ , $^{74}\text{W}$ , $^{75}\text{Re}$ , $^{78}\text{Pt}$ , $^{79}\text{Au}$ , $^{81}\text{Tl}$ , $^{82}\text{Pb}$ , $^{83}\text{Bi}$ , and $^{92}\text{U}$ . (Powdered samples containing pure elements along with a selection of their compounds: $\text{La}_2\text{O}_3$ , $\text{CeO}_2$ , $\text{YbO}_2$ , $\text{HgO}$ , $\text{ThO}_2$ ).	Si(Li) detector with 155 eV resolution at 5.96 keV.
[43]	$I_{L\alpha}/I_{\text{II}}, I_{L\alpha}/I_{L\beta}, I_{L\alpha}/I_{L\gamma}, I_{L\alpha}/I_{L\beta}, I_{L\alpha}/I_{L\gamma}, I_{L\alpha} / I_{L\gamma 2,3,6,8} \& I_{L\alpha}/I_{L\gamma 4,4}$	59.537 KeV photons emitted from an $^{241}\text{Am}$ radioisotope source with 100 mCi activity.	$^{72}\text{Hf}$ , $^{73}\text{Ta}$ , $^{74}\text{W}$ , $^{79}\text{Au}$ , $^{80}\text{Hg}$ , $^{81}\text{Tl}$ , $^{82}\text{Pb}$ , $^{83}\text{Bi}$ , $^{90}\text{Th}$ , and $^{92}\text{U}$ . (The samples are spectroscopically pure foils and powders).	A solid-state detector achieving a full-width at half-maximum (FWHM) resolution of 160 eV at 5.9 keV for Mn K $\alpha$ line.

(continued on next page)

Table 1 (continued)

References	Atomic parameters	Excitation sources	Target samples	Detectors
[70]	$I_{L\beta 4}/I_{L\beta 3}$ , $I_{L\gamma 1}/I_{L\beta 1}$ , $I_{L\gamma 1}/I_{L\alpha}$ , $I_{L\beta 6}/I_{L\alpha}$ & $I_{L\beta 2.15}/I_{L\alpha}$	Utilizing high-brilliance undulator radiation to generate synchrotron radiation spanning the range of 5.6 to 30 keV.	$^{56}\text{Ba}$ . (Target was pressed powder in the form of a disc).	Double crystal monochromator cooled by liquid-nitrogen.
[71]	$I_{L\gamma 1}/I_{L\alpha}$ , $I_{L\beta 1}/I_{L\alpha}$ & $I_{L\gamma 1}/I_{L\alpha}$	123.6 keV gamma rays produced from a $^{57}\text{Co}$ annular radioactive source.	$^{72}\text{Hf}$ . (Both the pure element and its corresponding compounds, all in powdered form, placed on a mylar film). Uranium ( $^{92}\text{U}$ ) and Thorium ( $^{90}\text{Th}$ ). (Spectroscopically pure powders with various magnetic field at 110° and 125° ( $B = 0, \pm 0.15\text{T}, \pm 0.30\text{T}, \pm 0.45\text{T}, \pm 0.60\text{T}$ , and $\pm 0.75\text{T}$ )).	Ultra-LEGe detector with a resolution of 150 eV at 5.9 keV.
[44]	$I_{L\gamma 1}/I_{L\gamma 2}$ , $I_{L\alpha}/I_{L\gamma 2}$ & $I_{L\beta 1}/I_{L\gamma 2}$	59.5 keV gamma photon sourced from a filtered point source of $^{241}\text{Am}$ with an intensity of $3.7 \times 10^8$ Bq was employed for direct excitation.	$^{73}\text{Ta}$ , $^{74}\text{W}$ , $^{79}\text{Au}$ , $^{80}\text{Hg}$ , $^{81}\text{Tl}$ , $^{82}\text{Pb}$ , $^{83}\text{Bi}$ , $^{90}\text{Th}$ , and $^{92}\text{U}$ . (Spectroscopically pure foil and powders with various magnetic field: $0\text{T}, \pm 0.15\text{T}, \pm 0.45\text{T}$ and $\pm 0.75\text{T}$ ).	Si(Li) detector with a resolution of 180 eV FWHM at 5.9 keV.
[45]	$I_{L\alpha}/I_{L\gamma 1}$ , $I_{L\alpha}/I_{L\beta 1}$ & $I_{L\alpha}/I_{L\gamma 2}$	59.54 keV gamma photon originating from a filtered point source of the radioisotope $^{241}\text{Am}$ was employed to directly excite.	$^{73}\text{Ta}$ , $^{74}\text{W}$ , $^{79}\text{Au}$ , $^{80}\text{Hg}$ , $^{81}\text{Tl}$ , $^{82}\text{Pb}$ , $^{83}\text{Bi}$ , $^{90}\text{Th}$ , and $^{92}\text{U}$ . (Spectroscopically pure foil and powders with various magnetic field: $0\text{T}, \pm 0.15\text{T}, \pm 0.45\text{T}$ and $\pm 0.75\text{T}$ ).	Si(Li) detector with a resolution of 180 eV FWHM at 5.9 keV.
[9]	$I_{L\gamma 1}/I_{L\alpha}$	A gamma photon with an energy of 59.54 keV, emitted from a specifically filtered point source containing the radioisotope $^{241}\text{Am}$ .	$^{73}\text{Ta}$ , $^{74}\text{W}$ , $^{79}\text{Au}$ , $^{80}\text{Hg}$ , $^{81}\text{Tl}$ , $^{82}\text{Pb}$ , $^{83}\text{Bi}$ , $^{90}\text{Th}$ , and $^{92}\text{U}$ . (Foil and powders with spectroscopic purity, subjected to magnetic fields of $\pm 0.75\text{T}$ and $0\text{T}$ ).	A Si(Li) detector exhibiting a 180 eV FWHM resolution at 5.9 keV.
[27]	$I_{L\alpha}$ , $I_{L\gamma 1}$ , $I_{L\beta 1}$ , $I_{L\beta 6}$ , $I_{L\beta 2.4}$ , $I_{L\beta 1.3}$ , $I_{L\beta 9.10}$ , $I_{L\gamma 2}$ , $I_{L\gamma 5}$ , $I_{L\gamma 1}$ , $I_{L\gamma 2.3}$ & $I_{L\gamma 4}$	Gamma rays with an energy of 59.54 keV generated by a radioactive point-source of $^{241}\text{Am}$ .	$^{78}\text{Pt}$ , $^{79}\text{Au}$ , $^{80}\text{Hg}$ , $^{81}\text{Tl}$ , $^{82}\text{Pb}$ , $^{83}\text{Bi}$ , $^{90}\text{Th}$ , and $^{92}\text{U}$ . (Samples of different thicknesses with high purity).	Collimated Si(Li) detector.
[72]	$I_{L\beta 1}/I_{L\alpha}$	Gamma rays with an energy of 59.54 keV emitted from a $^{241}\text{Am}$ point source at five angles ranging from 120° to 160°	$^{62}\text{Sm}$ , $^{63}\text{Eu}$ , $^{64}\text{Gd}$ , $^{65}\text{Tb}$ , $^{66}\text{Dy}$ , $^{67}\text{Ho}$ , and $^{68}\text{Er}$ . (Targets characterized by their spectroscopic purity).	Si(Li) detector having 160 eV FWHM resolution at 5.9 keV
[46]	$I_{L\gamma 1}/I_{L\gamma 2}$ , $I_{L\alpha}/I_{L\gamma 2}$ , $I_{L\beta 1}/I_{L\gamma 2}$ , $I_{L\alpha}/I_{L\gamma 1}$ & $I_{L\alpha}/I_{L\beta 1}$	Photons resulting from 59.5 KeV gamma rays were employed to excite the samples, utilizing an annular source of filtered radioisotope $^{241}\text{Am}$ (100mCi), as well as the radioactive decay of $^{160}\text{Tb}$ , $^{160}\text{Er}$ , $^{173}\text{Lu}$ , $^{182}\text{Re}$ , $^{201}\text{Tl}$ , $^{203}\text{Pb}$ , and $^{207}\text{Bi}$ .	$^{66}\text{Dy}$ , $^{67}\text{Ho}$ , $^{70}\text{Yb}$ , $^{74}\text{W}$ , $^{80}\text{Hg}$ , $^{81}\text{Tl}$ , and $^{82}\text{Pb}$ . (Samples that are pure and in the form of powder).	Si(Li) detector having 160 eV resolution at 5.9 keV.
[18]	$I_{L\gamma 1}/I_{L\alpha}$ , $I_{L\beta 1}/I_{L\alpha}$ , $I_{L\gamma 1}/I_{L\alpha}$ & $I_{L\gamma 1}/I_{L\alpha}$	Annular radioactive sources of $^{241}\text{Am}$ and $^{57}\text{Co}$ emitting gamma rays with energies of 59.5 keV and 123.6 keV, respectively.	$^{79}\text{Au}$ . (Both the elemental substance in its pure state and the associated compounds: $\text{AuCl}$ , $\text{Au}_2\text{O}_3$ and $\text{AuBr}_3$ , all presented as powders and affixed to a mylar film).	Ultra-LEGe detector with a resolution of 0.150 keV at 5.9 keV.
[73]	$I_{L\gamma 1}/I_{L\alpha}$ , $I_{L\beta 1}/I_{L\alpha}$ , $I_{L\gamma 1}/I_{L\alpha}$ & $I_{L\gamma 2.3}/I_{L\alpha}$	Gamma rays with an energy of 59.5 keV emitted by an annular radioactive source containing $^{241}\text{Am}$ .	$^{74}\text{W}$ , $^{75}\text{Re}$ , $^{76}\text{Os}$ , and $^{78}\text{Pt}$ . (Powder samples of pure elements and a variety of complexes).	Ultra-LEGe detector having 150 eV resolution at 5.9 keV.
[47]	$I_{L\alpha}/I_{L\gamma 1}$ , $I_{L\alpha}/I_{L\beta 1}$ , $I_{L\alpha}/I_{L\gamma 2}$ , $I_{L\alpha}/I_{L\gamma 1}$ , $I_{L\alpha}/I_{L\gamma 1}$ , $I_{L\alpha}/I_{L\gamma 5}$ , $I_{L\alpha}/I_{L\gamma 2.3.6.8}$ , $I_{L\alpha}/I_{L\gamma 4.4}$ , $I_{L\alpha}$ $/I_{L\beta 6}$ , $I_{L\alpha}/I_{L\beta 2.4.15}$ & $I_{L\alpha}/I_{L\beta 1.3}$	22.6 keV photons produced from a $^{109}\text{Cd}$ radioactive point source.	$^{66}\text{Dy}$ , $^{68}\text{Er}$ , $^{70}\text{Yb}$ , $^{71}\text{Lu}$ , $^{73}\text{Ta}$ , $^{74}\text{W}$ , $^{76}\text{Os}$ , $^{78}\text{Pt}$ , $^{79}\text{Au}$ , $^{80}\text{Hg}$ , $^{81}\text{Tl}$ , $^{82}\text{Pb}$ , $^{83}\text{Bi}$ , $^{90}\text{Th}$ , and $^{92}\text{U}$ . (Targets with spectroscopic purity, having thicknesses that vary between 0.018 and 0.36 g/cm <sup>2</sup> ).	Si(Li) detector having 160 eV FWHM resolution at 5.96 keV
[86]	$I_{L\gamma 1}/I_{L\alpha}$ , $I_{L\beta 1}/I_{L\alpha}$ , $I_{L\gamma 1}/I_{L\alpha}$ , $I_{L\gamma 1}/I_{L\alpha}$ , $I_{L\gamma 4}/I_{L\alpha}$ , $I_{L\gamma 2.3.6.8}/I_{L\alpha}$ , $I_{L\gamma 1.5}/I_{L\alpha}$ , $I_{L\beta 5.7}/I_{L\alpha}$ , $I_{L\beta 1.2.3.15}/I_{L\alpha}$ & $I_{L\beta 4.6}/I_{L\alpha}$	22.6 keV photons produced from a $^{109}\text{Cd}$ radioactive source. (Ag-K $\alpha$ ).	Mercury ( $^{80}\text{Hg}$ ) (Target in its pure liquid state).	Peltier cooled Si-PIN x-ray detector arranged in the 90° reflection geometry.
[48]	$I_{L\alpha}/I_{L\beta 1}$ & $I_{L\alpha}/I_{L\gamma 1}$	59.54 keV gamma rays produced from a $^{241}\text{Am}$ annular radioactive source of 100 mCi activity.	$^{57}\text{La}$ , $^{58}\text{Ce}$ , and $^{59}\text{Pr}$ . (The targets were readied as pellets, with the powdered materials compressed into circular disks for their ultimate utilization in the experiment).	Si(Li) detector.
[74]	$I_{L\gamma 1}/I_{L\alpha}$ , $I_{L\beta 1}/I_{L\alpha}$ , $I_{L\gamma 1}/I_{L\alpha}$ & $I_{L\gamma 2.3}/I_{L\alpha}$	59.5 keV gamma rays produced from a $^{241}\text{Am}$ annular radioactive source of 50 mCi activity.	$^{73}\text{Ta}$ and $^{74}\text{W}$ . (Powder samples of pure elements and their compounds: $\text{TaCl}_5$ , $\text{TaI}_5$ , $\text{TaF}_5$ , $\text{WS}_2$ , $\text{WSi}_2$ , $\text{W}_2\text{B}_5$ , $\text{WC}$ , $\text{WO}_3$ , $\text{Na}_2\text{WO}_4 \cdot 2(\text{H}_2\text{O})$ and $\text{WCl}_6$ ).	Ultra-LEGe detector having 150 eV resolution at 5.9 keV.
[87]	$I_{L\gamma 1}/I_{L\alpha}$ , $I_{L\beta 1}/I_{L\alpha}$ , $I_{L\beta 2}/I_{L\alpha}$ & $I_{L\gamma 1}/I_{L\alpha}$	Highly filtered gamma rays at an energy level of 59.543 keV, generated by a $^{241}\text{Am}$ radioisotope source with an activity of 75 mCi.	$^{62}\text{Sm}$ and $^{63}\text{Eu}$ . (Pure elemental samples and its compounds in powder form were prepared by placing them onto a mylar film for support).	Si(Li) detector which has a 155 eV resolution at 5.9 keV.
[75]	$I_{L\gamma 1}/I_{L\alpha}$ , $I_{L\beta 1}/I_{L\alpha}$ , $I_{L\beta 1.4}/I_{L\alpha}$ , $I_{L\beta 3.6}/I_{L\alpha}$ , $I_{L\beta 2.15.7}/I_{L\alpha}$ , $I_{L\beta 1.3.4.6}/I_{L\alpha}$ , $I_{L\gamma 2.3}/I_{L\alpha}$ , $I_{L\gamma 1.5}/I_{L\alpha}$ & $I_{L\gamma 4}/I_{L\alpha}$	The EDXRF spectrometer was employed to carry out measurements, utilizing disk-type radioactive sources of $^{109}\text{Cd}$ and $^{241}\text{Am}$ . Two incident	$^{66}\text{Dy}$ . (Spectroscopically pure self-supporting pressed pellets of $\text{Dy}_2\text{O}_3$ , $\text{Dy}_2(\text{CO}_3)_3$ ,	Peltier cooled Si-PIN detector having 152 eV resolution at 5.9 keV.

(continued on next page)

Table 1 (continued)

References	Atomic parameters	Excitation sources	Target samples	Detectors
[49]	$I_{La}/I_{Ll}, I_{La}/I_{L\beta} \text{ \& } I_{La}/I_{L\gamma}$	photon energies, namely 22.6 keV and 59.54 keV, were involved in the process. 59.5 keV gamma rays produced from a $^{241}\text{Am}$ annular radioactive source of 100 mCi activity.	$\text{Dy}_2(\text{SO}_4)_3 \cdot 8\text{H}_2\text{O}$ , $\text{DyI}_2$ and a pure Dy metallic foil. $^{66}\text{Dy}$ , $^{67}\text{Ho}$ , and $^{68}\text{Er}$ . (The target samples were created by compacting finely powdered compounds, ensuring both the purity and consistent pressure of the target).	Si(Li) detector with a resolution of 155 eV at 5.9 keV.
[76]	$I_{Ll}/I_{La}, I_{L\beta}/I_{La} \text{ \& } I_{L\gamma}/I_{La}$	Rhodium x-ray tube at an excitation energie of 20.48 keV.	$^{56}\text{Ba}$ , $^{59}\text{Pr}$ , $^{78}\text{Pt}$ , $^{80}\text{Hg}$ , and $^{83}\text{Bi}$ . (Pure elements in the form of powder).	Collimated Si(Li) detector having 167 eV resolution at 5.9 keV.
[50]	$I_{La}/I_{L\beta}$	x-ray tube by an Ag-anode.	$^{79}\text{Au}$ and $^{82}\text{Pb}$ . (Thin and thick).	Si-drift detector a resolution of 125 eV at 5.9 keV.
[51]	$I_{La}/I_{Ll}, I_{La}/I_{L\beta} \text{ \& } I_{La}/I_{L\gamma}$	Commercial $^{241}\text{Am}$ radioactive source was used with an activity 100mCi.	$^{57}\text{La}$ , $^{58}\text{Ce}$ , $^{59}\text{Pr}$ , $^{60}\text{Nd}$ , $^{62}\text{Sm}$ , $^{64}\text{Gd}$ , $^{65}\text{Tb}$ , $^{66}\text{Dy}$ , $^{67}\text{Ho}$ , and $^{68}\text{Er}$ . (Powder samples with magnetic field 0.6T and 1.2T).	Si(Li) detector having 155 eV resolution at 5.9 keV.
[1]	$I_{La}/I_{Ll}, I_{La}/I_{L\beta}, I_{La}/I_{L\gamma}, I_{Ll}/I_{L\beta}, I_{Ll}/I_{L\gamma} \text{ \& } I_{L\beta}/I_{L\gamma}$	59.54 keV gamma rays produced from a $^{241}\text{Am}$ annular radioactive source of 100 mCi activity.	$^{70}\text{Yb}$ , $^{73}\text{Ta}$ , $^{74}\text{W}$ , $^{80}\text{Hg}$ , $^{81}\text{Tl}$ , $^{82}\text{Pb}$ , $^{83}\text{Bi}$ , $^{90}\text{Th}$ , and $^{92}\text{U}$ . (Pure targets with high spectroscopic quality, initially in powdered state, later compacted into pellets).	Si(Li) detector having 160 eV FWHM resolution at 5.96 keV.
[10]	$I_{Ll}/I_{La}, I_{Ll}/I_{L\beta}, I_{L\gamma44}/I_{La}, I_{L\gamma1.8}/I_{La}, I_{L\gamma1}/I_{La}, I_{L\gamma5}/I_{La}, I_{L\gamma1.5.8}/I_{La}, \text{ \& } I_{L\gamma2.3}/I_{La}, I_{L\gamma2.3.6.8}/I_{La}, I_{L\gamma2.3.6}/I_{La}, I_{L\gamma2.3.7.15}/I_{La}, I_{L\beta2.15}/I_{La}, I_{L\beta2.4.15}/I_{La}, I_{L\beta9.10}/I_{La}, I_{L\beta1}/I_{La}, I_{L\beta1.4.6}/I_{La}, I_{L\beta6}/I_{La}, I_{L\beta1.3.7}/I_{La}, I_{L\beta1.3}/I_{La}, I_{L\beta1.3.4.6}/I_{La}, I_{L\beta1.4.6}/I_{La}, I_{L\beta1.4}/I_{La}, I_{L\beta3.6}/I_{La}, I_{L\beta3}/I_{La}, I_{L\beta2.7.9.10.15}/I_{La}, I_{Ll}/I_{La}, I_{L\beta}/I_{La}, I_{L\gamma1}/I_{La} \text{ \& } I_{L\gamma2.3}/I_{La}$	59.5 and 5.96 keV gamma-rays emitted by a $^{241}\text{Am}$ and $^{57}\text{Fe}$ annular source of 50 mCi activity, respectively. (The $^{57}\text{Fe}$ radioisotope for the elements in the range of $50 \leq Z \leq 53$ and $^{241}\text{Am}$ for $56 \leq Z \leq 92$ ).	$^{50}\text{Sn}$ , $^{51}\text{Sb}$ , $^{52}\text{Te}$ , $^{53}\text{I}$ , $^{56}\text{Ba}$ , $^{57}\text{La}$ , $^{58}\text{Ce}$ , $^{59}\text{Pr}$ , $^{60}\text{Nd}$ , $^{62}\text{Sm}$ , $^{63}\text{Eu}$ , $^{64}\text{Gd}$ , $^{65}\text{Tb}$ , $^{66}\text{Dy}$ , $^{67}\text{Ho}$ , $^{68}\text{Er}$ , $^{69}\text{Tm}$ , $^{71}\text{Lu}$ , $^{72}\text{Hf}$ , $^{73}\text{Ta}$ , $^{74}\text{W}$ , $^{75}\text{Re}$ , $^{76}\text{Os}$ , $^{77}\text{Ir}$ , $^{78}\text{Pt}$ , $^{79}\text{Au}$ , $^{80}\text{Hg}$ , $^{81}\text{Tl}$ , $^{82}\text{Pb}$ , $^{83}\text{Bi}$ , $^{90}\text{Th}$ , and $^{92}\text{U}$ .	Collimated Ultra-LEGE detector having 150 eV resolution at 5.96 keV.
[77]	$I_{Ll}/I_{La}, I_{L\beta}/I_{La}, I_{L\gamma1}/I_{La} \text{ \& } I_{L\gamma2.3}/I_{La}$	59.5 keV gamma photons emitted by a $^{241}\text{Am}$ annular radioactive source of 50 mCi activity.	$^{82}\text{Pb}$ . (Powdered samples containing a pure element and diverse complexes were readied by being placed onto a mylar film for support).	Ultra-LEGE detector having 150 eV resolution at 5.9 keV.
[52]	$I_{La}/I_{L\beta1.2}, I_{La}/I_{L\gamma} \text{ \& } I_{L\beta1.2}/I_{L\gamma}$	13.1 keV bremsstrahlung radiation from x-ray tube.	$^{73}\text{Ta}$ , $^{74}\text{W}$ , $^{79}\text{Au}$ , and $^{82}\text{Pb}$ .	AMPTEx production silicon Drift detector(XR-100SDD) having 125 eV resolution at 5.9 keV.
[78]	$I_{Ll}/I_{La}, I_{L\beta2.15}/I_{La}, I_{L\gamma1}/I_{L\beta1} \text{ \& } I_{L\gamma1.5}/I_{L\beta1}$	Photoionization triggered by synchrotron radiation in the energy range of 10.2 keV to 13.1 keV.	$^{74}\text{W}$ and $^{76}\text{Os}$ . (Spectroscopically, pure self-supporting $^{74}\text{W}$ (metallic foil) and thick pressed pellets of $^{76}\text{Os}$ ).	Silicon drift detector having an energy resolution~140 eV at 5.89 keV.
[53]	$I_{La}/I_{Ll}, I_{La}/I_{L\beta} \text{ \& } I_{La}/I_{L\gamma}$	Synchrotron radiation.	$^{64}\text{Gd}$ , $^{65}\text{Tb}$ , and $^{67}\text{Ho}$ . (Rare earth elements and their compounds).	Silicon drift detector having 130 eV resolution at 5.9 keV.
[54]	$I_{La}/I_{Ll}, I_{L\beta}/I_{Ll} \text{ \& } I_{L\gamma}/I_{Ll}$	Synchrotron radiation emitted at 17 distinct energy levels spanning from 8 keV to 17 keV, with intervals of 0.5 keV between each.	$^{66}\text{Dy}$ , $^{67}\text{Ho}$ , $^{68}\text{Er}$ , $^{71}\text{Lu}$ , $^{73}\text{Ta}$ , $^{74}\text{W}$ , $^{78}\text{Pt}$ , $^{79}\text{Au}$ , $^{80}\text{Hg}$ , $^{82}\text{Pb}$ , and $^{83}\text{Bi}$ . (Spectroscopically pure elements, Tantalum ( $^{73}\text{Ta}$ ), tungsten ( $^{74}\text{W}$ ), platinum ( $^{78}\text{Pt}$ ), gold ( $^{79}\text{Au}$ ), and lead ( $^{82}\text{Pb}$ ) were in a metallic state, whereas holmium ( $^{67}\text{Ho}$ ) was in powder form. Self-supporting targets of dysprosium ( $^{66}\text{Dy}$ ), erbium ( $^{68}\text{Er}$ ), lutetium ( $^{71}\text{Lu}$ ), mercury ( $^{80}\text{Hg}$ ), and bismuth ( $^{83}\text{Bi}$ ) were prepared directly from powder).	Peltier cooled Vortex solid state Silicon drift detector having an energy resolution~138 eV at 5.959 keV (Mn K $\alpha$ ) x-rays.
[91]	$I_{La}/I_{L\beta1} \text{ \& } I_{La}/I_{L\gamma}$	59.54 keV gamma rays emitted by a $^{133}\text{Ba}$ radioactive source of 100 mCi activity.	$^{60}\text{Nd}$ , $^{62}\text{Sm}$ , $^{64}\text{Gd}$ , and $^{65}\text{Tb}$ . 30 elements ( $^{60}\text{Nd}$ , $^{62}\text{Sm}$ , $^{64}\text{Gd}$ , $^{65}\text{Tb}$ and their compounds) with high purity starting as powders, they were subsequently compressed into thin, solid pellets.	Si(Li) detector having 155 eV resolution for 5.9 keV X-ray peak.
[92]	$I_{Ll}/I_{La}, I_{L\beta}/I_{La}, I_{L\gamma1.5}/I_{La}, I_{L\gamma2.3}/I_{La} \text{ \& } I_{L\gamma4}/I_{La}$	Emission of ELETTRA synchrotron radiation within the energy range of 7.8–10 keV.	$^{66}\text{Dy}$ . (Self-supporting pressed pellets of $^{66}\text{Dy}$ compounds namely $\text{Dy}_2\text{O}_3$ , $\text{Dy}_2(\text{CO}_3)_3$ , $\text{Dy}_2(\text{SO}_4)_3$ , $\cdot 8\text{H}_2\text{O}$ , $\text{DyI}_2$ and a pure Dy metallic foil).	Silicon drift detector having FWHM ~131 eV at 5.89 keV.
[55]	$I_{La}/I_{Ll}, I_{La}/I_{L\beta} \text{ \& } I_{La}/I_{L\gamma}$	Synchrotron radiation at energies of 15, 16, and 17 keV.	$^{80}\text{Hg}$ , $^{82}\text{Pb}$ , and $^{83}\text{Bi}$ . (Targets and their compounds which having different crystal structure with same chemical bonding and oxidation state).	Vortex-EX90 Silicon drift detector having 138 eV resolution at 5.9 keV.
[79]	$I_{Ll}/I_{La}, I_{L\beta2.15}/I_{La}, I_{L\gamma1}/I_{L\beta1}, I_{L\gamma1.5}/I_{L\beta1} \text{ \& } I_{L\gamma2.3}/I_{L\beta3}$	Emission of synchrotron radiation spanning energies within the range of 10.5 keV to 14 keV.	$^{75}\text{Re}$ . (A thin target with spectral purity deposited onto a thick mylar foil).	Silicon drift detector with FWHM ~131 eV at 5.89 keV.

(continued on next page)

Table 1 (continued)

References	Atomic parameters	Excitation sources	Target samples	Detectors
[80]	$I_{\text{Li}}/I_{\text{La}}, I_{\text{Li}\beta}/I_{\text{La}}, I_{\text{Li}\eta}/I_{\text{La}} \& I_{\text{Li}\gamma}/I_{\text{La}}$	50 W metal-ceramics Mo x-ray micro source working at 50 kV and 600 $\mu$ A.	$^{79}\text{Au}$ . The assessed chemical conditions encompassed metallic Au(0) as well as chloride Au(3+) phases, each featuring distinct oxidation states and varying crystal field surroundings.	XFlash silicon drift detector(SDD) with a resolution of 150 eV at 5.9 keV. (Mn K $\alpha$ ).
[19]	$I_{\text{Li}}/I_{\text{La}}, I_{\text{La}2}/I_{\text{La}1}, I_{\text{Li}\beta 15,2,3}/I_{\text{La}}, I_{\text{Li}\beta 5/2}/I_{\text{La}}, I_{\text{Li}\eta}/I_{\text{Li}\beta 1}, I_{\text{Li}\gamma 1}/I_{\text{Li}\beta 1}, I_{\text{Li}\gamma 5}/I_{\text{Li}\beta 1}, I_{\text{Li}\beta 6,4}/I_{\text{Li}\beta 4}, I_{\text{Li}\gamma 2,3,6}/I_{\text{Li}\beta 4} \& I_{\text{Li}\beta 1}/I_{\text{Li}\beta 1}$	X-rays generated using an x-ray tube equipped with a rhodium anode, operating at 60 kV and 50 mA.	$^{79}\text{Au}$ . Spectroscopically pure thin targets of pure $^{79}\text{Au}$ , AuCl, AuCl <sub>3</sub> , AuI, AuBr <sub>3</sub> and Au(OH) <sub>3</sub> .	Scintillation counter for high energy X-ray and proportional counter for low energy x-rays.
[81]	$I_{\text{Li}}/I_{\text{La}}, I_{\text{Li}\beta}/I_{\text{La}} \& I_{\text{Li}\gamma}/I_{\text{La}}$	18 and 23 keV synchrotron radiation.	$^{62}\text{Sm}, ^{64}\text{Gd}, ^{65}\text{Tb}, ^{68}\text{Er}, ^{73}\text{Ta}, ^{74}\text{W}, ^{75}\text{Re}, ^{80}\text{Hg}, ^{82}\text{Pb}, \text{ and } ^{83}\text{Bi}$ . (Pure metals).	KETEX silicon Drift detector(SDD) with an energy resolution of 138 eV at 5.96 keV Fe K $\alpha$ x-rays.

detectors. The resolution of these detectors may vary depending on the manufacturer and model.

### 1.3. Data analysis

$I_{\text{Li}}/I_{\text{Lj}}$  ( $i = \beta, \gamma, \eta, \text{ l, } \gamma_{5}, \gamma_{44}, \text{ and } \gamma_1; j = \alpha, \beta, \text{ and } \gamma$ ) intensity ratio data, sourced from referenced papers, have been tabulated in a four-digit format, accompanied by measurement error estimates at the standard deviation level. The compilation of these ratios is meticulously summarized in 10 tables (Table 2–11), encompassing elements within the atomic number range of  $^{39}\text{Y}$  to  $^{94}\text{Pu}$ . Each table includes not only the ratio data but also references to their origin. Additionally, comprehensive statistical analyses were conducted for each item and ratio, leading to the determination of weighted mean values  $(I_{\text{Li}}/I_{\text{Lj}})_w$ , mean z-scores ( $\bar{z}$ ), and combined standard deviations ( $z_i$ ), thereby enhancing the dataset's reliability and comprehensiveness [11]. The formula employed for computing the weighted average values in this study is as follows [82,83]:

$$(I_{\text{Li}}/I_{\text{Lj}})_w \pm \epsilon_{\text{ISD}} = \frac{1}{\sum_{n=1}^N \frac{1}{(\Delta(I_{\text{Li}}/I_{\text{Lj}})_{\text{EXP}-n})^2}} \sum_{n=1}^N \frac{(I_{\text{Li}}/I_{\text{Lj}})_{\text{EXP}-n}}{(\Delta(I_{\text{Li}}/I_{\text{Lj}})_{\text{EXP}-n})^2} \pm \frac{1}{\left( \sum_{n=1}^N \frac{1}{(\Delta(I_{\text{Li}}/I_{\text{Lj}})_{\text{EXP}-n})^2} \right)^{\frac{1}{2}}} \quad (7)$$

In Eq. (7),  $(I_{\text{Li}}/I_{\text{Lj}})_{\text{EXP}-n}$  represents the  $n^{\text{th}}$  experimental intensity ratio,  $N$  stands for the count of experimental data points,  $\Delta(I_{\text{Li}}/I_{\text{Lj}})_{\text{EXP}-n}$  denotes the uncertainty associated with the  $n^{\text{th}}$  experimental value, and  $\epsilon_{\text{ISD}}$  is the internal standard deviation.

A simple and natural way to visually present the deviation of the individual experimental points from the corresponding weighted mean for the element is to plot the signed deviation in multiples of the combined internal and external standard deviation defined by:

$$z_{i,\text{ISD}} = \frac{(I_{\text{Li}}/I_{\text{Lj}})_{\text{EXP}-n} - (I_{\text{Li}}/I_{\text{Lj}})_w}{\sqrt{(\Delta(I_{\text{Li}}/I_{\text{Lj}})_{\text{EXP}-n})^2 + (\Delta(I_{\text{Li}}/I_{\text{Lj}})_{\text{ISD}})^2}} \quad (8)$$

$$z_{i,\text{ESD}} = \frac{(I_{\text{Li}}/I_{\text{Lj}})_{\text{EXP}-n} - (I_{\text{Li}}/I_{\text{Lj}})_w}{\sqrt{(\Delta(I_{\text{Li}}/I_{\text{Lj}})_{\text{EXP}-n})^2 + (\Delta(I_{\text{Li}}/I_{\text{Lj}})_{\text{ESD}})^2}} \quad (9)$$

where  $(I_{\text{Li}}/I_{\text{Lj}})_{\text{EXP}-n}$  and  $(I_{\text{Li}}/I_{\text{Lj}})_w$  refer to the  $n^{\text{th}}$  experimental and corresponding elemental weighted average  $I_{\text{Li}}/I_{\text{Lj}}$  intensity ratio ( $i = \beta, \gamma, \eta, \text{ l, } \gamma_5, \gamma_{44}, \text{ and } \gamma_1; j = \alpha, \beta, \text{ and } \gamma$ ), respectively,  $\Delta(I_{\text{Li}}/I_{\text{Lj}})_{\text{ISD}} = \epsilon_{\text{ISD}}$  and  $\Delta(I_{\text{Li}}/I_{\text{Lj}})_{\text{ESD}} = \epsilon_{\text{ESD}}$  are the associated asserted standard deviations, with the external standard deviation is given by the equation:

$$\epsilon_{\text{ESD}} = \sqrt{\frac{\sum_n \left( (I_{\text{Li}}/I_{\text{Lj}})_{\text{EXP}-n} - (I_{\text{Li}}/I_{\text{Lj}})_w \right)^2 / \left( \Delta(I_{\text{Li}}/I_{\text{Lj}})_{\text{EXP}-n} \right)^2}{(n-1) \sum_n \frac{1}{(\Delta(I_{\text{Li}}/I_{\text{Lj}})_{\text{EXP}-n})^2}}} \quad (10)$$

The idea is to quantify the deviation of each point from the weighted mean in multiples of a distance measure comprising the quadrature sum of a contribution associated with the experiment and an estimate for how tightly the global average is defined. The metric is simple in the sense that we have not excluded the point in question from the internal and external standard deviation calculations, but hold them fixed across the data set. Note the internal and external standard deviations computed according to Eqs. (7) and (10) are referred to as internal and external standard errors, respectively, in the technical literature. They quantify confidence on the result based on all of the data rather than on an individual determination.

The average z-score is calculated as:

$$\bar{z}_{\text{ISD}} = \frac{\sum_{i=1}^n z_{i,\text{ISD}}}{n} \quad (11)$$

$$\bar{z}_{\text{ESD}} = \frac{\sum_{i=1}^n z_{i,\text{ESD}}}{n} \quad (12)$$

where  $n$  represents the number of experimental points for each element.

We note that Dhal and Padhi, [63] refers values from Shatandra *et al.*, [85] for the intensity ratios  $I_{\text{Li}\beta}/I_{\text{La}}, I_{\text{Li}\gamma}/I_{\text{La}}, \text{ and } I_{\text{Li}\eta}/I_{\text{La}}$  for the elements  $^{82}\text{Pb}$  and  $^{83}\text{Bi}$ . However, it is important to note that Shatandra *et al.*, [85] did not provide calculated values for these ratios. Instead, the focus of the article was on calculating cross sections.

Figs. 1 to 10 illustrate the distribution of experimental intensity ratio values, encompassing ratios such as  $I_{\text{Li}\beta}/I_{\text{La}}, I_{\text{Li}\gamma}/I_{\text{La}}, I_{\text{Li}\eta}/I_{\text{La}}, I_{\text{Li}\gamma}/I_{\text{Li}\beta}, I_{\text{Li}\eta}/I_{\text{Li}\beta}, I_{\text{Li}\gamma 5}/I_{\text{La}}, I_{\text{Li}\gamma 44}/I_{\text{La}}, I_{\text{Li}\eta}/I_{\text{La}}, \text{ and } I_{\text{Li}\gamma 1}/I_{\text{La}}$ , for elements of atomic number  $39 \leq Z \leq 94$ . These data were compiled within the scope of this study and are plotted against the atomic number  $Z$  of the target element.

The distribution of the number of data points for experimental intensity ratios  $I_{\text{Li}\beta}/I_{\text{La}}$  as a function of atomic number  $Z$  ( $39 \leq Z \leq 92$ ) is illustrated in Fig. 1. The analysis of this figure enables us to draw the following conclusions:

- Most of the elements from  $^{39}\text{Y}$  to  $^{92}\text{U}$  are included, except for  $^{43}\text{Tc}, ^{44}\text{Ru}, ^{45}\text{Rh}, ^{46}\text{Pd}, ^{48}\text{Cd}, ^{51}\text{Sb}, ^{52}\text{Te}, ^{84}\text{Po}, ^{85}\text{At}, ^{86}\text{Rn}, ^{87}\text{Fr}, ^{88}\text{Ra}, ^{89}\text{Ac}, \text{ and } ^{91}\text{Pa}$ , because data have not been reported for them yet due to the complexities associated with their handling. This presents a research opportunity.
- In certain isolated cases, the data contain fewer than two values, specifically  $^{39}\text{Y}, ^{40}\text{Zr}, ^{54}\text{Xe}, ^{55}\text{Cs}, \text{ and } ^{61}\text{Pm}$ . Additional measurements are needed to strengthen the data base.
- It is noteworthy that gold ( $^{79}\text{Au}$ ), lead ( $^{82}\text{Pb}$ ), and dysprosium ( $^{66}\text{Dy}$ ) are the most commonly measured materials, collectively representing 18.6% of the entire dataset, with 41, 44, and 41 data points

**Table 2**

Summary of the experimental  $I_{L\beta}/I_{L\alpha}$  intensity ratios from  $^{39}\text{Y}$  to  $^{92}\text{U}$  is presented according to their target atomic numbers. The weighted average values  $(I_{L\beta}/I_{L\alpha})_W$ , the references from which the databases are extracted,  $\epsilon_{ISD}$ ,  $\epsilon_{ESD}$ , the internal and external standard deviation ( $z_{ISD}$ ,  $z_{ESD}$ ), and their means ( $\bar{z}_{ISD}$ ,  $\bar{z}_{ESD}$ ) are also listed.

Z, Symbol	$\left(\frac{I_{L\beta}}{I_{L\alpha}}\right)_{EXP} \pm \Delta(I_{L\beta}/I_{L\alpha})_{EXP}$	References	$(I_{L\beta}/I_{L\alpha})_W \pm \epsilon_{ISD}$	$z_{ISD}$	$\bar{z}_{ISD}$	$\epsilon_{ESD}$	$Z_{ESD}$	$\bar{z}_{ESD}$
Z = 39, Y	0.893 ± 0.072	[8]	0.893 ± 0.072	0	0	–	–	–
Z = 40, Zr	0.909 ± 0.074	[8]	0.909 ± 0.074	0	0	–	–	–
Z = 41, Nb	0.943 ± 0.071	[8]	0.9578 ± 0.055	–0.16	0.03	0.0181	–0.20	0.02
	0.980 ± 0.087	[8]		0.22			0.25	
Z = 42, Mo	0.962 ± 0.083	[8]	0.951 ± 0.054	0.11	0.01	0.0094	0.13	0.01
	0.943 ± 0.071	[8]		–0.09			–0.11	
Z = 47, Ag	0.962 ± 0.083	[8]	1.0276 ± 0.0343	–0.73	–0.08	0.0230	–0.76	–0.08
	1.010 ± 0.082	[8]		–0.2			–0.21	
	1.075 ± 0.058	[8]		0.70			0.76	
	1.020 ± 0.062	[8]		–0.11			–0.11	
Z = 49, In	0.990 ± 0.078	[8]	0.9406 ± 0.0311	0.59	0.34	0.0710	0.47	0.32
	1.010 ± 0.092	[8]		0.71			0.60	
	1.099 ± 0.060	[8]		2.34			1.70	
	0.813 ± 0.046	[8]		–2.30			–1.51	
Z = 50, Sn	0.962 ± 0.083	[8]	1.0237 ± 0.0352	–0.68	–0.03	0.0183	–0.73	–0.03
	1.042 ± 0.076	[8]		0.22			0.23	
	1.053 ± 0.066	[8]		0.39			0.43	
	1.020 ± 0.062	[8]		–0.05			–0.06	
Z = 53, I	1.010 ± 0.082	[8]	1.0624 ± 0.036	–0.59	–0.06	0.0207	–0.04	0
	1.042 ± 0.087	[8]		–0.22			–0.01	
	1.111 ± 0.062	[8]		0.68			0.05	
	1.053 ± 0.066	[8]		–0.12			0	
Z = 54, Xe	0.793 ± 0.069	[24]	0.793 ± 0.069	0	0	–	–	–
Z = 55, Cs	1.00 ± 0.040	[56]	1.00 ± 0.040	0	0	–	–	–
Z = 56, Ba	0.980 ± 0.087	[8]	0.9093 ± 0.0124	0.80	0.53	0.0399	0.74	0.54
	0.990 ± 0.078	[8]		1.02			0.92	
	1.111 ± 0.062	[8]		3.19			2.74	
	1.053 ± 0.066	[8]		2.14			1.86	
	0.805 ± 0.045	[22]		–2.23			–1.73	
	0.760 ± 0.042	[12]		–3.41			–2.58	
	0.951 ± 0.052	[12]		0.78			0.64	
	1.020 ± 0.056	[12]		1.93			1.61	
	1.088 ± 0.060	[12]		2.92			2.48	
	0.969 ± 0.053	[12]		1.10			0.9	
	0.927 ± 0.046	[13]		0.37			0.29	
	1.022 ± 0.051	[13]		2.15			1.74	
	1.088 ± 0.054	[13]		3.23			2.66	
	0.951 ± 0.048	[13]		0.84			0.67	
	1.053 ± 0.042	[56]		3.28			2.48	
	0.620 ± 0.031	[84]		–8.66			–5.73	
	0.8565 ± 0.101	[76]		–0.52			–0.49	
Z = 57, La	0.971 ± 0.085	[8]	0.8730 ± 0.0128	1.14	0.50	0.0359	1.06	0.53
	1.064 ± 0.091	[8]		2.08			1.95	
	1.111 ± 0.074	[8]		3.17			2.89	
	1.031 ± 0.064	[8]		2.42			2.15	
	0.861 ± 0.047	[12]		–0.25			–0.2	
	1.034 ± 0.057	[12]		2.76			2.39	
	1.010 ± 0.056	[12]		2.39			2.06	
	1.133 ± 0.062	[12]		4.11			3.63	
	1.133 ± 0.062	[12]		4.11			3.63	
	0.909 ± 0.036	[56]		0.94			0.71	
	0.800 ± 0.071	[33]		–1.01			–0.92	
	0.682 ± 0.034	[84]		–5.26			–3.86	
	0.775 ± 0.060	[38]		–1.60			–1.4	
	0.7005 ± 0.056	[17]		–3.00			–2.59	
	0.96 ± 0.12	[67]		0.72			0.69	
	1.32 ± 0.15	[69]		2.97			2.9	
	0.742 ± 0.044	[51]		–2.86			–2.31	
	0.779 ± 0.049 (B = 0.6T)	[51]		–1.86			–1.55	
	0.789 ± 0.056 (B = 1.2T)	[51]		–1.46			–1.26	
Z = 58, Ce	1.010 ± 0.082	[8]	0.9062 ± 0.0121	1.25	0.47	0.0402	1.14	0.48
	1.053 ± 0.089	[8]		1.63			1.5	
	1.099 ± 0.072	[8]		2.64			2.34	
	1.042 ± 0.065	[8]		2.05			1.78	
	0.883 ± 0.049	[12]		–0.46			–0.37	
	0.978 ± 0.054	[12]		1.30			1.07	
	1.060 ± 0.058	[12]		2.60			2.18	
	1.186 ± 0.065	[12]		4.23			3.66	
	1.102 ± 0.061	[12]		3.15			2.68	
	0.952 ± 0.048	[13]		0.93			0.73	
	1.033 ± 0.052	[13]		2.38			1.93	
	1.186 ± 0.059	[13]		4.65			3.92	

(continued on next page)

Table 2 (continued)

Z, Symbol	$\left(\frac{I_{L\beta}}{I_{L\alpha}}\right)_{EXP} \pm \Delta(I_{L\beta}/I_{L\alpha})_{EXP}$	References	$(I_{L\beta}/I_{L\alpha})_W \pm \epsilon_{ISD}$	$z_{ISD}$	$\bar{z}_{ISD}$	$\epsilon_{ESD}$	$Z_{ESD}$	$\bar{Z}_{ESD}$
Z = 59, Pr	1.075 ± 0.054	[13]		3.05			2.51	
	0.926 ± 0.037	[56]		0.51			0.36	
	0.755 ± 0.066	[33]		-2.25			-1.96	
	0.629 ± 0.030	[84]		-8.57			-5.53	
	0.781 ± 0.061	[38]		-2.01			-1.71	
	0.724 ± 0.063	[51]		-2.84			-2.44	
	0.733 ± 0.059 (B = 0.6T)	[51]		-2.87			-2.43	
	0.773 ± 0.066 (B = 1.2T)	[51]		-1.98			-1.72	
	0.936 ± 0.051	[12]	0.9072 ± 0.013	0.55	0.21	0.0339	0.47	0.22
	0.966 ± 0.053	[12]		1.08			0.93	
	0.991 ± 0.055	[12]		1.48			1.3	
	1.131 ± 0.062	[12]		3.53			3.17	
	1.031 ± 0.057	[12]		2.12			1.87	
	0.943 ± 0.038	[56]		0.89			0.7	
	1.055 ± 0.042	[62]		3.36			2.74	
	1.076 ± 0.050	[88]		3.27			2.79	
	0.802 ± 0.071	[33]		-1.46			-1.34	
	0.794 ± 0.069	[38]		-1.61			-1.47	
	0.6832 ± 0.055	[17]		-3.96			-3.47	
0.98 ± 0.12	[67]		0.60			0.58		
1.15 ± 0.14	[69]		1.73			1.69		
1.0556 ± 0.1238	[76]		1.19			1.16		
0.744 ± 0.033	[51]		-4.60			-3.45		
0.777 ± 0.048 (B = 0.6T)	[51]		-2.62			-2.22		
0.797 ± 0.057 (B = 1.2T)	[51]		-1.89			-1.66		
Z = 60, Nd	0.835 ± 0.046	[12]	0.9181 ± 0.0132	-1.74	0.02	0.0248	-1.59	0.02
	0.920 ± 0.051	[12]		0.04			0.03	
	0.913 ± 0.050	[12]		-0.1			-0.09	
	1.115 ± 0.061	[12]		3.15			2.99	
	1.013 ± 0.056	[12]		1.65			1.55	
	0.901 ± 0.045	[13]		-0.36			-0.33	
	0.952 ± 0.048	[13]		0.68			0.63	
	1.115 ± 0.056	[13]		3.42			3.21	
	0.995 ± 0.050	[13]		1.49			1.38	
	0.935 ± 0.037	[56]		0.43			0.38	
	0.797 ± 0.072	[33]		-1.65			-1.59	
	0.781 ± 0.061	[38]		-2.2			-2.08	
	0.7570 ± 0.061	[17]		-2.58			-2.45	
	1.03 ± 0.12	[67]		0.93			0.91	
	1.20 ± 0.14	[69]		2.00			1.98	
	0.801 ± 0.064	[51]		-1.79			-1.71	
	0.810 ± 0.072 (B = 0.6T)	[51]		-1.48			-1.42	
	0.814 ± 0.066 (B = 1.2T)	[51]		-1.55			-1.48	
	Z = 61, Pm	1.031 ± 0.041	[56]	1.031 ± 0.041	0	0	-	-
Z = 62, Sm		1.010 ± 0.092	[8]	0.9214 ± 0.0181	0.95	0.38	0.0250	0.93
	1.064 ± 0.091	[8]		1.54			1.51	
	1.190 ± 0.085	[8]		3.09			3.03	
	1.075 ± 0.069	[8]		2.15			2.09	
	0.997 ± 0.055	[12]		1.31			1.25	
	1.090 ± 0.060	[12]		2.69			2.59	
	1.139 ± 0.063	[12]		3.32			3.21	
	1.145 ± 0.063	[12]		3.41			3.3	
	1.219 ± 0.067	[12]		4.29			4.16	
	1.020 ± 0.041	[56]		2.2			2.05	
	1.053 ± 0.100	[32]		1.3			1.28	
	0.789 ± 0.072	[33]		-1.78			-1.74	
	0.980 ± 0.077	[36]		0.74			0.72	
	0.781 ± 0.067	[38]		-2.02			-1.96	
	0.83328 ± 0.067	[17]		-1.27			-1.23	
	1.15 ± 0.11	[67]		2.05			2.03	
	1.12 ± 0.13	[69]		1.51			1.5	
	0.822 ± 0.049	[72]		-1.9			-1.81	
	0.810 ± 0.049	[72]		-2.13			-2.02	
	0.815 ± 0.049	[72]		-2.04			-1.93	
	0.826 ± 0.050	[72]		-1.79			-1.71	
	0.826 ± 0.050	[72]		-1.79			-1.71	
	0.836 ± 0.050	[72]		-1.61			-1.53	
	0.862 ± 0.040	[87]		-1.35			-1.26	
	0.861 ± 0.040	[87]		-1.37			-1.28	
	0.751 ± 0.040	[51]		-3.88			-3.61	
	0.883 ± 0.086 (B = 0.6T)	[51]		-0.44			-0.43	
	0.912 ± 0.075 (B = 1.2T)	[51]		-0.12			-0.12	
	1.119 ± 0.09	[81]		2.15			2.12	
	1.114 ± 0.09	[81]		2.1			2.06	

(continued on next page)

Table 2 (continued)

Z, Symbol	$\left(\frac{I_{L\beta}}{I_{L\alpha}}\right)_{EXP} \pm \Delta(I_{L\beta}/I_{L\alpha})_{EXP}$	References	$(I_{L\beta}/I_{L\alpha})_W \pm \epsilon_{ISD}$	$z_{ISD}$	$\bar{z}_{ISD}$	$\epsilon_{ESD}$	$Z_{ESD}$	$\bar{Z}_{ESD}$
Z = 63, Eu	0.822 ± 0.045	[12]	0.8827 ± 0.0111	-1.31	0.17	0.0208	-1.22	0.18
	0.934 ± 0.051	[12]		0.98				
	0.992 ± 0.055	[12]		1.95				
	1.038 ± 0.057	[12]		2.67				
	1.079 ± 0.059	[12]		3.27				
	1.065 ± 0.059	[12]		3.04				
	0.971 ± 0.039	[56]		2.18				
	0.857 ± 0.036	[26]		-0.68				
	0.891 ± 0.038	[26]		0.21				
	0.763 ± 0.067	[33]		-1.76				
	0.952 ± 0.091	[36]		0.76				
	0.8988 ± 0.072	[17]		0.22				
	1.16 ± 0.13	[67]		2.13				
	1.13 ± 0.13	[69]		1.9				
	0.825 ± 0.050	[72]		-1.13				
	0.813 ± 0.049	[72]		-1.39				
	0.816 ± 0.049	[72]		-1.33				
	0.826 ± 0.050	[72]		-1.11				
	0.837 ± 0.050	[72]		-0.89				
	0.833 ± 0.050	[72]		-0.97				
	0.758 ± 0.050	[87]		-2.43				
	0.753 ± 0.050	[87]		-2.53				
Z = 64, Gd	1.00 ± 0.090	[8]	0.9309 ± 0.0069	0.77	0.03	0.0208	0.75	0.02
	1.099 ± 0.085	[8]		1.97				
	1.163 ± 0.081	[8]		2.86				
	1.099 ± 0.060	[8]		2.78				
	1.053 ± 0.1	[8]		1.22				
	1.220 ± 0.119	[8]		2.43				
	1.190 ± 0.113	[8]		2.29				
	1.163 ± 0.112	[8]		2.07				
	0.886 ± 0.049	[12]		-0.91				
	0.932 ± 0.051	[12]		0.02				
	0.982 ± 0.054	[12]		0.94				
	1.050 ± 0.058	[12]		2.04				
	1.079 ± 0.059	[12]		2.49				
	1.140 ± 0.063	[12]		3.3				
	0.990 ± 0.040	[56]		1.46				
	0.781 ± 0.070	[33]		-2.13				
	0.629 ± 0.031	[84]		-9.51				
	0.7610 ± 0.061	[17]		-2.77				
	1.12 ± 0.13	[67]		1.45				
	1.13 ± 0.13	[69]		1.53				
	0.834 ± 0.050	[72]		-1.92				
	0.821 ± 0.049	[72]		-2.22				
	0.830 ± 0.050	[72]		-2				
	0.835 ± 0.050	[72]		-1.9				
	0.839 ± 0.050	[72]		-1.82				
	0.847 ± 0.050	[72]		-1.66				
	0.682 ± 0.056	[51]		-4.41				
0.712 ± 0.056 (B = 0.6T)	[51]	-3.88						
0.734 ± 0.054 (B = 1.2T)	[51]	-3.62						
0.962 ± 0.009	[53]	2.75						
1.277 ± 0.09	[81]	3.83						
1.248 ± 0.09	[81]	3.51						
Z = 65, Tb	0.856 ± 0.047	[12]	0.9276 ± 0.0071	-1.51	-0.002	0.0164	-1.44	0
	0.934 ± 0.051	[12]		0.12				
	0.992 ± 0.055	[12]		1.16				
	1.074 ± 0.059	[12]		2.46				
	1.148 ± 0.063	[12]		3.48				
	1.158 ± 0.064	[12]		3.58				
	0.917 ± 0.037	[56]		-0.28				
	0.791 ± 0.070	[33]		-1.94				
	1.0058 ± 0.080	[16]		0.97				
	1.0528 ± 0.084	[16]		1.49				
	1.0578 ± 0.085	[16]		1.53				
	0.826 ± 0.061	[38]		-1.65				
	0.9801 ± 0.078	[17]		0.67				
	1.06 ± 0.13	[67]		1.02				
	1.17 ± 0.09	[69]		2.69				
	0.815 ± 0.049	[72]		-2.27				
	0.804 ± 0.048	[72]		-2.55				
	0.808 ± 0.048	[72]		-2.46				
	0.819 ± 0.049	[72]		-2.19				
	0.820 ± 0.049	[72]		-2.17				

(continued on next page)

Table 2 (continued)

Z, Symbol	$\left(\frac{I_{L\beta}}{I_{L\alpha}}\right)_{EXP} \pm \Delta(I_{L\beta}/I_{L\alpha})_{EXP}$	References	$(I_{L\beta}/I_{L\alpha})_W \pm \epsilon_{ISD}$	$z_{ISD}$	$\bar{z}_{ISD}$	$\epsilon_{ESD}$	$Z_{ESD}$	$\bar{z}_{ESD}$
Z = 66, Dy	0.824 ± 0.049	[72]	0.8028 ± 0.0031	-2.09	2.11	0.0088	-2	2.13
	0.765 ± 0.053	[51]		-3.04			-2.93	
	0.769 ± 0.053 (B = 0.6T)	[51]		-2.97			-2.86	
	0.770 ± 0.065 (B = 1.2T)	[51]		-2.41			-2.35	
	0.943 ± 0.009	[53]		1.35			0.82	
	1.301 ± 0.10	[81]		3.72			3.68	
	1.254 ± 0.10	[81]		3.26			3.22	
	0.961 ± 0.057	[21]		2.77			2.74	
	0.918 ± 0.050	[12]		2.30			2.27	
	0.964 ± 0.053	[12]		3.04			3	
	1.014 ± 0.056	[12]		3.77			3.73	
	1.074 ± 0.059	[12]		4.59			4.55	
	1.143 ± 0.063	[12]		5.39			5.35	
	1.218 ± 0.067	[12]		6.19			6.14	
	0.926 ± 0.037	[56]		3.32			3.24	
	0.789 ± 0.070	[33]		-0.2			-0.2	
	1.0443 ± 0.084	[16]		2.87			2.86	
	1.0439 ± 0.084	[16]		2.87			2.86	
	1.0610 ± 0.085	[16]		3.04			3.02	
	0.826 ± 0.068	[38]		0.34			0.34	
	0.8077 ± 0.065	[17]		0.08			0.08	
	0.885 ± 0.141	[41]		0.58			0.58	
	1.07 ± 0.13	[67]		2.06			2.05	
	1.09 ± 0.12	[69]		2.39			2.39	
	0.843 ± 0.051	[72]		0.79			0.78	
	0.832 ± 0.050	[72]		0.58			0.58	
	0.835 ± 0.050	[72]		0.64			0.63	
	0.844 ± 0.051	[72]		0.81			0.8	
	0.852 ± 0.051	[72]		0.96			0.95	
	0.853 ± 0.051	[72]		0.98			0.97	
	0.841 ± 0.062	[46]		0.62			0.61	
	0.786 ± 0.003	[46]		-3.89			-1.8	
	1.161 ± 0.077	[47]		4.65			4.62	
	1.159 ± 0.078	[47]		4.56			4.54	
	1.17 ± 0.07	[75]		5.24			5.21	
	0.903 ± 0.054	[75]		1.85			1.83	
	0.808 ± 0.072	[49]		0.07			0.07	
	0.808 ± 0.072	[51]		0.07			0.07	
	0.810 ± 0.066 (B = 0.6T)	[51]		0.11			0.11	
	0.824 ± 0.068 (B = 1.2T)	[51]		0.31			0.31	
0.808 ± 0.024	[92]	0.22	0.2					
0.778 ± 0.023	[92]	-1.07	-1.01					
0.781 ± 0.023	[92]	-0.94	-0.88					
0.938 ± 0.028	[92]	4.80	4.61					
0.941 ± 0.028	[92]	4.91	4.71					
0.942 ± 0.028	[92]	4.94	4.74					
0.946 ± 0.028	[92]	5.08	4.88					
0.943 ± 0.028	[92]	4.98	4.78					
Z = 67, Ho	0.961 ± 0.048	[60]	0.9236 ± 0.0058	0.77	0.38	0.0173	0.73	0.40
	0.963 ± 0.048	[60]		0.82			0.77	
	1.048 ± 0.052	[60]		2.38			2.27	
	1.058 ± 0.053	[60]		2.52			2.41	
	1.199 ± 0.060	[60]		4.57			4.41	
	1.220 ± 0.061	[60]		4.84			4.67	
	0.990 ± 0.040	[56]		1.64			1.52	
	1.082 ± 0.039	[62]		4.02			3.71	
	1.072 ± 0.034	[62]		4.3			3.89	
	0.830 ± 0.075	[33]		-1.24			-1.22	
	1.1093 ± 0.089	[16]		2.08			2.05	
	1.0669 ± 0.085	[16]		1.68			1.65	
	1.1005 ± 0.088	[16]		2.01			1.97	
	0.862 ± 0.067	[38]		-0.92			-0.89	
	0.8170 ± 0.065	[17]		-1.63			-1.58	
	0.952 ± 0.118	[41]		0.24			0.24	
	1.11 ± 0.13	[67]		1.43			1.42	
	1.10 ± 0.13	[69]		1.36			1.35	
	0.848 ± 0.051	[72]		-1.47			-1.4	
	0.840 ± 0.050	[72]		-1.66			-1.58	
	0.843 ± 0.050	[72]		-1.6			-1.52	
	0.846 ± 0.050	[72]		-1.54			-1.47	
	0.852 ± 0.051	[72]		-1.39			-1.33	
	0.859 ± 0.051	[72]		-1.26			-1.2	
	0.905 ± 0.057	[46]		-0.32			-0.31	
	0.813 ± 0.011	[46]		-8.89			-5.39	

(continued on next page)

Table 2 (continued)

Z, Symbol	$\left(\frac{I_{L\beta}}{I_{L\alpha}}\right)_{EXP} \pm \Delta(I_{L\beta}/I_{L\alpha})_{EXP}$	References	$(I_{L\beta}/I_{L\alpha})_W \pm \epsilon_{ISD}$	$z_{ISD}$	$\bar{z}_{ISD}$	$\epsilon_{ESD}$	$Z_{ESD}$	$\bar{z}_{ESD}$	
Z = 68, Er	0.833 ± 0.062	[49]	0.6987 ± 0.0053	-1.45	4	0.0298	-1.41	3.77	
	0.833 ± 0.062	[51]		-1.45			-1.41		
	0.826 ± 0.075 (B = 0.6T)	[51]		-1.3			-1.27		
	0.836 ± 0.077 (B = 1.2T)	[51]		-1.13			-1.11		
	0.971 ± 0.009	[53]		4.43			2.43		
	0.939 ± 0.047	[60]		5.08			4.32		
	1.020 ± 0.051	[60]		6.27			5.44		
	1.104 ± 0.055	[60]		7.34			6.48		
	1.095 ± 0.055	[60]		7.17			6.33		
	1.137 ± 0.057	[60]		7.66			6.81		
	1.263 ± 0.063	[60]		8.93			8.1		
	1.061 ± 0.053	[24]		6.8			5.96		
	0.990 ± 0.040	[56]		7.22			5.84		
	0.815 ± 0.073	[33]		1.59			1.48		
	0.629 ± 0.006	[84]		-8.7			-2.29		
	0.840 ± 0.056	[38]		2.51			2.23		
	0.926 ± 0.129	[41]		1.76			1.72		
	0.852 ± 0.051	[72]		2.99			2.6		
	0.846 ± 0.051	[72]		2.87			2.49		
	0.852 ± 0.051	[72]		2.99			2.6		
	0.852 ± 0.051	[72]		2.99			2.6		
	0.853 ± 0.051	[72]		3.01			2.61		
	0.858 ± 0.051	[72]		3.11			2.7		
1.167 ± 0.076	[47]	6.15	5.74						
1.159 ± 0.075	[47]	6.12	5.7						
0.835 ± 0.063	[49]	2.16	1.96						
0.835 ± 0.063	[51]	2.16	1.96						
0.834 ± 0.049 (B = 0.6T)	[51]	2.75	2.36						
0.829 ± 0.055 (B = 1.2T)	[51]	2.36	2.08						
1.240 ± 0.08	[81]	6.75	6.34						
Z = 69, Tm	0.956 ± 0.039	[21]	1.0367 ± 0.0155	-1.92	0.16	0.0346	-1.55	0.17	
	1.035 ± 0.052	[14]	-0.03	-0.03					
	1.094 ± 0.055	[14]	1	0.88					
	1.156 ± 0.058	[14]	1.99	1.77					
	1.175 ± 0.059	[14]	2.27	2.02					
	1.280 ± 0.064	[14]	3.69	3.35					
	1.203 ± 0.060	[14]	2.68	2.4					
	0.962 ± 0.038	[56]	-1.82	-1.45					
	0.812 ± 0.073	[33]	-3.01	-2.78					
	1.0919 ± 0.087	[16]	0.63	0.59					
	1.0079 ± 0.081	[16]	-0.35	-0.33					
	1.0716 ± 0.086	[16]	0.4	0.38					
	0.77745 ± 0.062	[17]	-4.06	-3.65					
	1.08 ± 0.13	[67]	0.33	0.32					
	1.12 ± 0.13	[69]	0.64	0.62					
	Z = 70, Yb	1.052 ± 0.015	[20]	1.1907 ± 0.0082	-8.11	-0.31	0.0372	-3.45	-0.30
		1.003 ± 0.050	[60]	-3.7	-3.01				
1.043 ± 0.052		[60]	-2.81	-2.31					
1.125 ± 0.056		[60]	-1.16	-0.98					
1.138 ± 0.057		[60]	-0.91	-0.77					
1.212 ± 0.061		[60]	0.35	0.3					
1.356 ± 0.068		[60]	2.41	2.13					
0.980 ± 0.039		[56]	-5.29	-3.91					
1.137 ± 0.040		[62]	-1.31	-0.98					
1.060 ± 0.038		[62]	-3.36	-2.46					
1.449 ± 0.174		[33]	1.48	1.45					
1.1314 ± 0.091		[16]	-0.65	-0.6					
1.0852 ± 0.087		[16]	-1.21	-1.11					
1.1212 ± 0.090		[16]	-0.77	-0.71					
1.015 ± 0.051		[84]	-3.4	-2.78					
1.515 ± 0.184		[38]	1.76	1.73					
0.8221 ± 0.066		[17]	-5.54	-4.86					
1.553 ± 0.077		[40]	4.68	4.24					
1.12 ± 0.13		[67]	-0.54	-0.52					
1.14 ± 0.14		[69]	-0.36	-0.35					
1.458 ± 0.036		[46]	7.24	5.16					
1.420 ± 0.016		[46]	12.76	5.66					
1.147 ± 0.074		[47]	-0.59	-0.53					
1.166 ± 0.075	[47]	-0.33	-0.29						
1.299 ± 0.067	[1]	1.6	1.41						
Z = 71, Lu	1.024 ± 0.051	[14]	1.0861 ± 0.0160	-1.16	0.35	0.0416	-0.94	0.36	
	1.089 ± 0.054	[14]	0.05	0.04					
	1.141 ± 0.057	[14]	0.93	0.78					
	1.220 ± 0.061	[14]	2.12	1.81					

(continued on next page)

Table 2 (continued)

Z, Symbol	$\left(\frac{I_{L\beta}}{I_{L\alpha}}\right)_{EXP} \pm \Delta(I_{L\beta}/I_{L\alpha})_{EXP}$	References	$(I_{L\beta}/I_{L\alpha})_W \pm \epsilon_{ISD}$	$z_{ISD}$	$\bar{z}_{ISD}$	$\epsilon_{ESD}$	$Z_{ESD}$	$\bar{Z}_{ESD}$
	1.363 ± 0.068	[14]		3.96			3.47	
	1.485 ± 0.074	[14]		5.27			4.7	
	0.901 ± 0.036	[56]		-4.7			-3.37	
	1.342 ± 0.083	[33]		3.03			2.76	
	1.0891 ± 0.087	[16]		0.03			0.03	
	1.0702 ± 0.086	[16]		-0.18			-0.17	
	1.0954 ± 0.088	[16]		0.1			0.1	
	1.020 ± 0.083	[36]		-0.78			-0.71	
	0.8112 ± 0.065	[17]		-4.11			-3.56	
	1.11 ± 0.13	[67]		0.18			0.17	
	1.09 ± 0.12	[69]		0.03			0.03	
	1.133 ± 0.072	[47]		0.64			0.56	
	1.125 ± 0.072	[47]		0.53			0.47	
Z = 72, Hf	1.105 ± 0.025	[23]	1.1350 ± 0.0200	-0.93	0.54	0.0459	-0.57	0.54
	0.980 ± 0.106	[36]		-1.44			-1.34	
	1.429 ± 0.163	[38]		1.79			1.74	
	1.404 ± 0.063	[40]		4.07			3.45	
	1.031 ± 0.128	[41]		-0.80			-0.76	
	1.538 ± 0.189	[43]		2.12			2.07	
Z = 73, Ta	1.0826 ± 0.0487	[71]	1.1874 ± 0.0096	-0.99	0.59	0.0351	-0.78	0.61
	1.087 ± 0.025	[58]		-3.75			-2.33	
	1.184 ± 0.027	[58]		-0.12			-0.08	
	1.333 ± 0.038	[58]		3.71			2.81	
	1.380 ± 0.039	[58]		4.79			3.67	
	1.073 ± 0.025	[61]		-4.27			-2.66	
	1.230 ± 0.027	[61]		1.48			0.96	
	1.475 ± 0.041	[61]		6.83			5.33	
	0.926 ± 0.037	[56]		-6.84			-5.13	
	1.582 ± 0.198	[33]		1.99			1.96	
	1.460 ± 0.149	[35]		1.83			1.78	
	0.968 ± 0.052	[35]		-4.15			-3.5	
	1.116 ± 0.055	[84]		3.44			3.05	
	1.410 ± 0.064	[40]		1.08			1.06	
	1.370 ± 0.169	[43]		-1.28			-1.1	
	1.155 ± 0.072	[47]		-0.45			-0.41	
	1.153 ± 0.072	[47]		-0.47			-0.43	
	1.525 ± 0.078	[74]		4.3			3.95	
	1.429 ± 0.061	[1]		3.91			3.43	
	1.187 ± 0.07	[81]		-0.006			0.005	
Z = 74, W	1.163 ± 0.09	[81]	1.1917 ± 0.0097	-0.27	0.34	0.0376	-0.25	0.35
	1.043 ± 0.031	[59]		-4.58			-3.05	
	1.132 ± 0.034	[59]		-1.69			-1.18	
	1.288 ± 0.038	[59]		2.45			1.8	
	1.050 ± 0.031	[61]		-4.36			-2.91	
	1.178 ± 0.034	[61]		-0.39			-0.27	
	1.382 ± 0.038	[61]		4.85			3.56	
	0.885 ± 0.035	[56]		-8.44			-5.97	
	1.233 ± 0.053	[25]		0.77			0.64	
	1.592 ± 0.200	[33]		2			1.97	
	1.464 ± 0.129	[35]		2.1			2.03	
	1.019 ± 0.050	[35]		-3.39			-2.76	
	1.0121 ± 0.081	[16]		-2.2			-2.01	
	1.0378 ± 0.083	[16]		-1.84			-1.69	
	1.0328 ± 0.083	[16]		-1.9			-1.74	
	1.250 ± 0.109	[38]		0.53			0.51	
	1.477 ± 0.065	[40]		4.34			3.8	
	0.962 ± 0.092	[41]		-2.48			-2.31	
	1.198 ± 0.041	[68]		0.15			0.11	
	1.370 ± 0.188	[43]		0.95			0.93	
	1.600 ± 0.036	[46]		10.95			7.84	
	1.531 ± 0.167	[46]		2.03			1.98	
	1.461 ± 0.075	[73]		3.56			3.21	
	1.152 ± 0.065	[47]		-0.6			-0.53	
	1.174 ± 0.066	[47]		-0.27			-0.23	
	1.583 ± 0.080	[74]		4.86			4.43	
	1.429 ± 0.061	[1]		3.84			3.31	
	1.136 ± 0.08	[81]		-0.69			-0.63	
Z = 75, Re	1.092 ± 0.086	[81]	1.1367 ± 0.0148	-1.15	0.65	0.0378	-1.06	0.66
	1.029 ± 0.027	[61]		-3.50			-2.32	
	1.132 ± 0.025	[61]		-0.16			-0.1	
	1.299 ± 0.045	[61]		3.42			2.76	
	1.486 ± 0.181	[33]		1.92			1.89	
	1.344 ± 0.090	[35]		2.27			2.12	
	1.058 ± 0.060	[35]		-1.27			-1.11	

(continued on next page)

Table 2 (continued)

Z, Symbol	$\left(\frac{I_{L\beta}}{I_{L\alpha}}\right)_{EXP} \pm \Delta(I_{L\beta}/I_{L\alpha})_{EXP}$	References	$(I_{L\beta}/I_{L\alpha})_W \pm \epsilon_{ISD}$	$z_{ISD}$	$\bar{z}_{ISD}$	$\epsilon_{ESD}$	$Z_{ESD}$	$\bar{Z}_{ESD}$
Z = 76, Os	1.274 ± 0.067	[40]	1.0408 ± 0.0263	2.00	0.08	0.0557	1.78	0.08
	1.390 ± 0.071	[73]		3.49			3.15	
	1.086 ± 0.12	[81]		-0.42			-0.4	
	1.031 ± 0.08	[81]		-1.30			-1.19	
	1.040 ± 0.062	[21]		-0.01			-0.01	
	0.870 ± 0.060	[36]		-2.61			-2.09	
	1.064 ± 0.113	[38]		0.20			0.18	
	1.288 ± 0.066	[73]		3.48			2.86	
	1.019 ± 0.058	[47]		-0.34			-0.27	
	1.026 ± 0.058	[47]		-0.23			-0.18	
Z = 77, Ir	0.935 ± 0.037	[56]	0.9533 ± 0.0343	-0.36	0.39	0.0450	-0.31	0.39
	1.064 ± 0.091	[32]		1.14			1.09	
Z = 78, Pt	1.114 ± 0.039	[61]	1.0117 ± 0.0108	2.53	0.13	0.0256	2.19	0.14
	0.981 ± 0.021	[61]		-1.3			-0.93	
	1.031 ± 0.022	[61]		0.79			0.57	
	0.826 ± 0.034	[56]		-5.21			-4.36	
	1.121 ± 0.038	[63]		2.77			2.39	
	0.9739 ± 0.078	[16]		-0.48			-0.46	
	0.9623 ± 0.077	[16]		-0.64			-0.61	
	0.9868 ± 0.079	[16]		-0.31			-0.3	
	0.826 ± 0.068	[36]		-2.7			-2.56	
	1.144 ± 0.056	[40]		2.32			2.15	
	1 ± 0.099	[27]		-0.12			-0.11	
	1.274 ± 0.064	[73]		4.04			3.81	
	1.005 ± 0.057	[47]		-0.12			-0.11	
	1.010 ± 0.057	[47]		-0.03			-0.03	
	1.0713 ± 0.129	[76]		0.46			0.45	
	0.841 ± 0.011	[7]		-5.66			-4.61	
	0.848 ± 0.012	[7]		-5.07			-4.19	
	0.824 ± 0.013	[7]		-6.17			-5.14	
	0.834 ± 0.034	[7]		-2.9			-2.74	
	0.974 ± 0.017	[58]		1.55			1.35	
	1.008 ± 0.022	[58]		2.62			2.36	
	1.106 ± 0.080	[58]		2.04			2.02	
	1.097 ± 0.041	[58]		3.63			3.49	
	0.969 ± 0.019	[61]		1.23			1.09	
	1.009 ± 0.024	[61]		2.49			2.27	
	1.073 ± 0.056	[61]		2.3			2.25	
	0.926 ± 0.037	[56]		-0.36			-0.34	
1.010 ± 0.092	[32]	0.75	0.74					
1.1189 ± 0.048	[88]	3.58	3.47					
1.1149 ± 0.046	[88]	3.64	3.52					
1.1458 ± 0.044	[88]	4.46	4.31					
1.1660 ± 0.044	[88]	4.9	4.73					
1.1911 ± 0.042	[88]	5.68	5.47					
1.045 ± 0.044	[62]	2.28	2.2					
1.059 ± 0.046	[62]	2.48	2.4					
1.1144 ± 0.038	[64]	4.31	4.12					
1.1327 ± 0.034	[64]	5.25	4.98					
1.1583 ± 0.030	[64]	6.62	6.19					
1.078 ± 0.111	[33]	1.23	1.22					
0.979 ± 0.058	[35]	0.65	0.64					
1.037 ± 0.045	[35]	2.06	1.99					
0.9432 ± 0.075	[16]	0.04	0.04					
0.9521 ± 0.076	[16]	0.15	0.15					
0.9831 ± 0.079	[16]	0.54	0.53					
1.003 ± 0.050	[84]	1.21	1.18					
1.110 ± 0.059	[40]	2.8	2.75					
0.918 ± 0.042	[68]	-0.5	-0.48					
0.990 ± 0.127	[43]	0.39	0.39					
1.010 ± 0.100	[27]	0.69	0.69					
1.204 ± 0.084	[18]	3.1	3.07					
0.954 ± 0.054	[47]	0.25	0.24					
0.956 ± 0.054	[47]	0.28	0.28					
1.020 ± 0.042	[50]	1.81	1.74					
1.370 ± 0.056	[50]	7.46	7.29					
1.2 ± 0.1	[80]	2.57	2.55					
1.095 ± 0.055	[19]	2.73	2.67					
Z = 80, Hg	0.980 ± 0.035	[59]	1.0310 ± 0.0048	-1.44	-0.17	0.0134	-1.36	-0.17
	1.012 ± 0.037	[59]		-0.51			-0.48	
	1.086 ± 0.055	[59]		1			0.97	
	0.960 ± 0.032	[61]		-2.19			-2.05	
	0.995 ± 0.035	[61]		-1.02			-0.96	
	1.042 ± 0.055	[61]		0.2			0.19	

(continued on next page)

Table 2 (continued)

Z, Symbol	$\left(\frac{I_{L\beta}}{I_{L\alpha}}\right)_{EXP} \pm \Delta(I_{L\beta}/I_{L\alpha})_{EXP}$	References	$(I_{L\beta}/I_{L\alpha})_W \pm \epsilon_{ISD}$	$z_{ISD}$	$\bar{z}_{ISD}$	$\epsilon_{ESD}$	$Z_{ESD}$	$\bar{Z}_{ESD}$
	1.086 ± 0.045	[24]		1.22			1.17	
	1.184 ± 0.040	[24]		3.8			3.63	
	0.952 ± 0.038	[56]		-2.06			-1.96	
	0.990 ± 0.078	[32]		-0.52			-0.52	
	0.989 ± 0.098	[33]		-0.43			-0.42	
	1.055 ± 0.067	[35]		0.36			0.35	
	1.025 ± 0.034	[35]		-0.17			-0.16	
	1.099 ± 0.109	[38]		0.62			0.62	
	1.174 ± 0.058	[84]		2.46			2.4	
	1.062 ± 0.070	[40]		0.44			0.44	
	0.911 ± 0.040	[68]		-2.98			-2.84	
	0.990 ± 0.127	[43]		-0.32			-0.32	
	1.050 ± 0.104	[27]		0.18			0.18	
	1.193 ± 0.151	[46]		1.07			1.07	
	1.082 ± 0.015	[46]		3.24			2.54	
	0.951 ± 0.054	[47]		-1.48			-1.44	
	0.955 ± 0.054	[47]		-1.4			-1.37	
	1.06 ± 0.06	[86]		0.48			0.47	
	1.0328 ± 0.125	[76]		0.01			0.01	
	0.962 ± 0.037	[1]		-1.85			-1.75	
	0.932 ± 0.08	[81]		-1.23			-1.22	
	0.862 ± 0.08	[81]		-2.11			-2.08	
Z = 81, Tl	1.042 ± 0.057	[22]	1.0242 ± 0.0056	0.31	-0.39	0.0074	0.31	-0.39
	0.953 ± 0.029	[61]		-2.41			-2.38	
	0.986 ± 0.032	[61]		-1.18			-1.16	
	1.022 ± 0.037	[61]		-0.06			-0.06	
	1.034 ± 0.105	[33]		0.09			0.09	
	1.056 ± 0.022	[35]		1.4			1.37	
	1.036 ± 0.025	[35]		0.46			0.45	
	0.870 ± 0.068	[36]		-2.26			-2.25	
	1.042 ± 0.119	[38]		0.15			0.15	
	0.978 ± 0.059	[40]		-0.78			-0.78	
	0.840 ± 0.092	[41]		-2			-2	
	0.951 ± 0.045	[68]		-1.61			-1.61	
	0.962 ± 0.120	[43]		-0.52			-0.52	
	1.050 ± 0.104	[27]		0.25			0.25	
	1.066 ± 0.022	[46]		1.84			1.8	
	1.028 ± 0.007	[46]		0.42			0.37	
	0.953 ± 0.053	[47]		-1.34			-1.33	
	0.956 ± 0.053	[47]		-1.28			-1.27	
Z = 82, Pb	1.075 ± 0.046	[1]	1.0332 ± 0.0055	1.1	-0.002	0.0123	1.09	-0.003
	1.220 ± 0.059	[89]		3.15			3.1	
	1.043 ± 0.099	[58]		0.1			0.1	
	1.004 ± 0.018	[58]		-1.55			-1.34	
	1.040 ± 0.037	[58]		0.18			0.17	
	0.978 ± 0.036	[58]		-1.52			-1.45	
	1.203 ± 0.104	[85]		1.63			1.62	
	0.949 ± 0.043	[61]		-1.94			-1.88	
	0.984 ± 0.021	[61]		-2.27			-2.02	
	1.012 ± 0.033	[61]		-0.63			-0.6	
	1.020 ± 0.083	[32]		-0.16			-0.16	
	1.0190 ± 0.036	[88]		-0.39			-0.37	
	1.0382 ± 0.034	[88]		0.15			0.14	
	1.0462 ± 0.032	[88]		0.4			0.38	
	1.0531 ± 0.030	[88]		0.65			0.61	
	1.1465 ± 0.028	[88]		3.97			3.71	
	1.028 ± 0.048	[62]		-0.11			-0.1	
	1.023 ± 0.046	[62]		-0.22			-0.21	
	1.073 ± 0.025	[63]		1.56			1.43	
	0.9021 ± 0.046	[64]		-2.83			-2.75	
	0.9132 ± 0.044	[64]		-2.71			-2.63	
	1.0346 ± 0.040	[64]		0.03			0.03	
	1.065 ± 0.111	[33]		0.29			0.28	
	1.2464 ± 0.0311	[90]		6.75			6.38	
	1.059 ± 0.067	[35]		0.38			0.38	
	1.037 ± 0.020	[35]		0.18			0.16	
	1.053 ± 0.089	[36]		0.22			0.22	
	1.241 ± 0.062	[84]		3.34			3.29	
	1.031 ± 0.096	[38]		-0.02			-0.02	
	1.149 ± 0.119	[39]		0.97			0.97	
	1.078 ± 0.052	[40]		0.86			0.84	
	0.972 ± 0.044	[68]		-1.38			-1.34	
	0.980 ± 0.125	[43]		-0.43			-0.42	
	1.010 ± 0.100	[27]		-0.23			-0.23	

(continued on next page)

Table 2 (continued)

Z, Symbol	$\left(\frac{I_{L\beta}}{I_{L\alpha}}\right)_{EXP} \pm \Delta(I_{L\beta}/I_{L\alpha})_{EXP}$	References	$(I_{L\beta}/I_{L\alpha})_W \pm \epsilon_{ISD}$	$z_{ISD}$	$\bar{z}_{ISD}$	$\epsilon_{ESD}$	$Z_{ESD}$	$\bar{z}_{ESD}$	
Z = 83, Bi	1.093 ± 0.027	[46]		2.17			2.02		
	1.063 ± 0.017	[46]		1.67			1.42		
	0.941 ± 0.052	[47]		-1.76			-1.73		
	0.943 ± 0.053	[47]		-1.69			-1.66		
	0.962 ± 0.046	[50]		-1.54			-1.5		
	1.333 ± 0.053	[50]		5.63			5.51		
	0.952 ± 0.036	[1]		-2.23			-2.13		
	0.9087 ± 0.0509	[77]		-2.43			-2.38		
	0.917 ± 0.025	[55]		-4.54			-4.17		
	0.918 ± 0.08	[81]		-1.44			-1.42		
	0.845 ± 0.079	[81]		-2.38			-2.35		
	1.005 ± 0.030	[58]	1.0039 ± 0.0079	0.04	0.04	0.0146	0.03	0.04	
	1.039 ± 0.021	[58]		1.57			1.38		
	1.091 ± 0.048	[58]		1.79			1.74		
	1.140 ± 0.047	[58]		2.86			2.77		
	1.074 ± 0.098	[85]		0.71			0.71		
	0.947 ± 0.030	[61]		-1.83			-1.7		
	0.988 ± 0.018	[61]		-0.81			-0.68		
	1.012 ± 0.048	[61]		0.17			0.16		
	1.099 ± 0.038	[63]		2.45			2.34		
	1.055 ± 0.108	[33]		0.47			0.47		
	1.057 ± 0.056	[35]		0.94			0.92		
	1.057 ± 0.031	[35]		1.66			1.55		
	0.901 ± 0.065	[36]		-1.57			-1.54		
	1.314 ± 0.066	[84]		4.67			4.59		
	1.070 ± 0.058	[40]		1.13			1.11		
	0.855 ± 0.080	[41]		-1.85			-1.83		
	0.943 ± 0.042	[68]		-1.42			-1.37		
	1.020 ± 0.135	[43]		0.12			0.12		
	1.050 ± 0.104	[27]		0.44			0.44		
0.918 ± 0.050	[47]		-1.7			-1.65			
0.919 ± 0.050	[47]		-1.68			-1.63			
1.0505 ± 0.0926	[76]		0.5			0.5			
0.990 ± 0.039	[1]		-0.35			-0.33			
0.935 ± 0.026	[55]		-2.53			-2.31			
0.808 ± 0.075	[81]		-2.6			-2.56			
0.844 ± 0.077	[81]		-2.07			-2.04			
Z = 90, Th	1.190 ± 0.071	[89]	1.2413 ± 0.0094	-0.72	-0.39	0.0443	-0.61	-0.43	
	1.027 ± 0.051	[14]		-4.13			-3.17		
	1.058 ± 0.053	[14]		-3.41			-2.65		
	1.091 ± 0.055	[14]		-2.69			-2.13		
	1.114 ± 0.056	[14]		-2.24			-1.78		
	1.115 ± 0.056	[14]		-2.22			-1.77		
	1.116 ± 0.103	[33]		-1.21			-1.12		
	1.205 ± 0.030	[34]		-1.15			-0.68		
	1.319 ± 0.033	[34]		2.27			1.41		
	1.361 ± 0.033	[34]		3.49			2.17		
	1.462 ± 0.036	[34]		5.93			3.87		
	1.597 ± 0.041	[34]		8.46			5.89		
	1.669 ± 0.042	[34]		9.94			7.01		
	1.706 ± 0.044	[34]		10.33			7.44		
	1.129 ± 0.102	[35]		-1.1			-1.01		
	1.056 ± 0.027	[35]		-6.48			-3.57		
	1.111 ± 0.111	[38]		-1.17			-1.09		
	1.081 ± 0.051	[40]		-3.09			-2.37		
	0.909 ± 0.091	[41]		-3.63			-3.28		
	1.038 ± 0.045	[68]		-4.42			-3.22		
	1.010 ± 0.133	[43]		-1.73			-1.65		
	1.200 ± 0.119	[27]		-0.35			-0.33		
	1.011 ± 0.053	[47]		-4.28			-3.33		
	1.008 ± 0.053	[47]		-4.33			-3.38		
	1.163 ± 0.041	[1]		-1.86			-1.3		
	Z = 92, U	1.163 ± 0.068	[89]	1.0754 ± 0.0076	1.28	-0.05	0.0275	1.19	-0.07
		1.003 ± 0.050	[14]		-1.43			-1.27	
		1.008 ± 0.050	[14]		-1.33			-1.18	
		1.082 ± 0.054	[14]		0.12			0.11	
		1.083 ± 0.054	[14]		0.14			0.13	
1.108 ± 0.055		[14]		0.59			0.53		
0.847 ± 0.065		[32]		-3.49			-3.24		
1.183 ± 0.127		[34]		0.85			0.83		
1.015 ± 0.026		[34]		-2.23			-1.6		
1.096 ± 0.028		[34]		0.71			0.53		
1.198 ± 0.030		[34]		3.96			3.02		
1.232 ± 0.030		[34]		5.06			3.85		

(continued on next page)

Table 2 (continued)

Z, Symbol	$\left(\frac{I_{L\beta}}{I_{L\alpha}}\right)_{EXP} \pm \Delta(I_{L\beta}/I_{L\alpha})_{EXP}$	References	$(I_{L\beta}/I_{L\alpha})_W \pm \epsilon_{ISD}$	$z_{ISD}$	$\bar{z}_{ISD}$	$\epsilon_{ESD}$	$Z_{ESD}$	$\bar{z}_{ESD}$
	1.222 ± 0.030	[34]		4.74			3.61	
	1.282 ± 0.033	[34]		6.1			4.81	
	1.362 ± 0.033	[34]		8.46			6.68	
	1.085 ± 0.082	[35]		0.12			0.11	
	0.970 ± 0.020	[35]		-4.92			-3.1	
	1.042 ± 0.098	[38]		-0.34			-0.33	
	0.915 ± 0.026	[66]		-5.92			-4.24	
	0.884 ± 0.047	[40]		-4.02			-3.52	
	0.927 ± 0.047	[68]		-3.12			-2.73	
	0.980 ± 0.125	[43]		-0.76			-0.75	
	1.150 ± 0.114	[27]		0.65			0.64	
	0.892 ± 0.048	[47]		-3.77			-3.32	
	0.932 ± 0.050	[47]		-2.84			-2.51	
	1.075 ± 0.035	[1]		-0.01			-0.01	

Table 3

Summary of the experimental  $I_{L\gamma}/I_{L\alpha}$  intensity ratios from  $^{39}\text{Y}$  to  $^{92}\text{U}$  is presented according to their target atomic numbers. The weighted average values  $(I_{L\gamma}/I_{L\alpha})_W$ , the references from which the databases are extracted,  $\epsilon_{ISD}$ ,  $\epsilon_{ESD}$ , the internal and external standard deviation ( $z_{ISD}$ ,  $z_{ESD}$ ), and their means ( $\bar{z}_{ISD}$ ,  $\bar{z}_{ESD}$ ) are also listed.

Z, Symbol	$\left(\frac{I_{L\gamma}}{I_{L\alpha}}\right)_{EXP} \pm \Delta(I_{L\gamma}/I_{L\alpha})_{EXP}$	References	$(I_{L\gamma}/I_{L\alpha})_W \pm \epsilon_{ISD}$	$z_{ISD}$	$\bar{z}_{ISD}$	$\epsilon_{ESD}$	$Z_{ESD}$	$\bar{z}_{ESD}$
Z = 39, Y	0.176 ± 0.015	[8]	0.176 ± 0.015	0	0	-	-	-
Z = 40, Zr	0.181 ± 0.016	[8]	0.181 ± 0.016	0	0	-	-	-
Z = 41, Nb	0.184 ± 0.017	[8]	0.1861 ± 0.017	-0.10	-0.004	0.0020	-0.12	0
	0.188 ± 0.016	[8]		0.09			0.12	
Z = 42, Mo	0.192 ± 0.015	[8]	0.1955 ± 0.0112	-0.19	0.02	0.0040	-0.23	0.02
	0.200 ± 0.017	[8]		0.22			0.26	
Z = 47, Ag	0.205 ± 0.017	[8]	0.1965 ± 0.0067	0.46	0.37	0.0157	0.37	0.34
	0.213 ± 0.016	[8]		0.95			0.74	
	0.234 ± 0.014	[8]		2.42			1.78	
	0.168 ± 0.010	[8]		-2.37			-1.53	
Z = 49, In	0.206 ± 0.018	[8]	0.2317 ± 0.0090	-1.28	0.30	0.0168	-1.04	0.30
	0.227 ± 0.021	[8]		-0.21			-0.18	
	0.316 ± 0.029	[8]		2.78			2.51	
	0.230 ± 0.013	[8]		-0.11			-0.08	
Z = 50, Sn	0.209 ± 0.017	[8]	0.2331 ± 0.0085	-1.27	0.02	0.0093	-1.24	0.02
	0.231 ± 0.019	[8]		-0.10			-0.1	
	0.257 ± 0.020	[8]		1.1			1.08	
	0.239 ± 0.014	[8]		0.36			0.35	
Z = 53, I	0.222 ± 0.019	[8]	0.2380 ± 0.0085	-0.77	-0.04	0.0082	-0.77	-0.04
	0.228 ± 0.020	[8]		-0.46			-0.46	
	0.261 ± 0.017	[8]		1.21			1.22	
	0.236 ± 0.014	[8]		-0.12			-0.12	
Z = 54, Xe	0.099 ± 0.010	[24]	0.099 ± 0.010	0	0	-	-	-
Z = 55, Cs	0.144 ± 0.007	[56]	0.144 ± 0.007	0	0	-	-	-
Z = 56, Ba	0.212 ± 0.018	[8]	0.1486 ± 0.0027	3.48	1.43	0.0134	2.82	1.35
	0.233 ± 0.019	[8]		4.40			3.63	
	0.258 ± 0.015	[8]		7.18			5.43	
	0.226 ± 0.013	[8]		5.83			4.14	
	0.099 ± 0.007	[22]		-6.60			-3.27	
	0.144 ± 0.008	[12]		-0.54			-0.29	
	0.143 ± 0.008	[12]		-0.66			-0.36	
	0.194 ± 0.011	[12]		4.01			2.61	
	0.194 ± 0.010	[13]		4.38			2.71	
	0.145 ± 0.007	[56]		-0.48			-0.24	
	0.114 ± 0.006	[84]		-5.25			-2.35	
Z = 57, La	0.213 ± 0.017	[8]	0.1105 ± 0.0009	6.02	4.28	0.0053	5.75	4.04
	0.236 ± 0.019	[8]		6.6			6.36	
	0.267 ± 0.019	[8]		8.23			7.93	
	0.258 ± 0.015	[8]		9.81			9.26	
	0.136 ± 0.007	[12]		3.61			2.9	
	0.159 ± 0.009	[12]		5.36			4.64	
	0.181 ± 0.010	[12]		7.02			6.22	
	0.234 ± 0.013	[12]		9.48			8.79	
	0.153 ± 0.008	[56]		5.28			4.42	
	0.103 ± 0.001	[33]		-5.56			-1.39	
	0.148 ± 0.007	[84]		5.31			4.26	
	0.113 ± 0.012	[38]		0.21			0.19	
	0.20 ± 0.03	[67]		2.98			2.94	
	0.17 ± 0.02	[69]		2.97			2.87	

(continued on next page)

Table 3 (continued)

Z, Symbol	$\left(\frac{I_{Ly}}{I_{L\alpha}}\right)_{EXP} \pm \Delta(I_{Ly}/I_{L\alpha})_{EXP}$	References	$(I_{Ly}/I_{L\alpha})_W \pm \epsilon_{ISD}$	$z_{ISD}$	$\bar{z}_{ISD}$	$\epsilon_{ESD}$	$Z_{ESD}$	$\bar{z}_{ESD}$				
Z = 58, Ce	0.123 ± 0.006	[48]	0.1503 ± 0.0022	2.06	1.11	0.0104	2.09	1.14				
	0.123 ± 0.006	[51]		2.06								
	0.127 ± 0.005 (B = 0.6T)	[51]		3.24								
	0.152 ± 0.018 (B = 1.2T)	[51]		2.3								
	0.192 ± 0.017	[8]		2.43								
	0.249 ± 0.022	[8]		4.46								
	0.266 ± 0.021	[8]		5.48								
	0.216 ± 0.013	[8]		4.98								
	0.173 ± 0.010	[12]		2.21								
	0.197 ± 0.011	[12]		4.16								
	0.249 ± 0.014	[12]		6.96								
	0.191 ± 0.011	[12]		3.62								
	0.249 ± 0.012	[13]		8.08								
	0.185 ± 0.009	[13]		3.74								
	0.145 ± 0.007	[56]		-0.73								
	Z = 59, Pr	0.107 ± 0.008		[33]					-5.22	-0.69	0.0034	0.51
0.134 ± 0.007		[84]	-2.22									
0.114 ± 0.009		[38]	-3.92									
0.117 ± 0.007		[48]	-4.54									
0.117 ± 0.007		[51]	-4.54									
0.124 ± 0.007 (B = 0.6T)		[51]	-3.58									
0.131 ± 0.014 (B = 1.2T)		[51]	-1.36									
0.156 ± 0.001		[23]	1.31									
0.164 ± 0.009		[12]	1.08									
0.166 ± 0.009		[12]	1.3									
0.188 ± 0.010		[12]	3.36									
0.224 ± 0.012		[12]	5.8									
0.155 ± 0.008		[56]	0.1									
0.1743 ± 0.009		[62]	2.22									
0.1753 ± 0.010		[62]	2.1									
Z = 60, Nd		0.109 ± 0.009	[33]	-5	0.65	0.0086	0.09	0.67				
	0.122 ± 0.010	[38]	-3.21									
	0.17 ± 0.02	[67]	0.79									
	0.16 ± 0.02	[69]	0.29									
	0.107 ± 0.008	[48]	-5.86									
	0.1428 ± 0.0167	[76]	-0.68									
	0.107 ± 0.008	[51]	-5.86									
	0.109 ± 0.009 (B = 0.6T)	[51]	-5									
	0.110 ± 0.010 (B = 1.2T)	[51]	-4.4									
	0.130 ± 0.007	[12]	-0.63									
	0.141 ± 0.008	[12]	0.77									
	0.233 ± 0.013	[12]	7.46									
	0.148 ± 0.008	[12]	1.61									
	0.233 ± 0.012	[13]	8.06									
	0.145 ± 0.007	[13]	1.41									
	Z = 61, Pm	0.172 ± 0.009	[56]	4.03					0	-	3	-2.09
0.107 ± 0.010		[33]	-2.7									
0.118 ± 0.010		[38]	-1.62									
0.16 ± 0.02		[67]	1.26									
0.18 ± 0.02		[69]	2.25									
0.110 ± 0.006		[51]	-3.85									
0.111 ± 0.008 (B = 0.6T)		[51]	-2.85									
0.117 ± 0.011 (B = 1.2T)		[51]	-1.57									
0.110 ± 0.006		[91]	-3.85									
Z = 62, Sm		0.160 ± 0.008	[56]	0.160 ± 0.008	0.91	0.0073	2.83	0.96				
		0.196 ± 0.017	[8]	3.06								
		0.250 ± 0.021	[8]	5.04								
		0.279 ± 0.020	[8]	6.73								
		0.222 ± 0.013	[8]	5.95								
		0.121 ± 0.007	[12]	-3.08								
		0.136 ± 0.007	[12]	-1.04								
	0.170 ± 0.009	[12]	2.86									
	0.215 ± 0.012	[12]	5.86									
	0.165 ± 0.008	[56]	2.59									
	0.231 ± 0.020	[32]	4.35									
	0.114 ± 0.009	[33]	-3.2									
	0.141 ± 0.019	[36]	-0.13									
	0.131 ± 0.008	[38]	-1.52									
	0.17 ± 0.02	[67]	1.31									
	0.18 ± 0.03	[69]	1.21									
0.126 ± 0.006	[87]	-2.76										
0.124 ± 0.006	[87]	-3.07										
0.119 ± 0.013	[51]	-1.87										
0.121 ± 0.011 (B = 0.6T)	[51]	-2.01										

(continued on next page)

Table 3 (continued)

Z, Symbol	$\left(\frac{I_{L\gamma}}{I_{L\alpha}}\right)_{EXP} \pm \Delta(I_{L\gamma}/I_{L\alpha})_{EXP}$	References	$(I_{L\gamma}/I_{L\alpha})_W \pm \epsilon_{ISD}$	$z_{ISD}$	$\bar{z}_{ISD}$	$\epsilon_{ESD}$	$Z_{ESD}$	$\bar{z}_{ESD}$
Z = 63, Eu	0.127 ± 0.009 (B = 1.2T)	[51]	0.1412 ± 0.0025	-1.79	0.56	0.0072	-1.43	0.58
	0.119 ± 0.013	[91]		-1.87			-1.65	
	0.202 ± 0.027	[81]		2.16			2.09	
	0.188 ± 0.02	[81]		2.21			2.08	
	0.147 ± 0.008	[12]		0.69			0.54	
	0.122 ± 0.007	[12]		-2.58			-1.91	
	0.161 ± 0.009	[12]		2.12			1.71	
	0.162 ± 0.009	[12]		2.22			1.8	
	0.220 ± 0.012	[12]		6.42			5.62	
	0.146 ± 0.007	[56]		0.64			0.48	
	0.111 ± 0.007	[33]		-4.06			-3	
	0.147 ± 0.018	[36]		0.32			0.3	
	0.19 ± 0.03	[67]		1.62			1.58	
	0.19 ± 0.03	[69]		1.62			1.58	
Z = 64, Gd	0.133 ± 0.007	[87]	0.1452 ± 0.0014	-1.10	1.29	0.0056	-0.81	1.38
	0.132 ± 0.007	[87]		-1.24			-0.91	
	0.200 ± 0.017	[8]		3.21			3.06	
	0.251 ± 0.021	[8]		5.03			4.87	
	0.263 ± 0.021	[8]		5.6			5.42	
	0.238 ± 0.014	[8]		6.59			6.15	
	0.189 ± 0.015	[8]		2.91			2.73	
	0.254 ± 0.023	[8]		4.72			4.59	
	0.261 ± 0.023	[8]		5.02			4.89	
	0.271 ± 0.060	[8]		2.1			2.09	
	0.107 ± 0.006	[12]		-6.21			-4.65	
	0.136 ± 0.007	[12]		-1.29			-1.03	
	0.142 ± 0.008	[12]		-0.4			-0.33	
	0.183 ± 0.010	[12]		3.74			3.29	
Z = 65, Tb	0.171 ± 0.009	[12]	0.1450 ± 0.0017	2.83	0.66	0.0058	2.43	0.71
	0.207 ± 0.011	[12]		5.57			5	
	0.146 ± 0.007	[56]		0.11			0.09	
	0.113 ± 0.013	[33]		-2.46			-2.28	
	0.166 ± 0.008	[84]		2.56			2.13	
	0.20 ± 0.03	[67]		1.82			1.79	
	0.17 ± 0.02	[69]		1.24			1.19	
	0.113 ± 0.005	[51]		-6.21			-4.29	
	0.117 ± 0.007 (B = 0.6T)	[51]		-3.95			-3.15	
	0.133 ± 0.013 (B = 1.2T)	[51]		-0.93			-0.86	
	0.149 ± 0.002	[53]		1.55			0.63	
	0.113 ± 0.005	[91]		-6.21			-4.29	
	0.238 ± 0.028	[81]		3.31			3.25	
	0.209 ± 0.02	[81]		3.18			3.07	
Z = 66, Dy	0.145 ± 0.006	[12]	0.1194 ± 0.0002	-0.01	3.12	0.0008	-0.01	3.13
	0.134 ± 0.007	[12]		-1.54			-1.21	
	0.171 ± 0.008	[12]		3.18			2.62	
	0.168 ± 0.010	[12]		2.26			1.98	
	0.183 ± 0.009	[12]		4.15			3.54	
	0.248 ± 0.011	[12]		9.26			8.28	
	0.156 ± 0.008	[56]		1.34			1.11	
	0.116 ± 0.008	[33]		-3.56			-2.94	
	0.1571 ± 0.013	[16]		0.92			0.85	
	0.1875 ± 0.015	[16]		2.81			2.64	
	0.1899 ± 0.015	[16]		2.97			2.79	
	0.126 ± 0.008	[38]		-2.33			-1.93	
	0.19 ± 0.03	[67]		1.5			1.47	
	0.17 ± 0.02	[69]		1.24			1.2	
0.116 ± 0.006	[51]	-4.67	-3.48					
0.120 ± 0.006	[51]	-4.02	-3					
0.132 ± 0.010	[51]	-1.29	-1.13					
0.150 ± 0.003	[53]	1.45	0.76					
0.116 ± 0.006	[91]	-4.67	-3.48					
0.237 ± 0.03	[81]	3.06	3.01					
0.198 ± 0.028	[81]	1.89	1.85					
0.169 ± 0.010	[21]	4.96	4.95					
0.125 ± 0.007	[12]	0.8	0.8					
0.150 ± 0.008	[12]	3.83	3.81					
0.133 ± 0.007	[12]	1.95	1.94					
0.155 ± 0.009	[12]	3.96	3.94					
0.187 ± 0.010	[12]	6.76	6.74					
0.189 ± 0.010	[12]	6.96	6.94					
0.158 ± 0.008	[56]	4.83	4.81					
0.118 ± 0.007	[33]	-0.2	-0.19					
0.1700 ± 0.014	[16]	3.62	3.61					
0.1869 ± 0.015	[16]	4.5	4.5					

(continued on next page)

Table 3 (continued)

Z, Symbol	$\left(\frac{I_{Ly}}{I_{L\alpha}}\right)_{EXP} \pm \Delta(I_{Ly}/I_{L\alpha})_{EXP}$	References	$(I_{Ly}/I_{L\alpha})_W \pm \epsilon_{ISD}$	$z_{ISD}$	$\bar{z}_{ISD}$	$\epsilon_{ESD}$	$Z_{ESD}$	$\bar{z}_{ESD}$
Z = 67, Ho	0.1966 ± 0.016	[16]	0.1212 ± 0.0001	4.83	4.23	0.0005		4.20
	0.127 ± 0.007	[38]		1.09				
	0.156 ± 0.024	[41]		1.53				
	0.20 ± 0.03	[67]		2.69				
	0.17 ± 0.02	[69]		2.53				
	0.122 ± 0.001	[46]		2.58				
	0.119 ± 0.0002	[46]		-1.33				
	0.198 ± 0.014	[47]		5.62				
	0.190 ± 0.014	[47]		5.04				
	0.125 ± 0.008	[49]		0.7				
	0.248 ± 0.017	[75]		7.57				
	0.125 ± 0.008	[51]		0.7				
	0.130 ± 0.010 (B = 0.6T)	[51]		1.06				
	0.137 ± 0.012 (B = 1.2T)	[51]		1.47				
	0.127 ± 0.006	[60]		0.96				
	0.205 ± 0.010	[60]		8.38				
	0.176 ± 0.009	[60]		6.09				
	0.202 ± 0.010	[60]		8.08				
	0.199 ± 0.010	[60]		7.78				
	0.242 ± 0.012	[60]		10.06				
	0.149 ± 0.007	[56]		3.97				
	0.1854 ± 0.007	[62]		9.17				
	0.1852 ± 0.008	[62]		8				
	0.120 ± 0.007	[33]		-0.18				
	0.1937 ± 0.015	[16]		4.83				
0.1927 ± 0.015	[16]	4.76						
0.1909 ± 0.015	[16]	4.64						
0.136 ± 0.008	[38]	1.85						
0.159 ± 0.020	[41]	1.89						
0.19 ± 0.03	[67]	2.29						
0.18 ± 0.03	[69]	1.96						
0.123 ± 0.0004	[46]	4.3						
0.121 ± 0.0001	[46]	-1.66						
0.128 ± 0.012	[49]	0.56						
0.128 ± 0.012	[51]	0.56						
0.139 ± 0.015 (B = 0.6T)	[51]	1.18						
0.151 ± 0.017 (B = 1.2T)	[51]	1.75						
0.152 ± 0.003	[53]	10.25						
0.167 ± 0.008	[60]	0.61						
0.189 ± 0.009	[60]	2.92						
0.175 ± 0.009	[60]	1.41						
0.211 ± 0.011	[60]	4.37						
0.221 ± 0.011	[60]	5.26						
0.271 ± 0.014	[60]	7.7						
0.164 ± 0.010	[24]	0.2						
0.162 ± 0.008	[56]	0.007						
0.128 ± 0.007	[33]	-4.62						
0.167 ± 0.008	[84]	0.61						
0.131 ± 0.008	[38]	-3.73						
0.161 ± 0.023	[41]	-0.04						
0.214 ± 0.015	[47]	3.43						
0.204 ± 0.014	[47]	2.97						
0.132 ± 0.007	[49]	-4.08						
0.132 ± 0.007	[51]	-4.08						
0.136 ± 0.011 (B = 0.6T)	[51]	-2.31						
0.144 ± 0.015 (B = 1.2T)	[51]	-1.18						
0.227 ± 0.023	[81]	2.82						
0.159 ± 0.006	[21]	0.1642 ± 0.0024						
0.146 ± 0.007	[14]	-0.8						
0.191 ± 0.010	[14]	-2.45						
0.231 ± 0.012	[14]	2.61						
0.179 ± 0.009	[14]	5.46						
0.257 ± 0.013	[14]	1.59						
0.195 ± 0.010	[14]	7.02						
0.158 ± 0.008	[56]	2.99						
0.126 ± 0.005	[33]	-0.74						
0.1777 ± 0.014	[16]	-6.85						
0.1807 ± 0.014	[16]	0.95						
0.1977 ± 0.016	[16]	1.16						
0.20 ± 0.03	[67]	1.19						
0.18 ± 0.02	[69]	2.07						
0.170 ± 0.002	[20]	1.19						
0.121 ± 0.006	[60]	0.79						
0.203 ± 0.010	[60]	-5						
Z = 70, Yb			0.2533 ± 0.0011	-36.29	-2.50	0.0179	-4.63	-1.44
				-21.67			-7.01	
				-5			-2.45	

(continued on next page)

Table 3 (continued)

Z, Symbol	$\left(\frac{I_{Ly}}{I_{L\alpha}}\right)_{EXP} \pm \Delta(I_{Ly}/I_{L\alpha})_{EXP}$	References	$(I_{Ly}/I_{L\alpha})_W \pm \epsilon_{ISD}$	$z_{ISD}$	$\bar{z}_{ISD}$	$\epsilon_{ESD}$	$Z_{ESD}$	$\bar{z}_{ESD}$
	0.160 ± 0.008	[60]		-11.55			-4.76	
	0.233 ± 0.012	[60]		-1.69			-0.94	
	0.159 ± 0.008	[60]		-11.67			-4.81	
	0.227 ± 0.011	[60]		-2.38			-1.25	
	0.171 ± 0.009	[56]		-9.08			-4.11	
	0.2139 ± 0.012	[62]		-3.27			-1.83	
	0.2112 ± 0.007	[62]		-5.94			-2.19	
	0.339 ± 0.015	[33]		5.7			3.67	
	0.1924 ± 0.015	[16]		-4.05			-2.61	
	0.2106 ± 0.017	[16]		-2.51			-1.73	
	0.2124 ± 0.017	[16]		-2.4			-1.66	
	0.167 ± 0.008	[84]		-10.68			-4.4	
	0.300 ± 0.023	[38]		2.03			1.6	
	0.288 ± 0.014	[40]		2.47			1.53	
	0.21 ± 0.03	[67]		-1.44			-1.24	
	0.19 ± 0.03	[69]		-2.11			-1.81	
	0.356 ± 0.003	[46]		32.04			5.66	
	0.337 ± 0.002	[46]		36.45			4.65	
	0.205 ± 0.014	[47]		-3.44			-2.13	
	0.204 ± 0.014	[47]		-3.51			-2.17	
	0.254 ± 0.027	[1]		0.03			0.02	
Z = 71, Lu	0.142 ± 0.007	[14]	0.1927 ± 0.0030	-6.65	0.84	0.0117	-3.71	0.85
	0.185 ± 0.009	[14]		-0.81			-0.52	
	0.209 ± 0.010	[14]		1.57			1.06	
	0.217 ± 0.011	[14]		2.14			1.51	
	0.257 ± 0.013	[14]		4.82			3.67	
	0.367 ± 0.018	[14]		9.55			8.11	
	0.168 ± 0.008	[56]		-2.89			-1.74	
	0.322 ± 0.022	[33]		5.83			5.19	
	0.1866 ± 0.015	[16]		-0.4			-0.32	
	0.1764 ± 0.014	[16]		-1.14			-0.89	
	0.2119 ± 0.017	[16]		1.11			0.93	
	0.180 ± 0.012	[36]		-1.02			-0.75	
	0.21 ± 0.03	[67]		0.58			0.54	
	0.17 ± 0.02	[69]		-1.12			-0.98	
	0.207 ± 0.014	[47]		1			0.79	
Z = 72, Hf	0.204 ± 0.014	[47]		0.79			0.62	
	0.184 ± 0.006	[23]	0.1975 ± 0.0042	-1.84	0.95	0.0144	-0.86	0.90
	0.154 ± 0.017	[36]		-2.48			-1.95	
	0.274 ± 0.017	[38]		4.37			3.44	
	0.265 ± 0.013	[40]		4.95			3.48	
	0.204 ± 0.026	[41]		0.25			0.22	
	0.325 ± 0.042	[43]		3.02			2.87	
Z = 73, Ta	0.1825 ± 0.0082	[71]		-1.63			-0.9	
	0.201 ± 0.010	[58]	0.2353 ± 0.0046	-3.33	1.23	0.0133	-2.07	1.27
	0.230 ± 0.014	[58]		-0.38			-0.28	
	0.276 ± 0.022	[58]		1.84			1.58	
	0.265 ± 0.021	[58]		1.4			1.19	
	0.185 ± 0.010	[61]		-4.88			-3.03	
	0.225 ± 0.006	[61]		-1.59			-0.71	
	0.289 ± 0.008	[61]		6.4			3.46	
	0.164 ± 0.008	[56]		-8.51			-4.6	
	0.316 ± 0.020	[33]		4			3.36	
	0.297 ± 0.097	[35]		0.64			0.63	
	0.138 ± 0.018	[35]		-5.36			-4.35	
	0.170 ± 0.008	[84]		-7.79			-4.21	
	0.240 ± 0.011	[40]		0.41			0.27	
	0.315 ± 0.041	[43]		1.94			1.85	
	0.311 ± 0.012	[45]		6.17			4.23	
	0.399 ± 0.024 (B=+0.15T)	[45]		6.78			5.97	
	0.399 ± 0.024 (B=-0.15T)	[45]		6.78			5.97	
	0.403 ± 0.023 (B=+0.45T)	[45]		7.25			6.31	
	0.402 ± 0.023 (B=-0.45T)	[45]		7.2			6.27	
	0.406 ± 0.018 (B=+0.75T)	[45]		9.39			7.63	
	0.407 ± 0.021 (B=-0.75T)	[45]		8.12			6.91	
	0.207 ± 0.014	[47]		-1.99			-1.47	
	0.206 ± 0.014	[47]		-2.06			-1.52	
	0.329 ± 0.024	[1]		3.88			3.41	
	0.282 ± 0.028	[52]		1.66			1.51	
	0.198 ± 0.02	[81]		-1.85			-1.56	
	0.183 ± 0.018	[81]		-2.88			-2.34	
Z = 74, W	0.206 ± 0.010	[59]	0.2502 ± 0.0022	-4.32	0.04	0.0120	-2.83	0.09
	0.233 ± 0.011	[59]		-1.54			-1.06	
	0.348 ± 0.017	[59]		5.7			4.7	

(continued on next page)

Table 3 (continued)

Z, Symbol	$\left(\frac{I_{Ly}}{I_{L\alpha}}\right)_{EXP} \pm \Delta(I_{Ly}/I_{L\alpha})_{EXP}$	References	$(I_{Ly}/I_{L\alpha})_W \pm \epsilon_{ISD}$	$z_{ISD}$	$\bar{z}_{ISD}$	$\epsilon_{ESD}$	$Z_{ESD}$	$\bar{z}_{ESD}$
	0.178 ± 0.010	[61]		-7.05			-4.62	
	0.212 ± 0.011	[61]		-3.41			-2.35	
	0.266 ± 0.017	[61]		0.92			0.76	
	0.153 ± 0.008	[56]		-11.72			-6.74	
	0.182 ± 0.009	[25]		-7.36			-4.55	
	0.360 ± 0.027	[33]		4.05			3.72	
	0.305 ± 0.112	[35]		0.49			0.49	
	0.133 ± 0.017	[35]		-6.84			-5.63	
	0.1787 ± 0.014	[16]		-5.05			-3.88	
	0.1826 ± 0.015	[16]		-4.46			-3.52	
	0.1961 ± 0.016	[16]		-3.35			-2.71	
	0.331 ± 0.027	[38]		2.98			2.73	
	0.242 ± 0.010	[40]		-0.8			-0.53	
	0.169 ± 0.017	[41]		-4.74			-3.9	
	0.277 ± 0.020	[68]		1.33			1.15	
	0.324 ± 0.006	[46]		11.54			5.5	
	0.311 ± 0.007	[46]		8.28			4.38	
	0.326 ± 0.042	[43]		1.8			1.73	
	0.313 ± 0.014	[45]		4.43			3.4	
	0.334 ± 0.017 (B=+0.15T)	[45]		4.89			4.03	
	0.334 ± 0.018 (B=-0.15T)	[45]		4.62			3.87	
	0.337 ± 0.016 (B=+0.45T)	[45]		5.37			4.34	
	0.337 ± 0.016 (B=-0.45T)	[45]		5.37			4.34	
	0.340 ± 0.014 (B=+0.75T)	[45]		6.33			4.87	
	0.340 ± 0.014 (B=-0.75T)	[45]		6.33			4.87	
	0.199 ± 0.013	[47]		-3.88			-2.9	
	0.205 ± 0.014	[47]		-3.19			-2.45	
	0.272 ± 0.022	[1]		0.98			0.87	
	0.296 ± 0.030	[52]		1.52			1.42	
	0.190 ± 0.018	[81]		-3.32			-2.78	
	0.173 ± 0.017	[81]		-4.5			-3.71	
Z = 75, Re	0.173 ± 0.009	[61]	0.1892 ± 0.0043	-1.62	0.35	0.0113	-1.12	0.36
	0.201 ± 0.009	[61]		1.19			0.82	
	0.246 ± 0.018	[61]		3.07			2.67	
	0.304 ± 0.022	[33]		5.12			4.64	
	0.247 ± 0.062	[35]		0.93			0.92	
	0.135 ± 0.018	[35]		-2.93			-2.55	
	0.183 ± 0.008	[40]		-0.68			-0.44	
	0.182 ± 0.023	[81]		-0.31			-0.28	
Z = 76, Os	0.161 ± 0.017	[81]	0.1756 ± 0.0052	-1.61	1.12	0.0229	-1.38	0.78
	0.145 ± 0.007	[36]		-3.52			-1.28	
	0.260 ± 0.014	[38]		5.65			3.15	
	0.193 ± 0.013	[47]		1.24			0.66	
	0.191 ± 0.013	[47]		1.10			0.59	
Z = 77, Ir	0.153 ± 0.008	[56]	0.1601 ± 0.0069	-0.67	0.36	0.0125	-0.48	0.34
	0.182 ± 0.014	[32]		1.40			1.17	
Z = 78, Pt	0.165 ± 0.008	[61]	0.1797 ± 0.0025	-1.76	-0.07	0.0055	-1.52	-0.08
	0.181 ± 0.005	[61]		0.22			0.17	
	0.205 ± 0.015	[61]		1.66			1.58	
	0.170 ± 0.009	[56]		-1.04			-0.92	
	0.217 ± 0.007	[63]		5.02			4.18	
	0.1623 ± 0.013	[16]		-1.32			-1.24	
	0.1673 ± 0.013	[16]		-0.94			-0.88	
	0.1906 ± 0.015	[16]		0.71			0.68	
	0.157 ± 0.007	[36]		-3.06			-2.55	
	0.193 ± 0.009	[40]		1.42			1.26	
	0.204 ± 0.020	[27]		1.20			1.17	
	0.181 ± 0.012	[47]		0.10			0.1	
	0.180 ± 0.012	[47]		0.02			0.02	
Z = 79, Au	0.1290 ± 0.0154	[76]	0.1861 ± 0.0016	-3.25	0.12	0.0026	-3.1	0.12
	0.194 ± 0.005	[7]		1.51			1.4	
	0.194 ± 0.006	[7]		1.27			1.2	
	0.207 ± 0.007	[7]		2.91			2.79	
	0.184 ± 0.021	[7]		-0.1			-0.1	
	0.174 ± 0.016	[58]		-0.75			-0.75	
	0.181 ± 0.009	[58]		-0.56			-0.55	
	0.193 ± 0.023	[58]		0.3			0.3	
	0.227 ± 0.066	[58]		0.62			0.62	
	0.165 ± 0.009	[61]		-2.31			-2.25	
	0.178 ± 0.010	[61]		-0.8			-0.78	
	0.199 ± 0.012	[61]		1.06			1.05	
	0.159 ± 0.008	[56]		-3.33			-3.22	
	0.183 ± 0.014	[32]		-0.22			-0.22	
	0.1776 ± 0.012	[62]		-0.7			-0.69	

(continued on next page)

Table 3 (continued)

Z, Symbol	$\left(\frac{I_{L\gamma}}{I_{L\alpha}}\right)_{EXP} \pm \Delta(I_{L\gamma}/I_{L\alpha})_{EXP}$	References	$(I_{L\gamma}/I_{L\alpha})_W \pm \epsilon_{ISD}$	$z_{ISD}$	$\bar{z}_{ISD}$	$\epsilon_{ESD}$	$Z_{ESD}$	$\bar{z}_{ESD}$
	0.1768 ± 0.010	[62]		-0.92			-0.9	
	0.1951 ± 0.018	[88]		0.5			0.49	
	0.2155 ± 0.016	[88]		1.83			1.81	
	0.2150 ± 0.016	[88]		1.8			1.78	
	0.2145 ± 0.014	[88]		2.02			1.99	
	0.2133 ± 0.012	[88]		2.25			2.21	
	0.1803 ± 0.018	[64]		-0.32			-0.32	
	0.2108 ± 0.016	[64]		1.54			1.52	
	0.2053 ± 0.014	[64]		1.36			1.35	
	0.195 ± 0.016	[33]		0.55			0.55	
	0.187 ± 0.044	[35]		0.02			0.02	
	0.138 ± 0.018	[35]		-2.66			-2.65	
	0.1587 ± 0.013	[16]		-2.09			-2.07	
	0.1717 ± 0.014	[16]		-1.02			-1.01	
	0.1989 ± 0.016	[16]		0.8			0.79	
	0.224 ± 0.011	[84]		3.41			3.35	
	0.172 ± 0.009	[40]		-1.54			-1.51	
	0.175 ± 0.015	[68]		-0.74			-0.73	
	0.201 ± 0.026	[43]		0.57			0.57	
	0.205 ± 0.011	[45]		1.7			1.67	
	0.203 ± 0.010 (B=+0.15T)	[45]		1.67			1.63	
	0.203 ± 0.011 (B=-0.15T)	[45]		1.52			1.49	
	0.182 ± 0.008 (B=+0.45T)	[45]		-0.5			-0.49	
	0.182 ± 0.008 (B=-0.45T)	[45]		-0.5			-0.49	
	0.167 ± 0.006 (B=+0.75T)	[45]		-3.08			-2.92	
	0.167 ± 0.006 (B=-0.75T)	[45]		-3.08			-2.92	
	0.173 ± 0.017	[27]		-0.77			-0.76	
	0.219 ± 0.015	[18]		2.18			2.16	
	0.175 ± 0.011	[47]		-1			-0.98	
	0.173 ± 0.011	[47]		-1.18			-1.16	
	0.218 ± 0.022	[52]		1.45			1.44	
	0.15 ± 0.03	[80]		-1.2			-1.2	
	0.210 ± 0.011	[19]		2.15			2.11	
Z = 80, Hg	0.180 ± 0.010	[59]	0.2021 ± 0.0009	-2.2	-1.16	0.0023	-2.16	-1.17
	0.169 ± 0.009	[59]		-3.66			-3.57	
	0.182 ± 0.010	[59]		-2			-1.96	
	0.166 ± 0.011	[61]		-3.27			-3.21	
	0.177 ± 0.009	[61]		-2.78			-2.7	
	0.195 ± 0.010	[61]		-0.71			-0.69	
	0.209 ± 0.010	[24]		0.69			0.67	
	0.236 ± 0.009	[24]		3.75			3.65	
	0.161 ± 0.008	[56]		-5.11			-4.94	
	0.192 ± 0.014	[32]		-0.72			-0.71	
	0.179 ± 0.010	[33]		-2.3			-2.25	
	0.212 ± 0.047	[35]		0.21			0.21	
	0.164 ± 0.025	[35]		-1.52			-1.52	
	0.279 ± 0.092	[84]		0.84			0.84	
	0.203 ± 0.013	[38]		0.07			0.07	
	0.189 ± 0.013	[40]		-1.01			-0.99	
	0.174 ± 0.015	[68]		-1.87			-1.85	
	0.204 ± 0.027	[43]		0.07			0.07	
	0.212 ± 0.011	[45]		0.9			0.88	
	0.210 ± 0.011 (B=+0.15T)	[45]		0.71			0.7	
	0.210 ± 0.011 (B=-0.15T)	[45]		0.71			0.7	
	0.206 ± 0.010 (B=+0.45T)	[45]		0.39			0.38	
	0.206 ± 0.010 (B=-0.45T)	[45]		0.39			0.38	
	0.166 ± 0.006 (B=+0.75T)	[45]		-5.96			-5.62	
	0.167 ± 0.006 (B=-0.75T)	[45]		-5.79			-5.46	
	0.192 ± 0.019	[27]		-0.53			-0.53	
	0.216 ± 0.014	[46]		0.99			0.98	
	0.207 ± 0.001	[46]		3.66			1.94	
	0.185 ± 0.012	[47]		-1.42			-1.4	
	0.180 ± 0.012	[47]		-1.84			-1.81	
	0.193 ± 0.012	[86]		-0.76			-0.75	
	0.1312 ± 0.0155	[76]		-4.57			-4.53	
	0.185 ± 0.010	[1]		-1.71			-1.67	
	0.174 ± 0.018	[81]		-1.56			-1.55	
	0.159 ± 0.017	[81]		-2.53			-2.51	
Z = 81, Tl	0.207 ± 0.012	[22]	0.2095 ± 0.0014	-0.21	-0.42	0.0033	-0.2	-0.43
	0.173 ± 0.007	[61]		-5.12			-4.72	
	0.180 ± 0.012	[61]		-2.45			-2.37	
	0.195 ± 0.008	[61]		-1.79			-1.68	
	0.181 ± 0.011	[33]		-2.57			-2.48	
	0.213 ± 0.046	[35]		0.08			0.07	

(continued on next page)

Table 3 (continued)

Z, Symbol	$\left(\frac{I_{L\gamma}}{I_{L\alpha}}\right)_{EXP} \pm \Delta(I_{L\gamma}/I_{L\alpha})_{EXP}$	References	$(I_{L\gamma}/I_{L\alpha})_W \pm \epsilon_{ISD}$	$z_{ISD}$	$\bar{z}_{ISD}$	$\epsilon_{ESD}$	$Z_{ESD}$	$\bar{z}_{ESD}$
	0.172 ± 0.025	[35]		-1.5			-1.49	
	0.163 ± 0.013	[36]		-3.56			-3.47	
	0.214 ± 0.015	[38]		0.3			0.29	
	0.199 ± 0.011	[40]		-0.95			-0.92	
	0.151 ± 0.017	[41]		-3.43			-3.38	
	0.178 ± 0.017	[68]		-1.85			-1.82	
	0.188 ± 0.024	[43]		-0.9			-0.89	
	0.217 ± 0.007	[45]		1.04			0.96	
	0.228 ± 0.008 (B=+0.15T)	[45]		2.27			2.13	
	0.228 ± 0.008 (B=-0.15T)	[45]		2.27			2.13	
	0.230 ± 0.007 (B=+0.45T)	[45]		2.87			2.64	
	0.230 ± 0.007 (B=-0.45T)	[45]		2.87			2.64	
	0.231 ± 0.006 (B=+0.75T)	[45]		3.48			3.13	
	0.231 ± 0.006 (B=-0.75T)	[45]		3.48			3.13	
	0.183 ± 0.018	[27]		-1.47			-1.45	
	0.232 ± 0.016	[46]		1.4			1.37	
	0.209 ± 0.002	[46]		-0.23			-0.14	
	0.184 ± 0.012	[47]		-2.11			-2.05	
	0.184 ± 0.012	[47]		-2.11			-2.05	
	0.204 ± 0.008	[1]		-0.68			-0.64	
Z = 82, Pb	0.254 ± 0.014	[89]	0.2008 ± 0.0013	3.79	0.03	0.0040	3.65	0.03
	0.213 ± 0.011	[58]		1.1			1.04	
	0.180 ± 0.020	[58]		-1.04			-1.02	
	0.211 ± 0.017	[58]		0.6			0.59	
	0.197 ± 0.030	[58]		-0.13			-0.12	
	0.235 ± 0.022	[85]		1.55			1.53	
	0.173 ± 0.007	[61]		-3.9			-3.44	
	0.184 ± 0.010	[61]		-1.66			-1.56	
	0.198 ± 0.009	[61]		-0.31			-0.28	
	0.183 ± 0.013	[32]		-1.36			-1.31	
	0.1697 ± 0.008	[62]		-3.84			-3.47	
	0.1898 ± 0.010	[62]		-1.09			-1.02	
	0.1996 ± 0.009	[88]		-0.13			-0.12	
	0.2133 ± 0.010	[88]		1.24			1.16	
	0.2188 ± 0.010	[88]		1.79			1.67	
	0.2230 ± 0.012	[88]		1.84			1.76	
	0.2130 ± 0.014	[88]		0.87			0.84	
	0.217 ± 0.006	[63]		2.64			2.25	
	0.1804 ± 0.008	[64]		-2.51			-2.28	
	0.1833 ± 0.010	[64]		-1.73			-1.62	
	0.2094 ± 0.012	[64]		0.71			0.68	
	0.198 ± 0.016	[33]		-0.17			-0.17	
	0.2970 ± 0.0074	[90]		12.81			11.44	
	0.209 ± 0.044	[35]		0.19			0.19	
	0.184 ± 0.029	[35]		-0.58			-0.57	
	0.166 ± 0.008	[36]		-4.29			-3.89	
	0.299 ± 0.015	[84]		6.52			6.33	
	0.236 ± 0.017	[38]		2.07			2.02	
	0.192 ± 0.019	[39]		-0.46			-0.45	
	0.177 ± 0.009	[40]		-2.62			-2.41	
	0.184 ± 0.017	[68]		-0.98			-0.96	
	0.236 ± 0.031	[43]		1.14			1.13	
	0.208 ± 0.005	[45]		1.4			1.13	
	0.206 ± 0.006 (B=+0.15T)	[45]		0.85			0.72	
	0.206 ± 0.006 (B=-0.15T)	[45]		0.85			0.72	
	0.204 ± 0.006 (B=+0.45T)	[45]		0.52			0.45	
	0.204 ± 0.006 (B=-0.45T)	[45]		0.52			0.45	
	0.199 ± 0.005 (B=+0.75T)	[45]		-0.34			-0.28	
	0.199 ± 0.005 (B=-0.75T)	[45]		-0.34			-0.28	
	0.170 ± 0.017	[27]		-1.81			-1.76	
	0.240 ± 0.018	[46]		2.17			2.13	
	0.219 ± 0.006	[46]		2.97			2.53	
	0.184 ± 0.012	[47]		-1.39			-1.33	
	0.182 ± 0.012	[47]		-1.56			-1.48	
	0.207 ± 0.010	[1]		0.62			0.58	
	0.151 ± 0.006	[55]		-8.11			-6.9	
	0.151 ± 0.016	[81]		-3.1			-3.02	
	0.143 ± 0.015	[81]		-3.84			-3.72	
Z = 83, Bi	0.206 ± 0.010	[58]	0.1959 ± 0.0017	1	0.08	0.0039	0.94	0.08
	0.207 ± 0.017	[58]		0.65			0.64	
	0.218 ± 0.028	[58]		0.79			0.78	
	0.230 ± 0.024	[85]		1.42			1.4	
	0.177 ± 0.005	[61]		-3.58			-2.97	
	0.190 ± 0.008	[61]		-0.72			-0.66	

(continued on next page)

Table 3 (continued)

Z, Symbol	$\left(\frac{I_{Ly}}{I_{L\alpha}}\right)_{EXP} \pm \Delta(I_{Ly}/I_{L\alpha})_{EXP}$	References	$(I_{Ly}/I_{L\alpha})_W \pm \epsilon_{ISD}$	$z_{ISD}$	$\bar{z}_{ISD}$	$\epsilon_{ESD}$	$Z_{ESD}$	$\bar{z}_{ESD}$
	0.205 ± 0.008	[61]		1.11			1.02	
	0.234 ± 0.007	[63]		5.29			4.74	
	0.209 ± 0.014	[33]		0.93			0.9	
	0.225 ± 0.052	[35]		0.56			0.56	
	0.194 ± 0.031	[35]		-0.06			-0.06	
	0.174 ± 0.009	[36]		-2.39			-2.23	
	0.263 ± 0.013	[84]		5.12			4.94	
	0.219 ± 0.011	[40]		2.08			1.98	
	0.160 ± 0.016	[41]		-2.23			-2.18	
	0.185 ± 0.016	[68]		-0.68			-0.66	
	0.229 ± 0.030	[43]		1.1			1.09	
	0.207 ± 0.006	[45]		1.78			1.55	
	0.205 ± 0.008 (B=+0.15T)	[45]		1.11			1.02	
	0.205 ± 0.008 (B=-0.15T)	[45]		1.11			1.02	
	0.200 ± 0.007 (B=+0.45T)	[45]		0.57			0.51	
	0.200 ± 0.007 (B=-0.45T)	[45]		0.57			0.51	
	0.199 ± 0.007 (B=+0.75T)	[45]		0.43			0.39	
	0.199 ± 0.007 (B=-0.75T)	[45]		0.43			0.39	
	0.186 ± 0.018	[27]		-0.55			-0.54	
	0.174 ± 0.011	[47]		-1.97			-1.87	
	0.173 ± 0.011	[47]		-2.06			-1.96	
	0.210 ± 0.009	[1]		1.54			1.44	
	0.153 ± 0.007	[55]		-5.96			-5.34	
	0.160 ± 0.016	[81]		-2.23			-2.18	
	0.153 ± 0.015	[81]		-2.84			-2.77	
Z = 90, Th	0.261 ± 0.016	[89]	0.2500 ± 0.0003	0.69	-0.17	0.0014	0.69	-0.17
	0.220 ± 0.011	[14]		-2.72			-2.71	
	0.243 ± 0.012	[14]		-0.58			-0.58	
	0.236 ± 0.012	[14]		-1.17			-1.16	
	0.252 ± 0.013	[14]		0.16			0.15	
	0.247 ± 0.021	[33]		-0.14			-0.14	
	0.217 ± 0.005	[34]		-6.59			-6.37	
	0.215 ± 0.005	[34]		-6.99			-6.75	
	0.231 ± 0.006	[34]		-3.16			-3.09	
	0.252 ± 0.006	[34]		0.34			0.33	
	0.286 ± 0.007	[34]		5.14			5.05	
	0.282 ± 0.007	[34]		4.57			4.49	
	0.292 ± 0.007	[34]		6			5.89	
	0.258 ± 0.070	[35]		0.11			0.11	
	0.192 ± 0.030	[35]		-1.93			-1.93	
	0.246 ± 0.018	[38]		-0.22			-0.22	
	0.269 ± 0.013	[40]		1.46			1.45	
	0.188 ± 0.019	[41]		-3.26			-3.25	
	0.216 ± 0.015	[68]		-2.27			-2.26	
	0.198 ± 0.026	[43]		-2			-2	
	0.249 ± 0.001	[44]		-0.95			-0.58	
	0.257 ± 0.001	[44]		6.76			4.17	
	0.258 ± 0.002 (B=+0.75T)	[44]		3.97			3.32	
	0.265 ± 0.001 (B=+0.75T)	[44]		14.46			8.91	
	0.248 ± 0.002 (B=+0.60T)	[44]		-0.98			-0.82	
	0.254 ± 0.002 (B=+0.60T)	[44]		1.99			1.66	
	0.241 ± 0.002 (B=+0.45T)	[44]		-4.45			-3.72	
	0.247 ± 0.001 (B=+0.45T)	[44]		-2.87			-1.77	
	0.238 ± 0.001 (B=+0.30T)	[44]		-11.54			-7.11	
	0.243 ± 0.002 (B=+0.30T)	[44]		-3.46			-2.89	
	0.241 ± 0.002 (B=+0.15T)	[44]		-4.45			-3.72	
	0.247 ± 0.001 (B=+0.15T)	[44]		-2.87			-1.77	
	0.257 ± 0.002 (B=-0.75T)	[44]		3.47			2.9	
	0.266 ± 0.001 (B=-0.75T)	[44]		15.43			9.51	
	0.247 ± 0.002 (B=-0.60T)	[44]		-1.48			-1.24	
	0.255 ± 0.002 (B=-0.60T)	[44]		2.48			2.08	
	0.241 ± 0.001 (B=-0.45T)	[44]		-8.65			-5.33	
	0.247 ± 0.002 (B=-0.45T)	[44]		-1.48			-1.24	
	0.238 ± 0.002 (B=-0.30T)	[44]		-5.93			-4.96	
	0.243 ± 0.002 (B=-0.30T)	[44]		-3.46			-2.89	
	0.242 ± 0.002 (B=-0.15T)	[44]		-3.95			-3.3	
	0.247 ± 0.002 (B=-0.15T)	[44]		-1.48			-1.24	
	0.249 ± 0.001	[44]		-0.95			-0.58	
	0.270 ± 0.009 (B=+0.15T)	[44]		2.22			2.2	
	0.270 ± 0.009 (B=-0.15T)	[44]		2.22			2.2	
	0.273 ± 0.008 (B=+0.45T)	[44]		2.88			2.84	
	0.273 ± 0.008 (B=-0.45T)	[44]		2.88			2.84	
	0.276 ± 0.007 (B=+0.75T)	[44]		3.71			3.65	
	0.276 ± 0.006 (B=-0.75T)	[44]		4.33			4.23	

(continued on next page)

Table 3 (continued)

Z, Symbol	$\left(\frac{I_{L\gamma}}{I_{L\alpha}}\right)_{EXP} \pm \Delta(I_{L\gamma}/I_{L\alpha})_{EXP}$	References	$(I_{L\gamma}/I_{L\alpha})_W \pm \epsilon_{ISD}$	$z_{ISD}$	$\bar{z}_{ISD}$	$\epsilon_{ESD}$	$Z_{ESD}$	$\bar{z}_{ESD}$
Z = 92, U	0.232 ± 0.023	[27]	0.2376 ± 0.0002	-0.78	0.57	0.0013	-0.78	0.59
	0.221 ± 0.014	[47]		-2.07			-2.06	
	0.218 ± 0.014	[47]		-2.28			-2.27	
	0.262 ± 0.012	[1]		1			0.99	
	0.271 ± 0.017	[89]		1.96			1.96	
	0.207 ± 0.010	[14]		-3.06			-3.04	
	0.234 ± 0.012	[14]		-0.3			-0.3	
	0.235 ± 0.012	[14]		-0.22			-0.22	
	0.229 ± 0.011	[14]		-0.78			-0.78	
	0.274 ± 0.022	[33]		1.65			1.65	
	0.237 ± 0.006	[34]		-0.1			-0.1	
	0.246 ± 0.006	[34]		1.4			1.37	
	0.275 ± 0.001	[34]		36.64			23.25	
	0.282 ± 0.007	[34]		6.34			6.24	
	0.280 ± 0.007	[34]		6.05			5.96	
	0.311 ± 0.008	[34]		9.17			9.06	
	0.315 ± 0.008	[34]		9.67			9.56	
	0.246 ± 0.063	[35]		0.13			0.13	
	0.213 ± 0.039	[35]		-0.63			-0.63	
	0.233 ± 0.016	[38]		-0.29			-0.29	
	0.241 ± 0.006	[66]		0.56			0.55	
	0.241 ± 0.013	[40]		0.26			0.26	
	0.202 ± 0.017	[68]		-2.1			-2.09	
	0.228 ± 0.030	[43]		-0.32			-0.32	
	0.236 ± 0.001	[44]		-1.59			-1.01	
	0.240 ± 0.001	[44]		2.33			1.48	
	0.239 ± 0.001 (B=+0.75T)	[44]		1.35			0.86	
	0.241 ± 0.001 (B=+0.75T)	[44]		3.31			2.1	
	0.235 ± 0.001 (B=+0.60T)	[44]		-2.57			-1.63	
	0.237 ± 0.001 (B=+0.60T)	[44]		-0.61			-0.38	
	0.233 ± 0.001 (B=+0.45T)	[44]		-4.53			-2.87	
	0.235 ± 0.001 (B=+0.45T)	[44]		-2.57			-1.63	
	0.231 ± 0.001 (B=+0.30T)	[44]		-6.49			-4.12	
	0.234 ± 0.001 (B=+0.30T)	[44]		-3.55			-2.25	
	0.233 ± 0.001 (B=+0.15T)	[44]		-4.53			-2.87	
	0.236 ± 0.001 (B=+0.15T)	[44]		-1.59			-1.01	
	0.239 ± 0.001 (B=-0.75T)	[44]		1.35			0.86	
	0.241 ± 0.001 (B=-0.75T)	[44]		3.31			2.1	
	0.236 ± 0.001 (B=-0.60T)	[44]		-1.59			-1.01	
	0.238 ± 0.001 (B=-0.60T)	[44]		0.37			0.24	
0.233 ± 0.001 (B=-0.45T)	[44]	-4.53	-2.87					
0.235 ± 0.001 (B=-0.45T)	[44]	-2.57	-1.63					
0.232 ± 0.001 (B=-0.30T)	[44]	-5.51	-3.49					
0.234 ± 0.001 (B=-0.30T)	[44]	-3.55	-2.25					
0.233 ± 0.001 (B=-0.15T)	[44]	-4.53	-2.87					
0.236 ± 0.001 (B=-0.15T)	[44]	-1.59	-1.01					
0.236 ± 0.001	[45]	-1.59	-1.01					
0.239 ± 0.007 (B=+0.15T)	[45]	0.2	0.19					
0.239 ± 0.007 (B=-0.15T)	[45]	0.2	0.19					
0.241 ± 0.006 (B=+0.45T)	[45]	0.56	0.55					
0.241 ± 0.006 (B=-0.45T)	[45]	0.56	0.55					
0.244 ± 0.005 (B=+0.75T)	[45]	1.28	1.24					
0.244 ± 0.005 (B=-0.75T)	[45]	1.28	1.24					
0.230 ± 0.023	[27]	-0.33	-0.33					
0.242 ± 0.009	[1]	0.49	0.48					

allocated to them, respectively. The scatter of results for these elements is therefore, in a sense, indicative of the quality of such ratio measurements. Future measurements could well include one of more of these elements as an internal reference standard to help gauge quality.

- The elements within the lanthanide series, falling within the atomic number range  $57 \leq Z \leq 71$ , tend to have comprehensive data coverage, typically featuring between seventeen and forty-three experimental values per element. However, it is important to note that  ${}_{61}\text{Pm}$  is an exception, with only a single reported value. This is a prime candidate for redetermination.

We have compiled an extensive database comprising 696 values for the experimental intensity ratios  $I_{L\gamma}/I_{L\alpha}$ , and these data have been

graphically shown in Fig. 2, with atomic number  $Z$  as the independent variable. To gain a comprehensive understanding of the insights conveyed by this figure, it is necessary to offer some commentary, including the following points:

- With the exception of specific cases where data are unavailable ( ${}_{43}\text{Tc}$ ,  ${}_{44}\text{Ru}$ ,  ${}_{45}\text{Rh}$ ,  ${}_{46}\text{Pd}$ ,  ${}_{48}\text{Cd}$ ,  ${}_{51}\text{Sb}$ ,  ${}_{52}\text{Te}$ ,  ${}_{84}\text{Po}$ ,  ${}_{85}\text{At}$ ,  ${}_{86}\text{Rn}$ ,  ${}_{87}\text{Fr}$ ,  ${}_{88}\text{Ra}$ ,  ${}_{89}\text{Ac}$ , and  ${}_{91}\text{Pa}$ ), our coverage extends to all targets within the range of  ${}_{39}\text{Y}$  to  ${}_{92}\text{U}$ .
- In certain instances, there exists just a solitary value, as seen in  ${}_{39}\text{Y}$ ,  ${}_{40}\text{Zr}$ ,  ${}_{54}\text{Xe}$ ,  ${}_{55}\text{Cs}$ , and  ${}_{61}\text{Pm}$ , while for others, there are merely two values available, notably for  ${}_{41}\text{Nb}$ ,  ${}_{42}\text{Mo}$ , and  ${}_{77}\text{Ir}$ . Again this suggests a need for new and improved experimental campaigns.

Table 4

Summary of the experimental  $I_{L1}/I_{L\alpha}$  intensity ratios from  $^{39}\text{Y}$  to  $^{94}\text{Pu}$  is presented according to their target atomic numbers. The weighted average values  $(I_{L1}/I_{L\alpha})_W$ , the references from which the databases are extracted,  $\epsilon_{ISD}$ ,  $\epsilon_{ESD}$ , the internal and external standard deviation ( $z_{ISD}$ ,  $z_{ESD}$ ), and their means ( $\bar{z}_{ISD}$ ,  $\bar{z}_{ESD}$ ) are also listed.

Z, Symbol	$\left(\frac{I_{L1}}{I_{L\alpha}}\right)_{EXP} \pm \Delta(I_{L1}/I_{L\alpha})_{EXP}$	References	$(I_{L1}/I_{L\alpha})_W \pm \epsilon_{ISD}$	$z_{ISD}$	$\bar{z}_{ISD}$	$\epsilon_{ESD}$	$z_{ESD}$	$\bar{z}_{ESD}$
Z = 39, Y	0.041 ± 0.004	[8]	0.041 ± 0.004	0	0	–	–	–
Z = 40, Zr	0.051 ± 0.005	[8]	0.051 ± 0.005	0	0	–	–	–
Z = 41, Nb	0.049 ± 0.005	[8]	0.0515 ± 0.0035	–0.41	0	0.0025	–0.45	0
	0.054 ± 0.005	[8]		0.41			0.45	
Z = 42, Mo	0.058 ± 0.005	[8]	0.0513 ± 0.0031	1.14	0.15	0.0054	0.91	0.14
	0.047 ± 0.004	[8]		–0.85			–0.64	
Z = 44, Ru	0.021 ± 0.004	[57]	0.021 ± 0.004	0	0	–	–	–
Z = 45, Rh	0.023 ± 0.0045	[57]	0.023 ± 0.0045	0	0	–	–	–
Z = 46, Pd	0.020 ± 0.0044	[57]	0.020 ± 0.0044	0	0	–	–	–
Z = 47, Ag	0.041 ± 0.0057	[57]	0.0517 ± 0.0020	–1.77	0.002	0.0037	–1.57	–0.12
	0.052 ± 0.005	[8]		0.06			0.06	
	0.043 ± 0.004	[8]		–1.94			–1.58	
	0.060 ± 0.004	[8]		1.87			1.53	
	0.057 ± 0.004	[8]		1.20			0.98	
Z = 48, Cd	0.031 ± 0.0047	[57]	0.031 ± 0.0047	0	0	–	–	–
Z = 49, In	0.039 ± 0.006	[57]	0.0568 ± 0.0018	–2.84	–0.22	0.0040	–2.46	–0.22
	0.050 ± 0.004	[8]		–1.55			–1.2	
	0.059 ± 0.005	[8]		0.41			0.34	
	0.068 ± 0.004	[8]		2.55			1.97	
	0.058 ± 0.003	[8]		0.34			0.24	
Z = 50, Sn	0.0305 ± 0.005	[57]	0.0587 ± 0.0019	–5.27	1.19	0.0127	–2.07	0.95
	0.051 ± 0.004	[8]		–1.73			–0.58	
	0.051 ± 0.004	[8]		–1.73			–0.58	
	0.068 ± 0.005	[8]		1.74			0.69	
	0.063 ± 0.004	[8]		0.98			0.33	
	0.1834 ± 0.0093	[10]		13.14			7.94	
Z = 51, Sb	0.039 ± 0.006	[57]	0.0809 ± 0.0051	–5.33	2.21	0.0663	–0.63	0.47
	0.1858 ± 0.0095	[10]		9.74			1.57	
Z = 52, Te	0.043 ± 0.0065	[57]	0.0880 ± 0.0055	–5.29	2.20	0.0713	–0.63	0.47
	0.2010 ± 0.0103	[10]		9.68			1.57	
Z = 53, I	0.039 ± 0.006	[57]	0.0570 ± 0.0018	–2.87	1.46	0.0119	–1.35	1.27
	0.056 ± 0.005	[8]		–0.18			–0.07	
	0.050 ± 0.004	[8]		–1.59			–0.55	
	0.054 ± 0.003	[8]		–0.85			–0.24	
	0.057 ± 0.004	[8]		0.008			0.003	
	0.2172 ± 0.0111	[10]		14.25			9.84	
Z = 54, Xe	0.039 ± 0.006	[24]	0.039 ± 0.006	0	0	–	–	–
Z = 55, Cs	0.038 ± 0.006	[57]	0.0371 ± 0.0019	0.14	0.05	0.0003	0.15	0.05
	0.037 ± 0.002	[30]		–0.04			–0.05	
Z = 56, Ba	0.040 ± 0.0055	[57]	0.0419 ± 0.0010	–0.35	0.84	0.0037	–0.29	0.83
	0.053 ± 0.005	[8]		2.17			1.77	
	0.071 ± 0.006	[8]		4.78			4.11	
	0.058 ± 0.003	[8]		5.10			3.34	
	0.065 ± 0.004	[8]		5.60			4.2	
	0.029 ± 0.003	[22]		–4.11			–2.7	
	0.037 ± 0.002	[30]		–2.23			–1.16	
	0.0364 ± 0.0022	[70]		–2.31			–1.28	
	0.0396 ± 0.0020	[10]		–1.06			–0.55	
Z = 57, La	0.0365 ± 0.0052	[57]	0.0438 ± 0.0011	–1.37	0.69	0.0041	–1.11	0.61
	0.056 ± 0.005	[8]		2.38			1.89	
	0.044 ± 0.004	[8]		0.05			0.03	
	0.062 ± 0.003	[8]		5.69			3.6	
	0.059 ± 0.004	[8]		3.66			2.66	
	0.0359 ± 0.002	[65]		–3.46			–1.74	
	0.0389 ± 0.0020	[10]		–2.14			–1.08	
Z = 58, Ce	0.039 ± 0.0055	[57]	0.0430 ± 0.0010	–0.72	1	0.0037	–0.61	0.96
	0.043 ± 0.004	[8]		–0.003			–0.002	
	0.062 ± 0.005	[8]		3.73			3.07	
	0.067 ± 0.004	[8]		5.82			4.43	
	0.065 ± 0.004	[8]		5.34			4.06	
	0.039 ± 0.002	[30]		–1.80			–0.96	
	0.0378 ± 0.002	[65]		–2.34			–1.25	
	0.0387 ± 0.0019	[10]		–2.02			–1.05	
Z = 59, Pr	0.039 ± 0.0055	[57]	0.0400 ± 0.0011	–0.18	0.24	0.0011	–0.18	0.24
	0.039 ± 0.002	[30]		–0.44			–0.44	
	0.0392 ± 0.002	[65]		–0.35			–0.35	
	0.0512 ± 0.006	[76]		1.83			1.83	
	0.0408 ± 0.0021	[10]		0.33			0.33	
Z = 60, Nd	0.035 ± 0.005	[57]	0.0392 ± 0.0014	–0.81	–0.12	0.0008	–0.83	–0.12
	0.039 ± 0.002	[30]		–0.09			–0.1	
	0.0401 ± 0.002	[65]		0.37			0.41	
	0.0400 ± 0.020	[10]		0.04			0.04	

(continued on next page)

Table 4 (continued)

Z, Symbol	$\left(\frac{I_{L1}}{I_{L\alpha}}\right)_{EXP} \pm \Delta(I_{L1}/I_{L\alpha})_{EXP}$	References	$(I_{L1}/I_{L\alpha})_W \pm \epsilon_{ISD}$	$z_{ISD}$	$\bar{z}_{ISD}$	$\epsilon_{ESD}$	$z_{ESD}$	$\bar{z}_{ESD}$
Z = 61, Pm	0.040 ± 0.002	[30]	0.040 ± 0.002	0	0	–	–	–
Z = 62, Sm	0.035 ± 0.005	[57]	0.0411 ± 0.0006	–1.2	0.58	0.0017	–1.14	0.60
	0.055 ± 0.005	[8]		2.77			2.64	
	0.057 ± 0.005	[8]		3.16			3.01	
	0.064 ± 0.004	[8]		5.67			5.26	
	0.067 ± 0.005	[8]		5.15			4.9	
	0.040 ± 0.002	[30]		–0.5			–0.4	
	0.029 ± 0.003	[32]		–3.93			–3.48	
	0.0388 ± 0.001	[65]		–1.9			–1.12	
	0.046 ± 0.005	[36]		0.98			0.93	
	0.040 ± 0.003	[42]		–0.34			–0.3	
	0.042 ± 0.002	[87]		0.45			0.36	
	0.042 ± 0.002	[87]		0.45			0.36	
	0.0418 ± 0.0021	[10]		0.34			0.27	
	0.031 ± 0.008	[81]		–1.25			–1.23	
	0.032 ± 0.008	[81]		–1.13			–1.11	
	0.040 ± 0.003	[30]		–0.22			–0.22	
	Z = 63, Eu	0.039 ± 0.002		[26]			0.0407 ± 0.0007	
0.045 ± 0.002		[26]	2.03	2.04				
0.0392 ± 0.002		[65]	–0.69	–0.69				
0.042 ± 0.003		[36]	0.43	0.43				
0.040 ± 0.003		[42]	–0.22	–0.22				
0.039 ± 0.002		[87]	–0.78	–0.78				
0.040 ± 0.002		[87]	–0.31	–0.31				
0.0419 ± 0.0021		[10]	0.55	0.56				
0.042 ± 0.004		[8]	–0.48	–0.44				
0.049 ± 0.004		[8]	1.24	1.14				
Z = 64, Gd	0.058 ± 0.003	[8]	0.0440 ± 0.0007	4.56	0.98	0.0019	3.95	1
	0.065 ± 0.004	[8]		5.18			4.75	
	0.053 ± 0.006	[8]		1.5			1.44	
	0.055 ± 0.005	[8]		2.19			2.06	
	0.069 ± 0.007	[8]		3.56			3.45	
	0.067 ± 0.008	[8]		2.87			2.8	
	0.041 ± 0.003	[30]		–0.96			–0.83	
	0.0400 ± 0.002	[65]		–1.87			–1.43	
	0.0429 ± 0.0022	[10]		–0.46			–0.36	
	0.041 ± 0.001	[53]		–2.42			–1.37	
	0.038 ± 0.009	[81]		–0.66			–0.65	
	0.039 ± 0.009	[81]		–0.55			–0.54	
	0.038 ± 0.003	[28]		–0.70			–0.7	
	0.041 ± 0.003	[30]		0.27			0.27	
	0.0420 ± 0.002	[65]		0.86			0.86	
	0.041 ± 0.003	[38]		0.27			0.27	
	0.0445 ± 0.0023	[10]		1.79			1.8	
Z = 65, Tb	0.039 ± 0.001	[53]	0.0402 ± 0.0007	–0.94	0.13	0.0007	–0.42	0.13
	0.036 ± 0.01	[81]		–0.42			–0.1	
	0.039 ± 0.012	[81]		–0.1			–0.95	
	0.058 ± 0.005	[21]		3			3	
	0.042 ± 0.003	[30]		–0.33			–0.33	
	0.0422 ± 0.002	[65]		–0.40			–0.4	
	0.043 ± 0.003	[38]		–0.001			–0.001	
	0.044 ± 0.007	[41]		0.14			0.14	
	0.043 ± 0.0002	[46]		–0.02			–0.02	
	0.043 ± 0.0001	[46]		–0.03			–0.03	
	0.040 ± 0.003	[47]		–1			–1	
	0.040 ± 0.003	[47]		–1			–1	
	0.042 ± 0.003	[49]		–0.33			–0.33	
	0.0416 ± 0.0037	[75]		–0.38			–0.38	
	0.0453 ± 0.0045	[75]		0.51			0.51	
	0.042 ± 0.003	[51]		–0.33			–0.33	
	0.043 ± 0.003 (B = 0.6T)	[51]		–0.001			–0.001	
0.044 ± 0.003 (B = 1.2T)	[51]	0.33	0.33					
0.0468 ± 0.0024	[10]	1.58	1.58					
Z = 66, Dy	0.050 ± 0.004	[54]	0.0430 ± 0.0001	1.75	0.21	0.0001	1.75	0.21
	0.050 ± 0.003	[54]		2.33			2.33	
	0.047 ± 0.003	[54]		1.33			1.33	
	0.0416 ± 0.002	[92]		–0.70			–0.7	
	0.0409 ± 0.002	[92]		–1.05			–1.05	
	0.0413 ± 0.002	[92]		–0.85			–0.85	
	0.040 ± 0.002	[29]		–1.04			–1.04	
	0.042 ± 0.003	[30]		–0.03			–0.03	
	0.045 ± 0.004	[62]		0.73			0.73	
	0.045 ± 0.004	[62]		0.73			0.73	
	0.0439 ± 0.003	[65]		0.60			0.6	
Z = 67, Ho	0.040 ± 0.002	[29]	0.0421 ± 0.0001	–1.04	0.08	0.0001	–1.04	0.08
	0.042 ± 0.003	[30]		–0.03			–0.03	
	0.045 ± 0.004	[62]		0.73			0.73	
	0.045 ± 0.004	[62]		0.73			0.73	
	0.0439 ± 0.003	[65]		0.60			0.6	

(continued on next page)

Table 4 (continued)

Z, Symbol	$\left(\frac{I_{L1}}{I_{L\alpha}}\right)_{EXP} \pm \Delta(I_{L1}/I_{L\alpha})_{EXP}$	References	$(I_{L1}/I_{L\alpha})_W \pm \epsilon_{ISD}$	$z_{ISD}$	$\bar{z}_{ISD}$	$\epsilon_{ESD}$	$z_{ESD}$	$\bar{z}_{ESD}$
Z = 68, Er	0.043 ± 0.003	[38]	0.0428 ± 0.0007	0.30	0.06	0.0065	0.3	0.04
	0.045 ± 0.006	[41]		0.49			0.49	
	0.042 ± 0.004	[42]		-0.02			-0.02	
	0.043 ± 0.0003	[46]		2.91			2.78	
	0.042 ± 0.0001	[46]		-0.63			-0.52	
	0.043 ± 0.002	[49]		0.46			0.46	
	0.043 ± 0.002	[51]		0.46			0.46	
	0.044 ± 0.002	[51]		0.96			0.95	
	0.045 ± 0.003	[51]		0.97			0.97	
	0.0469 ± 0.0024	[10]		2			2	
	0.041 ± 0.001	[53]		-1.08			-1.36	
	0.038 ± 0.003	[54]		-1.36			-1.36	
	0.038 ± 0.003 (B = 0.6T)	[54]		-1.36			-3.54	
	0.035 ± 0.002 (B = 1.2T)	[54]		-3.54			-1.08	
	0.041 ± 0.003	[30]		-0.58			-0.25	
	0.037 ± 0.002	[24]		-2.74			-0.85	
	0.0440 ± 0.003	[65]		0.4			0.17	
	0.045 ± 0.003	[38]		0.72			0.31	
	0.047 ± 0.007	[41]		0.6			0.44	
	0.043 ± 0.003	[42]		0.07			0.03	
0.041 ± 0.003	[47]	-0.58	-0.25					
0.041 ± 0.003	[47]	-0.58	-0.25					
0.043 ± 0.002	[49]	0.11	0.03					
0.043 ± 0.002	[51]	0.11	0.03					
0.046 ± 0.003 (B = 0.6T)	[51]	1.05	0.45					
0.046 ± 0.003 (B = 1.2T)	[51]	1.05	0.45					
0.0479 ± 0.0024	[10]	2.05	0.74					
0.050 ± 0.003	[54]	2.35	1.01					
0.041 ± 0.003	[54]	-0.58	-0.25					
0.036 ± 0.003	[54]	-2.20	-0.95					
0.041 ± 0.008	[81]	-0.22	-0.17					
Z = 69, Tm	0.055 ± 0.002	[21]	0.0506 ± 0.0008	1.99	0.49	0.0030	1.25	0.4
	0.045 ± 0.002	[14]		-2.62			-1.64	
	0.061 ± 0.003	[14]		3.31			2.5	
	0.057 ± 0.003	[14]		2.03			1.53	
	0.046 ± 0.002	[14]		-2.16			-1.35	
	0.046 ± 0.002	[14]		-2.16			-1.35	
	0.0441 ± 0.003	[65]		-2.11			-1.6	
	0.0722 ± 0.0037	[10]		5.67			4.62	
	0.043 ± 0.003	[28]		-0.63			-0.63	
	0.042 ± 0.001	[20]		-2.84			-2.89	
Z = 70, Yb	0.045 ± 0.004	[62]	0.0449 ± 0.0002	0.03	-0.31	0.0002	0.03	-0.30
	0.045 ± 0.004	[62]		0.03			0.03	
	0.0446 ± 0.003	[65]		-0.1			-0.1	
	0.045 ± 0.003	[38]		0.04			0.04	
	0.045 ± 0.0005	[46]		0.21			0.22	
	0.045 ± 0.0002	[46]		0.41			0.56	
	0.044 ± 0.003	[47]		-0.3			-0.3	
	0.045 ± 0.003	[47]		0.04			0.04	
	0.042 ± 0.009	[1]		-0.32			-0.32	
	0.042 ± 0.003	[30]		-0.82			-0.62	
	0.035 ± 0.002	[14]		-4.47			-2.83	
	0.034 ± 0.002	[14]		-4.94			-3.12	
	0.064 ± 0.003	[14]		6.31			4.82	
	0.048 ± 0.002	[14]		1.63			1.03	
	0.054 ± 0.003	[14]		3.07			2.34	
Z = 71, Lu	0.0451 ± 0.003	[65]	0.0445 ± 0.0007	0.19	0.46	0.0027	0.14	0.47
	0.047 ± 0.005	[36]		0.49			0.44	
	0.043 ± 0.003	[47]		-0.49			-0.38	
	0.044 ± 0.003	[47]		-0.17			-0.13	
	0.0766 ± 0.0039	[10]		8.08			6.75	
	0.040 ± 0.003	[54]		-1.46			-1.12	
	0.044 ± 0.003	[54]		-0.17			-0.13	
	0.042 ± 0.003	[54]		-0.82			-0.62	
	0.055 ± 0.002	[23]		2.42			1.5	
	0.041 ± 0.002	[15]		-3.97			-2.46	
	0.051 ± 0.005	[36]		0.26			0.23	
	0.045 ± 0.003	[38]		-1.5			-1.12	
	0.045 ± 0.002	[40]		-2.14			-1.33	
	0.047 ± 0.006	[41]		-0.44			-0.4	
	0.045 ± 0.004	[42]		-1.14			-0.95	
Z = 72, Hf	0.046 ± 0.006	[43]	0.0497 ± 0.0009	-0.61	0.26	0.0029	-0.55	0.26
	0.0571 ± 0.0025	[71]		2.79			1.93	
	0.0781 ± 0.0040	[10]		6.93			5.74	

(continued on next page)

Table 4 (continued)

Z, Symbol	$\left(\frac{I_{LL}}{I_{La}}\right)_{EXP} \pm \Delta(I_{LL}/I_{La})_{EXP}$	References	$(I_{LL}/I_{La})_W \pm \epsilon_{ISD}$	$z_{ISD}$	$\bar{z}_{ISD}$	$\epsilon_{ESD}$	$z_{ESD}$	$\bar{z}_{ESD}$
Z = 73, Ta	0.044 ± 0.002	[28]	0.0474 ± 0.0006	-1.64	0.08	0.0010	-1.51	0.08
	0.0475 ± 0.009	[58]		0.009			0.01	
	0.0464 ± 0.018	[58]		-0.06			-0.06	
	0.0524 ± 0.009	[58]		0.55			0.55	
	0.0438 ± 0.012	[58]		-0.3			-0.3	
	0.042 ± 0.003	[29]		-1.77			-1.7	
	0.045 ± 0.003	[30]		-0.79			-0.76	
	0.0465 ± 0.004	[65]		-0.23			-0.22	
	0.045 ± 0.005	[35]		-0.48			-0.47	
	0.044 ± 0.002	[40]		-1.64			-1.51	
	0.046 ± 0.004	[42]		-0.35			-0.34	
	0.045 ± 0.006	[43]		-0.4			-0.4	
	0.046 ± 0.003	[45]		-0.46			-0.45	
	0.051 ± 0.003 (B=+0.15T)	[45]		1.17			1.13	
	0.051 ± 0.003 (B=-0.15T)	[45]		1.17			1.13	
	0.051 ± 0.003 (B=+0.45T)	[45]		1.17			1.13	
	0.051 ± 0.003 (B=-0.45T)	[45]		1.17			1.13	
	0.051 ± 0.003 (B=+0.75T)	[45]		1.17			1.13	
	0.051 ± 0.003 (B=-0.75T)	[45]		1.17			1.13	
	0.0462 ± 0.002	[9]		-0.58			-0.54	
	0.0513 ± 0.003 (B=+0.75T)	[9]		1.27			1.22	
	0.0513 ± 0.003 (B=-0.75T)	[9]		1.27			1.22	
	0.046 ± 0.003	[47]		-0.46			-0.45	
	0.047 ± 0.003	[47]		-0.14			-0.13	
	0.0500 ± 0.0028	[74]		0.9			0.86	
	0.047 ± 0.008	[1]		-0.05			-0.05	
	0.0800 ± 0.0041	[10]		7.87			7.7	
	0.038 ± 0.003	[54]		-3.08			-2.96	
	0.047 ± 0.003	[54]		-0.14			-0.13	
	0.043 ± 0.003	[54]		-1.45			-1.39	
	0.039 ± 0.006	[81]		-1.4			-1.38	
	0.041 ± 0.006	[81]		-1.06			-1.05	
	Z = 74, W	0.047 ± 0.004		[59]			0.0470 ± 0.00001	
0.050 ± 0.004		[59]	0.75	0.75				
0.054 ± 0.004		[59]	1.75	1.75				
0.047 ± 0.003		[30]	0.0001	0.0001				
0.040 ± 0.003		[26]	-2.33	-2.33				
0.0471 ± 0.004		[65]	0.03	0.03				
0.050 ± 0.004		[35]	0.75	0.75				
0.047 ± 0.003		[38]	0.0001	0.0001				
0.047 ± 0.005		[41]	0.0001	0.0001				
0.038 ± 0.001		[40]	-9	-9				
0.053 ± 0.005		[68]	1.2	1.2				
0.046 ± 0.004		[42]	-0.25	-0.25				
0.054 ± 0.007		[43]	1	1				
0.048 ± 0.003		[45]	0.33	0.33				
0.052 ± 0.004		[45]	1.25	1.25				
0.052 ± 0.004		[45]	1.25	1.25				
0.052 ± 0.004		[45]	1.25	1.25				
0.052 ± 0.004		[45]	1.25	1.25				
0.053 ± 0.004		[45]	1.5	1.5				
0.053 ± 0.004		[45]	1.5	1.5				
0.0478 ± 0.003		[9]	0.27	0.27				
0.0526 ± 0.005 (B=+0.75T)		[9]	1.12	1.12				
0.0527 ± 0.005 (B=-0.75T)		[9]	1.14	1.14				
0.047 ± 0.00001		[46]	0.02	0.01				
0.047 ± 0.00004		[46]	0.01	0.01				
0.0524 ± 0.0027		[73]	2	2				
0.047 ± 0.003		[47]	0.01	0.0001				
0.048 ± 0.003		[47]	0.33	0.33				
0.0486 ± 0.0027		[74]	0.59	0.59				
0.049 ± 0.007		[1]	0.29	0.29				
0.0831 ± 0.0042		[10]	8.6	8.6				
0.043 ± 0.003		[54]	-1.33	-1.33				
0.052 ± 0.004		[54]	1.25	1.25				
0.048 ± 0.003	[54]	0.33	0.33					
0.051 ± 0.004	[92]	1	1					
0.043 ± 0.006	[81]	-0.67	-0.67					
0.047 ± 0.007	[81]	0	0					
Z = 75, Re	0.043 ± 0.002	[15]	0.0476 ± 0.0009	-2.1	0.65	0.0031	-1.25	0.66
	0.0469 ± 0.004	[65]		-0.18			-0.14	
	0.059 ± 0.004	[35]		2.77			2.25	
	0.043 ± 0.002	[40]		-2.1			-1.25	
	0.047 ± 0.004	[42]		-0.15			-0.12	

(continued on next page)

Table 4 (continued)

Z, Symbol	$\left(\frac{I_{L1}}{I_{L\alpha}}\right)_{EXP} \pm \Delta(I_{L1}/I_{L\alpha})_{EXP}$	References	$(I_{L1}/I_{L\alpha})_W \pm \epsilon_{ISD}$	$z_{ISD}$	$\bar{z}_{ISD}$	$\epsilon_{ESD}$	$z_{ESD}$	$\bar{z}_{ESD}$					
Z = 76, Os	0.0482 ± 0.0025	[73]	0.0281 ± 0.0008	0.22	4.96	0.0078	0.14	2.47					
	0.0885 ± 0.0045	[10]		8.9			7.48						
	0.046 ± 0.002	[79]		-0.74			-0.44						
	0.045 ± 0.007	[81]		-0.37			-0.34						
	0.050 ± 0.008	[81]		0.29			0.28						
	0.012 ± 0.001	[21]		-12.72			-2.04						
	0.050 ± 0.004	[36]		5.38			2.49						
	0.049 ± 0.003	[38]		6.75			2.49						
	0.0491 ± 0.0025	[73]		8.03			2.56						
	0.049 ± 0.003	[47]		6.75			2.49						
Z = 77, Ir	0.0881 ± 0.0045	[10]	0.0530 ± 0.0019	13.14	0.33	0.0089	6.64	0.23					
	0.051 ± 0.004	[92]		5.62			2.6						
	0.042 ± 0.004	[28]		-2.5			-1.13						
	0.048 ± 0.003	[15]		-1.42			-0.53						
	0.046 ± 0.004	[32]		-1.59			-0.72						
	0.0856 ± 0.0044	[10]		6.82			3.28						
Z = 78, Pt	0.048 ± 0.002	[28]	0.0494 ± 0.0007	-0.64	0.38	0.0017	-0.51	0.40					
	0.050 ± 0.003	[30]		0.21			0.19						
	0.049 ± 0.003	[15]		-0.11			-0.1						
	0.0491 ± 0.0015	[63]		-0.15			-0.11						
	0.052 ± 0.004	[36]		0.65			0.61						
	0.042 ± 0.002	[40]		-3.48			-2.77						
	0.048 ± 0.003	[42]		-0.44			-0.39						
	0.060 ± 0.006	[27]		1.76			1.7						
	0.0514 ± 0.0026	[73]		0.76			0.66						
	0.049 ± 0.003	[47]		-0.11			-0.1						
	0.049 ± 0.003	[47]		-0.11			-0.1						
	0.0435 ± 0.0052	[76]		-1.12			-1.07						
	0.0867 ± 0.0044	[10]		8.39			7.89						
	0.056 ± 0.004	[54]		1.64			1.52						
	0.046 ± 0.003	[54]		-1.09			-0.97						
	0.049 ± 0.003	[54]		-0.11			-0.1						
	Z = 79, Au	0.0672 ± 0.0042		[7]			0.0463 ± 0.0005		4.93	0.56	0.0012	4.78	0.58
		0.0638 ± 0.005		[7]					3.47			3.4	
		0.0757 ± 0.009		[7]					3.26			3.23	
		0.0465 ± 0.009		[58]					0.02			0.02	
0.0462 ± 0.012		[58]	-0.01	-0.01									
0.069 ± 0.035		[58]	0.65	0.65									
0.0668 ± 0.122		[58]	0.17	0.17									
0.048 ± 0.004		[29]	0.41	0.4									
0.050 ± 0.003		[30]	1.2	1.13									
0.053 ± 0.004		[32]	1.65	1.6									
0.052 ± 0.005		[88]	1.13	1.1									
0.052 ± 0.005		[88]	1.13	1.1									
0.052 ± 0.005		[88]	1.13	1.1									
0.052 ± 0.005		[88]	1.13	1.1									
0.053 ± 0.005		[88]	1.33	1.3									
0.048 ± 0.004		[62]	0.41	0.4									
0.049 ± 0.004		[62]	0.66	0.64									
0.052 ± 0.005		[64]	1.13	1.1									
0.052 ± 0.005		[64]	1.13	1.1									
0.053 ± 0.005		[64]	1.33	1.3									
0.0514 ± 0.005		[65]	1.01	0.98									
0.054 ± 0.004		[35]	1.9	1.84									
0.045 ± 0.002		[40]	-0.65	-0.58									
0.046 ± 0.004		[68]	-0.08	-0.08									
0.051 ± 0.004		[42]	1.16	1.12									
0.048 ± 0.006		[43]	0.28	0.27									
0.051 ± 0.007		[45]	0.66	0.66									
0.038 ± 0.004		[45]	-2.07	-2									
0.038 ± 0.004		[45]	-2.07	-2									
0.038 ± 0.004		[45]	-2.07	-2									
0.038 ± 0.004	[45]	-2.07	-2										
0.038 ± 0.003	[45]	-2.74	-2.59										
0.038 ± 0.003	[45]	-2.74	-2.59										
0.0511 ± 0.005	[9]	0.95	0.93										
0.0379 ± 0.004	[9]	-2.09	-2.02										
0.0379 ± 0.004	[9]	-2.09	-2.02										
0.052 ± 0.005	[27]	1.13	1.1										
0.0532 ± 0.004	[18]	1.7	1.64										
0.051 ± 0.003	[47]	1.53	1.44										
0.051 ± 0.003	[47]	1.53	1.44										
0.0905 ± 0.0046	[10]	9.54	9.3										

(continued on next page)

Table 4 (continued)

Z, Symbol	$\left(\frac{I_{L1}}{I_{L\alpha}}\right)_{EXP} \pm \Delta(I_{L1}/I_{L\alpha})_{EXP}$	References	$(I_{L1}/I_{L\alpha})_W \pm \epsilon_{ISD}$	$z_{ISD}$	$\bar{z}_{ISD}$	$\epsilon_{ESD}$	$z_{ESD}$	$\bar{z}_{ESD}$	
Z = 80, Hg	0.045 ± 0.003	[54]		-0.44			-0.42		
	0.048 ± 0.003	[54]		0.55			0.51		
	0.047 ± 0.003	[54]		0.22			0.2		
	0.040 ± 0.001	[80]		-5.68			-4.09		
	0.049 ± 0.002	[19]		1.29			1.14		
	0.0507 ± 0.003	[19]		1.43			1.35		
	0.052 ± 0.004	[59]	0.0520 ± 0.0001	0.002	-0.71	0.0002	0.002	-0.72	
	0.054 ± 0.004	[59]		0.5			0.5		
	0.052 ± 0.004	[59]		0.002			0.002		
	0.052 ± 0.003	[30]		0.003			0.003		
	0.046 ± 0.005	[24]		-1.2			-1.2		
	0.045 ± 0.003	[24]		-2.33			-2.32		
	0.058 ± 0.005	[32]		1.2			1.2		
	0.0502 ± 0.005	[65]		-0.36			-0.36		
	0.056 ± 0.003	[35]		1.34			1.33		
	0.055 ± 0.005	[37]		0.6			0.6		
	0.052 ± 0.004	[38]		0.002			0.002		
	0.055 ± 0.003	[40]		1			1		
	0.049 ± 0.005	[68]		-0.6			-0.6		
	0.052 ± 0.007	[43]		0.001			0.001		
	0.052 ± 0.005	[45]		0.002			0.002		
	0.043 ± 0.003 (B=+0.15T)	[45]		-3			-2.99		
	0.043 ± 0.003 (B=-0.15T)	[45]		-3			-2.99		
	0.043 ± 0.003 (B=+0.45T)	[45]		-3			-2.99		
	0.043 ± 0.003 (B=-0.45T)	[45]		-3			-2.99		
	0.043 ± 0.003 (B=+0.75T)	[45]		-3			-2.99		
	0.043 ± 0.003 (B=-0.75T)	[45]		-3			-2.99		
	0.0523 ± 0.004	[9]		0.08			0.08		
	0.0428 ± 0.002 (B=+0.75T)	[9]		-4.59			-4.57		
	0.0429 ± 0.002 (B=-0.75T)	[9]		-4.54			-4.52		
	0.055 ± 0.005	[27]		0.6			0.6		
	0.053 ± 0.0003	[46]		3.21			2.71		
	0.052 ± 0.0001	[46]		0.06			0.04		
	0.050 ± 0.003	[47]		-0.66			-0.66		
	0.050 ± 0.003	[47]		-0.66			-0.66		
	0.0480 ± 0.0034	[86]		-1.17			-1.17		
	0.0485 ± 0.0057	[76]		-0.61			-0.61		
	0.049 ± 0.005	[1]		-0.6			-0.6		
	0.0880 ± 0.0045	[10]		8			7.99		
	0.043 ± 0.003	[54]		-3			-2.99		
0.045 ± 0.003	[54]		-2.33			-2.32			
0.049 ± 0.003	[54]		-1			-0.99			
0.044 ± 0.005	[81]		-1.6			-1.6			
0.050 ± 0.006	[81]		-0.33			-0.33			
Z = 81, Tl	0.046 ± 0.002	[28]	0.0540 ± 0.0001	-4.01	0.43	0.0002	-3.99	0.43	
	0.049 ± 0.003	[22]		-1.68			-1.67		
	0.0515 ± 0.005	[65]		-0.51			-0.51		
	0.055 ± 0.004	[35]		0.24			0.24		
	0.058 ± 0.003	[36]		1.32			1.32		
	0.055 ± 0.004	[38]		0.24			0.24		
	0.049 ± 0.002	[40]		-2.52			-2.5		
	0.052 ± 0.006	[41]		-0.34			-0.34		
	0.048 ± 0.005	[68]		-1.21			-1.21		
	0.053 ± 0.005	[42]		-0.21			-0.21		
	0.051 ± 0.007	[43]		-0.43			-0.43		
	0.051 ± 0.004	[45]		-0.76			-0.76		
	0.060 ± 0.004 (B=+0.15T)	[45]		1.49			1.49		
	0.060 ± 0.004 (B=-0.15T)	[45]		1.49			1.49		
	0.060 ± 0.004 (B=+0.45T)	[45]		1.49			1.49		
	0.060 ± 0.004 (B=-0.45T)	[45]		1.49			1.49		
	0.060 ± 0.004 (B=+0.75T)	[45]		1.49			1.49		
	0.060 ± 0.004 (B=-0.75T)	[45]		1.49			1.49		
	0.0514 ± 0.004	[9]		-0.66			-0.66		
	0.0599 ± 0.003 (B=+0.75T)	[9]		1.95			1.95		
	0.0599 ± 0.003 (B=-0.75T)	[9]		1.95			1.95		
	0.054 ± 0.005	[27]		-0.01			-0.01		
	0.057 ± 0.001	[46]		2.95			2.9		
	0.054 ± 0.0001	[46]		-0.26			-0.15		
	0.052 ± 0.003	[47]		-0.68			-0.68		
	0.052 ± 0.003	[47]		-0.68			-0.68		
	0.054 ± 0.004	[1]		-0.01			-0.01		
	Z = 82, Pb	0.0942 ± 0.0048	[10]		8.37			8.36	
		0.049 ± 0.001	[28]	0.0529 ± 0.0002	-3.82	-0.20	0.0004	-3.69	-0.20
		0.055 ± 0.003	[89]		0.69			0.69	

(continued on next page)

Table 4 (continued)

Z, Symbol	$\left(\frac{I_{LL}}{I_{L\alpha}}\right)_{EXP} \pm \Delta(I_{LL}/I_{L\alpha})_{EXP}$	References	$(I_{LL}/I_{L\alpha})_W \pm \epsilon_{ISD}$	$z_{ISD}$	$\bar{z}_{ISD}$	$\epsilon_{ESD}$	$z_{ESD}$	$\bar{z}_{ESD}$
	0.0560 ± 0.019	[58]		0.16			0.16	
	0.0482 ± 0.013	[58]		-0.36			-0.36	
	0.0599 ± 0.013	[58]		0.54			0.54	
	0.0470 ± 0.010	[58]		-0.59			-0.59	
	0.051 ± 0.004	[85]		-0.48			-0.48	
	0.051 ± 0.003	[29]		-0.64			-0.63	
	0.049 ± 0.003	[15]		-1.3			-1.29	
	0.055 ± 0.005	[32]		0.42			0.42	
	0.053 ± 0.005	[88]		0.02			0.02	
	0.052 ± 0.005	[88]		-0.18			-0.18	
	0.053 ± 0.005	[88]		0.02			0.02	
	0.055 ± 0.005	[88]		0.42			0.42	
	0.054 ± 0.005	[88]		0.22			0.22	
	0.047 ± 0.004	[62]		-1.48			-1.47	
	0.047 ± 0.004	[62]		-1.48			-1.47	
	0.0517 ± 0.0015	[63]		-0.8			-0.79	
	0.053 ± 0.005	[64]		0.02			0.02	
	0.053 ± 0.005	[64]		0.02			0.02	
	0.053 ± 0.005	[64]		0.02			0.02	
	0.0549 ± 0.005	[65]		0.4			0.4	
	0.056 ± 0.005	[35]		0.62			0.62	
	0.056 ± 0.004	[36]		0.77			0.77	
	0.053 ± 0.003	[38]		0.03			0.03	
	0.050 ± 0.005	[39]		-0.58			-0.58	
	0.045 ± 0.003	[40]		-2.63			-2.62	
	0.049 ± 0.004	[68]		-0.98			-0.97	
	0.055 ± 0.005	[42]		0.42			0.42	
	0.053 ± 0.007	[43]		0.01			0.01	
	0.053 ± 0.007	[45]		0.01			0.01	
	0.047 ± 0.005 (B=+0.15T)	[45]		-1.18			-1.18	
	0.047 ± 0.005 (B=-0.15T)	[45]		-1.18			-1.18	
	0.047 ± 0.005 (B=+0.45T)	[45]		-1.18			-1.18	
	0.047 ± 0.005 (B=-0.45T)	[45]		-1.18			-1.18	
	0.047 ± 0.005 (B=+0.75T)	[45]		-1.18			-1.18	
	0.047 ± 0.005 (B=-0.75T)	[45]		-1.18			-1.18	
	0.0531 ± 0.003	[9]		0.06			0.06	
	0.0465 ± 0.003 (B=+0.75T)	[9]		-2.13			-2.12	
	0.0466 ± 0.003 (B=-0.75T)	[9]		-2.1			-2.09	
	0.057 ± 0.006	[27]		0.68			0.68	
	0.054 ± 0.0004	[46]		2.4			2.04	
	0.053 ± 0.0003	[46]		0.24			0.19	
	0.054 ± 0.004	[47]		0.27			0.27	
	0.054 ± 0.004	[47]		0.27			0.27	
	0.050 ± 0.004	[1]		-0.73			-0.72	
	0.0936 ± 0.0048	[10]		8.47			8.45	
	0.0509 ± 0.0029	[77]		-0.69			-0.69	
	0.060 ± 0.004	[54]		1.77			1.77	
	0.054 ± 0.004	[54]		0.27			0.27	
	0.047 ± 0.003	[54]		-1.97			-1.96	
	0.051 ± 0.003	[55]		-0.64			-0.63	
	0.049 ± 0.006	[81]		-0.65			-0.65	
	0.065 ± 0.008	[81]		1.51			1.51	
Z = 83, Bi	0.050 ± 0.001	[28]	0.0525 ± 0.0006	-2.18	0.17	0.0010	-1.74	0.18
	0.0504 ± 0.018	[58]		-0.12			-0.12	
	0.0588 ± 0.010	[58]		0.63			0.63	
	0.0591 ± 0.014	[58]		0.47			0.47	
	0.0653 ± 0.050	[58]		0.26			0.26	
	0.062 ± 0.005	[85]		1.89			1.86	
	0.054 ± 0.003	[29]		0.5			0.48	
	0.057 ± 0.016	[23]		0.28			0.28	
	0.0557 ± 0.0015	[63]		2.01			1.77	
	0.0562 ± 0.005	[65]		0.74			0.73	
	0.055 ± 0.005	[35]		0.5			0.49	
	0.058 ± 0.003	[36]		1.81			1.74	
	0.058 ± 0.005	[37]		1.1			1.08	
	0.047 ± 0.004	[40]		-1.36			-1.33	
	0.054 ± 0.005	[41]		0.3			0.3	
	0.053 ± 0.005	[68]		0.1			0.1	
	0.056 ± 0.005	[42]		0.7			0.69	
	0.056 ± 0.007	[43]		0.5			0.5	
	0.054 ± 0.006	[45]		0.25			0.25	
	0.048 ± 0.005 (B=+0.15T)	[45]		-0.89			-0.88	
	0.048 ± 0.005 (B=-0.15T)	[45]		-0.89			-0.88	
	0.047 ± 0.005 (B=+0.45T)	[45]		-1.09			-1.07	

(continued on next page)

Table 4 (continued)

Z, Symbol	$\left(\frac{I_{LL}}{I_{L\alpha}}\right)_{EXP} \pm \Delta(I_{LL}/I_{L\alpha})_{EXP}$	References	$(I_{LL}/I_{L\alpha})_W \pm \epsilon_{ISD}$	$z_{ISD}$	$\bar{z}_{ISD}$	$\epsilon_{ESD}$	$z_{ESD}$	$\bar{z}_{ESD}$
	0.047 ± 0.005 (B=-0.45T)	[45]		-1.09			-1.07	
	0.047 ± 0.005 (B=+0.75T)	[45]		-1.09			-1.07	
	0.047 ± 0.005 (B=-0.75T)	[45]		-1.09			-1.07	
	0.0544 ± 0.004	[9]		0.47			0.46	
	0.0473 ± 0.004 (B=+0.75T)	[9]		-1.28			-1.26	
	0.0473 ± 0.004 (B=-0.75T)	[9]		-1.28			-1.26	
	0.054 ± 0.005	[27]		0.3			0.3	
	0.055 ± 0.004	[47]		0.62			0.61	
	0.055 ± 0.004	[47]		0.62			0.61	
	0.0423 ± 0.005	[76]		-2.02			-2	
	0.057 ± 0.004	[1]		1.12			1.09	
	0.1005 ± 0.0051	[10]		9.36			9.23	
	0.056 ± 0.004	[54]		0.87			0.85	
	0.048 ± 0.003	[54]		-1.47			-1.41	
	0.048 ± 0.003	[54]		-1.47			-1.41	
	0.052 ± 0.003	[55]		-0.16			-0.15	
	0.049 ± 0.005	[81]		-0.69			-0.68	
	0.051 ± 0.006	[81]		-0.25			-0.24	
Z = 90, Th	0.069 ± 0.004	[89]	0.0651 ± 0.0005	0.98	-0.14	0.0013	0.94	-0.15
	0.060 ± 0.004	[29]		-1.26			-1.2	
	0.062 ± 0.003	[14]		-1.01			-0.94	
	0.053 ± 0.003	[14]		-3.97			-3.69	
	0.056 ± 0.003	[14]		-2.98			-2.77	
	0.054 ± 0.003	[14]		-3.64			-3.39	
	0.057 ± 0.003	[14]		-2.65			-2.47	
	0.054 ± 0.005	[31]		-2.2			-2.14	
	0.0712 ± 0.006	[65]		1.02			1	
	0.079 ± 0.002	[34]		6.78			5.85	
	0.076 ± 0.002	[34]		5.32			4.59	
	0.074 ± 0.002	[34]		4.35			3.75	
	0.070 ± 0.002	[34]		2.4			2.07	
	0.069 ± 0.002	[34]		1.92			1.65	
	0.062 ± 0.002	[34]		-1.49			-1.28	
	0.063 ± 0.002	[34]		-1			-0.86	
	0.060 ± 0.006	[35]		-0.84			-0.82	
	0.060 ± 0.007	[35]		-0.72			-0.71	
	0.065 ± 0.004	[37]		-0.01			-0.01	
	0.059 ± 0.005	[38]		-1.21			-1.17	
	0.058 ± 0.002	[40]		-3.44			-2.96	
	0.062 ± 0.006	[41]		-0.51			-0.5	
	0.052 ± 0.005	[68]		-2.6			-2.53	
	0.061 ± 0.008	[43]		-0.51			-0.5	
	0.061 ± 0.003	[45]		-1.34			-1.24	
	0.064 ± 0.004 (B=+0.15T)	[45]		-0.26			-0.25	
	0.064 ± 0.004 (B=-0.15T)	[45]		-0.26			-0.25	
	0.064 ± 0.004 (B=+0.45T)	[45]		-0.26			-0.25	
	0.064 ± 0.004 (B=-0.45T)	[45]		-0.26			-0.25	
	0.065 ± 0.004 (B=+0.75T)	[45]		-0.01			-0.01	
	0.064 ± 0.004 (B=-0.75T)	[45]		-0.26			-0.25	
	0.0607 ± 0.002	[9]		-2.12			-1.83	
	0.0645 ± 0.002 (B=+0.75T)	[9]		-0.27			-0.23	
	0.0643 ± 0.002 (B=-0.75T)	[9]		-0.37			-0.32	
	0.067 ± 0.007	[27]		0.28			0.27	
	0.062 ± 0.004	[47]		-0.76			-0.73	
	0.062 ± 0.004	[47]		-0.76			-0.73	
	0.063 ± 0.003	[1]		-0.68			-0.63	
Z = 92, U	0.1248 ± 0.0064	[10]	0.0580 ± 0.0004	9.31	1.57	0.0022	9.15	1.56
	0.061 ± 0.003	[28]		0.99			0.81	
	0.067 ± 0.004	[89]		2.24			1.98	
	0.061 ± 0.003	[29]		0.99			0.81	
	0.063 ± 0.003	[14]		1.65			1.35	
	0.060 ± 0.003	[14]		0.66			0.54	
	0.061 ± 0.003	[14]		0.99			0.81	
	0.055 ± 0.003	[14]		-0.99			-0.81	
	0.052 ± 0.003	[14]		-1.98			-1.62	
	0.053 ± 0.005	[31]		-1			-0.92	
	0.058 ± 0.005	[32]		-0.001			-0.001	
	0.0712 ± 0.006	[65]		2.19			2.07	
	0.101 ± 0.003	[34]		14.18			11.61	
	0.085 ± 0.002	[34]		13.19			9.14	
	0.067 ± 0.002	[34]		4.39			3.05	
	0.065 ± 0.002	[34]		3.42			2.37	
	0.061 ± 0.002	[34]		1.46			1.01	
	0.046 ± 0.001	[34]		-11.01			-5.02	

(continued on next page)

Table 4 (continued)

Z, Symbol	$\left(\frac{I_{L\alpha}}{I_{L\alpha}}\right)_{EXP} \pm \Delta(I_{L\alpha}/I_{L\alpha})_{EXP}$	References	$(I_{L\alpha}/I_{L\alpha})_W \pm \epsilon_{ISD}$	$z_{ISD}$	$\bar{z}_{ISD}$	$\epsilon_{ESD}$	$z_{ESD}$	$\bar{z}_{ESD}$
	0.043 ± 0.001	[34]		-13.76			-6.27	
	0.062 ± 0.007	[35]		0.57			0.55	
	0.062 ± 0.007	[35]		0.57			0.55	
	0.067 ± 0.004	[37]		2.24			1.98	
	0.060 ± 0.004	[38]		0.5			0.44	
	0.062 ± 0.003	[66]		1.32			1.08	
	0.062 ± 0.003	[40]		1.32			1.08	
	0.060 ± 0.005	[68]		0.4			0.37	
	0.062 ± 0.006	[42]		0.66			0.63	
	0.065 ± 0.008	[43]		0.87			0.84	
	0.065 ± 0.006	[45]		1.16			1.1	
	0.074 ± 0.007 (B=+0.15T)	[45]		2.28			2.18	
	0.074 ± 0.008 (B=-0.15T)	[45]		2			1.93	
	0.075 ± 0.008 (B=+0.45T)	[45]		2.12			2.05	
	0.075 ± 0.008 (B=-0.45T)	[45]		2.12			2.05	
	0.075 ± 0.007 (B=+0.75T)	[45]		2.42			2.32	
	0.075 ± 0.007 (B=-0.75T)	[45]		2.42			2.32	
	0.0651 ± 0.004	[9]		1.76			1.56	
	0.0749 ± 0.004 (B=+0.75T)	[9]		4.2			3.71	
	0.0747 ± 0.004 (B=-0.75T)	[9]		4.15			3.67	
	0.066 ± 0.007	[27]		1.14			1.09	
	0.063 ± 0.004	[47]		1.24			1.1	
	0.063 ± 0.004	[47]		1.24			1.1	
	0.059 ± 0.002	[1]		0.49			0.34	
	0.1329 ± 0.0068	[10]		10.99			10.49	
Z = 93, Np	0.061 ± 0.002	[28]	0.061 ± 0.002	0	0	-	-	-
Z = 94, Pu	0.061 ± 0.002	[28]	0.061 ± 0.002	0	0	-	-	-

Table 5

Summary of the experimental  $I_{L\gamma}/I_{L\beta}$  intensity ratios from  $^{54}\text{Xe}$  to  $^{92}\text{U}$  is presented according to their target atomic numbers. The weighted average values  $(I_{L\gamma}/I_{L\beta})_W$ , the references from which the databases are extracted,  $\epsilon_{ISD}$ ,  $\epsilon_{ESD}$ , the internal and external standard deviation ( $z_{ISD}$ ,  $z_{ESD}$ ), and their means ( $\bar{z}_{ISD}$ ,  $\bar{z}_{ESD}$ ) are also listed.

Z, Symbol	$\left(\frac{I_{L\gamma}}{I_{L\beta}}\right)_{EXP} \pm \Delta(I_{L\gamma}/I_{L\beta})_{EXP}$	References	$(I_{L\gamma}/I_{L\beta})_W \pm \epsilon_{ISD}$	$z_{ISD}$	$\bar{z}_{ISD}$	$\epsilon_{ESD}$	$z_{ESD}$	$\bar{z}_{ESD}$
Z = 54, Xe	0.125 ± 0.013	[24]	0.125 ± 0.013	0	0	-	-	-
Z = 56, Ba	0.122 ± 0.008	[22]	0.122 ± 0.008	0	0	-	-	-
Z = 57, La	0.129 ± 0.009	[33]	0.129 ± 0.009	0	0	-	-	-
Z = 58, Ce	0.145 ± 0.012	[33]	0.145 ± 0.012	0	0	-	-	-
Z = 59, Pr	0.135 ± 0.008	[33]	0.135 ± 0.008	0	0	-	-	-
Z = 60, Nd	0.139 ± 0.006	[33]	0.139 ± 0.006	0	0	-	-	-
Z = 62, Sm	0.140 ± 0.005	[33]	0.140 ± 0.005	0	0	-	-	-
Z = 63, Eu	0.135 ± 0.010	[33]	0.135 ± 0.010	0	0	-	-	-
Z = 64, Gd	0.134 ± 0.010	[33]	0.134 ± 0.010	0	0	-	-	-
Z = 65, Tb	0.147 ± 0.012	[33]	0.147 ± 0.012	0	0	-	-	-
Z = 66, Dy	0.176 ± 0.010	[21]	0.1511 ± 0.0007	2.48	0.62	0.0011	2.47	0.63
	0.150 ± 0.015	[33]		-0.08			-0.08	
	0.176 ± 0.027	[41]		0.92			0.92	
	0.152 ± 0.001	[46]		0.70			0.59	
	0.150 ± 0.001	[46]		-0.93			-0.78	
Z = 67, Ho	0.143 ± 0.011	[33]	0.1500 ± 0.0001	-0.64	0.64	0.0002	-0.64	0.65
	0.167 ± 0.021	[41]		0.81			0.81	
	0.155 ± 0.002	[46]		2.49			2.49	
	0.150 ± 0.0001	[46]		-0.09			-0.07	
Z = 68, Er	0.155 ± 0.009	[24]	0.1571 ± 0.0072	-0.18	0.15	0.0037	-0.22	0.15
	0.157 ± 0.014	[33]		-0.01			-0.01	
	0.174 ± 0.025	[41]		0.65			0.67	
Z = 69, Tm	0.166 ± 0.007	[21]	0.1612 ± 0.0053	0.54	-0.05	0.0055	0.54	-0.05
	0.155 ± 0.008	[33]		-0.65			-0.64	
Z = 70, Yb	0.162 ± 0.002	[20]	0.2278 ± 0.0009	-30.27	-2.80	0.0156	-4.18	-0.59
	0.234 ± 0.015	[33]		0.41			0.28	
	0.249 ± 0.003	[46]		6.79			1.33	
	0.242 ± 0.001	[46]		10.77			0.9	
	0.196 ± 0.019	[1]		-1.67			-1.29	
Z = 71, Lu	0.240 ± 0.018	[33]	0.240 ± 0.018	0	0	-	-	-
Z = 72, Hf	0.167 ± 0.005	[23]	0.1679 ± 0.0049	-0.14	0.36	0.0044	-0.14	0.36
	0.188 ± 0.023	[41]		0.85			0.86	
Z = 73, Ta	0.214 ± 0.014	[33]	0.2204 ± 0.0111	-0.36	0.07	0.0082	-0.39	0.07
	0.231 ± 0.018	[1]		0.50			0.54	
Z = 74, W	0.147 ± 0.007	[25]	0.2051 ± 0.0010	-8.23	-1.04	0.0039	-7.26	-1.01
	0.248 ± 0.020	[33]		2.14			2.1	
	0.176 ± 0.018	[41]		-1.62			-1.58	

(continued on next page)

Table 5 (continued)

Z, Symbol	$\left(\frac{I_{L\gamma}}{I_{L\beta}}\right)_{EXP} \pm \Delta(I_{L\gamma}/I_{L\beta})_{EXP}$	References	$(I_{L\gamma}/I_{L\beta})_W \pm \epsilon_{ISD}$	$z_{ISD}$	$\bar{z}_{ISD}$	$\epsilon_{ESD}$	$z_{ESD}$	$\bar{z}_{ESD}$
Z = 75, Re	0.214 ± 0.005	[46]	0.205 ± 0.013	1.74	0	-	1.4	-
	0.206 ± 0.001	[46]		0.63			0.22	
	0.191 ± 0.015	[1]		-0.94			-0.94	
Z = 78, Pt	0.204 ± 0.020	[27]	0.204 ± 0.020	0	0	-	-	-
Z = 79, Au	0.181 ± 0.014	[33]	0.1770 ± 0.0108	0.23	-0.03	0.0049	0.27	-0.03
	0.171 ± 0.017	[27]		-0.30			-0.34	
Z = 80, Hg	0.193 ± 0.010	[24]	0.1918 ± 0.0108	0.11	0.12	0.0013	0.12	0.12
	0.199 ± 0.007	[24]		0.99			1.01	
	0.182 ± 0.017	[33]		-0.58			-0.58	
	0.183 ± 0.018	[27]		-0.49			-0.49	
	0.203 ± 0.010	[46]		1.10			1.11	
	0.191 ± 0.002	[46]		-0.31			-0.35	
	0.192 ± 0.010	[1]		0.02			0.02	
	0.199 ± 0.011	[22]		0.13			0.13	
Z = 81, Tl	0.175 ± 0.019	[33]	0.1975 ± 0.0018	-1.18	-0.74	0.0025	-1.18	-0.75
	0.180 ± 0.020	[41]		-0.87			-0.87	
	0.174 ± 0.017	[27]		-1.38			-1.37	
	0.200 ± 0.002	[46]		0.91			0.78	
	0.184 ± 0.006	[46]		-2.16			-2.09	
	0.191 ± 0.010	[1]		-0.64			-0.63	
Z = 82, Pb	0.186 ± 0.015	[33]	0.2086 ± 0.0053	-1.42	-0.27	0.0086	-1.31	-0.27
	0.168 ± 0.017	[27]		-2.28			-2.13	
	0.223 ± 0.013	[46]		1.03			0.93	
	0.215 ± 0.008	[46]		0.67			0.55	
	0.218 ± 0.013	[1]		0.67			0.6	
Z = 83, Bi	0.198 ± 0.010	[33]	0.1993 ± 0.0062	-0.11	-0.23	0.0066	-0.11	-0.23
	0.187 ± 0.019	[41]		-0.62			-0.61	
	0.177 ± 0.018	[27]		-1.17			-1.17	
	0.211 ± 0.010	[1]		0.99			0.97	
Z = 90, Th	0.172 ± 0.020	[33]	0.2216 ± 0.0002	-2.48	-2.10	0.0014	-2.47	-2.22
	0.180 ± 0.004	[34]		-10.37			-9.84	
	0.163 ± 0.004	[34]		-14.62			-13.86	
	0.171 ± 0.004	[34]		-12.62			-11.97	
	0.172 ± 0.004	[34]		-12.37			-11.73	
	0.179 ± 0.004	[34]		-10.62			-10.07	
	0.169 ± 0.004	[34]		-13.12			-12.44	
	0.171 ± 0.004	[34]		-12.62			-11.97	
	0.207 ± 0.021	[41]		-0.69			-0.69	
	0.222 ± 0.001	[44]		0.44			0.26	
	0.224 ± 0.001	[44]		2.39			1.45	
	0.227 ± 0.001 (B=+0.75T)	[44]		5.33			3.23	
	0.229 ± 0.001 (B=+0.75T)	[44]		7.29			4.41	
	0.223 ± 0.001 (B=+0.60T)	[44]		1.42			0.86	
	0.225 ± 0.001 (B=+0.60T)	[44]		3.37			2.04	
	0.221 ± 0.001 (B=+0.45T)	[44]		-0.54			-0.33	
	0.222 ± 0.001 (B=+0.45T)	[44]		0.44			0.26	
	0.218 ± 0.001 (B=+0.30T)	[44]		-3.48			-2.11	
	0.220 ± 0.001 (B=+0.30T)	[44]		-1.52			-0.92	
	0.220 ± 0.001 (B=+0.15T)	[44]		-1.52			-0.92	
	0.221 ± 0.001 (B=+0.15T)	[44]		-0.54			-0.33	
	0.227 ± 0.001 (B=-0.75T)	[44]		5.33			3.23	
	0.229 ± 0.001 (B=-0.75T)	[44]		7.29			4.41	
	0.223 ± 0.001 (B=-0.60T)	[44]		1.42			0.86	
	0.224 ± 0.001 (B=-0.60T)	[44]		2.39			1.45	
	0.220 ± 0.001 (B=-0.45T)	[44]		-1.52			-0.92	
	0.222 ± 0.001 (B=-0.45T)	[44]		0.44			0.26	
	0.218 ± 0.001 (B=-0.30T)	[44]		-3.48			-2.11	
	0.220 ± 0.001 (B=-0.30T)	[44]		-1.52			-0.92	
	0.220 ± 0.001 (B=-0.15T)	[44]		-1.52			-0.92	
0.221 ± 0.001 (B=-0.15T)	[44]	-0.54	-0.33					
0.193 ± 0.019	[27]	-1.5	-1.5					
0.226 ± 0.011	[1]	0.4	0.4					
Z = 92, U	0.232 ± 0.017	[33]	0.2181 ± 0.0002	0.82	0.58	0.0004	0.82	0.60
	0.233 ± 0.006	[34]		2.48			2.48	
	0.224 ± 0.006	[34]		0.98			0.98	
	0.230 ± 0.006	[34]		1.98			1.98	
	0.229 ± 0.006	[34]		1.82			1.81	
	0.229 ± 0.006	[34]		1.82			1.81	
	0.242 ± 0.006	[34]		3.98			3.97	
	0.232 ± 0.006	[34]		2.32			2.31	
	0.218 ± 0.001	[44]		-0.10			-0.1	
	0.221 ± 0.001	[44]		2.86			2.65	
	0.221 ± 0.001 (B=+0.75T)	[44]		2.86			2.65	

(continued on next page)

Table 5 (continued)

Z, Symbol	$\left(\frac{I_{L\gamma}}{I_{L\beta}}\right)_{EXP} \pm \Delta(I_{L\gamma}/I_{L\beta})_{EXP}$	References	$(I_{L\gamma}/I_{L\beta})_W \pm \epsilon_{ISD}$	$z_{ISD}$	$\bar{z}_{ISD}$	$\epsilon_{ESD}$	$z_{ESD}$	$\bar{z}_{ESD}$
	0.224 ± 0.001 (B=+0.75T)	[44]		5.81			5.39	
	0.218 ± 0.001 (B=+0.60T)	[44]		-0.10			-0.1	
	0.221 ± 0.001 (B=+0.60T)	[44]		2.86			2.65	
	0.216 ± 0.001 (B=+0.45T)	[44]		-2.08			-1.92	
	0.218 ± 0.001 (B=+0.45T)	[44]		-0.10			-0.1	
	0.215 ± 0.001 (B=+0.30T)	[44]		-3.06			-2.84	
	0.216 ± 0.001 (B=+0.30T)	[44]		-2.08			-1.92	
	0.216 ± 0.001 (B=+0.15T)	[44]		-2.08			-1.92	
	0.217 ± 0.001 (B=+0.15T)	[44]		-1.09			-1.01	
	0.221 ± 0.001 (B=-0.75T)	[44]		2.86			2.65	
	0.224 ± 0.001 (B=-0.75T)	[44]		5.81			5.39	
	0.218 ± 0.0003 (B=-0.60T)	[44]		-0.30			-0.2	
	0.221 ± 0.001 (B=-0.60T)	[44]		2.86			2.65	
	0.216 ± 0.001 (B=-0.45T)	[44]		-2.08			-1.92	
	0.218 ± 0.001 (B=-0.45T)	[44]		-0.10			-0.1	
	0.215 ± 0.001 (B=-0.30T)	[44]		-3.06			-2.84	
	0.216 ± 0.001 (B=-0.30T)	[44]		-2.08			-1.92	
	0.216 ± 0.0005 (B=-0.15T)	[44]		-3.99			-3.15	
	0.217 ± 0.001 (B=-0.15T)	[44]		-1.09			-1.01	
	0.200 ± 0.020	[27]		-0.91			-0.9	
	0.226 ± 0.009	[1]		0.88			0.88	

Table 6

Summary of the experimental  $I_{L1}/I_{L\gamma}$  intensity ratios from  $^{54}\text{Xe}$  to  $^{92}\text{U}$  is presented according to their target atomic numbers. The weighted average values  $(I_{L1}/I_{L\gamma})_W$ , the references from which the databases are extracted,  $\epsilon_{ISD}$ ,  $\epsilon_{ESD}$ , the internal and external standard deviation ( $z_{ISD}$ ,  $z_{ESD}$ ), and their means ( $\bar{z}_{ISD}$ ,  $\bar{z}_{ESD}$ ) are also listed.

Z, Symbol	$\left(\frac{I_{L1}}{I_{L\gamma}}\right)_{EXP} \pm \Delta(I_{L1}/I_{L\gamma})_{EXP}$	References	$(I_{L1}/I_{L\gamma})_W \pm \epsilon_{ISD}$	$z_{ISD}$	$\bar{z}_{ISD}$	$\epsilon_{ESD}$	$z_{ESD}$	$\bar{z}_{ESD}$
Z = 54, Xe	0.389 ± 0.064	[24]	0.389 ± 0.064	0	0	-	-	-
Z = 56, Ba	0.291 ± 0.030	[22]	0.291 ± 0.030	0	0	-	-	-
Z = 57, La	0.3480 ± 0.019	[33]	0.3480 ± 0.019	0	0	-	-	-
Z = 58, Ce	0.3450 ± 0.021	[33]	0.3450 ± 0.021	0	0	-	-	-
Z = 59, Pr	0.3610 ± 0.022	[33]	0.3610 ± 0.022	0	0	-	-	-
Z = 60, Nd	0.3610 ± 0.022	[33]	0.3610 ± 0.022	0	0	-	-	-
Z = 62, Sm	0.3690 ± 0.031	[33]	0.3690 ± 0.031	0	0	-	-	-
Z = 63, Eu	0.3510 ± 0.026	[33]	0.3510 ± 0.026	0	0	-	-	-
Z = 64, Gd	0.3550 ± 0.019	[33]	0.3550 ± 0.019	0	0	-	-	-
Z = 65, Tb	0.3620 ± 0.017	[33]	0.3620 ± 0.017	0	0	-	-	-
Z = 66, Dy	0.344 ± 0.027	[21]	0.3130 ± 0.0075	1.11	0.08	0.0191	0.94	0.08
	0.3570 ± 0.023	[33]		1.82			1.47	
	0.29 ± 0.05	[41]		-0.46			-0.43	
	0.313 ± 0.019	[46]		-0.001			-0.001	
	0.348 ± 0.014	[46]		2.20			1.48	
	0.326 ± 0.021	[54]		0.58			0.46	
	0.230 ± 0.016	[54]		-4.70			-3.33	
Z = 67, Ho	0.3660 ± 0.023	[33]	0.3385 ± 0.0051	1.17	-1.29	0.0206	0.89	-1.03
	0.29 ± 0.04	[41]		-1.20			-1.08	
	0.293 ± 0.029	[46]		-1.54			-1.28	
	0.362 ± 0.006	[46]		3			1.09	
	0.302 ± 0.018	[54]		-1.95			-1.33	
	0.224 ± 0.015	[54]		-7.23			-4.49	
Z = 68, Er	0.225 ± 0.013	[24]	0.2597 ± 0.0083	-2.25	0.55	0.0215	-1.38	0.53
	0.3450 ± 0.025	[33]		3.24			2.58	
	0.29 ± 0.04	[41]		0.74			0.67	
	0.305 ± 0.019	[54]		2.18			1.58	
	0.238 ± 0.017	[54]		-1.15			-0.79	
Z = 69, Tm	0.344 ± 0.006	[21]	0.3284 ± 0.0058	1.86	-4.57	0.0677	0.23	-1.91
	0.0351 ± 0.026	[33]		-11			-4.05	
Z = 70, Yb	0.244 ± 0.003	[20]	0.2096 ± 0.0025	8.75	-3.95	0.0272	1.26	-1.60
	0.1316 ± 0.011	[33]		-6.91			-2.66	
	0.119 ± 0.006	[46]		-13.91			-3.26	
	0.132 ± 0.011	[46]		-6.88			-2.65	
	0.17 ± 0.05	[1]		-0.79			-0.7	
Z = 71, Lu	0.1400 ± 0.090	[33]	0.2940 ± 0.0125	-1.69	-0.45	0.0166	-1.68	-0.46
	0.307 ± 0.019	[54]		0.57			0.52	
	0.289 ± 0.017	[54]		-0.23			-0.21	
Z = 72, Hf	0.298 ± 0.010	[23]	0.2912 ± 0.0095	0.49	-0.73	0.0204	0.3	-0.69
	0.23 ± 0.03	[41]		-1.95			-1.69	
Z = 73, Ta	0.1470 ± 0.099	[33]	0.2175 ± 0.0116	-0.71	0.17	0.0425	-0.65	0.02
	0.14 ± 0.04	[1]		-1.86			-1.33	

(continued on next page)

Table 6 (continued)

Z, Symbol	$\left(\frac{I_{LL}}{I_{L\gamma}}\right)_{EXP} \pm \Delta(I_{LL}/I_{L\gamma})_{EXP}$	References	$(I_{LL}/I_{L\gamma})_W \pm \epsilon_{ISD}$	$z_{ISD}$	$\bar{z}_{ISD}$	$\epsilon_{ESD}$	$z_{ESD}$	$\bar{z}_{ESD}$
Z = 74, W	0.356 ± 0.025	[54]	0.1627 ± 0.0033	5.02	1.52	0.0140	2.81	1.47
	0.185 ± 0.014	[54]		-1.79			-0.73	
	0.220 ± 0.015	[25]		3.73			2.79	
	0.1310 ± 0.010	[33]		-3.02			-1.85	
	0.28 ± 0.03	[41]		3.89			3.54	
	0.127 ± 0.011	[46]		-3.11			-2.01	
	0.156 ± 0.004	[46]		-1.30			-0.46	
	0.18 ± 0.04	[1]		0.43			0.41	
Z = 75, Re	0.322 ± 0.021	[54]	0.1544 ± 0.010	7.49	0	-	6.31	-
	0.225 ± 0.015	[54]		4.06			3.04	
	0.1544 ± 0.010	[33]		0			-	
	0.2630 ± 0.015	[33]		-0.52			-0.01	
Z = 78, Pt	0.286 ± 0.016	[54]	0.2723 ± 0.0097	0.73	0.13	0.0190	0.78	0.12
	0.267 ± 0.021	[54]		-0.23			-0.24	
Z = 79, Au	0.280 ± 0.016	[54]	0.2952 ± 0.0125	-0.75	0.13	0.0190	-0.61	0.12
	0.319 ± 0.020	[54]		1			0.86	
Z = 80, Hg	0.218 ± 0.026	[24]	0.2484 ± 0.0044	-1.15	-0.11	0.0115	-1.07	-0.08
	0.189 ± 0.011	[24]		-5.02			-3.73	
	0.2801 ± 0.016	[33]		1.91			1.61	
	0.218 ± 0.015	[46]		-1.95			-1.61	
	0.261 ± 0.006	[46]		1.70			0.97	
	0.26 ± 0.03	[1]		0.38			0.36	
	0.282 ± 0.016	[54]		2.03			1.7	
	0.277 ± 0.023	[54]		1.22			1.11	
	0.236 ± 0.015	[22]		-1.39			-1.24	
	0.2840 ± 0.016	[33]		1.55			1.4	
Z = 81, Tl	0.35 ± 0.04	[41]	0.2580 ± 0.005	2.28	0.19	0.0094	2.24	0.21
	0.230 ± 0.011	[46]		-2.31			-1.93	
	0.266 ± 0.007	[46]		0.94			0.68	
	0.26 ± 0.02	[1]		0.1			0.09	
	0.2780 ± 0.017	[33]		0.67			0.55	
Z = 82, Pb	0.218 ± 0.017	[46]	0.2655 ± 0.0077	-2.55	-0.02	0.0149	-2.1	-0.02
	0.243 ± 0.018	[46]		-1.15			-0.96	
	0.24 ± 0.03	[1]		-0.82			-0.76	
	0.304 ± 0.019	[54]		1.88			1.59	
	0.302 ± 0.018	[54]		1.86			1.56	
	0.2690 ± 0.017	[33]		-1.31			-1.16	
Z = 83, Bi	0.34 ± 0.03	[41]	0.2941 ± 0.009	1.46	0.18	0.0133	1.4	0.19
	0.27 ± 0.02	[1]		-1.1			-1	
	0.329 ± 0.022	[54]		1.47			1.36	
	0.302 ± 0.018	[54]		0.39			0.35	
Z = 90, Th	0.2880 ± 0.018	[33]	0.1758 ± 0.003	6.15	0.1	0.0092	5.55	0.10
	0.32 ± 0.03	[41]		4.78			4.59	
	0.178 ± 0.021	[44]		0.10			0.1	
	0.245 ± 0.017	[44]		4			3.58	
	0.099 ± 0.022 (B=+0.75T)	[44]		-3.46			-3.22	
	0.137 ± 0.021 (B=+0.75T)	[44]		-1.83			-1.69	
	0.129 ± 0.012 (B=+0.60T)	[44]		-3.78			-3.09	
	0.159 ± 0.018 (B=+0.60T)	[44]		-0.92			-0.83	
	0.151 ± 0.014 (B=+0.45T)	[44]		-1.73			-1.48	
	0.176 ± 0.011 (B=+0.45T)	[44]		0.02			0.02	
	0.170 ± 0.015 (B=+0.30T)	[44]		-0.38			-0.33	
	0.192 ± 0.014 (B=+0.30T)	[44]		1.13			0.97	
	0.186 ± 0.027 (B=+0.15T)	[44]		0.38			0.36	
	0.214 ± 0.019 (B=+0.15T)	[44]		1.99			1.81	
	0.099 ± 0.012 (B=-0.75T)	[44]		-6.21			-5.07	
	0.138 ± 0.020 (B=-0.75T)	[44]		-1.87			-1.72	
	0.131 ± 0.015 (B=-0.60T)	[44]		-2.93			-2.54	
	0.159 ± 0.011 (B=-0.60T)	[44]		-1.47			-1.17	
	0.152 ± 0.018 (B=-0.45T)	[44]		-1.30			-1.18	
	0.178 ± 0.015 (B=-0.45T)	[44]		0.14			0.13	
0.171 ± 0.012 (B=-0.30T)	[44]	-0.39	-0.32					
0.192 ± 0.016 (B=-0.30T)	[44]	1	0.88					
0.185 ± 0.015 (B=-0.15T)	[44]	0.60	0.52					
0.215 ± 0.017 (B=-0.15T)	[44]	2.27	2.03					
0.24 ± 0.01	[1]	6.15	4.72					
Z = 92, U	0.2600 ± 0.017	[33]	0.1836 ± 0.0015	4.47	-0.78	0.0060	4.24	-0.74
	0.176 ± 0.024	[44]		-0.32			-0.31	
	0.265 ± 0.021	[44]		3.86			3.73	
	0.116 ± 0.010 (B=+0.75T)	[44]		-6.69			-5.81	
	0.128 ± 0.009 (B=+0.75T)	[44]		-6.09			-5.16	
	0.153 ± 0.011 (B=+0.60T)	[44]		-2.76			-2.45	
	0.135 ± 0.011 (B=+0.60T)	[44]		-4.38			-3.89	
	0.183 ± 0.014 (B=+0.45T)	[44]		-0.05			-0.04	

(continued on next page)

Table 6 (continued)

Z, Symbol	$\left(\frac{I_{L1}}{I_{L\gamma}}\right)_{EXP} \pm \Delta(I_{L1}/I_{L\gamma})_{EXP}$	References	$(I_{L1}/I_{L\gamma})_W \pm \epsilon_{ISD}$	$z_{ISD}$	$\bar{z}_{ISD}$	$\epsilon_{ESD}$	$z_{ESD}$	$\bar{z}_{ESD}$
	0.157 ± 0.012 (B=+0.45T)	[44]		-2.20			-1.99	
	0.203 ± 0.015 (B=+0.30T)	[44]		1.28			1.2	
	0.180 ± 0.015 (B=+0.30T)	[44]		-0.24			-0.23	
	0.194 ± 0.002 (B=+0.15T)	[44]		4.10			1.65	
	0.206 ± 0.010 (B=+0.15T)	[44]		2.21			1.92	
	0.114 ± 0.010 (B=-0.75T)	[44]		-6.88			-5.98	
	0.124 ± 0.011 (B=-0.75T)	[44]		-5.37			-4.77	
	0.157 ± 0.011 (B=-0.60T)	[44]		-2.40			-2.13	
	0.134 ± 0.010 (B=-0.60T)	[44]		-4.91			-4.27	
	0.185 ± 0.016 (B=-0.45T)	[44]		0.08			0.08	
	0.153 ± 0.011 (B=-0.45T)	[44]		-2.76			-2.45	
	0.203 ± 0.015 (B=-0.30T)	[44]		1.28			1.2	
	0.179 ± 0.014 (B=-0.30T)	[44]		-0.33			-0.31	
	0.194 ± 0.009 (B=-0.15T)	[44]		1.13			0.96	
	0.207 ± 0.009 (B=-0.15T)	[44]		2.56			2.16	
	0.24 ± 0.01	[1]		5.57			4.84	

Table 7

Summary of the experimental  $I_{L1}/I_{L\beta}$  intensity ratios from  $_{54}\text{Xe}$  to  $_{92}\text{U}$  is presented according to their target atomic numbers. The weighted average values  $(I_{L1}/I_{L\beta})_W$ , the references from which the databases are extracted,  $\epsilon_{ISD}$ ,  $\epsilon_{ESD}$ , the internal and external standard deviation ( $z_{ISD}$ ,  $z_{ESD}$ ), and their means ( $\bar{z}_{ISD}$ ,  $\bar{z}_{ESD}$ ) are also listed.

Z, Symbol	$\left(\frac{I_{L1}}{I_{L\beta}}\right)_{EXP} \pm \Delta(I_{L1}/I_{L\beta})_{EXP}$	References	$(I_{L1}/I_{L\beta})_W \pm \epsilon_{ISD}$	$z_{ISD}$	$\bar{z}_{ISD}$	$\epsilon_{ESD}$	$z_{ESD}$	$\bar{z}_{ESD}$
Z = 54, Xe	0.049 ± 0.008	[24]	0.049 ± 0.008	0	0	-	-	-
Z = 56, Ba	0.036 ± 0.003	[22]	0.036 ± 0.003	0	0	-	-	-
Z = 57, La	0.0449 ± 0.003	[33]	0.0449 ± 0.003	0	0	-	-	-
Z = 58, Ce	0.0501 ± 0.003	[33]	0.0501 ± 0.003	0	0	-	-	-
Z = 59, Pr	0.0489 ± 0.002	[33]	0.0489 ± 0.002	0	0	-	-	-
Z = 60, Nd	0.0515 ± 0.004	[33]	0.0515 ± 0.004	0	0	-	-	-
Z = 62, Sm	0.0531 ± 0.005	[33]	0.0531 ± 0.005	0	0	-	-	-
Z = 63, Eu	0.045 ± 0.002	[26]	0.0485 ± 0.0013	-1.46	0.18	0.0022	-1.17	0.18
	0.051 ± 0.002	[26]		1.04			0.83	
	0.0526 ± 0.004	[33]		0.97			0.89	
Z = 64, Gd	0.0528 ± 0.004	[33]	0.0528 ± 0.004	0	0	-	-	-
Z = 65, Tb	0.0531 ± 0.004	[33]	0.0531 ± 0.004	0	0	-	-	-
Z = 66, Dy	0.060 ± 0.005	[21]	0.0632 ± 0.0009	-0.64	-1.77	0.0034	-0.54	-1.53
	0.0535 ± 0.004	[33]		-2.38			-1.86	
	0.05 ± 0.01	[41]		-1.32			-1.25	
	0.067 ± 0.001	[54]		2.83			1.07	
	0.051 ± 0.004	[54]		-2.99			-2.34	
	0.044 ± 0.003	[54]		-6.15			-4.27	
Z = 67, Ho	0.0529 ± 0.005	[33]	0.0633 ± 0.0009	-2.05	-2.09	0.0040	-1.62	-1.67
	0.05 ± 0.01	[41]		-1.33			-1.23	
	0.067 ± 0.001	[54]		2.74			0.89	
	0.051 ± 0.004	[54]		-3			-2.17	
	0.042 ± 0.003	[54]		-6.80			-4.24	
Z = 68, Er	0.035 ± 0.001	[24]	0.0514 ± 0.0007	-13.70	-0.37	0.0072	-2.26	-0.18
	0.0540 ± 0.005	[33]		0.51			0.29	
	0.05 ± 0.01	[41]		-0.14			-0.12	
	0.069 ± 0.001	[54]		14.63			2.42	
	0.049 ± 0.003	[54]		-0.79			-0.31	
	0.043 ± 0.003	[54]		-2.75			-1.08	
Z = 69, Tm	0.057 ± 0.002	[21]	0.0557 ± 0.0014	0.55	0	0.0014	0.56	0
	0.0543 ± 0.002	[33]		-0.55			-0.56	
Z = 70, Yb	0.039 ± 0.001	[20]	0.0373 ± 0.0009	1.28	-0.77	0.0023	0.67	-0.67
	0.0308 ± 0.002	[33]		-2.97			-2.11	
	0.033 ± 0.007	[1]		-0.61			-0.58	
Z = 71, Lu	0.0336 ± 0.002	[33]	0.0611 ± 0.0009	-12.65	-2.65	0.0079	-3.36	-1.05
	0.069 ± 0.001	[54]		6			0.99	
	0.053 ± 0.004	[54]		-1.98			-0.91	
	0.053 ± 0.004	[54]		-1.98			-0.91	
Z = 72, Hf	0.050 ± 0.002	[23]	0.05 ± 0.002	0	0	0	0	0
	0.05 ± 0.01	[41]		0			0	
Z = 73, Ta	0.0315 ± 0.003	[33]	0.0631 ± 0.0009	-10.13	-3.51	0.0066	-4.38	-2.04
	0.033 ± 0.006	[1]		-4.97			-3.39	
	0.070 ± 0.001	[54]		5.17			1.03	
	0.057 ± 0.004	[54]		-1.50			-0.8	
	0.044 ± 0.003	[54]		-6.13			-2.65	
Z = 74, W	0.032 ± 0.002	[25]	0.0568 ± 0.0008	-11.55	-2.52	0.0070	-3.39	-1.16
	0.0326 ± 0.002	[33]		-11.27			-3.31	

(continued on next page)

Table 7 (continued)

Z, Symbol	$\left(\frac{I_{L1}}{I_{L\beta}}\right)_{EXP} \pm \Delta(I_{L1}/I_{L\beta})_{EXP}$	References	$(I_{L1}/I_{L\beta})_W \pm \epsilon_{ISD}$	$z_{ISD}$	$\bar{z}_{ISD}$	$\epsilon_{ESD}$	$z_{ESD}$	$\bar{z}_{ESD}$
	0.05 ± 0.01	[41]		-0.67			-0.55	
	0.034 ± 0.005	[1]		-4.50			-2.64	
	0.070 ± 0.001	[54]		10.48			1.87	
	0.058 ± 0.004	[54]		0.30			0.15	
	0.055 ± 0.004	[54]		-0.43			-0.22	
Z = 75, Re	0.0316 ± 0.002	[33]	0.0316 ± 0.002	0	0	-	-	-
Z = 76, Os	0.012 ± 0.001	[21]	0.012 ± 0.001	0	0	-	-	-
Z = 78, Pt	0.072 ± 0.002	[54]	0.0686 ± 0.0017	1.31	-0.59	0.0048	0.66	-0.49
	0.070 ± 0.005	[54]		0.27			0.2	
	0.054 ± 0.004	[54]		-3.356			-2.33	
Z = 79, Au	0.0477 ± 0.002	[33]	0.0656 ± 0.0009	-8.22	-1.05	0.0051	-3.26	-0.46
	0.070 ± 0.001	[54]		3.34			0.85	
	0.060 ± 0.004	[54]		-1.37			-0.86	
	0.076 ± 0.005	[54]		2.05			1.46	
Z = 80, Hg	0.038 ± 0.002	[24]	0.0547 ± 0.0011	-7.24	0.16	0.0060	-2.66	0.14
	0.042 ± 0.005	[24]		-2.48			-1.63	
	0.0508 ± 0.003	[33]		-1.21			-0.58	
	0.051 ± 0.006	[1]		-0.61			-0.44	
	0.071 ± 0.002	[54]		7.07			2.59	
	0.072 ± 0.005	[54]		3.37			2.22	
	0.066 ± 0.005	[54]		2.20			1.45	
Z = 81, Tl	0.047 ± 0.003	[22]	0.0491 ± 0.0018	-0.61	0.21	0.0014	-0.64	0.21
	0.0498 ± 0.003	[33]		0.19			0.2	
	0.06 ± 0.01	[41]		1.07			1.08	
	0.050 ± 0.004	[1]		0.20			0.2	
Z = 82, Pb	0.0516 ± 0.003	[33]	0.0663 ± 0.0015	-4.40	-0.30	0.0050	-2.5	-0.20
	0.053 ± 0.005	[1]		-2.55			-1.87	
	0.073 ± 0.002	[54]		2.71			1.23	
	0.069 ± 0.005	[54]		0.52			0.38	
	0.080 ± 0.006	[54]		2.22			1.75	
Z = 83, Bi	0.050 ± 0.014	[23]	0.0655 ± 0.0014	-1.1	-0.73	0.0034	-1.07	-0.71
	0.0533 ± 0.004	[33]		-2.86			-2.32	
	0.06 ± 0.01	[41]		-0.54			-0.52	
	0.058 ± 0.004	[1]		-1.75			-1.42	
	0.073 ± 0.002	[54]		3.07			1.91	
	0.067 ± 0.005	[54]		0.30			0.26	
	0.056 ± 0.004	[54]		-2.23			-1.8	
Z = 90, Th	0.0496 ± 0.004	[33]	0.0534 ± 0.0023	-0.81	0.23	0.0032	-0.74	0.33
	0.07 ± 0.01	[41]		1.62			1.58	
	0.054 ± 0.003	[1]		0.16			0.14	
Z = 92, U	0.0602 ± 0.004	[33]	0.0560 ± 0.0018	0.95	0.28	0.0021	0.92	0.28
	0.055 ± 0.002	[1]		-0.39			-0.36	

Table 8

. Summary of the experimental  $I_{L75}/I_{L\alpha}$  intensity ratios from  $_{56}\text{Ba}$  to  $_{92}\text{U}$  is presented according to their target atomic numbers. The weighted average values  $(I_{L75}/I_{L\alpha})_W$ , the references from which the databases are extracted,  $\epsilon_{ISD}$ ,  $\epsilon_{ESD}$ , the internal and external standard deviation ( $z_{ISD}$ ,  $z_{ESD}$ ), and their means ( $\bar{z}_{ISD}$ ,  $\bar{z}_{ESD}$ ) are also listed.

Z, Symbol	$\left(\frac{I_{L75}}{I_{L\alpha}}\right)_{EXP} \pm \Delta(I_{L75}/I_{L\alpha})_{EXP}$	References	$(I_{L75}/I_{L\alpha})_W \pm \epsilon_{ISD}$	$z_{ISD}$	$\bar{z}_{ISD}$	$\epsilon_{ESD}$	$z_{ESD}$	$\bar{z}_{ESD}$
Z = 56, Ba	0.0033 ± 0.0002	[10]	0.0033 ± 0.0002	0	0	-	-	-
Z = 57, La	0.0035 ± 0.0002	[10]	0.0035 ± 0.0002	0	0	-	-	-
Z = 58, Ce	0.0034 ± 0.0002	[10]	0.0034 ± 0.0002	0	0	-	-	-
Z = 59, Pr	0.0035 ± 0.0002	[10]	0.0035 ± 0.0002	0	0	-	-	-
Z = 60, Nd	0.0035 ± 0.0002	[10]	0.0035 ± 0.0002	0	0	-	-	-
Z = 62, Sm	0.0036 ± 0.0002	[10]	0.0036 ± 0.0002	0	0	-	-	-
Z = 63, Eu	0.0036 ± 0.0002	[10]	0.0036 ± 0.0002	0	0	-	-	-
Z = 64, Gd	0.0037 ± 0.0002	[10]	0.0037 ± 0.0002	0	0	-	-	-
Z = 65, Tb	0.0040 ± 0.0002	[10]	0.0040 ± 0.0002	0	0	-	-	-
Z = 66, Dy	0.0040 ± 0.0002	[10]	0.0040 ± 0.0002	0	0	-	-	-
Z = 67, Ho	0.0042 ± 0.0002	[10]	0.0042 ± 0.0002	0	0	-	-	-
Z = 68, Er	0.0043 ± 0.0002	[10]	0.0043 ± 0.0002	0	0	-	-	-
Z = 69, Tm	0.0077 ± 0.0004	[10]	0.0077 ± 0.0004	0	0	-	-	-
Z = 71, Lu	0.0087 ± 0.0004	[10]	0.0087 ± 0.0004	0	0	-	-	-
Z = 72, Hf	0.007 ± 0.001	[43]	0.0085 ± 0.0004	-1.39	-0.41	0.0008	-1.21	-0.40
	0.0089 ± 0.0005	[10]		0.57			0.42	
Z = 73, Ta	0.005 ± 0.001	[43]	0.0060 ± 0.0002	-0.96	0.20	0.0010	-0.68	0.11
	0.005 ± 0.0004	[47]		-2.10			-0.88	
	0.005 ± 0.0004	[47]		-2.11			-0.88	
	0.0093 ± 0.0005	[10]		5.99			2.87	

(continued on next page)

Table 8 (continued)

Z, Symbol	$\left(\frac{I_{L\gamma 5}}{I_{L\alpha}}\right)_{EXP} \pm \Delta(I_{L\gamma 5}/I_{L\alpha})_{EXP}$	References	$(I_{L\gamma 5}/I_{L\alpha})_W \pm \epsilon_{ISD}$	$z_{ISD}$	$\bar{z}_{ISD}$	$\epsilon_{ESD}$	$z_{ESD}$	$\bar{z}_{ESD}$
Z = 74, W	0.004 ± 0.001 0.005 ± 0.0004 0.005 ± 0.0004 0.0094 ± 0.0005	[43] [47] [47] [10]	0.0059 ± 0.0002	-1.90 -2.04 -2.04 6.23	0.07	0.0011	-1.32 -0.82 -0.82 2.87	-0.02
Z = 75, Re	0.0089 ± 0.0005	[10]	0.0089 ± 0.0005	0	0	-	-	-
Z = 76, Os	0.005 ± 0.0004 0.005 ± 0.0004 0.0081 ± 0.0004	[47] [47] [10]	0.0060 ± 0.0002	-2.4 -2.24 4.47	0	0.0010	-0.93 -0.93 1.87	0
Z = 77, Ir	0.0083 ± 0.0004	[10]	0.0083 ± 0.0004	0	0	-	-	-
Z = 78, Pt	0.005 ± 0.0004 0.004 ± 0.0004 0.0077 ± 0.0004	[47] [47] [10]	0.0056 ± 0.0002	-1.23 -3.39 4.62	0	0.0011	-0.48 -1.33 1.82	0
Z = 79, Au	0.004 ± 0.001 0.004 ± 0.0003 0.004 ± 0.0003 0.0078 ± 0.0004	[43] [47] [47] [10]	0.0048 ± 0.0002	-0.79 -2.29 -2.29 6.80	0.36	0.0009	-0.6 -0.85 -0.85 3.05	0.19
Z = 80, Hg	0.003 ± 0.0004 0.004 ± 0.0004 0.004 ± 0.0004 0.0078 ± 0.0004	[43] [47] [47] [10]	0.0047 ± 0.0002	-3.80 -1.57 -1.57 6.93	0	0.0011	-1.5 -0.62 -0.62 2.74	0
Z = 81, Tl	0.005 ± 0.001 0.004 ± 0.0003 0.004 ± 0.0003 0.0078 ± 0.0004	[43] [47] [47] [10]	0.0048 ± 0.0002	0.16 -2.39 -2.39 6.72	0.53	0.0009	0.12 -0.89 -0.89 3.03	0.34
Z = 82, Pb	0.005 ± 0.001 0.005 ± 0.0004 0.004 ± 0.0004 0.0081 ± 0.0004	[43] [47] [47] [10]	0.0057 ± 0.0002	-0.65 -1.45 -3.63 5.31	-0.10	0.0010	-0.47 -0.62 -1.56 2.29	-0.09
Z = 83, Bi	0.005 ± 0.001 0.004 ± 0.0003 0.004 ± 0.0003 0.0082 ± 0.0004	[43] [47] [47] [10]	0.0049 ± 0.0002	0.07 -2.63 -2.63 7.44	0.56	0.0010	0.05 -0.9 -0.9 3.08	0.33
Z = 90, Th	0.004 ± 0.001 0.005 ± 0.0004 0.005 ± 0.0004 0.0106 ± 0.0005	[43] [47] [47] [10]	0.0062 ± 0.0002	-2.16 -2.62 -2.62 7.90	0.12	0.0014	-1.3 -0.85 -0.85 2.98	-0.01
Z = 92, U	0.005 ± 0.001 0.004 ± 0.0003 0.004 ± 0.0003 0.01101 ± 0.0006	[43] [47] [47] [10]	0.0048 ± 0.0002	0.21 -2.20 -2.20 9.86	1.42	0.0012	0.13 -0.61 -0.61 4.5	0.85

Table 9

Summary of the experimental  $I_{L\gamma 44}/I_{L\alpha}$  intensity ratios from  $^{50}\text{Sn}$  to  $^{92}\text{U}$  is presented according to their target atomic numbers. The weighted average values  $(I_{L\gamma 44}/I_{L\alpha})_W$ , the references from which the databases are extracted,  $\epsilon_{ISD}$ ,  $\epsilon_{ESD}$ , the internal and external standard deviation ( $z_{ISD}$ ,  $z_{ESD}$ ), and their means ( $\bar{z}_{ISD}$ ,  $\bar{z}_{ESD}$ ) are also listed.

Z, Symbol	$\left(\frac{I_{L\gamma 44}}{I_{L\alpha}}\right)_{EXP} \pm \Delta(I_{L\gamma 44}/I_{L\alpha})_{EXP}$	References	$(I_{L\gamma 44}/I_{L\alpha})_W \pm \epsilon_{ISD}$	$z_{ISD}$	$\bar{z}_{ISD}$	$\epsilon_{ESD}$	$z_{ESD}$	$\bar{z}_{ESD}$
Z = 50, Sn	0.0037 ± 0.0002	[10]	0.0037 ± 0.0002	0	0	-	-	-
Z = 51, Sb	0.0086 ± 0.0004	[10]	0.0086 ± 0.0004	0	0	-	-	-
Z = 52, Te	0.0139 ± 0.0007	[10]	0.0139 ± 0.0007	0	0	-	-	-
Z = 53, I	0.0202 ± 0.0010	[10]	0.0202 ± 0.0010	0	0	-	-	-
Z = 56, Ba	0.0041 ± 0.0002	[10]	0.0041 ± 0.0002	0	0	-	-	-
Z = 57, La	0.0043 ± 0.0002	[10]	0.0043 ± 0.0002	0	0	-	-	-
Z = 58, Ce	0.0038 ± 0.0002	[10]	0.0038 ± 0.0002	0	0	-	-	-
Z = 59, Pr	0.0037 ± 0.0002	[10]	0.0037 ± 0.0002	0	0	-	-	-
Z = 60, Nd	0.0034 ± 0.0002	[10]	0.0034 ± 0.0002	0	0	-	-	-
Z = 62, Sm	0.0031 ± 0.0002	[10]	0.0031 ± 0.0002	0	0	-	-	-
Z = 63, Eu	0.0032 ± 0.0002	[10]	0.0032 ± 0.0002	0	0	-	-	-
Z = 64, Gd	0.0033 ± 0.0002	[10]	0.0033 ± 0.0002	0	0	-	-	-
Z = 65, Tb	0.0032 ± 0.0002	[10]	0.0032 ± 0.0002	0	0	-	-	-
Z = 66, Dy	0.009 ± 0.001 0.009 ± 0.001 0.0033 ± 0.0002	[47] [47] [10]	0.0037 ± 0.0002	5.18 5.18 -1.52	2.95	0.0011	3.63 3.63 -0.39	2.29
Z = 67, Ho	0.0033 ± 0.0002	[10]	0.0033 ± 0.0002	0	0	-	-	-
Z = 68, Er	0.010 ± 0.001 0.010 ± 0.001 0.0033 ± 0.0002	[47] [47] [10]	0.0038 ± 0.0002	6.09 6.09 -1.79	3.47	0.0012	3.89 3.89 -0.39	2.46
Z = 69, Tm	0.0284 ± 0.0014	[10]	0.0284 ± 0.0014	0	0	-	-	-

(continued on next page)

Table 9 (continued)

Z, Symbol	$\left(\frac{I_{L\gamma 44}}{I_{L\alpha}}\right)_{EXP} \pm \Delta(I_{L\gamma 44}/I_{L\alpha})_{EXP}$	References	$(I_{L\gamma 44}/I_{L\alpha})_W \pm \epsilon_{ISD}$	$z_{ISD}$	$\bar{z}_{ISD}$	$\epsilon_{ESD}$	$z_{ESD}$	$\bar{z}_{ESD}$
Z = 70, Yb	0.009 ± 0.001	[47]	0.0090 ± 0.0007	0	0	0	0	0
	0.009 ± 0.001	[47]		0			0	
Z = 71, Lu	0.009 ± 0.001	[47]	0.0128 ± 0.0006	-3.20	1.36	0.0057	-0.66	0.53
	0.009 ± 0.001	[47]		-3.20			-0.66	
	0.0299 ± 0.0015	[10]		10.49			2.9	
Z = 72, Hf	0.019 ± 0.002	[43]	0.0264 ± 0.0012	-3.13	-0.40	0.0059	-1.18	-0.21
	0.0311 ± 0.0016	[10]		2.33			0.77	
Z = 73, Ta	0.019 ± 0.002	[43]	0.0140 ± 0.0006	2.37	1.61	0.0047	0.97	0.81
	0.010 ± 0.001	[47]		-3.43			-0.84	
	0.010 ± 0.001	[47]		-3.43			-0.84	
	0.0338 ± 0.0017	[10]		10.92			3.94	
Z = 74, W	0.023 ± 0.003	[43]	0.0133 ± 0.0007	3.17	2.28	0.0054	1.58	1.17
	0.009 ± 0.001	[47]		-3.58			-0.78	
	0.010 ± 0.001	[47]		-2.74			-0.6	
	0.0391 ± 0.0020	[10]		12.28			4.49	
Z = 75, Re	0.0346 ± 0.0018	[10]	0.0346 ± 0.0018	0	0	-	-	-
Z = 76, Os	0.008 ± 0.001	[47]	0.0120 ± 0.0006	-3.35	1.14	0.0055	-0.7	0.44
	0.008 ± 0.001	[47]		-3.35			-0.7	
	0.0275 ± 0.0014	[10]		10.12			2.71	
Z = 77, Ir	0.0232 ± 0.0012	[10]	0.0232 ± 0.0012	0	0	-	-	-
Z = 78, Pt	0.006 ± 0.001	[47]	0.0104 ± 0.0006	-3.74	0.31	0.0048	-0.89	0.12
	0.006 ± 0.001	[47]		-3.74			-0.89	
	0.0209 ± 0.0011	[10]		8.43			2.14	
Z = 79, Au	0.011 ± 0.001	[43]	0.0078 ± 0.0003	3.04	1.92	0.0023	1.25	1.05
	0.006 ± 0.0005	[47]		-3.06			-0.76	
	0.006 ± 0.0005	[47]		-3.06			-0.76	
	0.0191 ± 0.0010	[10]		10.76			4.44	
Z = 80, Hg	0.010 ± 0.001	[43]	0.0078 ± 0.0003	2.09	1.92	0.0025	0.82	1
	0.006 ± 0.0005	[47]		-3.06			-0.72	
	0.006 ± 0.0005	[47]		-3.06			-0.72	
	0.0201 ± 0.0010	[10]		11.72			4.62	
Z = 81, Tl	0.010 ± 0.001	[43]	0.0078 ± 0.0003	2.09	1.92	0.0025	0.82	1
	0.006 ± 0.0005	[47]		-3.06			-0.72	
	0.006 ± 0.0005	[47]		-3.06			-0.72	
	0.0201 ± 0.0010	[10]		11.72			4.62	
Z = 82, Pb	0.013 ± 0.002	[43]	0.0067 ± 0.0003	3.13	2.76	0.0022	2.1	1.62
	0.006 ± 0.0004	[47]		-1.43			-0.3	
	0.005 ± 0.0004	[47]		-3.51			-0.74	
	0.0200 ± 0.0010	[10]		12.85			5.41	
Z = 83, Bi	0.012 ± 0.002	[43]	0.0061 ± 0.0003	2.90	2.96	0.0023	1.91	1.73
	0.005 ± 0.0004	[47]		-2.36			-0.48	
	0.005 ± 0.0004	[47]		-2.36			-0.48	
	0.0216 ± 0.0011	[10]		13.65			5.99	
Z = 90, Th	0.012 ± 0.002	[43]	0.0104 ± 0.0006	0.77	1.23	0.0050	0.3	0.55
	0.006 ± 0.001	[47]		-3.76			-0.87	
	0.006 ± 0.001	[47]		-3.76			-0.87	
	0.0293 ± 0.0015	[10]		11.67			3.65	
Z = 92, U	0.013 ± 0.002	[43]	0.0239 ± 0.0012	-4.69	-0.74	0.0082	-1.3	-0.28
	0.0301 ± 0.0015	[10]		3.20			0.74	

• Elements like <sup>62</sup>Sm, <sup>64</sup>Gd, <sup>65</sup>Tb, <sup>66</sup>Dy, <sup>67</sup>Ho, <sup>68</sup>Er, <sup>70</sup>Yb, <sup>73</sup>Ta, <sup>74</sup>W, <sup>80</sup>Hg, <sup>81</sup>Tl, and <sup>83</sup>Bi are associated with a substantial amount of data. Additionally, it is worth highlighting that the elements <sup>79</sup>Au, <sup>82</sup>Pb, <sup>90</sup>Th, and <sup>92</sup>U have a notable significant quantity of data, specifically 47, 48, 53, and 51 data points, respectively.

Fig. 3 illustrates the distribution of data points concerning experimental intensity ratios  $I_{L1}/I_{L\alpha}$  across the atomic number range from <sup>39</sup>Y to <sup>94</sup>Pu. These data points have been extracted from a compilation of 66 cited research papers. Analyzing this figure provides us with the opportunity to offer some observations:

• Almost all the elements, ranging from <sup>39</sup>Y to <sup>94</sup>Pu, are included in the dataset, with the exception of eight elements: <sup>43</sup>Tc, <sup>84</sup>Po, <sup>85</sup>At, <sup>86</sup>Rn, <sup>87</sup>Fr, <sup>88</sup>Ra, <sup>89</sup>Ac, and <sup>91</sup>Pa. The absence of data for these elements can be attributed to their radioactive nature, which makes them challenging to work with and study.

• For some elements there is only a single value (<sup>39</sup>Y, <sup>40</sup>Zr, <sup>44</sup>Ru, <sup>45</sup>Rh, <sup>46</sup>Pd, <sup>48</sup>Cd, <sup>54</sup>Xe, <sup>61</sup>Pm, <sup>93</sup>Np, and <sup>94</sup>Pu) while others have only two values, including <sup>41</sup>Nb, <sup>42</sup>Mo, <sup>51</sup>Sb, <sup>52</sup>Te, and <sup>55</sup>Cs.

• The number of measurements for the following elements is between two and twenty: <sup>47</sup>Ag, <sup>49</sup>In, <sup>50</sup>Sn, <sup>53</sup>I, <sup>56</sup>Ba, <sup>57</sup>La, <sup>58</sup>Ce, <sup>59</sup>Pr, <sup>60</sup>Nd, <sup>62</sup>Sm, <sup>63</sup>Eu, <sup>64</sup>Gd, <sup>65</sup>Tb, <sup>67</sup>Ho, <sup>68</sup>Er, <sup>69</sup>Tm, <sup>70</sup>Yb, <sup>71</sup>Lu, <sup>72</sup>Hf, <sup>75</sup>Re, <sup>76</sup>Os, <sup>77</sup>Ir, and <sup>78</sup>Pt.

• The extensively studied elements are primarily found within the atomic number range of  $62 \leq Z \leq 92$ , encompassing a notable group of elements, including <sup>66</sup>Dy, <sup>73</sup>Ta, <sup>74</sup>W, <sup>79</sup>Au, <sup>80</sup>Hg, <sup>81</sup>Tl, <sup>82</sup>Pb, <sup>83</sup>Bi, <sup>90</sup>Th, and <sup>92</sup>U. It is worth noting that three elements, <sup>79</sup>Au, <sup>82</sup>Pb, and <sup>92</sup>U, particularly stand out with the highest number of data points, featuring 47, 54, and 42 data values, respectively. Remarkably, these three elements are the focus of approximately 41 publications, collectively constituting 62.1% of all the cited references.

The distribution of the number of experimental intensity ratios data points for  $I_{L\gamma}/I_{L\beta}$ ,  $I_{L1}/I_{L\gamma}$ , and  $I_{L1}/I_{L\beta}$  as a function of the atomic number Z ( $54 \leq Z \leq 92$ ) is presented in Figs. 4, 5, and 6, respectively. Analyzing

**Table 10**

Summary of the experimental  $I_{L\eta}/I_{L\alpha}$  intensity ratios from  ${}_{50}\text{Sn}$  to  ${}_{92}\text{U}$  is presented according to their target atomic numbers. The weighted average values  $(I_{L\eta}/I_{L\alpha})_W$ , the references from which the databases are extracted,  $\varepsilon_{ISD}$ ,  $\varepsilon_{ESD}$ , the internal and external standard deviation ( $z_{ISD}$ ,  $z_{ESD}$ ), and their means ( $\bar{z}_{ISD}$ ,  $\bar{z}_{ESD}$ ) are also listed.

Z, Symbol	$\left(\frac{I_{L\eta}}{I_{L\alpha}}\right)_{EXP} \pm \Delta(I_{L\eta}/I_{L\alpha})_{EXP}$	References	$(I_{L\eta}/I_{L\alpha})_W \pm \varepsilon_{ISD}$	$z_{ISD}$	$\bar{z}_{ISD}$	$\varepsilon_{ESD}$	$z_{ESD}$	$\bar{z}_{ESD}$
Z = 50, Sn	0.0729 ± 0.0037	[10]	0.0729 ± 0.0037	0	0	–	–	–
Z = 51, Sb	0.0723 ± 0.0037	[10]	0.0723 ± 0.0037	0	0	–	–	–
Z = 52, Te	0.0810 ± 0.0041	[10]	0.0810 ± 0.0041	0	0	–	–	–
Z = 53, I	0.0847 ± 0.0043	[10]	0.0847 ± 0.0043	0	0	–	–	–
Z = 56, Ba	0.0145 ± 0.0007	[10]	0.0145 ± 0.0007	0	0	–	–	–
Z = 57, La	0.0146 ± 0.0007	[10]	0.0146 ± 0.0007	0	0	–	–	–
Z = 58, Ce	0.0142 ± 0.0007	[10]	0.0142 ± 0.0007	0	0	–	–	–
Z = 59, Pr	0.0150 ± 0.0008	[10]	0.0150 ± 0.0008	0	0	–	–	–
Z = 60, Nd	0.0144 ± 0.0007	[10]	0.0144 ± 0.0007	0	0	–	–	–
Z = 62, Sm	0.0148 ± 0.0008	[10]	0.0148 ± 0.0008	0	0	–	–	–
Z = 63, Eu	0.0154 ± 0.0008	[10]	0.0154 ± 0.0008	0	0	–	–	–
Z = 64, Gd	0.0152 ± 0.0008	[10]	0.0152 ± 0.0008	0	0	–	–	–
Z = 65, Tb	0.0170 ± 0.0009	[10]	0.0170 ± 0.0009	0	0	–	–	–
Z = 66, Dy	0.0163 ± 0.0008	[10]	0.0163 ± 0.0008	0	0	–	–	–
Z = 67, Ho	0.0175 ± 0.0009	[10]	0.0175 ± 0.0009	0	0	–	–	–
Z = 68, Er	0.0173 ± 0.0009	[10]	0.0173 ± 0.0009	0	0	–	–	–
Z = 69, Tm	0.0332 ± 0.0017	[10]	0.0332 ± 0.0017	0	0	–	–	–
Z = 71, Lu	0.0370 ± 0.0019	[10]	0.0370 ± 0.0019	0	0	–	–	–
Z = 72, Hf	0.0374 ± 0.0019	[10]	0.0374 ± 0.0019	0	0	–	–	–
Z = 73, Ta	0.0373 ± 0.0019	[10]	0.0373 ± 0.0019	0	0	–	–	–
Z = 74, W	0.0377 ± 0.0019	[10]	0.0377 ± 0.0019	0	0	–	–	–
Z = 75, Re	0.0365 ± 0.0019	[10]	0.0365 ± 0.0019	0	0	–	–	–
Z = 76, Os	0.019 ± 0.002	[47]	0.02518 ± 0.0010	–2.71	–0.33	0.0052	–1.1	–0.19
	0.019 ± 0.002	[47]		–2.71			–1.1	
	0.0341 ± 0.0017	[10]		4.42			1.62	
Z = 77, Ir	0.019 ± 0.002	[32]	0.02626 ± 0.0013	–3.08	–0.39	0.0058	–1.18	–0.21
	0.0309 ± 0.0016	[10]		2.29			0.77	
Z = 78, Pt	0.018 ± 0.001	[47]	0.02016 ± 0.0006	–1.82	0.78	0.0032	–0.64	0.48
	0.018 ± 0.001	[47]		–1.82			–0.64	
	0.0299 ± 0.0015	[10]		5.97			2.72	
Z = 79, Au	0.018 ± 0.001	[32]	0.01854 ± 0.0004	–0.50	0.40	0.0014	–0.31	0.40
	0.0179 ± 0.001	[18]		–0.59			–0.37	
	0.018 ± 0.001	[47]		–0.50			–0.31	
	0.017 ± 0.001	[47]		–1.42			–0.89	
	0.0302 ± 0.0015	[10]		7.49			5.66	
	0.019 ± 0.002	[80]		0.23			0.19	
	0.0165 ± 0.001	[19]		–1.88			–1.18	
Z = 80, Hg	0.015 ± 0.002	[59]	0.01794 ± 0.0005	–1.43	0.13	0.0014	–1.19	0.13
	0.022 ± 0.003	[59]		1.34			1.22	
	0.012 ± 0.002	[59]		–2.90			–2.41	
	0.018 ± 0.020	[24]		0.003			0.003	
	0.018 ± 0.003	[24]		0.02			0.02	
	0.019 ± 0.001	[32]		0.97			0.61	
	0.016 ± 0.001	[47]		–1.76			–1.1	
	0.016 ± 0.001	[47]		–1.76			–1.1	
	0.0166 ± 0.0012	[86]		–1.04			–0.71	
	0.0303 ± 0.0015	[10]		7.89			5.95	
Z = 81, Tl	0.016 ± 0.001	[22]	0.01772 ± 0.0005	–1.51	0.82	0.0027	–0.59	0.60
	0.016 ± 0.001	[47]		–1.51			–0.59	
	0.016 ± 0.001	[47]		–1.51			–0.59	
	0.0309 ± 0.0016	[10]		7.80			4.15	
Z = 82, Pb	0.020 ± 0.002	[32]	0.01826 ± 0.0005	0.84	0.77	0.0024	0.55	0.61
	0.015 ± 0.001	[39]		–2.88			–1.23	
	0.017 ± 0.001	[47]		–1.11			–0.47	
	0.017 ± 0.001	[47]		–1.11			–0.47	
	0.0319 ± 0.0016	[10]		8.10			4.67	
Z = 83, Bi	0.007 ± 0.002	[23]	0.0175 ± 0.0006	–5.02	0.21	0.0038	–2.46	0.07
	0.016 ± 0.001	[47]		–1.28			–0.38	
	0.016 ± 0.001	[47]		–1.28			–0.38	
	0.0319 ± 0.0016	[10]		8.40			3.51	
Z = 90, Th	0.017 ± 0.002	[43]	0.01923 ± 0.0006	–1.07	0.94	0.0032	–0.59	0.68
	0.019 ± 0.002	[27]		–0.11			–0.06	
	0.017 ± 0.001	[47]		–1.91			–0.66	
	0.017 ± 0.001	[47]		–1.91			–0.66	
	0.0395 ± 0.0020	[10]		9.70			5.35	
Z = 92, U	0.016 ± 0.001	[32]	0.01767 ± 0.0005	–1.49	0.88	0.0026	–0.61	0.72
	0.017 ± 0.002	[43]		–0.33			–0.21	
	0.017 ± 0.002	[27]		–0.33			–0.21	
	0.016 ± 0.001	[47]		–1.49			–0.61	
	0.016 ± 0.001	[47]		–1.49			–0.61	
	0.0391 ± 0.0020	[10]		10.37			6.59	

**Table 11**

. Summary of the experimental  $I_{L\gamma 1}/I_{L\alpha}$  intensity ratios from  ${}_{66}\text{Dy}$  to  ${}_{92}\text{U}$  is presented according to their target atomic numbers. The weighted average values  $(I_{L\gamma 1}/I_{L\alpha})_W$ , the references from which the databases are extracted,  $\epsilon_{ISD}$ ,  $\epsilon_{ESD}$ , the internal and external standard deviation ( $z_{ISD}$ ,  $z_{ESD}$ ), and their means ( $\bar{z}_{ISD}$ ,  $\bar{z}_{ESD}$ ) are also listed.

Z, Symbol	$\left(\frac{I_{L\gamma 1}}{I_{L\alpha}}\right)_{EXP} \pm \Delta(I_{L\gamma 1}/I_{L\alpha})_{EXP}$	References	$(I_{L\gamma 1}/I_{L\alpha})_W \pm \epsilon_{ISD}$	$z_{ISD}$	$\bar{z}_{ISD}$	$\epsilon_{ESD}$	$z_{ESD}$	$\bar{z}_{ESD}$
Z = 66, Dy	0.119 ± 0.009	[47]	0.1151 ± 0.060	0.36	0.03	0.0035	0.41	0.03
	0.112 ± 0.008	[47]		-0.31				
Z = 68, Er	0.127 ± 0.009	[47]	0.1235 ± 0.0064	0.32	0	0.0035	0.36	0
	0.120 ± 0.009	[47]		-0.32				
Z = 70, Yb	0.122 ± 0.009	[47]	0.121 ± 0.0064	0.09	0	0.001	0.11	0
	0.120 ± 0.009	[47]		-0.09				
Z = 71, Lu	0.124 ± 0.009	[47]	0.125 ± 0.0064	-0.09	0	0.001	-0.11	0
	0.126 ± 0.009	[47]		0.09				
Z = 72, Hf	0.148 ± 0.019	[43]	0.148 ± 0.019	0	0	-	-	-
Z = 73, Ta	0.147 ± 0.019	[43]	0.1475 ± 0.005	-0.03	-0.11	0.0082	-0.02	-0.11
	0.137 ± 0.010	[47]		-0.94				
	0.134 ± 0.009	[47]		-1.31				
	0.165 ± 0.008	[74]		1.86				
	0.156 ± 0.020	[43]		0.48				
Z = 74, W	0.129 ± 0.009	[47]	0.1462 ± 0.0041	-1.74	0.03	0.0067	0.46	0.03
	0.136 ± 0.009	[47]		-1.03				
	0.149 ± 0.007	[74]		0.35				
	0.167 ± 0.009	[73]		2.10				
	0.154 ± 0.008	[73]		0				
Z = 75, Re	0.154 ± 0.008	[73]	0.154 ± 0.008	0	0	-	-	-
Z = 76, Os	0.130 ± 0.009	[47]	0.1387 ± 0.005	1.62	-0.09	0.0086	1.3	-0.08
	0.128 ± 0.009	[47]		-0.84				
	0.124 ± 0.006	[73]		-1.04				
Z = 78, Pt	0.127 ± 0.009	[47]	0.1376 ± 0.0041	-1.87	0.63	0.0179	-0.72	0.47
	0.126 ± 0.009	[47]		-1.07				
	0.2147 ± 0.0109	[10]		-1.17				
	0.117 ± 0.015	[43]		-1.17				
Z = 79, Au	0.115 ± 0.008	[47]	0.1348 ± 0.0048	6.63	0.47	0.0238	3.69	0.30
	0.116 ± 0.008	[47]		-1.13				
	0.2234 ± 0.0114	[10]		-2.12				
	0.110 ± 0.008	[47]		-2.01				
Z = 80, Hg	0.120 ± 0.016	[43]	0.1400 ± 0.0049	7.16	0.49	0.0237	3.36	0.31
	0.123 ± 0.008	[47]		-1.20				
	0.120 ± 0.008	[47]		-1.82				
	0.2300 ± 0.0117	[10]		-2.14				
Z = 81, Tl	0.109 ± 0.014	[43]	0.1389 ± 0.0048	7.10	0.42	0.0237	3.41	0.26
	0.123 ± 0.008	[47]		-2.02				
	0.122 ± 0.008	[47]		-1.71				
	0.2300 ± 0.0117	[10]		-1.81				
Z = 82, Pb	0.140 ± 0.018	[43]	0.1415 ± 0.0049	7.21	0.49	0.0211	3.45	0.34
	0.123 ± 0.008	[47]		-0.08				
	0.119 ± 0.008	[47]		-1.97				
	0.2350 ± 0.0120	[10]		-2.40				
	0.1214 ± 0.0679	[77]		7.21				
Z = 83, Bi	0.130 ± 0.017	[43]	0.1327 ± 0.0044	7.21	0.97	0.0240	3.85	0.62
	0.116 ± 0.007	[47]		-0.16				
	0.115 ± 0.007	[47]		-2.02				
	0.2389 ± 0.0122	[10]		-2.14				
Z = 90, Th	0.130 ± 0.017	[43]	0.1655 ± 0.0056	8.18	0.83	0.0322	3.95	0.52
	0.148 ± 0.009	[47]		-1.98				
	0.146 ± 0.009	[47]		-1.65				
	0.3157 ± 0.0161	[10]		-1.84				
Z = 92, U	0.132 ± 0.017	[43]	0.1426 ± 0.0051	8.81	1.45	0.0345	4.17	0.86
	0.123 ± 0.008	[47]		-0.60				
	0.122 ± 0.008	[47]		-2.07				
	0.3283 ± 0.0167	[10]		-2.17				

these figures leads us to the following conclusions:

- The majority of targets are included in the dataset, with only a few isolated cases having either no data or fewer than two available data points.
- The elements listed below have a measurement count ranging from two to ten:  ${}_{59}\text{Pr}$ ,  ${}_{66}\text{Dy}$ ,  ${}_{67}\text{Ho}$ ,  ${}_{68}\text{Er}$ ,  ${}_{69}\text{Tm}$ ,  ${}_{70}\text{Yb}$ ,  ${}_{72}\text{Hf}$ ,  ${}_{73}\text{Ta}$ ,  ${}_{74}\text{W}$ ,  ${}_{79}\text{Au}$ ,  ${}_{80}\text{Hg}$ ,  ${}_{81}\text{Tl}$ ,  ${}_{82}\text{Pb}$ , and  ${}_{83}\text{Bi}$  (for  $I_{L\gamma}/I_{L\beta}$ ), as well as  ${}_{66}\text{Dy}$ ,  ${}_{67}\text{Ho}$ ,  ${}_{68}\text{Er}$ ,  ${}_{69}\text{Tm}$ ,  ${}_{70}\text{Yb}$ ,  ${}_{71}\text{Lu}$ ,  ${}_{72}\text{Hf}$ ,  ${}_{73}\text{Ta}$ ,  ${}_{74}\text{W}$ ,  ${}_{78}\text{Pt}$ ,  ${}_{79}\text{Au}$ ,  ${}_{80}\text{Hg}$ ,  ${}_{81}\text{Tl}$ ,  ${}_{82}\text{Pb}$ , and  ${}_{83}\text{Bi}$  (for  $I_{L\gamma}/I_{L\gamma}$ ), and similarly, for  ${}_{63}\text{Eu}$ ,  ${}_{66}\text{Dy}$ ,  ${}_{67}\text{Ho}$ ,  ${}_{68}\text{Er}$ ,  ${}_{69}\text{Tm}$ ,  ${}_{70}\text{Yb}$ ,  ${}_{71}\text{Lu}$ ,  ${}_{72}\text{Hf}$ ,  ${}_{73}\text{Ta}$ ,  ${}_{78}\text{Pt}$ ,  ${}_{79}\text{Au}$ ,  ${}_{81}\text{Tl}$ ,  ${}_{82}\text{Pb}$ ,  ${}_{90}\text{Th}$ , and  ${}_{92}\text{U}$  (for  $I_{L\beta}/I_{L\beta}$ ).
- Thorium ( ${}_{90}\text{Th}$ ) holds the largest number of experimental data points, with 33 values for  $I_{L\gamma}/I_{L\beta}$  and 25 values for  $I_{L\beta}/I_{L\gamma}$ . In the case of  $I_{L\beta}/I_{L\beta}$ , the elements  ${}_{74}\text{W}$ ,  ${}_{80}\text{Hg}$ , and  ${}_{83}\text{Bi}$  each have the largest number of experimental data points, with 7 values.

We compiled a database comprising three research papers for  $I_{L\gamma 44}/I_{L\alpha}$  and fourteen for  $I_{L\beta}/I_{L\alpha}$ , which we have presented in Figs. 8 and 9, respectively, as a function of atomic number  $Z$  ( $50 \leq Z \leq 92$ ). These figures warrant some comments, specifically:

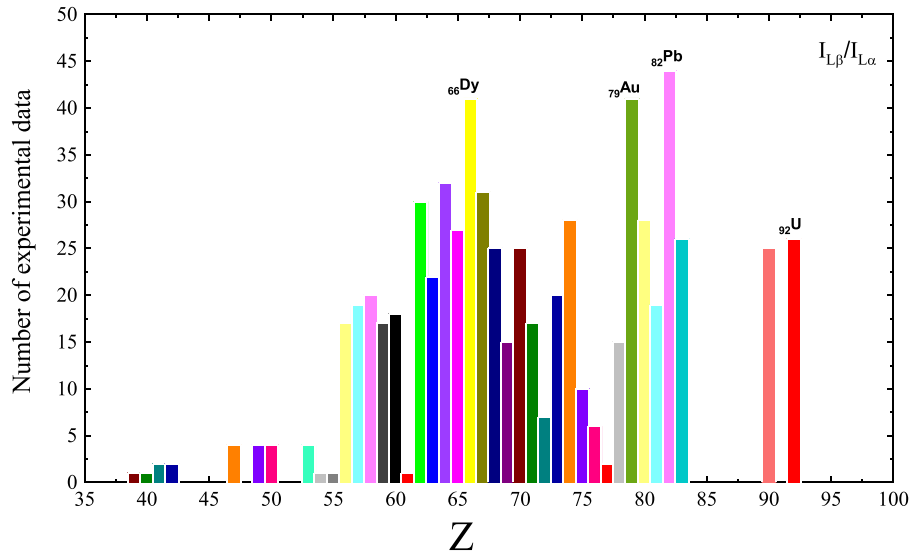


Fig. 1. Distribution of the experimental  $I_{L\beta}/I_{L\alpha}$  values according to the atomic number  $Z$ .

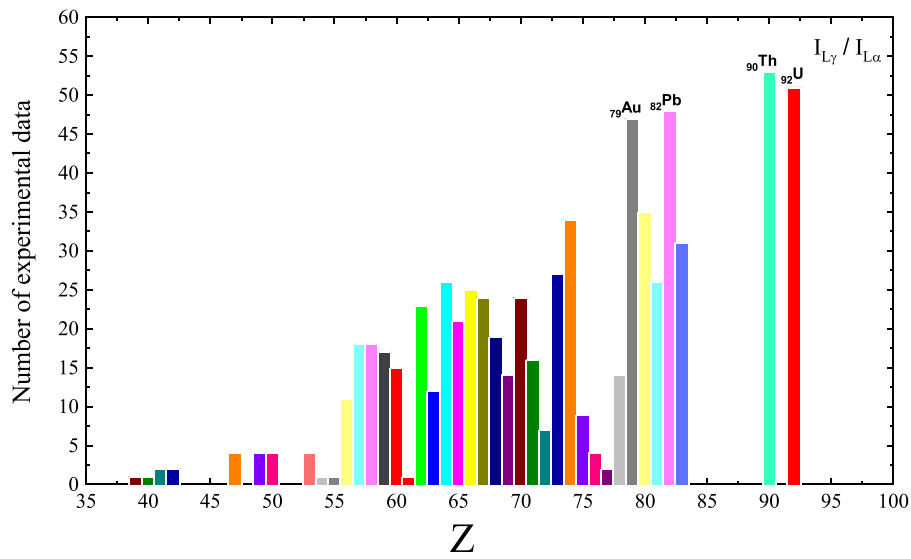


Fig. 2. Distribution of the experimental  $I_{L\gamma}/I_{L\alpha}$  values according to the atomic number  $Z$ .

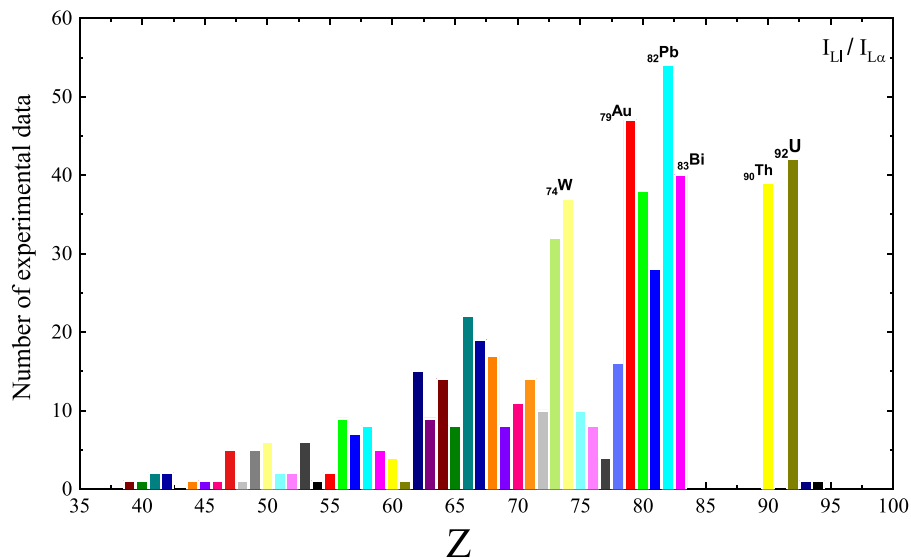


Fig. 3. Distribution of the experimental  $I_{L1}/I_{L\alpha}$  values according to the atomic number  $Z$ .

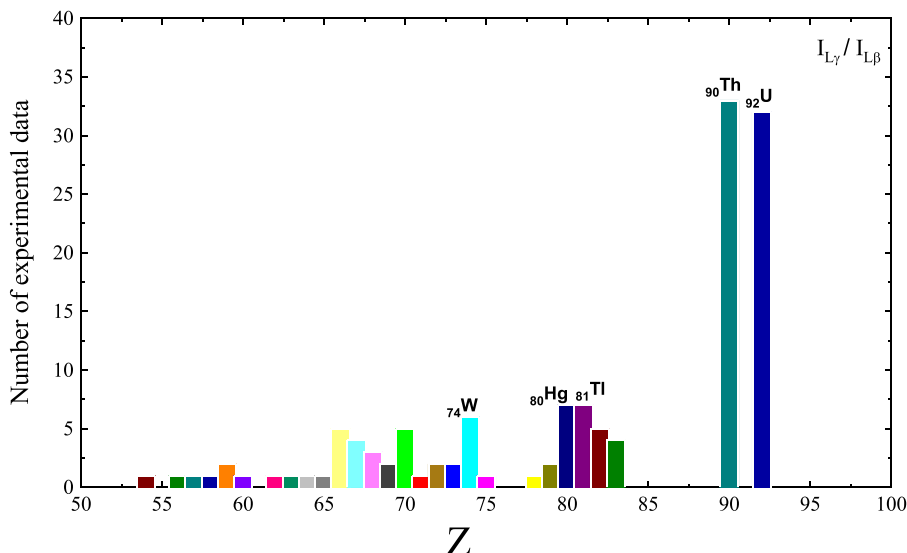


Fig. 4. Distribution of the experimental  $I_{L\gamma}/I_{L\beta}$  values according to the atomic number  $Z$ .

- For  $I_{L\eta}/I_{L\alpha}$  only ten elements lack published values, while for some elements, there is just a single recorded value ( $_{50}\text{Sn}$ ,  $_{51}\text{Sb}$ ,  $_{52}\text{Te}$ ,  $_{53}\text{I}$ ,  $_{56}\text{Ba}$ ,  $_{57}\text{La}$ ,  $_{58}\text{Ce}$ ,  $_{59}\text{Pr}$ ,  $_{60}\text{Nd}$ ,  $_{62}\text{Sm}$ ,  $_{63}\text{Eu}$ ,  $_{64}\text{Gd}$ ,  $_{65}\text{Tb}$ ,  $_{66}\text{Dy}$ ,  $_{67}\text{Ho}$ ,  $_{68}\text{Er}$ ,  $_{69}\text{Tm}$ ,  $_{71}\text{Lu}$ ,  $_{72}\text{Hf}$ ,  $_{73}\text{Ta}$ ,  $_{74}\text{W}$ , and  $_{75}\text{Re}$ ).
- $_{76}\text{Os}$ ,  $_{77}\text{Ir}$ ,  $_{78}\text{Pt}$ ,  $_{79}\text{Au}$ ,  $_{81}\text{Tl}$ ,  $_{82}\text{Pb}$ ,  $_{83}\text{Bi}$ ,  $_{90}\text{Th}$ , and  $_{92}\text{U}$ , with more than two and less than ten intensity ratio measurements per element for  $I_{L\eta}/I_{L\alpha}$ .
- $_{66}\text{Dy}$ ,  $_{70}\text{Yb}$ ,  $_{71}\text{Lu}$ ,  $_{72}\text{Hf}$ ,  $_{73}\text{Ta}$ ,  $_{74}\text{W}$ ,  $_{76}\text{Os}$ ,  $_{78}\text{Pt}$ ,  $_{79}\text{Au}$ ,  $_{80}\text{Hg}$ ,  $_{81}\text{Tl}$ ,  $_{82}\text{Pb}$ ,  $_{83}\text{Bi}$ ,  $_{90}\text{Th}$ , and  $_{92}\text{U}$ , with more than two and less than five intensity ratios measurements per element for  $I_{L\gamma44}/I_{L\alpha}$ .

- The lanthanides ( $56 \leq Z \leq 71$ ) are sparsely documented, with only one experimental value per element, except for  $_{61}\text{Pm}$  and  $_{70}\text{Yb}$ , which lack any recorded values for  $I_{L\gamma5}/I_{L\alpha}$ .
- For  $I_{L\gamma5}/I_{L\alpha}$ , elements  $_{72}\text{Hf}$ ,  $_{73}\text{Ta}$ ,  $_{74}\text{W}$ ,  $_{76}\text{Os}$ ,  $_{78}\text{Pt}$ ,  $_{79}\text{Au}$ ,  $_{80}\text{Hg}$ ,  $_{81}\text{Tl}$ ,  $_{82}\text{Pb}$ ,  $_{83}\text{Bi}$ ,  $_{90}\text{Th}$ , and  $_{92}\text{U}$  exhibit a range of experimental data values between two and five. Additionally, for  $I_{L\gamma1}/I_{L\alpha}$ ,  $_{66}\text{Dy}$ ,  $_{68}\text{Er}$ ,  $_{70}\text{Yb}$ ,  $_{71}\text{Lu}$ ,  $_{73}\text{Ta}$ ,  $_{74}\text{W}$ ,  $_{76}\text{Os}$ ,  $_{78}\text{Pt}$ ,  $_{79}\text{Au}$ ,  $_{80}\text{Hg}$ ,  $_{81}\text{Tl}$ ,  $_{82}\text{Pb}$ ,  $_{83}\text{Bi}$ ,  $_{90}\text{Th}$ , and  $_{92}\text{U}$  display a range of experimental data values between two and six.

The distribution of experimental intensity ratio data points for  $I_{L\gamma5}/I_{L\alpha}$  and  $I_{L\gamma1}/I_{L\alpha}$  as functions of atomic number  $Z$ , within the respective ranges of  $56 \leq Z \leq 92$  and  $66 \leq Z \leq 92$ , is depicted in Figs. 7 and 10. The analysis of these figures allows us to make some comments:

The data distribution study for all intensity ratios as a function of atomic number  $Z$  concludes that there is an important amount of data for the lanthanides ( $56 \leq Z \leq 71$ ). However, it is especially important to draw attention to the absence of published data on these elements:  $_{84}\text{Po}$ ,  $_{85}\text{At}$ ,  $_{86}\text{Rn}$ ,  $_{87}\text{Fr}$ ,  $_{88}\text{Ra}$ ,  $_{89}\text{Ac}$ , and  $_{91}\text{Pa}$ .

Figs. 11 to 20 present histograms representing the count of articles that contain experimental data. There are 64 publications for  $I_{L\beta}/I_{L\alpha}$ , 61

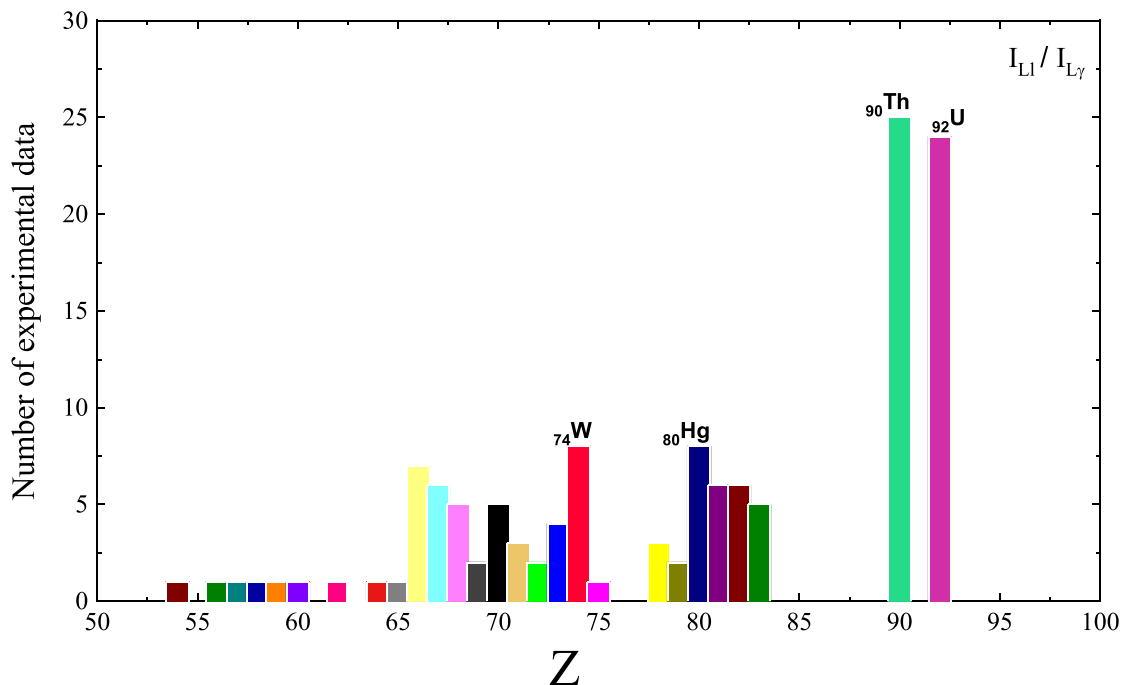


Fig. 5. Distribution of the experimental  $I_{L1}/I_{L\gamma}$  values according to the atomic number  $Z$ .

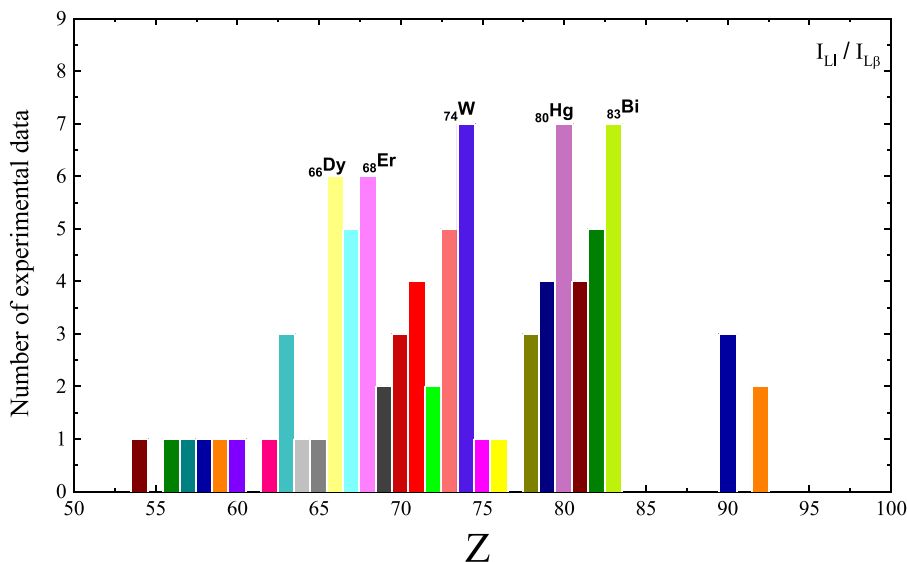


Fig. 6. Distribution of the experimental  $I_{L1}/I_{L\beta}$  values according to the atomic number Z.

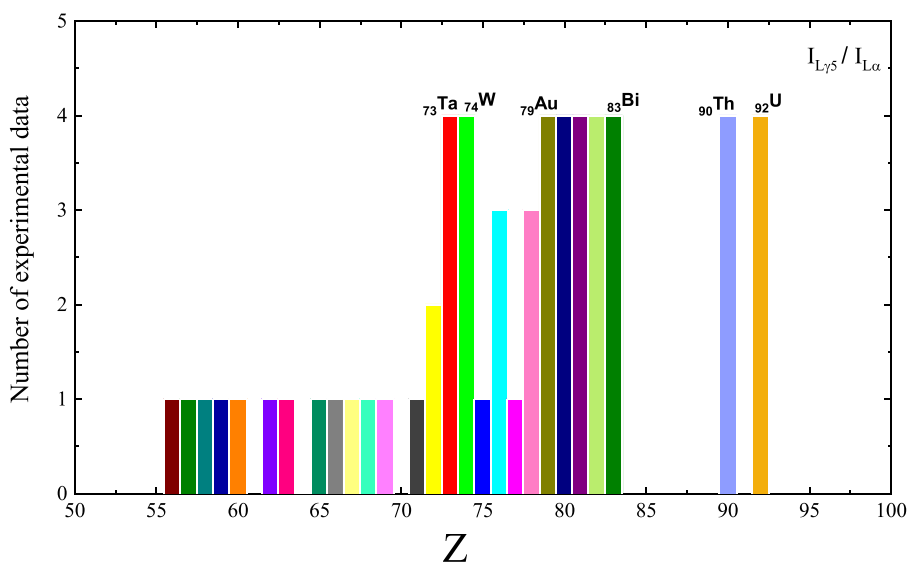


Fig. 7. Distribution of the experimental  $I_{L\gamma5}/I_{L\alpha}$  values according to the atomic number Z.

for  $I_{L\gamma}/I_{L\alpha}$ , 66 for  $I_{L1}/I_{L\alpha}$ , 14 for  $I_{L\eta}/I_{L\alpha}$ , 13 for  $I_{L\gamma}/I_{L\beta}$ , 12 for  $I_{L1}/I_{L\gamma}$ , 11 for  $I_{L1}/I_{L\beta}$ , 3 for  $I_{L\gamma5}/I_{L\alpha}$  and  $I_{L\gamma44}/I_{L\alpha}$ , and 6 for  $I_{L\gamma1}/I_{L\alpha}$ . These histograms are organized based on the publication year of the original work. Studying these figures, we can discern that:

- The publication years for  $I_{L\beta}/I_{L\alpha}$  span from 1978 to 2023: In the initial decade, starting in 1978, the average number of intensity ratio  $I_{L\beta}/I_{L\alpha}$  measurements ranged from 3 to 46, with a peak of 91 values observed in 1987. However, between 1989 and 2010, there was a substantial increase in the number of measurements, accounting for roughly 50% of all published data. It is worth noting that 1991 and 2009 were exceptions, with no recorded experimental values for this parameter during those years. Moving forward to the period from 2011 to 2023, there has been a significant reduction in the availability of experimental data. Specifically, in 2011 and 2013, there were 69 experimental values for the intensity ratios  $I_{L\beta}/I_{L\alpha}$ , distributed as 31 and 38, respectively. In contrast, in 2021 and 2022, only one value was reported for each of those years. Furthermore, in the most recent year, 2023, a single paper was published containing 19 values.
- The publication years for  $I_{L\gamma}/I_{L\alpha}$  span from 1978 to 2023: In the decades 1978–1990 there was a gradual increase in the number of measurements, with a total of 226 data points published. There were no new values published in the years 1979, 1980, and 1981, while the maximum number of data points, 75 in total, were reached in 1987. In the two decades following 1990 (from 1991 to 2010), there was an exponential growth in the number of measurements, accounting for approximately 50.9% of all published data. The only exception was in 2009 when no new publications were recorded. The remarkable growth rate in the 2000's and early 2010's peaked in 2007, with a total of 175 data points. This substantial increase was mainly attributed to the works of Demir and Sahin [44,45]. Specifically, these authors contributed 59, 50, 32, and 66 experimental data points, respectively, during this year. In the recent period from 2011 to 2023, the number of data points gradually started to decrease. We can observe years with only one data point. Notably, in the last year, particularly in the month of April, there is one article [81], while in 2014 and 2018, no new data are mentioned.
- The publication years for  $I_{L1}/I_{L\alpha}$  span from 1971 to 2023: During the period from 1971 to the end of 2000, there are an important number

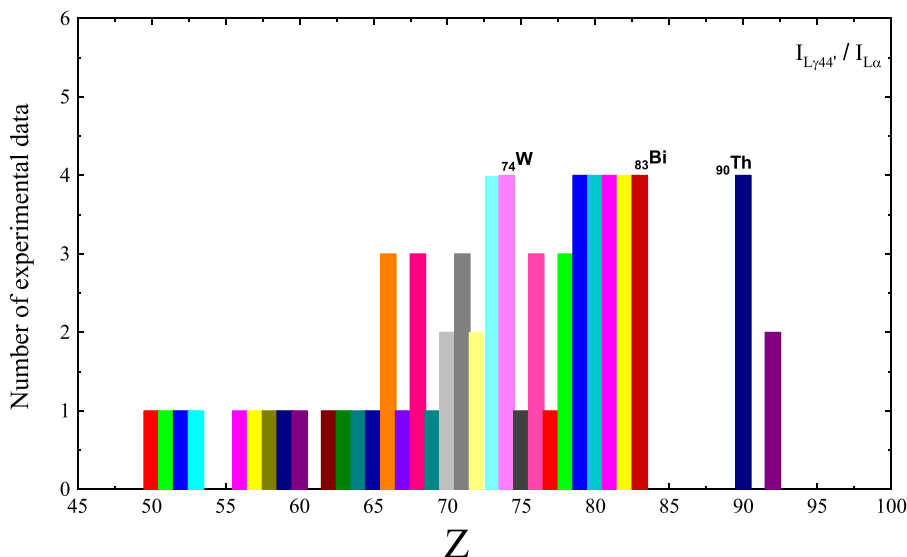


Fig. 8. Distribution of the experimental  $I_{L\gamma 44}/I_{L\alpha}$  values according to the atomic number  $Z$ .

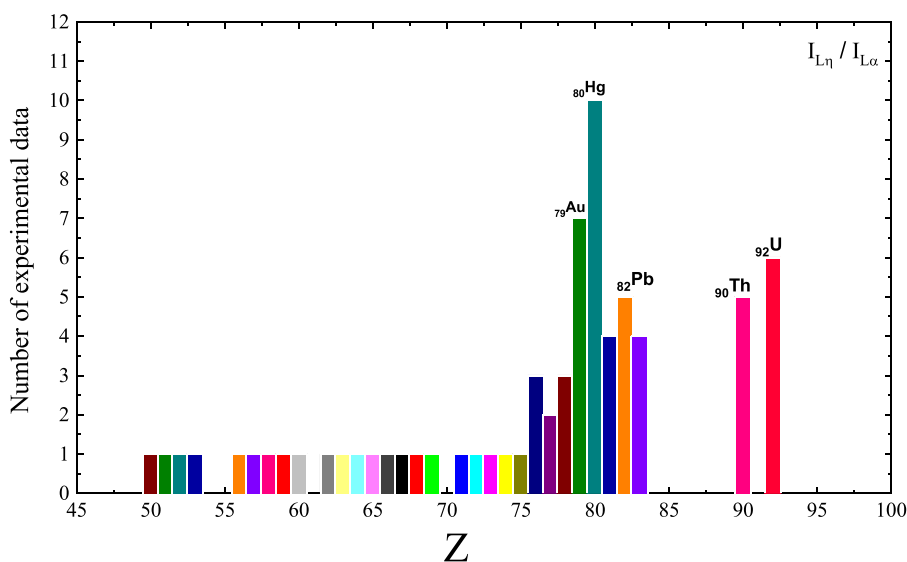


Fig. 9. Distribution of the experimental  $I_{L\eta}/I_{L\alpha}$  values according to the atomic number  $Z$ .

of published data, but during the years 1972, 1973, 1975, 1976, 1977, 1979, 1980, 1981, 1991 there are no published data. Also, we note that the two years 1983 and 1987 contain the largest number of published data with values of 42 and 50 respectively. In the decades 2001–2023, 317 data points were published with a maximum in the year 2007 (64 data points).

- For  $I_{L\gamma}/I_{L\beta}$ , articles spanning 1985 to 2015 reveal a slight gap in this intensity ratio, featuring a single value for the years 1998 and 1992. Nevertheless, between 1996 and 2015, there are a notable surge in measurements, constituting 92.4% of the total published values. As for  $I_{L\beta}/I_{L\gamma}$  and  $I_{L\beta}/I_{L\alpha}$ , data are available from 1985 to 2017. The early years (1985–1992) show limited values, but starting in 1996, there is a significant increase, peaking at 44 in 2007 for  $I_{L\beta}/I_{L\gamma}$  and 33 in 2017 for  $I_{L\beta}/I_{L\alpha}$ . Concerning the  $I_{L\eta}/I_{L\alpha}$  ratio, articles are spread across the years 1985 to 2022. Notably, 71.8% of the total values are concentrated in 2011 and 2015, while other years typically provide 1 to 5 data points.

- For  $I_{L\gamma 5}/I_{L\alpha}$ ,  $I_{L\gamma 44}/I_{L\alpha}$ , and  $I_{L\gamma 1}/I_{L\alpha}$ , the values have been published from 2006 to 2015. It is evident that these intensity ratios have garnered attention from several authors in the past decade.

Following the calculation of the weighted average value  $(Li/Lj)_w$  for all elements and intensity ratios using Eq. (7), we proceeded to determine the ratio of experimental  $Li/Lj$  intensity ratios relative to their corresponding weighted averages values for each element. This ratio, denoted as  $S = \frac{(Li/Lj)_{exp}}{(Li/Lj)_w}$ , was then graphed as a function of the atomic number  $Z$ , as illustrated in Fig. 21 for  $I_{L\beta}/I_{L\alpha}$ , Fig. 22 for  $I_{L\gamma}/I_{L\alpha}$ , Fig. 23 for  $I_{L\beta}/I_{L\alpha}$ , Fig. 24 for  $I_{L\gamma}/I_{L\beta}$ , Fig. 25 for  $I_{L\beta}/I_{L\gamma}$ , Fig. 26 for  $I_{L\beta}/I_{L\alpha}$ , Fig. 27 for  $I_{L\gamma 5}/I_{L\alpha}$ , Fig. 28 for  $I_{L\gamma 44}/I_{L\alpha}$ , Fig. 29 for  $I_{L\eta}/I_{L\alpha}$ , and Fig. 30 for  $I_{L\gamma 1}/I_{L\alpha}$ .

For  $I_{L\beta}/I_{L\alpha}$ : It is important to note that the majority values of  $S$  ratio are close to the range [0.7, 1.4], and it should be noted that some  $(I_{L\beta}/I_{L\alpha})_{EXP}$  values show a remarkably high disparity compared to the weighted values, particularly the values of Singh et al. [12], Al Salah and Saleh [16], Salah and Al-Jundi, [69] and Kumar and Puri [75] for the  $^{66}\text{Dy}$  element, as well as the values of Garg et al. [60], Kaçal et al. [47]

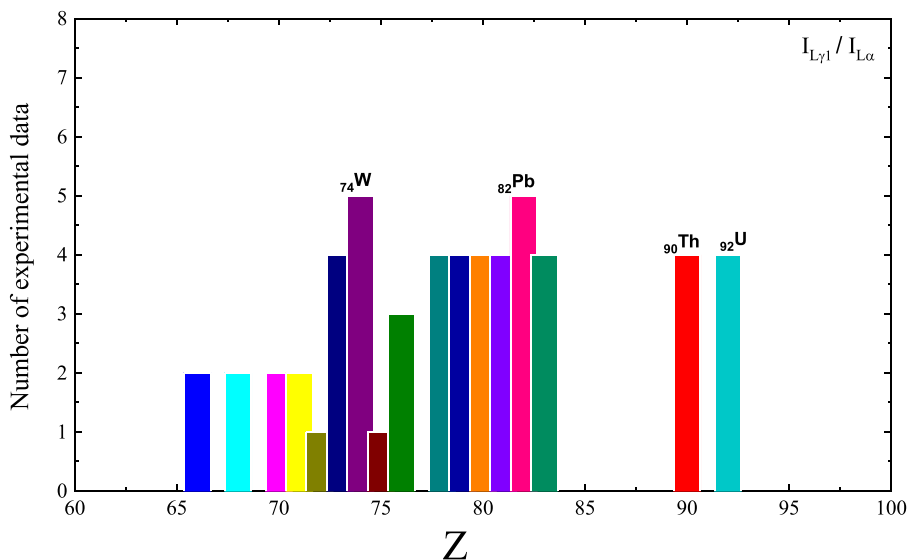


Fig. 10. Distribution of the experimental  $I_{L\gamma}/I_{L\alpha}$  values according to the atomic number  $Z$ .

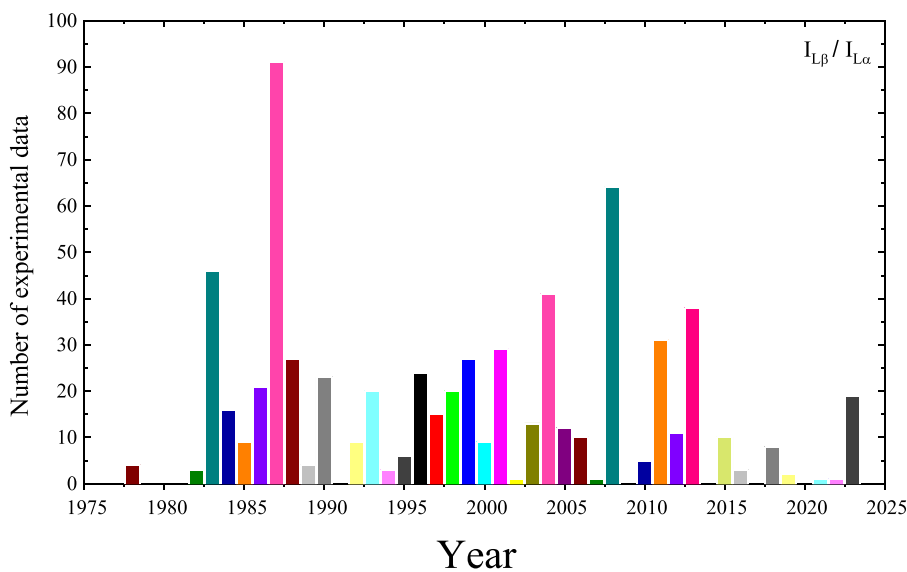


Fig. 11. Histogram of data for experimental photon-induced  $I_{L\beta}/I_{L\alpha}$  intensity ratios. The vertical lines indicate the annual number of published intensity ratios as compiled in this work.

and Alqadi et al. [81] for the  ${}_{68}\text{Er}$  and the value of Salah and Al-Jundi, [69] for  ${}_{57}\text{La}$ , where the  $S$  ratio exceeds the range  $[1, 1.4]$ . Additionally, the  $S$  ratios of Baydaş et al. [84] for  $Z = 56, 58$  and  $64$ , as well as those of Saad [17] for  ${}_{70}\text{Yb}$ , lie outside the range  $[1, 1.4]$ . This notable variation is due to the large number of experimental values published for these elements.

For  $I_{L\gamma}/I_{L\alpha}$ : It is noticeable that a few  $(I_{L\gamma}/I_{L\alpha})_{\text{EXP}}$  values have an unexpectedly large disparity when compared to the weighted values, especially the values obtained by Shatendra et al. [8] for the elements  ${}_{56}\text{Ba}$ ,  ${}_{57}\text{La}$ ,  ${}_{58}\text{Ce}$ ,  ${}_{62}\text{Sm}$ , and  ${}_{64}\text{Gd}$ ; Garg et al. [60] for  ${}_{67}\text{Ho}$ ; Ertugrul [33] for  ${}_{71}\text{Lu}$ ,  ${}_{75}\text{Re}$ ; Singh et al. [14] for  ${}_{71}\text{Lu}$ ; Salah [67] for  ${}_{57}\text{La}$ ; Kumar and Puri [75] for  ${}_{66}\text{Dy}$ , in which the ratio  $S = \frac{(I_{L\gamma}/I_{L\alpha})_{\text{EXP}}}{(I_{L\gamma}/I_{L\alpha})_w}$  is outside the range  $[0.8, 1.5]$ , and also with a few other values ( $[12, 13, 16, 32, 43, 47, 81]$ ). In addition, the ratio  $S$  of the values of Garg et al. [60] for  ${}_{70}\text{Yb}$ , Mehta et al. [22] for  ${}_{56}\text{Ba}$ , Saleh et al. [61] for  ${}_{73}\text{Ta}$ , Raghavaiah et al. [56] for  ${}_{70}\text{Yb}$ , and  ${}_{74}\text{W}$ , Dogan et al. [35] for  ${}_{73}\text{Ta}$ , and  ${}_{74}\text{W}$ , Baydaş et al. [84] for  ${}_{70}\text{Yb}$ , Öz et al. [41] for  ${}_{74}\text{W}$ , Alqadi et al. [76] for  ${}_{80}\text{Hg}$ , and Alqadi et al. [81] for  ${}_{74}\text{W}$ , are below the range  $[0.7, 1.2]$ . Nevertheless, it is evident that

most of the  $S$  values (ranging from 0.8 to 1.4) are close to unity, which would be expected for consistent data (unbiased with a reasonable uncertainty assignment).

For  $I_{L\beta}/I_{L\alpha}$ : It is clear that the vast majority of  $S$  values (in the range of 0.8 to 1.2) are near unity. Furthermore, the surprisingly notable difference in certain  $(I_{L\beta}/I_{L\alpha})_{\text{EXP}}$  values from the weighted values should be highlighted. This is particularly apparent in the research of Shatendra et al. [8] for  ${}_{56}\text{Ba}$ ,  ${}_{57}\text{La}$ , Ismail and Malhi [36], Durak and Özdemir [38], Cengiz et al. [73], Kaçal et al. [47], and Kaur et al. [78] for  ${}_{76}\text{Re}$ , and in the work of Aylikci et al. [10] for  $50 \leq Z \leq 53$  and  $71 \leq Z \leq 92$ , where the ratio  $S$  is over the range  $[0.7, 1.5]$ . Also, in Salem and Wichell [57] for  $49 \leq Z \leq 53$ , Mehta et al. [21] for  ${}_{76}\text{Re}$ , and Mehta et al. [22] for  ${}_{56}\text{Ba}$ , the values of  $S$  are outside the range  $[0.7, 1.3]$ .

Concerning  $I_{L\gamma}/I_{L\beta}$ , which has been studied in 13 different papers, it is clear that the majority of the  $S$  ratio values fall within a very close range of  $[0.7, 1.2]$ . And when we turn to  $I_{L\beta}/I_{L\gamma}$ , most of the  $S$  values are found in  $[0.6, 1.4]$ , it should be mentioned that some studies vary from the norm such as those by Ertuğrul [33] for  ${}_{69}\text{Tm}$ ,  ${}_{71}\text{Lu}$ , and  ${}_{90}\text{Th}$ , Öz et al. [41] for  ${}_{74}\text{W}$ , and  ${}_{90}\text{Th}$ , along with a few others ( $[44, 46, 54]$ ). In

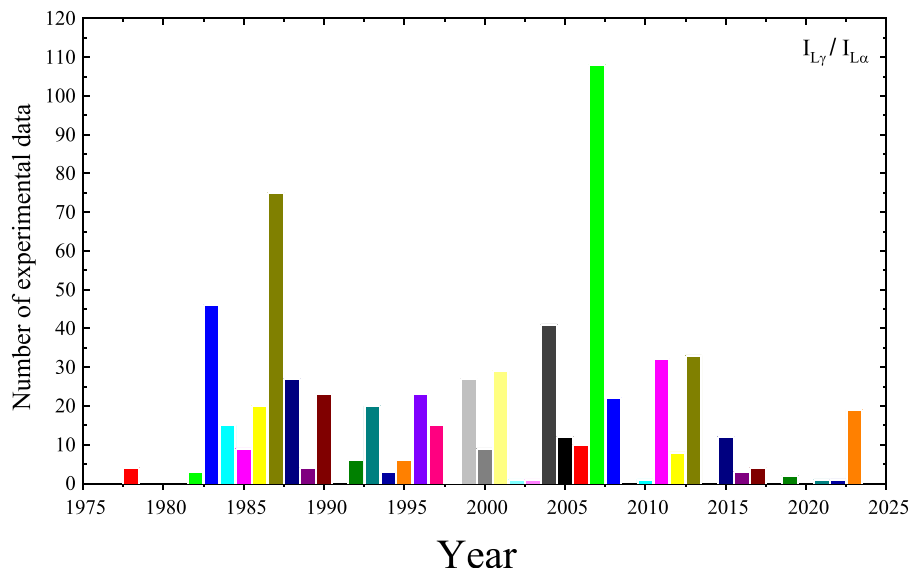


**Fig. 12.** Histogram of data for experimental photon-induced  $I_{L\gamma}/I_{L\alpha}$  intensity ratios. The vertical lines indicate the annual number of published intensity ratios as compiled in this work.

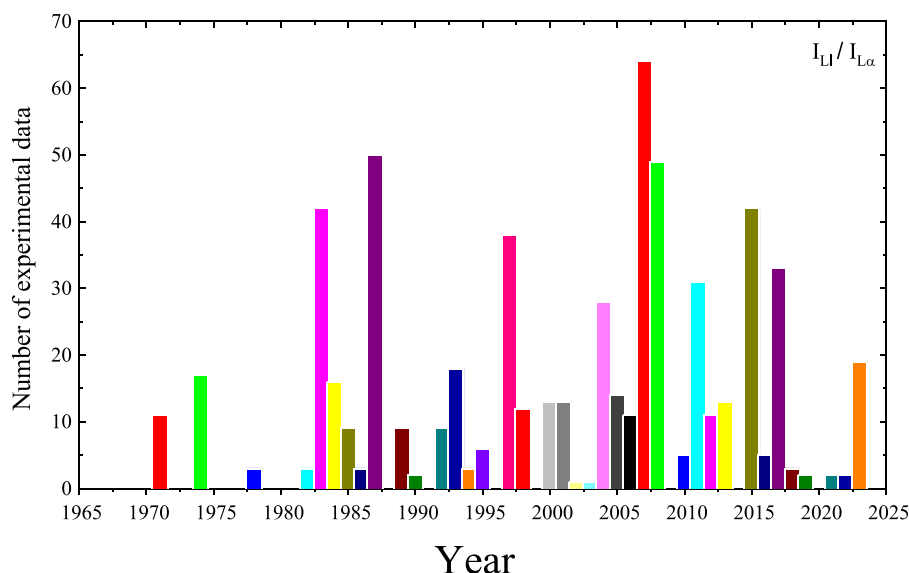


**Fig. 13.** Histogram of data for experimental photon-induced  $I_{L1}/I_{L\alpha}$  intensity ratios. The vertical lines indicate the annual number of published intensity ratios as compiled in this work.

what concerns  $I_{L1}/I_{L\beta}$ , in general the majority of the  $S$  values falls within  $[0.6, 1.3]$ , but some deviations are noted in the work of Ertuğrul [33] for the elements  $_{71}\text{Lu}$ ,  $_{73}\text{Ta}$ , and  $_{74}\text{W}$ , and also in the work of Akman et al. [1] for  $_{73}\text{Ta}$ , and  $_{74}\text{W}$ . In nearly all of the  $S$  values for  $I_{L\gamma5}/I_{L\alpha}$ ,  $I_{L\eta}/I_{L\alpha}$ , and  $I_{L\gamma1}/I_{L\alpha}$ , which have been reported in 3, 14, and 6 publications respectively, most of the  $S$  values tend to be within  $[0.7, 1.3]$ . However, there is a remarkable exception in the research of Aylikci et al. [10], where the results depart considerably from this range. Regarding  $I_{L\gamma44}/I_{L\alpha}$  it is noteworthy that the values of  $S$  reported by Karabulut and Gürol [43] for  $_{74}\text{W}$ ,  $_{82}\text{Pb}$ ,  $_{83}\text{Bi}$ , and  $_{92}\text{U}$ , and Kaçal et al. [47] for the elements  $_{66}\text{Dy}$ ,  $_{68}\text{Er}$ ,  $_{78}\text{Pt}$ , and  $_{90}\text{Th}$ , as well as Aylikci et al. [10] for  $_{71}\text{Lu}$ ,  $_{73}\text{Ta}$ ,  $_{74}\text{W}$ ,  $_{76}\text{Os}$ ,  $_{78}\text{Pt}$ ,  $_{79}\text{Au}$ ,  $_{80}\text{Hg}$ ,  $_{81}\text{Tl}$ ,  $_{82}\text{Pb}$ ,  $_{83}\text{Bi}$  and  $_{90}\text{Th}$  are significantly outside of the range  $[0.6, 1.3]$ . The considerable dispersion in experimental data can be attributed in part to the extensive use of papers for data collection without taking in account variations in experimental conditions and methods.

Plotting the signed deviation in multiples of the combined standard

deviation was calculated using formula (8) and (9), which is the divergence of the individual experimental points from the associated weighted mean for the element.

For each ratio, the distribution of Eqs. (8) and (11) as a function of the atomic number  $Z$  are represented in Figs. 31 to 40. The values of  $z_{i,ISD}$  and the average  $\bar{z}_{ISD}$  are also mentioned in the ten databases. Based on the published experimental uncertainties of certain atomic elements, the analysis of these figures shows a scatter that is far larger than expected. For instance, considering the  $I_{L\beta}/I_{L\alpha}$  ratio we observe that the values of internal standard deviation  $z_{i,ISD}$  vary between  $-9.5$  for the element  $_{64}\text{Gd}$  [84] to  $12.8$  for  $_{70}\text{Yb}$  [46] and the majority of the  $z_{i,ISD}$  values are located in the range  $[-4, 4]$  with some exceptions [20,34,46,56], where the values of  $\bar{z}_{ISD}$  range from 0 to 4. Then, moving on to the  $I_{L\gamma}/I_{L\alpha}$  ratio, where the  $z_{i,ISD}$  values are from  $-36.3$  [34] to  $36.6$  [46], it is important to note there are a few  $z_{i,ISD}$  values that appear to be significantly different from the rest and fall outside the range  $[-3, 3]$  [60,84]. After analyzing Fig. 33 for the  $I_{L1}/I_{L\alpha}$  ratio, it is evident that the average

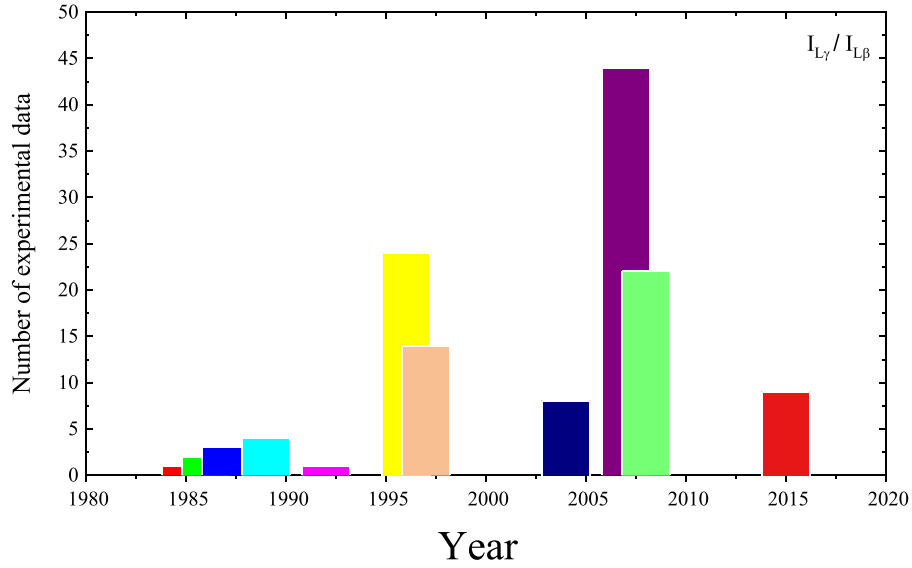


Fig. 14. Histogram of data for experimental photon-induced  $I_{L\gamma}/I_{L\beta}$  intensity ratios. The vertical lines indicate the annual number of published intensity ratios as compiled in this work.

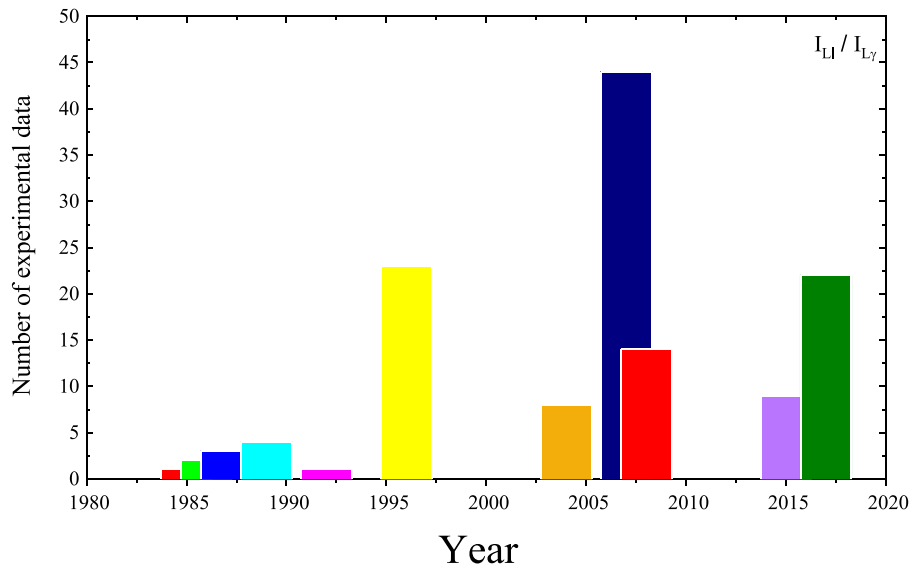


Fig. 15. Histogram of data for experimental photon-induced  $I_{LI}/I_{L\gamma}$  intensity ratios. The vertical lines indicate the annual number of published intensity ratios as compiled in this work.

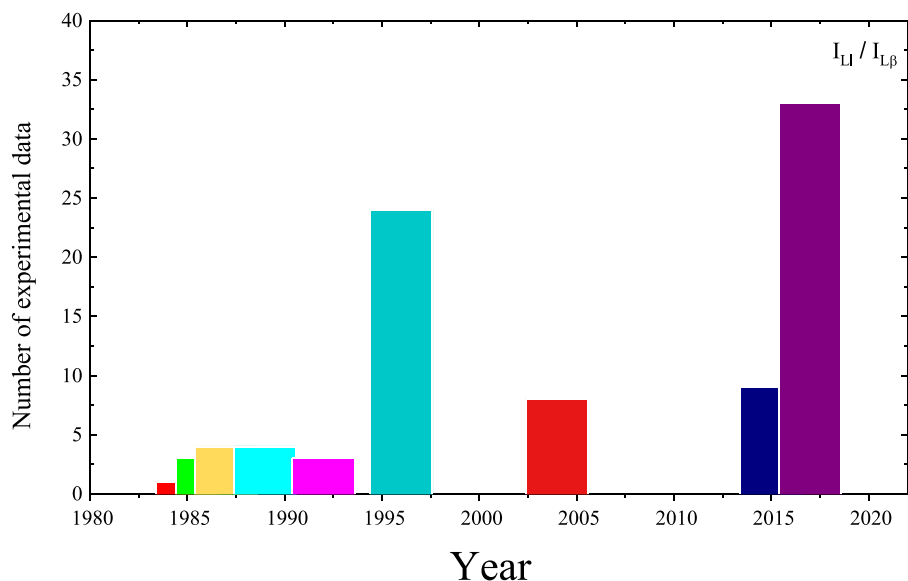


Fig. 16. Histogram of data for experimental photon-induced  $I_{L1}/I_{L\beta}$  intensity ratios. The vertical lines indicate the annual number of published intensity ratios as compiled in this work.

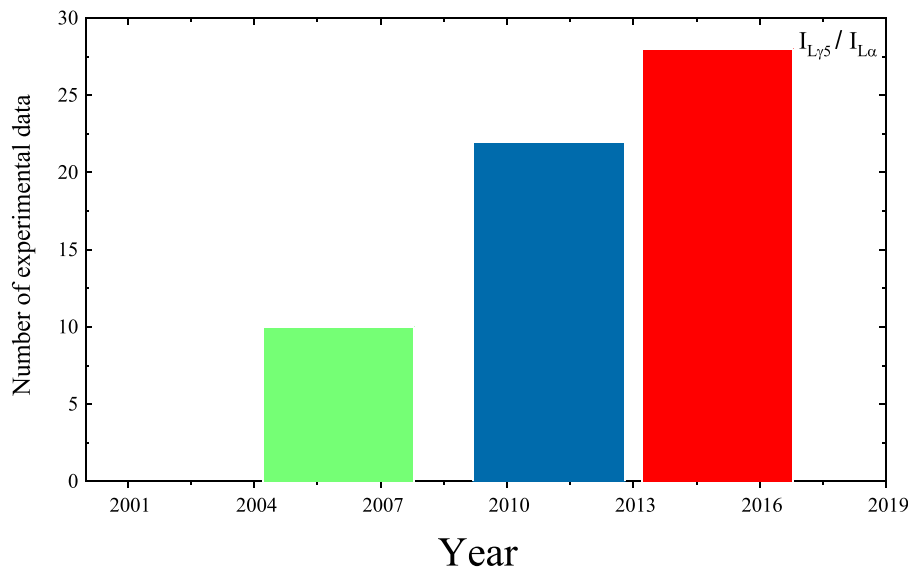


Fig. 17. Histogram of data for experimental photon-induced  $I_{L\gamma5}/I_{L\alpha}$  intensity ratios. The vertical lines indicate the annual number of published intensity ratios as compiled in this work.

z-score values range from 0 to 4.9, with for the combined internal standard deviation the majority of values falling in the  $[-3, 3]$  range. The two points observed which are located very far from this range are  $-13.8$  and  $14.2$  for  ${}_{92}\text{U}$  [34]. With a few notable exceptions [20,34,46,54], almost all of standard deviation  $z_{i,ESD}$  values for the  $I_{L\gamma}/I_{L\beta}$ ,  $I_{L1}/I_{L\gamma}$ , and  $I_{L1}/I_{L\beta}$  ratios are in the range  $[-4, 4]$ . Except for [10] data, all other values for the  $I_{L\gamma5}/I_{L\alpha}$ ,  $I_{L\gamma44}/I_{L\alpha}$ ,  $I_{L\eta}/I_{L\alpha}$ , and  $I_{L\gamma1}/I_{L\alpha}$  ratios are inside the range  $[-5, 5]$ .

Figs. 41 to 50 present the distribution of Eqs. (9) and (12) according to the atomic number  $Z$ . Additionally, in the two last columns of the ten databases the values of both  $z_{i,ESD}$  and  $\bar{z}_{ESD}$  are also included. After analyzing these figures, we notice that for the  $I_{L\beta}/I_{L\alpha}$  ratio the values of external standard deviation  $z_{i,ESD}$  vary between  $-8$  for the element  ${}_{64}\text{Gd}$  [84] to 8 for  ${}_{68}\text{Er}$  [60], and nearly all the values fall within the range of  $[-4, 4]$ , and for  $\bar{z}_{ESD}$  span the range from 0 to 3. For the  $I_{L\gamma}/I_{L\alpha}$  ratio, it is clear that majority of the values of  $z_{i,ESD}$  are located in the range  $[-3, 3]$ , with a few exceptions [14,34,53,60,62,90]. Next, turning one's

attention to the  $I_{L1}/I_{L\alpha}$  ratio, it is remarkable that one value of  $z_{i,ESD}$  seems to significantly diverge from the others by being in the range  $[-4, 4]$  [34]. Examination of Figs. 44–49, and Fig. 50 for  $I_{L\gamma}/I_{L\beta}$ ,  $I_{L1}/I_{L\gamma}$ ,  $I_{L1}/I_{L\beta}$ ,  $I_{L\gamma5}/I_{L\alpha}$ ,  $I_{L\gamma44}/I_{L\alpha}$ ,  $I_{L\eta}/I_{L\alpha}$ , and  $I_{L\gamma1}/I_{L\alpha}$ , respectively, shows it is evident that a most of the values of  $z_{i,ESD}$  are located inside the range  $[-3, 3]$ .

This dispersion (z-scores exceeding 2 or 3 in magnitude) means that the experimenters reported uncertainties that may not be well evaluated and may include contributions from hidden errors. Figs. 31 to 50 indicate that in order to help resolve inconsistencies and improve the quality of experimental guidance, further high-quality experimental data will be needed, along with accurate uncertainty evaluations, precise explanations, and uncertainty quantifications. Our effort reported here is the first step toward enabling a thorough assessment. The original publications listed in the references are available to researchers who are interested in a specific element.

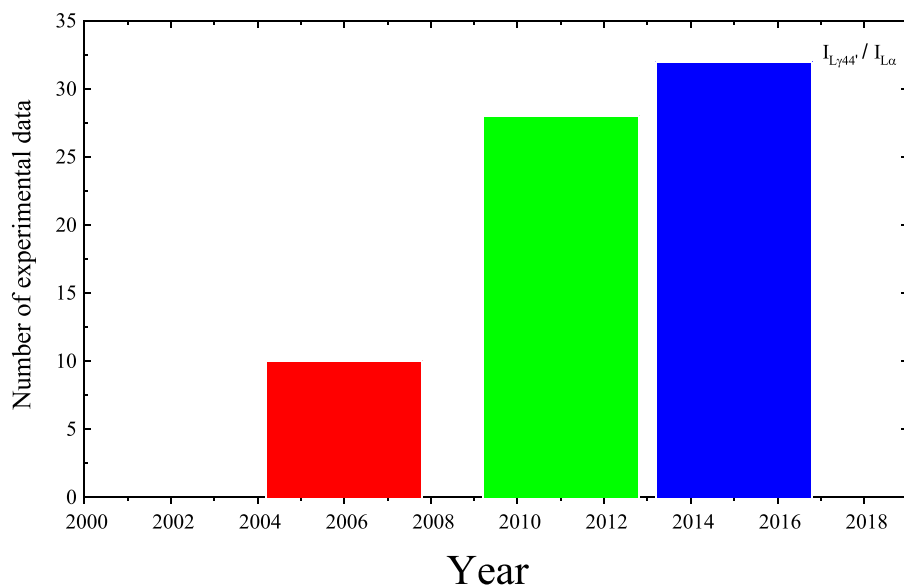


Fig. 18. Histogram of data for experimental photon-induced  $I_{L\gamma 44} / I_{L\alpha}$  intensity ratios. The vertical lines indicate the annual number of published intensity ratios as compiled in this work.

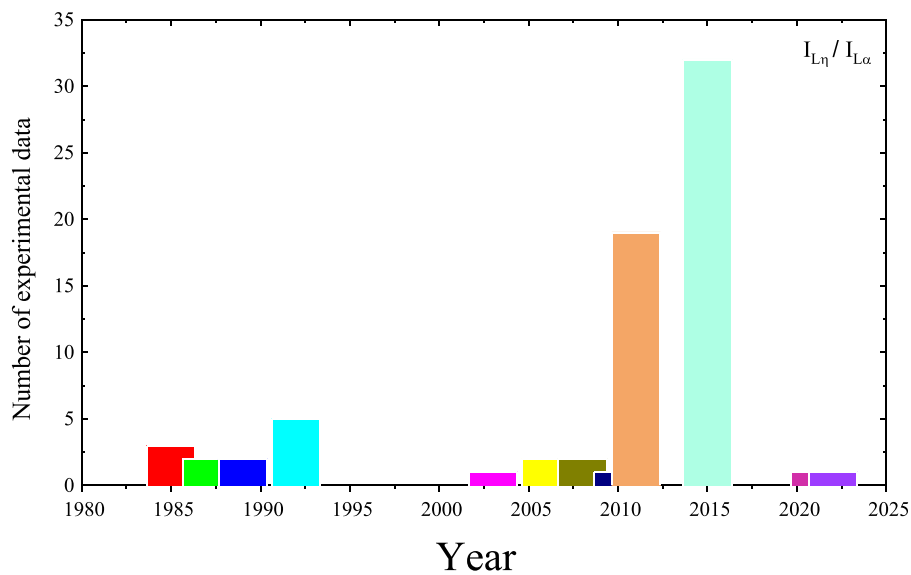


Fig. 19. Histogram of data for experimental photon-induced  $I_{L\eta} / I_{L\alpha}$  intensity ratios. The vertical lines indicate the annual number of published intensity ratios as compiled in this work.

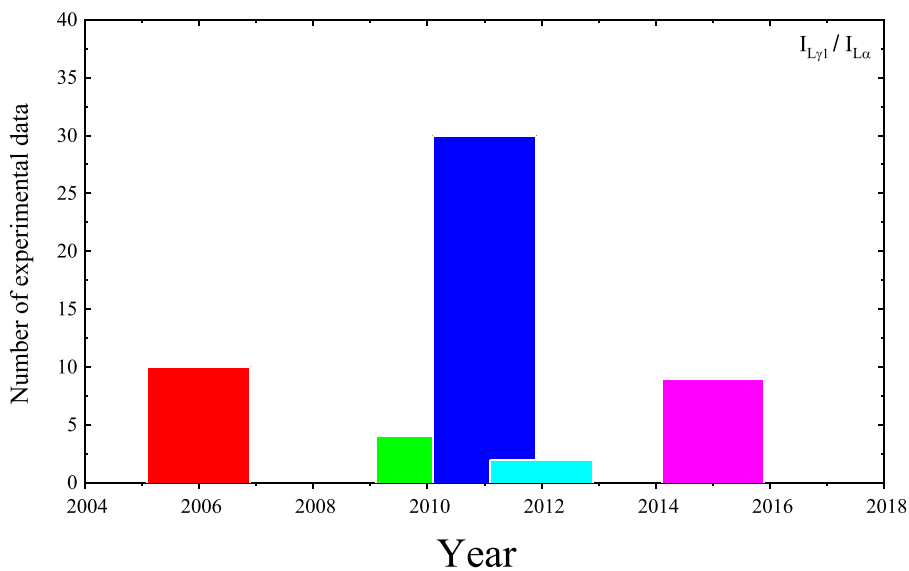


Fig. 20. Histogram of data for experimental photon-induced  $I_{L\beta 1}/I_{L\alpha}$  intensity ratios. The vertical lines indicate the annual number of published intensity ratios as compiled in this work.

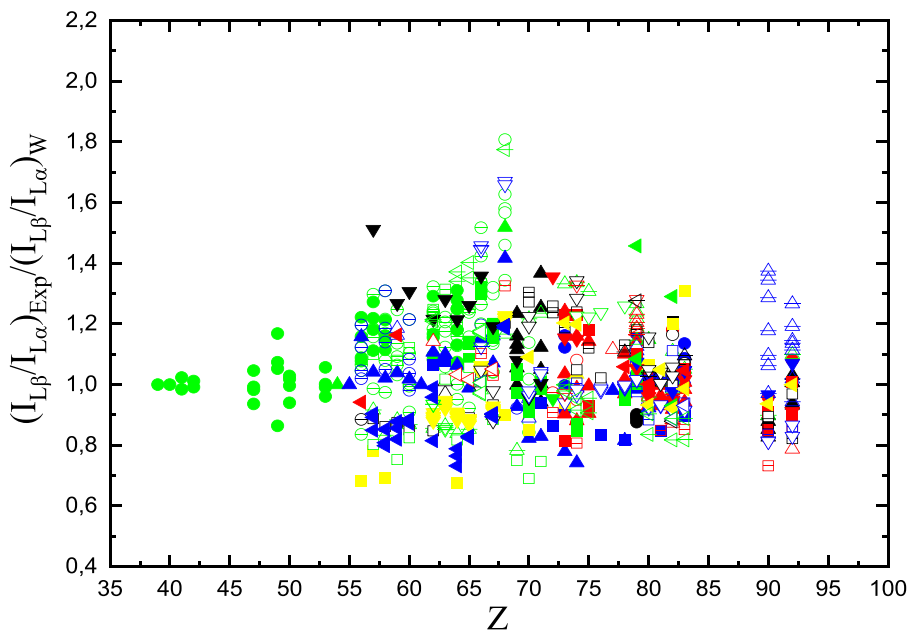
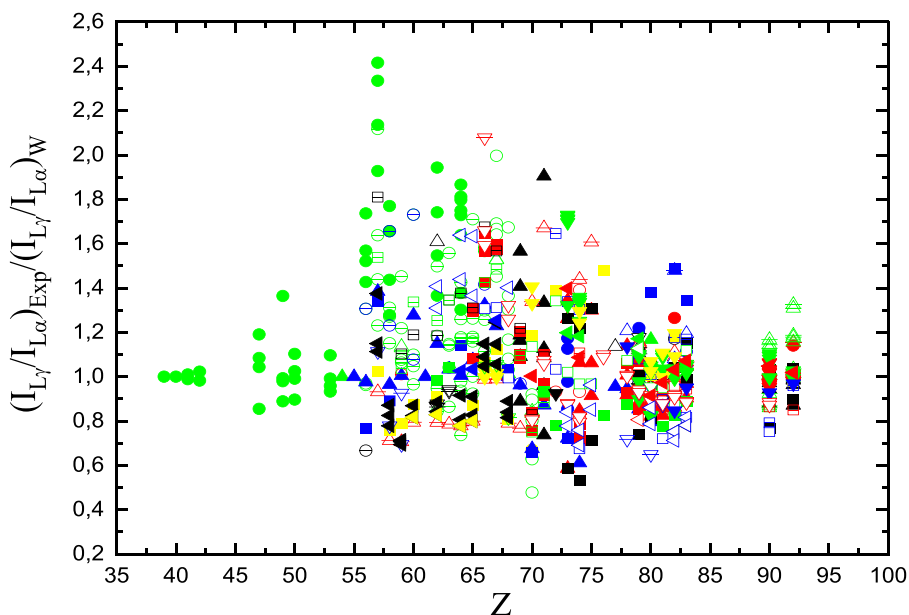
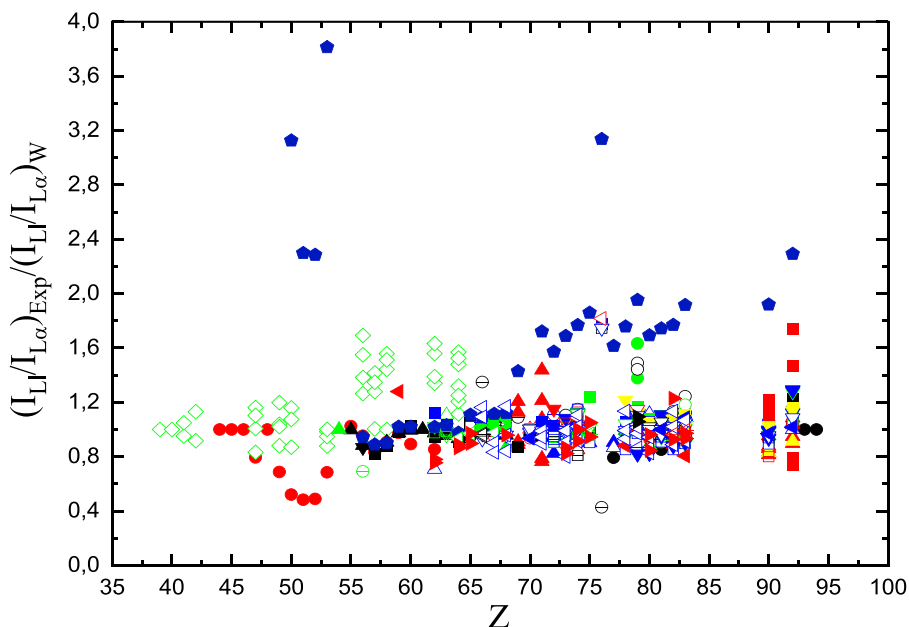


Fig. 21. The distribution of  $(I_{L\beta}/I_{L\alpha})_{EXP} / (I_{L\beta}/I_{L\alpha})_W$  for each reference from which the databases are extracted according to the atomic number  $Z$  (from 1978 to 2023). ●: [7]; ●: [89]; ●: [8]; ●: [58]; ●: [20]; ○: [85]; ○: [59]; ○: [60]; ○: [21]; ⊖: [22]; ⊖: [23]; ⊖: [12]; ⊖: [13]; ▲: [14]; ▲: [61]; ▲: [24]; ▲: [56]; ▲: [25]; △: [26]; △: [32]; △: [88]; △: [62]; △: [63]; △: [64]; △: [33]; △: [34]; ■: [90]; ■: [35]; ■: [16]; ■: [36]; ■: [84]; □: [38]; □: [66]; □: [17]; □: [39]; □: [40]; □: [41]; □: [67]; □: [68]; ▼: [69]; ▼: [43]; ▼: [71]; ▼: [27]; ▼: [72]; ▼: [46]; ▼: [18]; ▼: [73]; ▼: [47]; ▼: [86]; ▼: [74]; ▼: [87]; ▼: [75]; ◀: [49]; ◀: [76]; ◀: [50]; ◀: [51]; ◀: [1]; ◀: [77]; ◀: [53]; ◀: [92]; ◀: [55]; ◀: [80]; ◀: [19]; ◀: [81].



**Fig. 22.** The distribution of  $(I_{L\gamma}/I_{L\alpha})_{Exp} / (I_{L\gamma}/I_{L\alpha})_W$  for each reference from which the databases are extracted according to the atomic number  $Z$  (from 1978 to 2023).  
 ●: [7]; ●: [89]; ●: [8]; ●: [58]; ●: [20]; ○: [85]; ○: [59]; ○: [60]; ○: [21]; ⊖: [22]; ⊖: [23]; ⊖: [12]; ⊖: [13]; ▲: [14]; ▲: [61]; ▲: [24]; ▲: [56];  
 ▲: [25]; △: [32]; △: [88]; △: [62]; △: [63]; △: [64]; △: [33]; △: [34]; △: [90]; ■: [35]; ■: [16]; ■: [36]; ■: [84]; ■: [38]; □: [66]; □: [39]; □: [40]; □: [41]; □: [67]; □: [68]; □: [69]; □: [43]; ▼: [71]; ▼: [44]; ▼: [45]; ▼: [27]; ▼: [46]; ▼: [18]; ▼: [47]; ▼: [86]; ▼: [48]; ▼: [87]; ▼: [75]; ▼: [49]; ▼: [76]; ▼: [51]; ▼: [1]; ▼: [52]; ▼: [53]; ▼: [91]; ▼: [55]; ▼: [80]; ▼: [19]; ▼: [81].



**Fig. 23.** The distribution of  $(I_{L1}/I_{L\alpha})_{Exp} / (I_{L1}/I_{L\alpha})_W$  for each reference from which the databases are extracted according to the atomic number  $Z$  (from 1971 to 2023).  
 ●: [28]; ●: [57]; ●: [7]; ●: [89]; ◇: [8]; ○: [58]; ○: [20]; ○: [85]; ○: [59]; ⊖: [21]; ⊖: [29]; ⊖: [22]; ⊖: [23]; ▲: [30]; ▲: [14]; ▲: [24]; ▲: [15];  
 ▲: [31]; △: [25]; △: [26]; △: [32]; △: [88]; △: [62]; △: [63]; △: [64]; ■: [65]; ■: [34]; ■: [35]; ■: [36]; ■: [37]; □: [38]; □: [66]; □: [39]; □: [40]; □: [41]; □: [68]; □: [42]; □: [43]; ▼: [70]; ▼: [71]; ▼: [45]; ▼: [9]; ▼: [27]; ▼: [46]; ▼: [18]; ▼: [73]; ▼: [47]; ▼: [86]; ▼: [74]; ▼: [87]; ▼: [75]; ▼: [49]; ▼: [76]; ▼: [51]; ▼: [1]; ▼: [10]; ▼: [77]; ▼: [78]; ▼: [53]; ▼: [54]; ▼: [92]; ▼: [55]; ▼: [79]; ▼: [80]; ▼: [19]; ▼: [81].

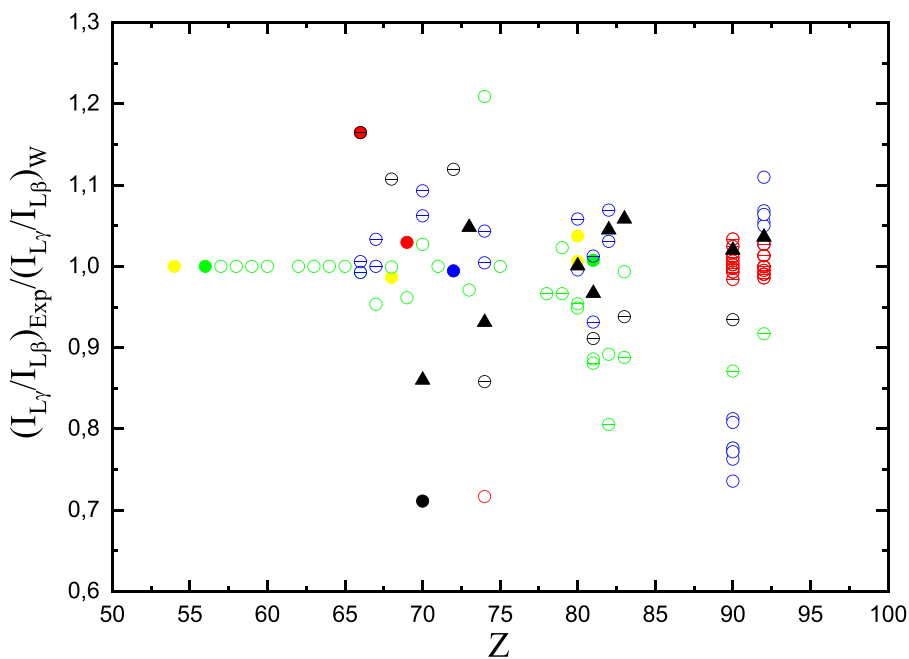


Fig. 24. The distribution of  $(I_{L\gamma}/I_{L\beta})_{Exp}/(I_{L\gamma}/I_{L\beta})_W$  for each reference from which the databases are extracted according to the atomic number  $Z$  (from 1985 to 2015).  
 ●: [20]; ●: [21]; ●: [22]; ●: [23]; ●: [24]; ○: [25]; ○: [33]; ○: [34]; ⊖: [41]; ⊖: [44]; ⊖: [27]; ⊖: [46]; ▲: [1].

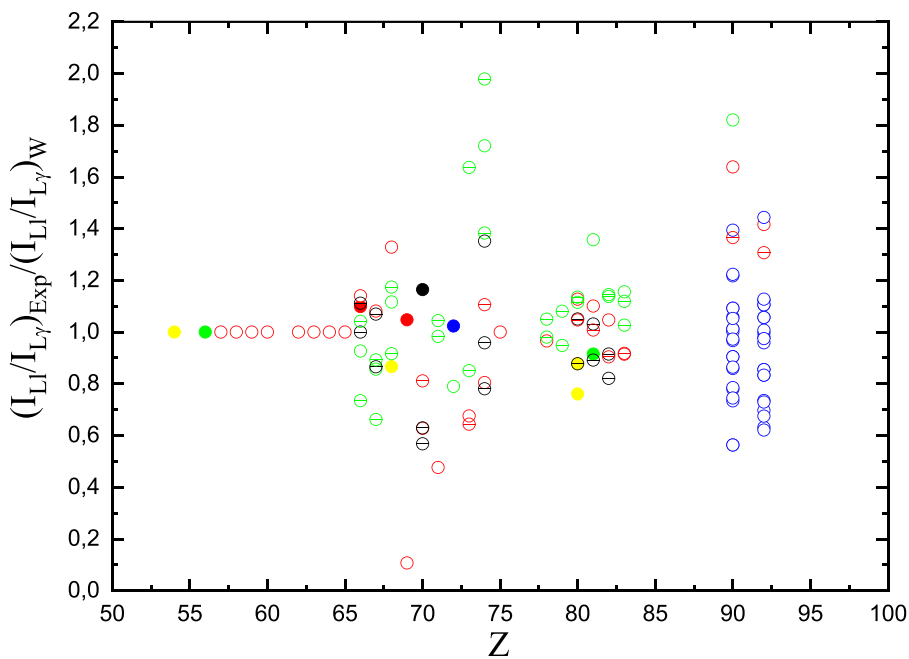


Fig. 25. The distribution of  $(I_{L1}/I_{L\gamma})_{Exp}/(I_{L1}/I_{L\gamma})_W$  for each reference from which the databases are extracted according to the atomic number  $Z$  (from 1985 to 2017).  
 ●: [20]; ●: [21]; ●: [22]; ●: [23]; ●: [24]; ○: [25]; ○: [33]; ○: [41]; ○: [44]; ⊖: [46]; ⊖: [1]; ⊖: [54].

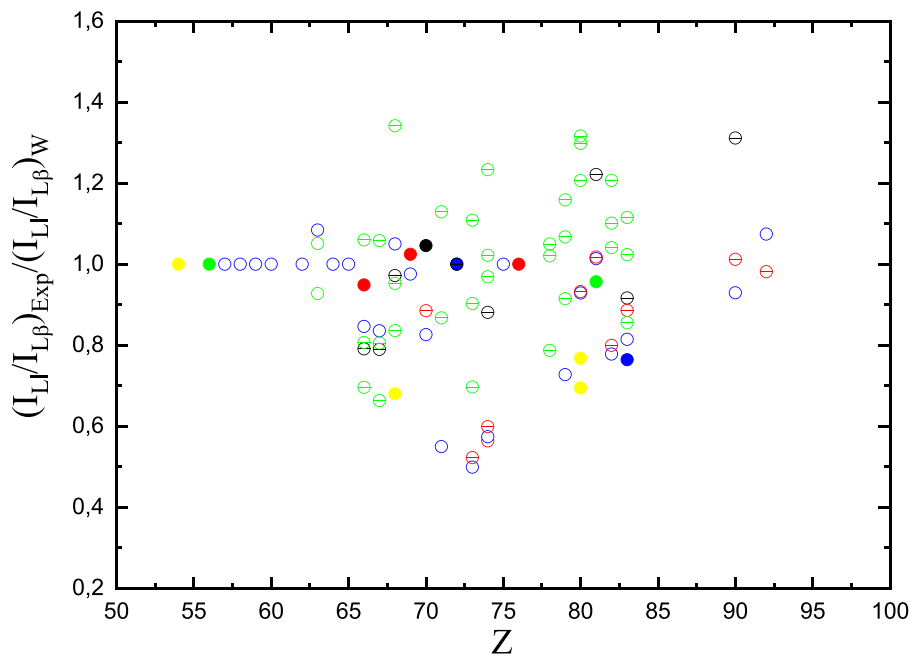


Fig. 26. The distribution of  $(I_{L1}/I_{L\beta})_{EXP}/(I_{L1}/I_{L\beta})_W$  for each reference from which the databases are extracted according to the atomic number  $Z$  (from 1985 to 2017). ●: [20]; ●: [21]; ●: [22]; ●: [23]; ●: [24]; ○: [25]; ○: [26]; ○: [33]; ⊖: [41]; ⊖: [1]; ⊖: [54].

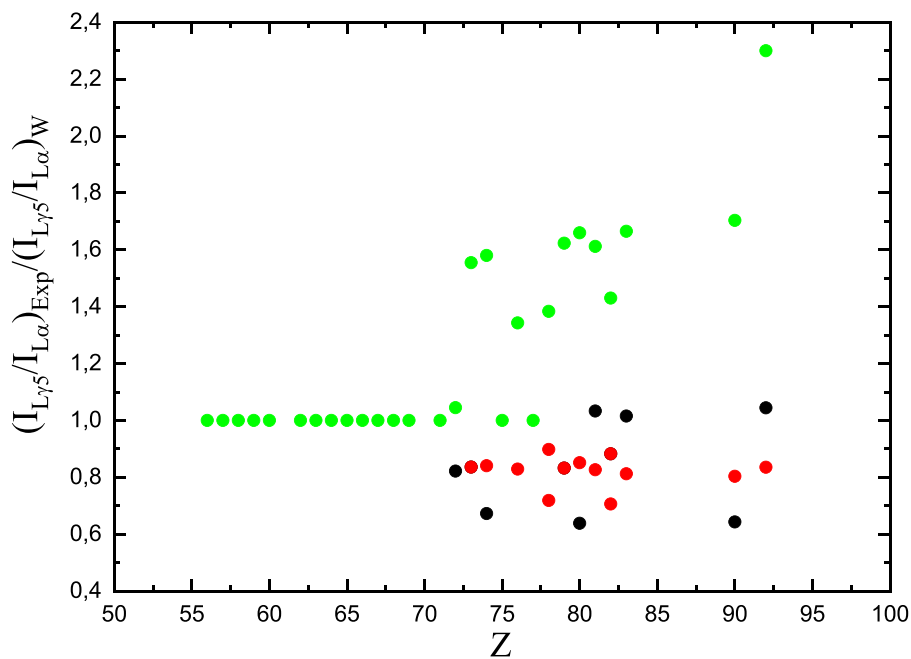


Fig. 27. The distribution of  $(I_{L\gamma5}/I_{L\alpha})_{EXP}/(I_{L\gamma5}/I_{L\alpha})_W$  for each reference from which the databases are extracted according to the atomic number  $Z$  (from 2006 to 2015). ●: [43]; ●: [47]; ●: [10].

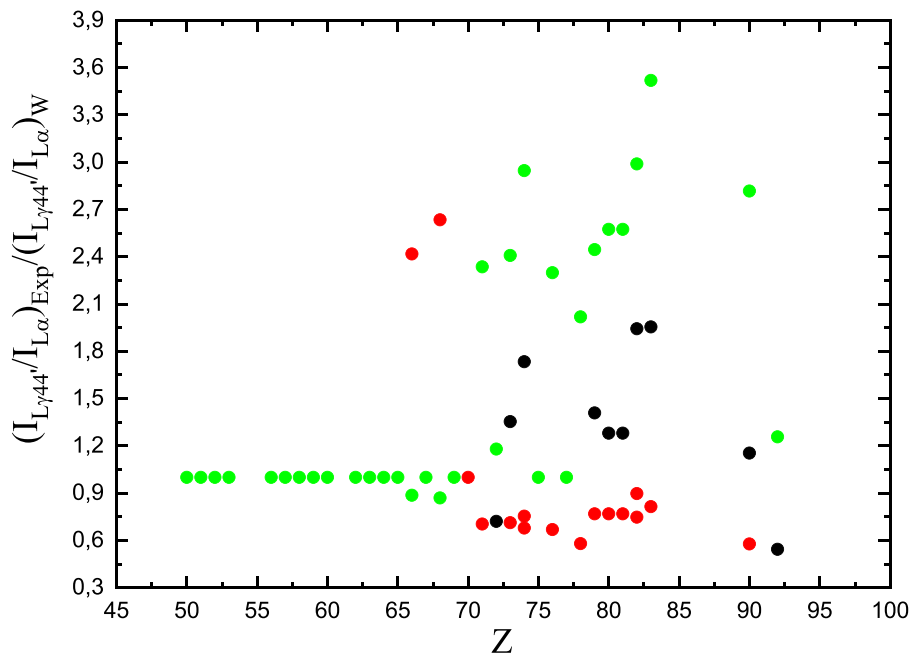


Fig. 28. The distribution of  $(I_{Ly44}/I_{L\alpha})_{Exp} / (I_{Ly44}/I_{L\alpha})_W$  for each reference from which the databases are extracted according to the atomic number  $Z$  (from 2006 to 2015). ●: [43]; ●: [47]; ●: [10].

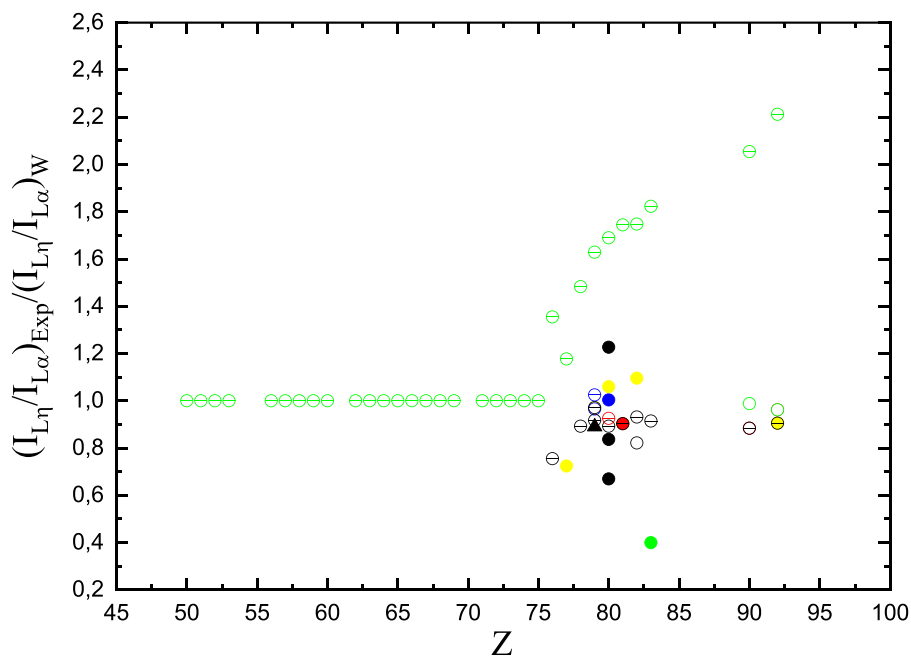


Fig. 29. The distribution of  $(I_{Ln}/I_{L\alpha})_{Exp} / (I_{Ln}/I_{L\alpha})_W$  for each reference from which the databases are extracted according to the atomic number  $Z$  (from 1985 to 2022). ●: [59]; ●: [22]; ●: [23]; ●: [24]; ●: [32]; ○: [39]; ○: [43]; ○: [27]; ○: [18]; ○: [47]; ○: [86]; ○: [10]; ○: [80]; ▲: [19].

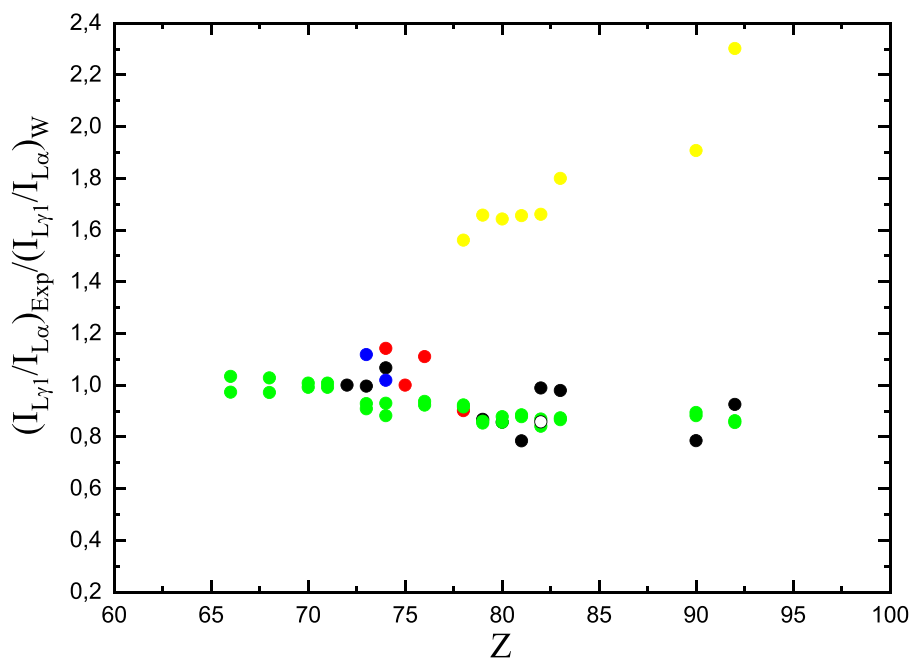


Fig. 30. The distribution of  $(I_{L\gamma 1}/I_{L\alpha})_{Exp}/(I_{L\gamma 1}/I_{L\alpha})_W$  for each reference from which the databases are extracted according to the atomic number  $Z$  (from 2006 to 2015). ●: [43]; ●: [73]; ●: [22]; ●: [23]; ●: [10]; ○: [77].

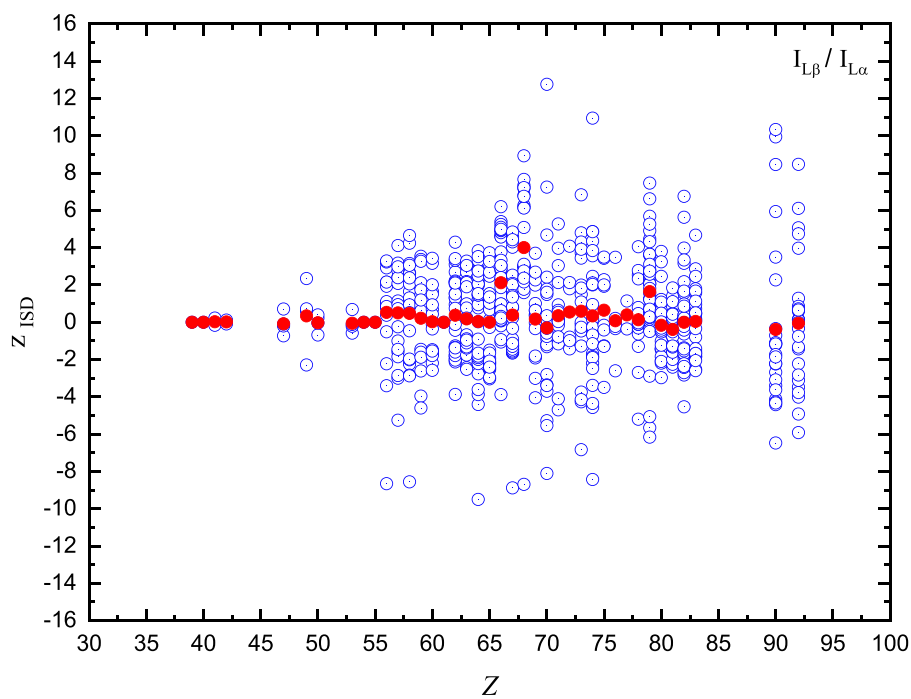


Fig. 31. Distribution of Eqs. (8) and (11) for  $I_{L\beta}/I_{L\alpha}$  according to the atomic number  $Z$ .

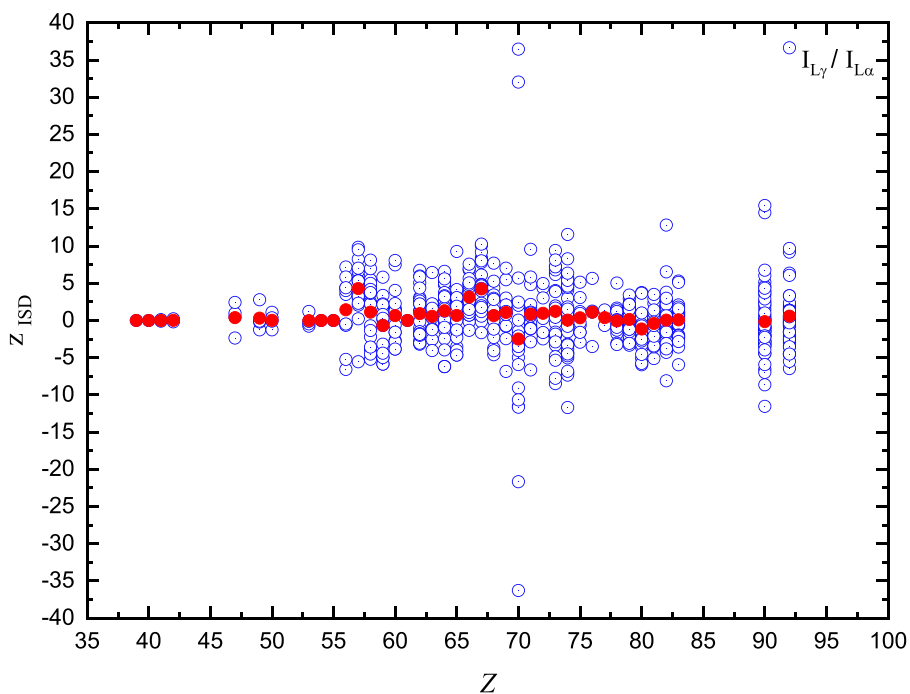


Fig. 32. Distribution of Eqs. (8) and (11) for  $I_{L\gamma}/I_{L\alpha}$  according to the atomic number  $Z$ .

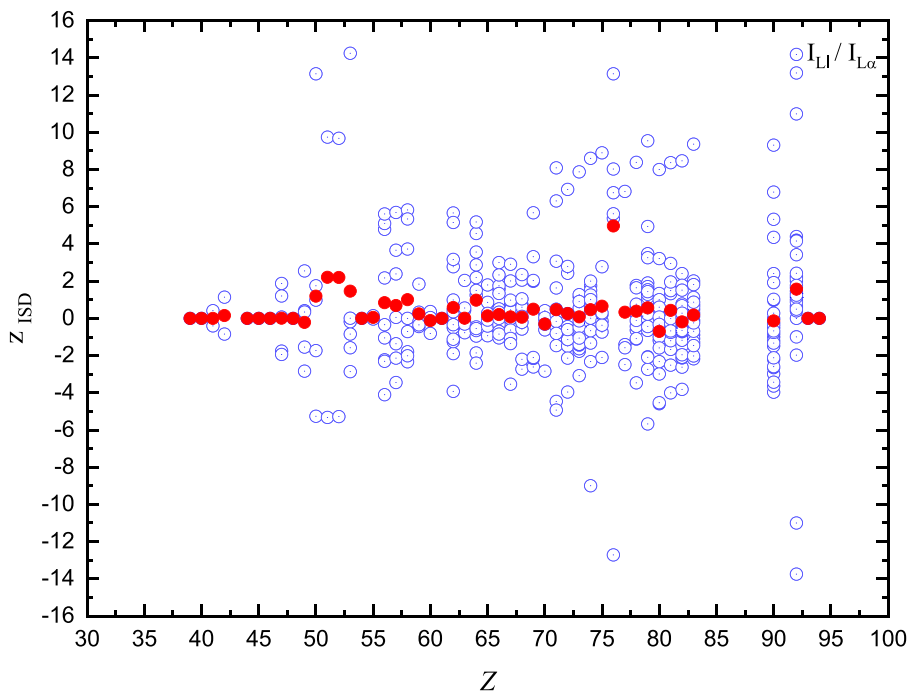


Fig. 33. Distribution of Eqs. (8) and (11) for  $I_{L1}/I_{L\alpha}$  according to the atomic number  $Z$ .

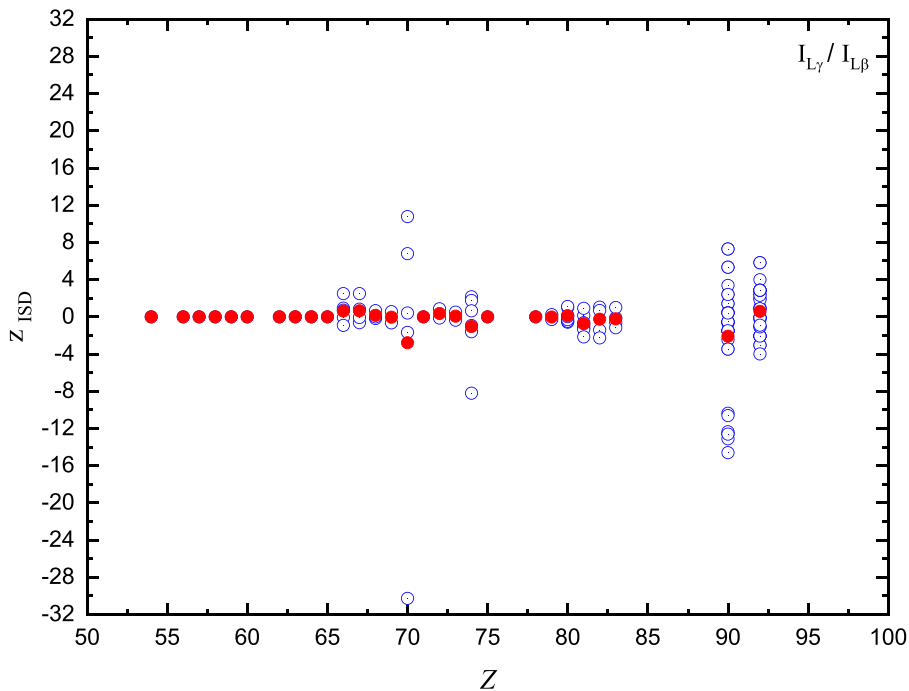


Fig. 34. Distribution of Eqs. (8) and (11) for  $I_{L\gamma}/I_{L\beta}$  according to the atomic number  $Z$ .

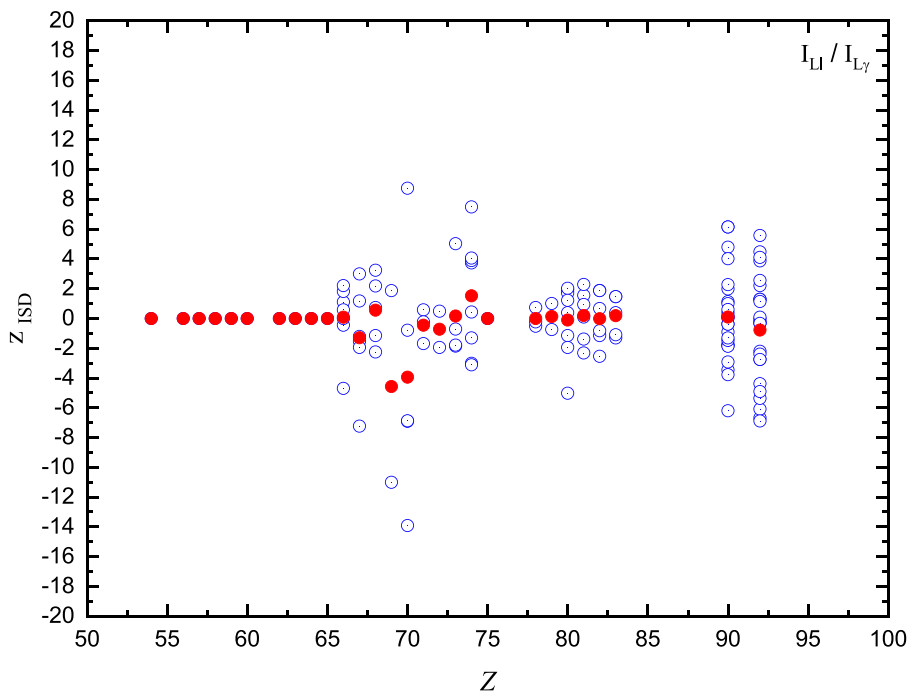


Fig. 35. Distribution of Eqs. (8) and (11) for  $I_{L1}/I_{L\gamma}$  according to the atomic number  $Z$ .

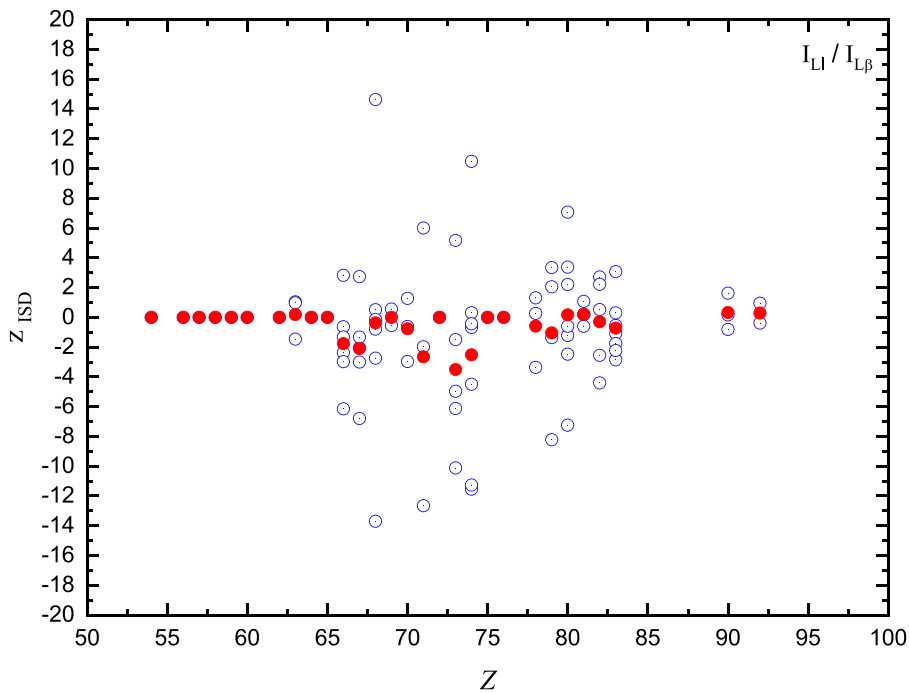


Fig. 36. Distribution of Eqs. (8) and (11) for  $I_{L1}/I_{L\beta}$  according to the atomic number  $Z$ .

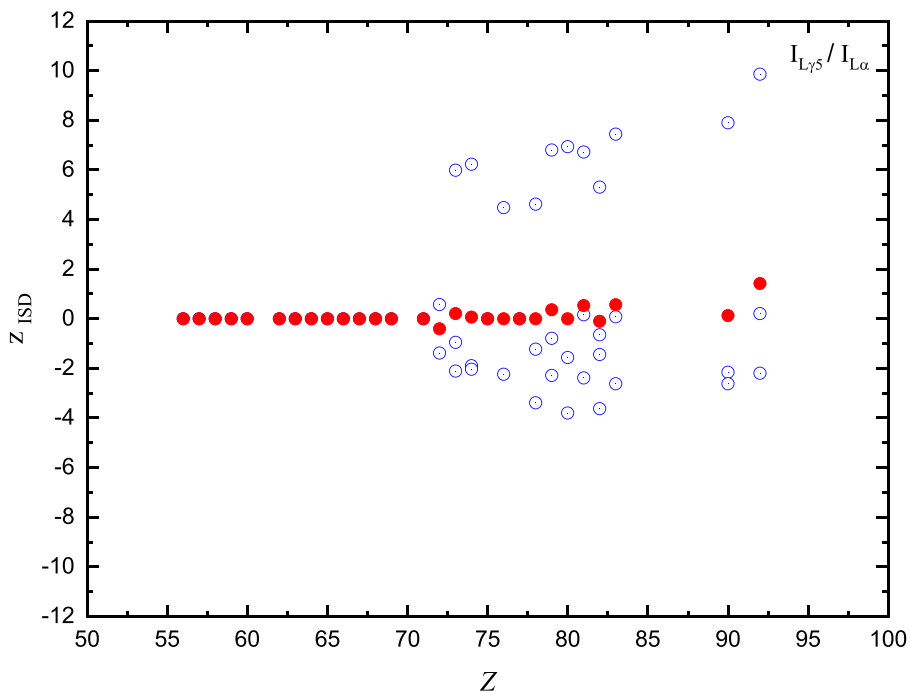


Fig. 37. Distribution of Eqs. (8) and (11) for  $I_{L\gamma5}/I_{L\alpha}$  according to the atomic number  $Z$ .

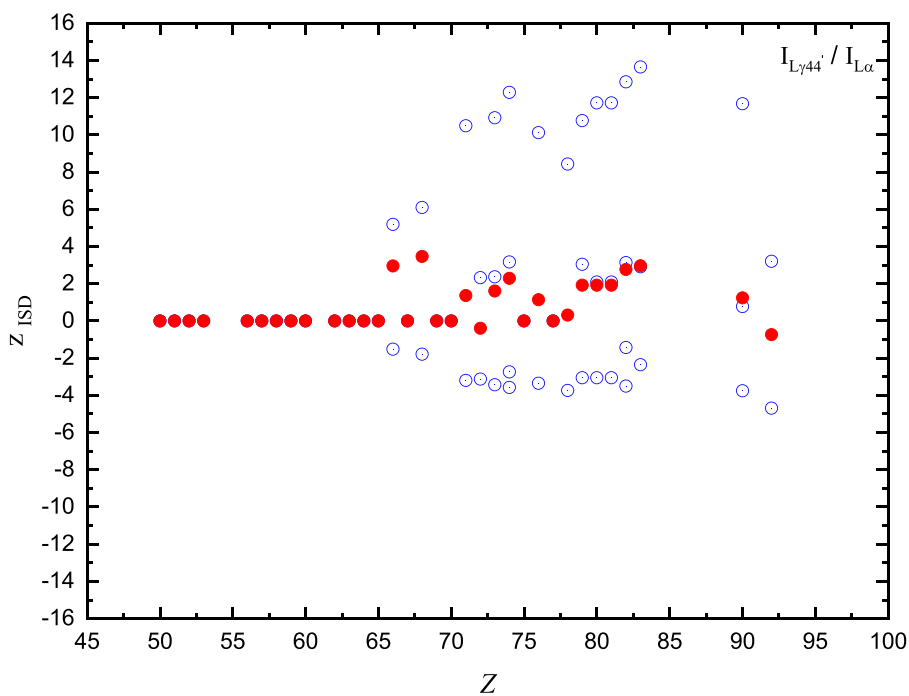


Fig. 38. Distribution of Eqs. (8) and (11) for  $I_{L\gamma44}/I_{L\alpha}$  according to the atomic number  $Z$ .

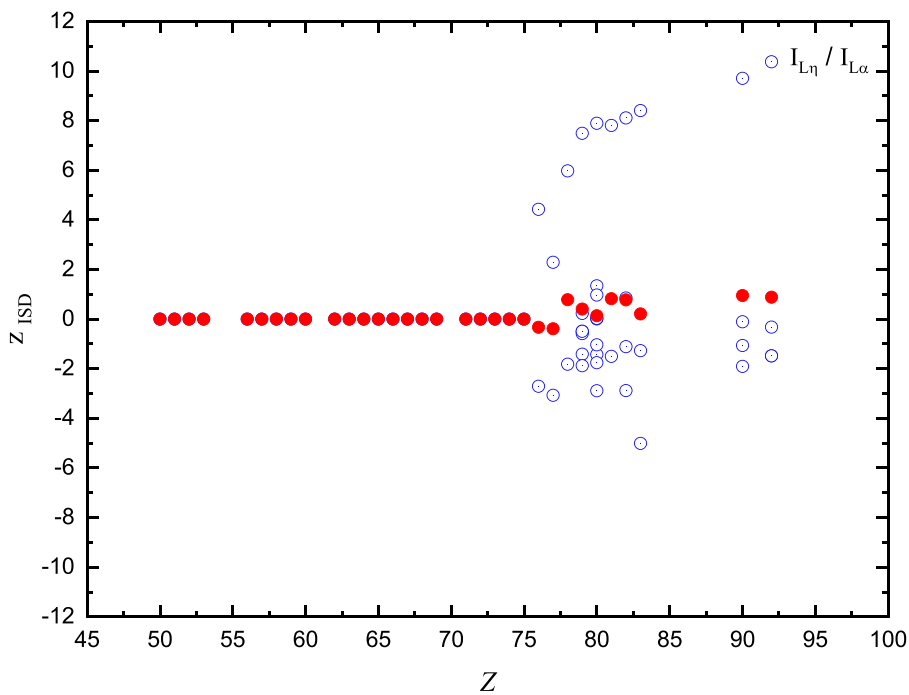


Fig. 39. Distribution of Eqs. (8) and (11) for  $I_{L\eta}/I_{L\alpha}$  according to the atomic number  $Z$ .

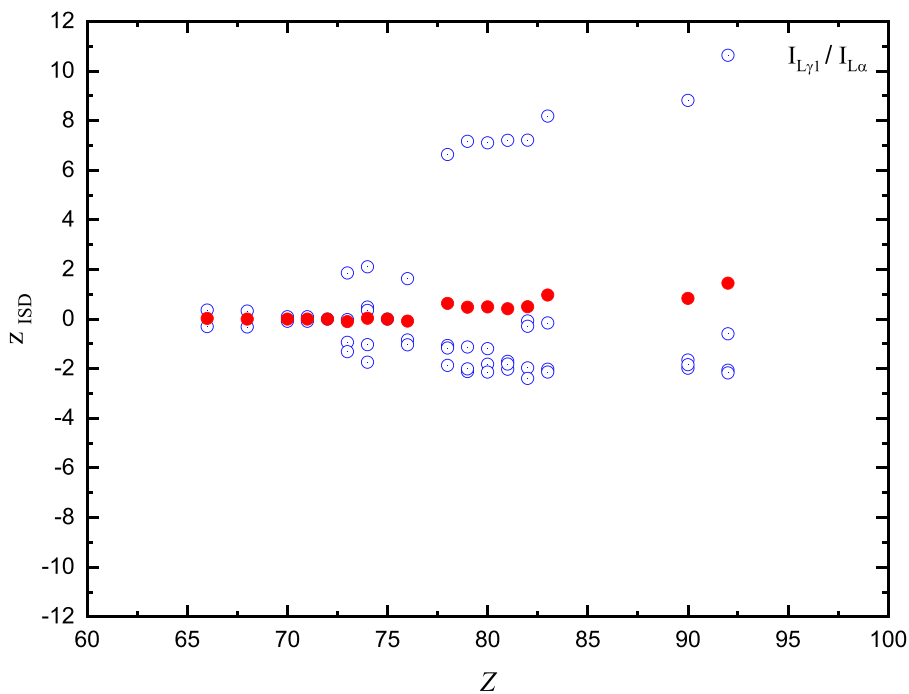


Fig. 40. Distribution of Eqs. (8) and (11) for  $I_{L\gamma 1}/I_{L\alpha}$  according to the atomic number  $Z$ .

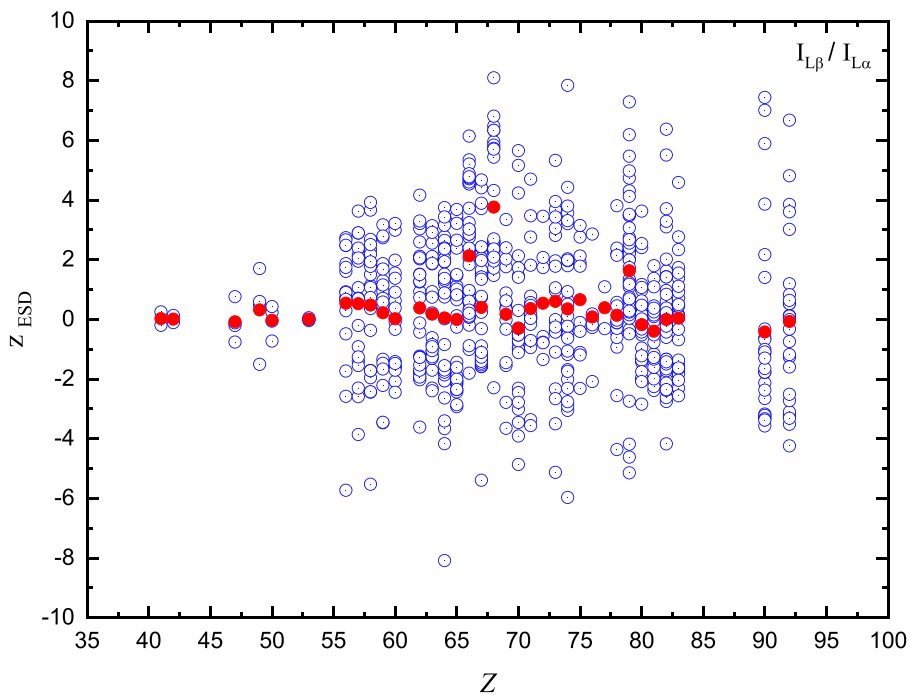


Fig. 41. Distribution of Eqs. (9) and (12) for  $I_{L\beta}/I_{L\alpha}$  according to the atomic number  $Z$ .

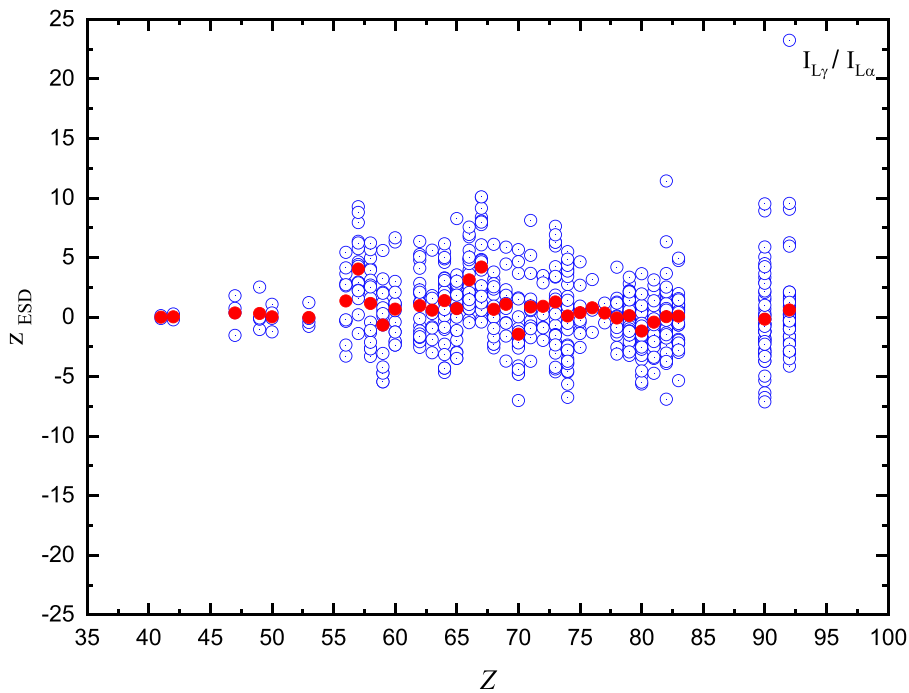


Fig. 42. Distribution of Eqs. (9) and (12) for  $I_{L\gamma} / I_{L\alpha}$  according to the atomic number  $Z$ .

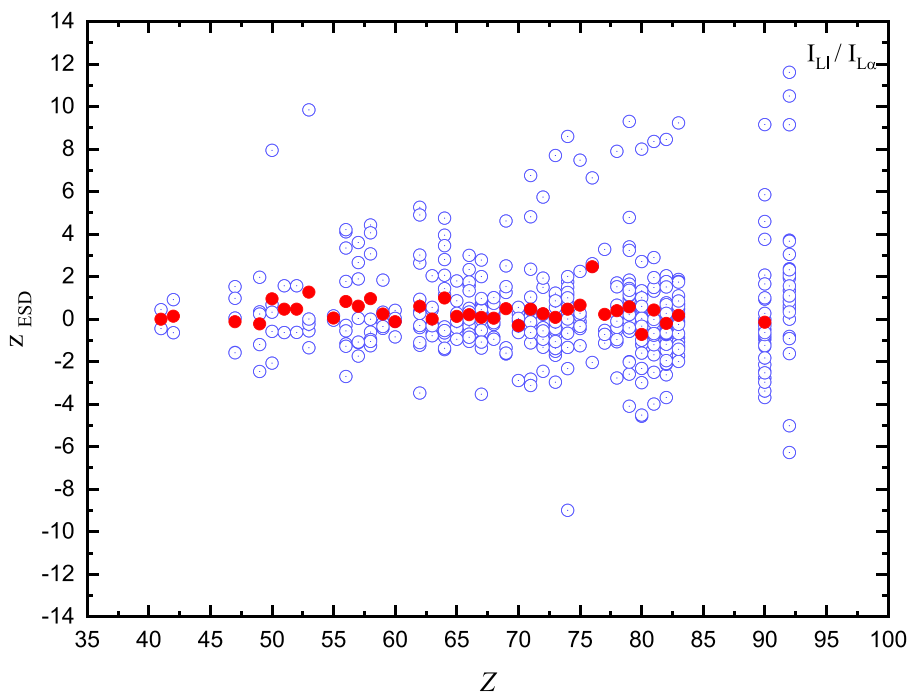


Fig. 43. Distribution of Eqs. (9) and (12) for  $I_{L1} / I_{L\alpha}$  according to the atomic number  $Z$ .

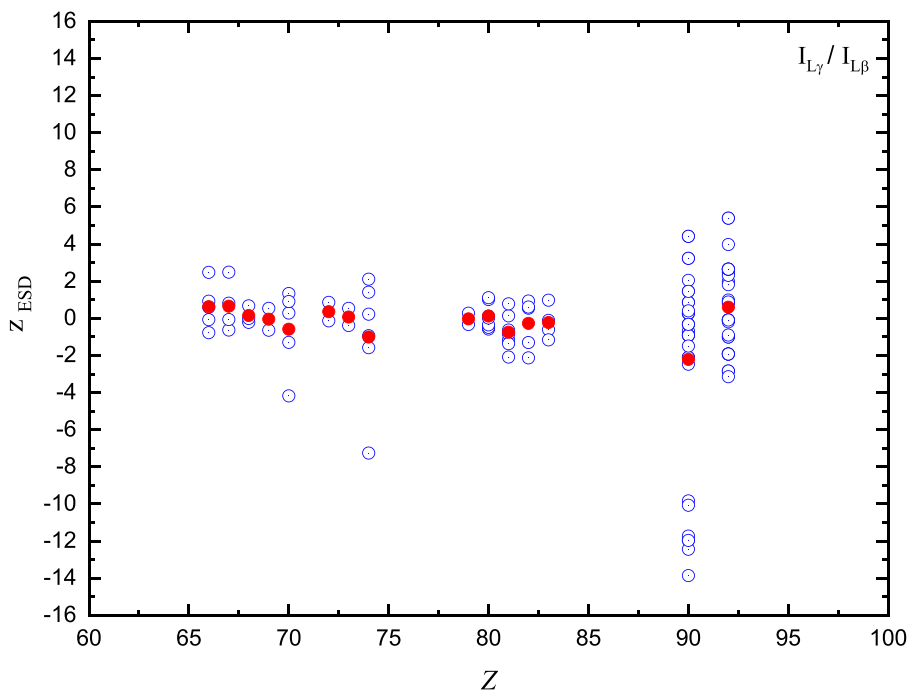


Fig. 44. Distribution of Eqs. (9) and (12) for  $I_{L\gamma} / I_{L\beta}$  according to the atomic number  $Z$ .

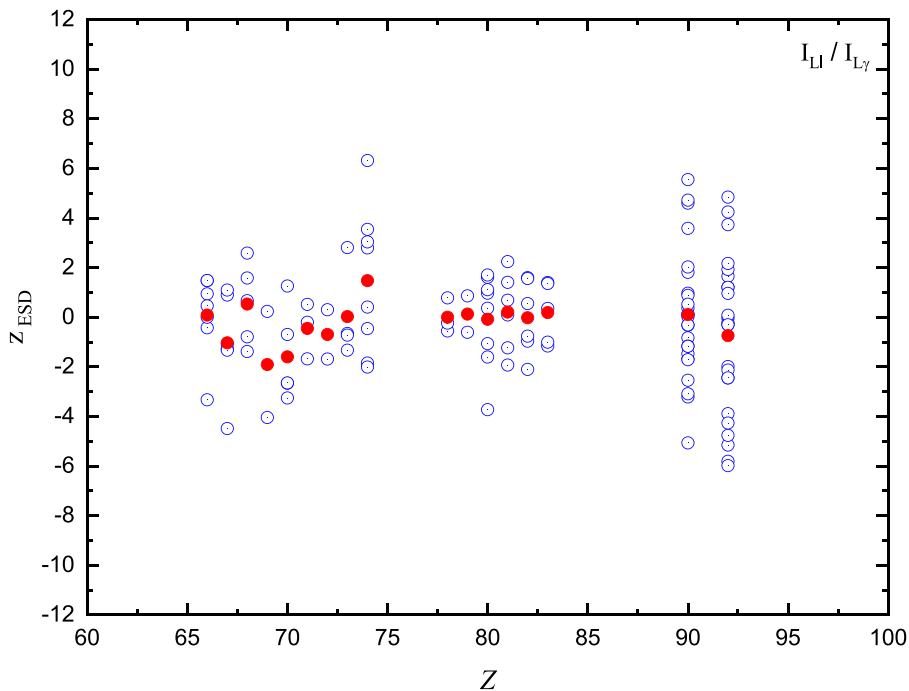


Fig. 45. Distribution of Eqs. (9) and (12) for  $I_{L1} / I_{L\gamma}$  according to the atomic number  $Z$ .

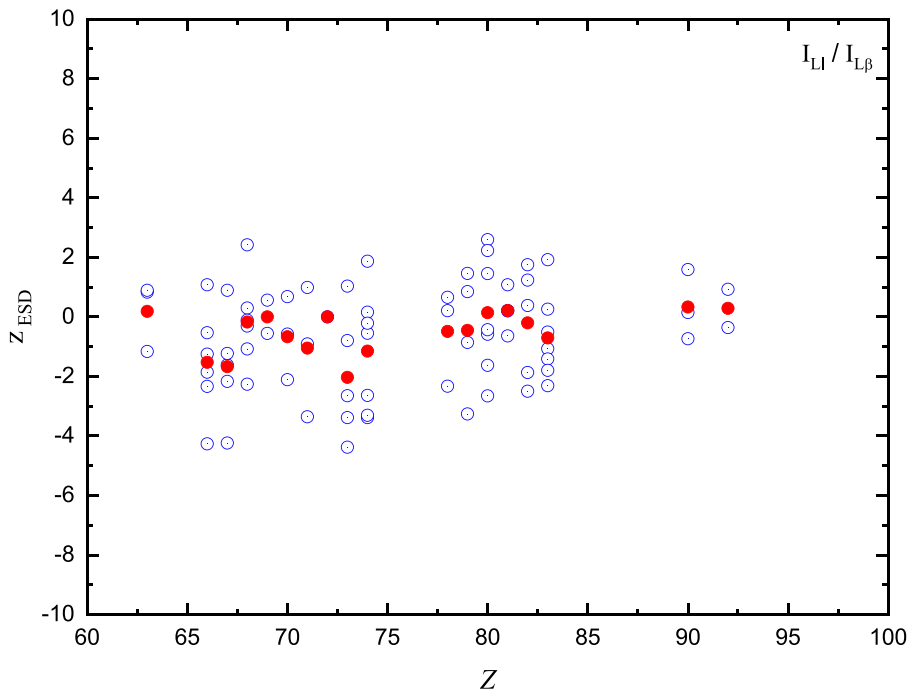


Fig. 46. Distribution of Eqs. (9) and (12) for  $I_{L1}/I_{L\beta}$  according to the atomic number  $Z$ .

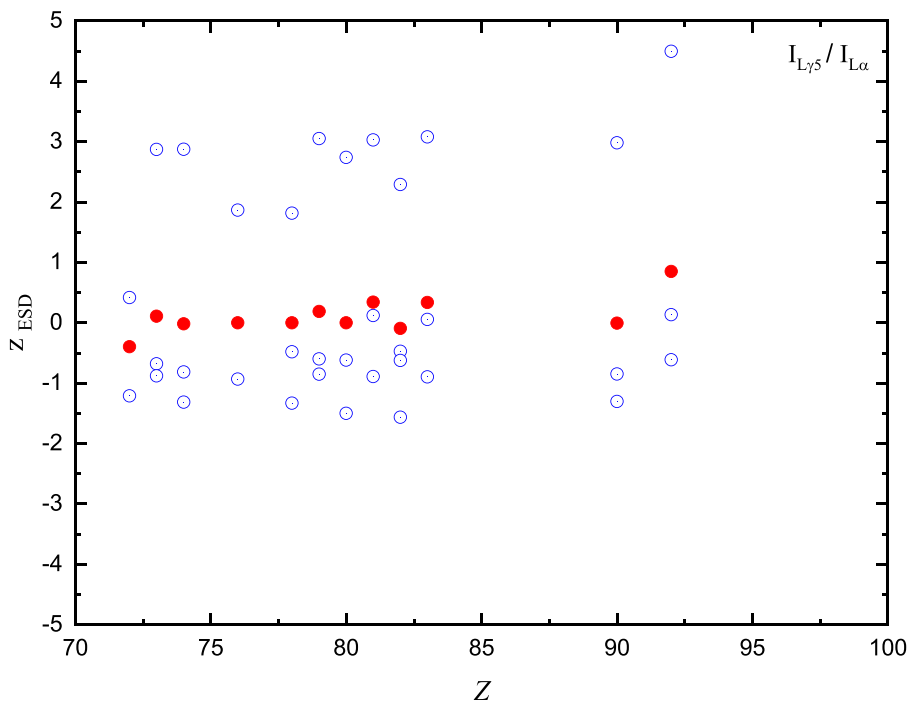


Fig. 47. Distribution of Eqs. (9) and (12) for  $I_{L75}/I_{L\alpha}$  according to the atomic number  $Z$ .

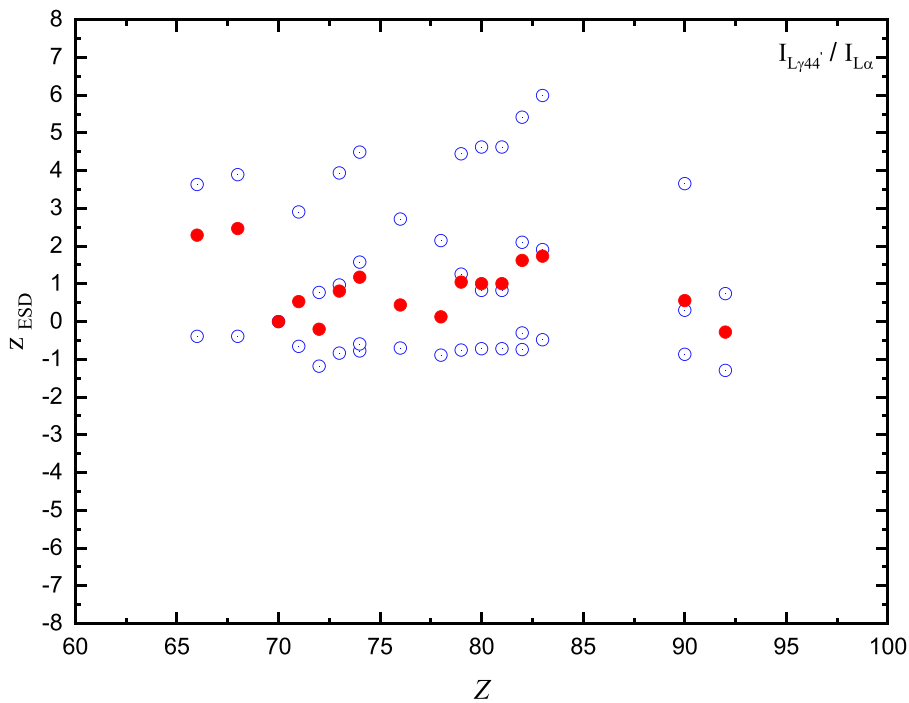


Fig. 48. Distribution of Eqs. (9) and (12) for  $I_{L\gamma44}/I_{L\alpha}$  according to the atomic number  $Z$ .

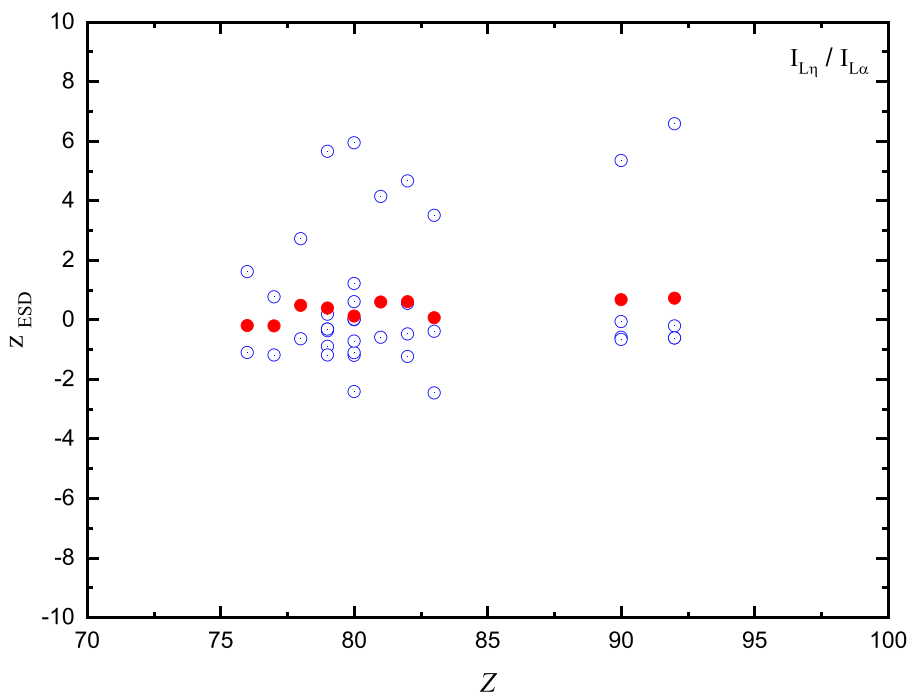


Fig. 49. Distribution of Eqs. (9) and (12) for  $I_{L\eta}/I_{L\alpha}$  according to the atomic number  $Z$ .

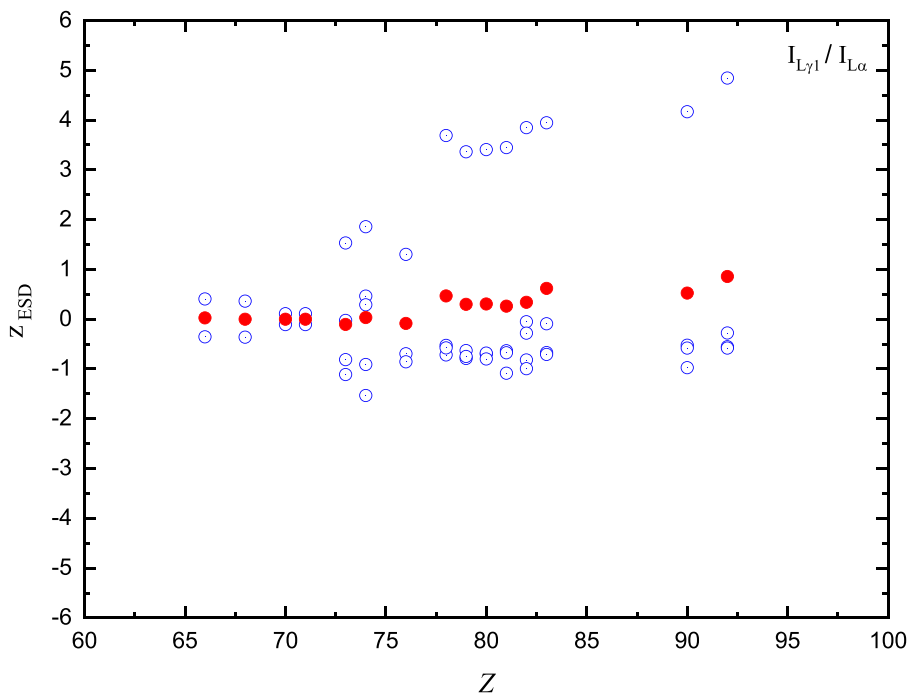


Fig. 50. Distribution of Eqs. (9) and (12) for  $I_{L\gamma 1}/I_{L\alpha}$  according to the atomic number  $Z$ .

## 2. Conclusion

A detailed review and presentation in the form of tables of intensity ratios data  $I_{L_i}/I_{L_j}$  induced by photons has been completed. A total of 2600 values have been published in the period from 1971 to April 2023. To the best of our knowledge, this is the first attempt to provide a comprehensive summary of experimental data values for intensity ratios of L lines in the atomic range  $39 \leq Z \leq 92$  for  $I_{L\beta}/I_{L\alpha}$  and  $I_{L\gamma}/I_{L\alpha}$ ,  $39 \leq Z \leq 94$  for  $I_{L\delta}/I_{L\alpha}$ ,  $54 \leq Z \leq 92$  for  $I_{L\gamma}/I_{L\beta}$ ,  $I_{L\delta}/I_{L\gamma}$ , and  $I_{L\delta}/I_{L\beta}$ ,  $50 \leq Z \leq 92$  for  $I_{L\gamma 44}/I_{L\alpha}$ , and  $I_{L\eta}/I_{L\alpha}$ ,  $56 \leq Z \leq 92$  for  $I_{L\gamma 5}/I_{L\alpha}$ , and  $66 \leq Z \leq 92$  for  $I_{L\gamma 1}/I_{L\alpha}$ . Weighted means, combined standard deviations, and average z-score values were calculated for each element. Research gaps and needs have been identified.

## Declaration of competing interest

The authors declare that they have no known competing financial interests or personal relationships that could have appeared to influence

the work reported in this paper.

## Data availability

Data will be made available on request.

## Acknowledgements

We gratefully acknowledge the support of the DGRSDT, Ministry of Higher Education and Scientific Research, Algeria. This work was done with the support of Mohamed El Bachir El Ibrahim University, under project (PRFU) N<sup>o</sup>: B00L02UN340120230004. This work was also supported by the Fundação para a Ciência e Tecnologia (FCT), Portugal through contracts UIDP/50007/2020 (LIP) and UID/FIS/04559/2020 (LIBPhys). S.C. warmly acknowledges the financial support of Lancaster University, and A.F. gratefully acknowledges the support of the Joint Research Centre of the European Commission.

## Appendix

Table A

. Correspondence between Siegbahn, IUPAC notation diagram lines, and the  $Z$  values associated with the appearance of these lines.

Siegbahns		IUPAC	$Z$
$L_{\alpha}$	$L_{\alpha 1}$	$L_3 - M_5$	$Z \geq 23$
	$L_{\alpha 2}$	$L_3 - M_4$	$Z \geq 19$
$L_{\beta}$	$L_{\beta 1}$	$L_2 - M_4$	$Z \geq 19$
	$L_{\beta 2}$	$L_3 - N_5$	$Z \geq 41$
	$L_{\beta 3}$	$L_1 - M_3$	$Z \geq 15$
	$L_{\beta 4}$	$L_1 - M_2$	$Z \geq 13$
	$L_{\beta 5}$	$L_3 - O_4$	$Z \geq 69$
	$L_{\beta 5}$	$L_3 - O_5$	$Z \geq 73$
	$L_{\beta 6}$	$L_3 - N_1$	$Z \geq 29$
	$L_{\beta 7}$	$L_3 - O_1$	$Z \geq 61$
	$L_{\beta 7}$	$L_3 - N_6$	$Z \geq 47$
	$L_{\beta 7}$	$L_3 - N_7$	$Z \geq 53$
	$L_{\beta 7}$	$L_1 - M_5$	$Z \geq 23$

(continued on next page)

Table A (continued)

Siegbahns		IUPAC	Z
	$L_{\beta 9}$	$L_1 - M_4$	$Z \geq 19$
	$L_{\beta 10}$	$L_3 - N_4$	$Z \geq 37$
	$L_{\beta 15}$	$L_2 - M_3$	$Z \geq 15$
	$L_{\beta 17}$		
$L_{\gamma}$	$L_{\gamma 1}$	$L_2 - N_4$	$Z \geq 37$
	$L_{\gamma 2}$	$L_1 - N_2$	$Z \geq 31$
	$L_{\gamma 3}$	$L_1 - N_3$	$Z \geq 33$
	$L_{\gamma 4}$	$L_1 - O_3$	$Z \geq 65$
	$L_{\gamma 4'}$	$L_1 - O_2$	$Z \geq 63$
	$L_{\gamma 5}$	$L_2 - N_1$	$Z \geq 29$
	$L_{\gamma 6}$	$L_2 - O_4$	$Z \geq 69$
	$L_{\gamma 8}$	$L_2 - O_1$	$Z \geq 61$
	$L_{\gamma 8'}$	$L_2 - N_6^{(7)}$	$Z \geq 47$
	$L_I$	$L_I$	$L_3 - M_1$
$L_{\eta}$	$L_{\eta}$	$L_2 - M_1$	$Z \geq 11$

## References

- [1] F. Akman, R. Durak, M.R. Kaçal, M.F. Turhan, Measurement of Li X-ray fluorescence production cross sections and intensity ratios of some elements at 59.54 keV, *Can. J. Phys.* 93 (10) (2015) 1057–1066.
- [2] R. Jenkins, R. Manne, R. Robin, C. Senemaud, Nomenclature system for x-ray spectroscopy, *Pure Appl. Chem.* 63 (5) (1991) 735–746.
- [3] J.H. Scofield, Relativistic Hartree-Slater values for K and L X-ray emission rates, *At. Data Nucl. Data Tables* 14 (2) (1974) 121–137.
- [4] J.L. Campbell, J.-X. Wang, Interpolated Dirac-Fock values of L-subshell x-ray emission rates including overlap and exchange effects", *At. Data Nucl. Data Tables* 43 (2) (1989) 281–291.
- [5] A. Kumar, Y. Chauhan, S. Puri, Incident photon energy and Z dependence of L X-ray relative intensities, *At. Data Nucl. Data Tables* 96 (6) (2010) 567–585.
- [6] S. Puri, X-ray relative intensities at incident photon energies across the Li ( $i=1-3$ ) absorption edges of elements with', *At. Data Nucl. Data Tables* 100 (4) (2014) 847–858.
- [7] Chu-Nan Chang & Wen-Herng Su, The relative photoionization cross section measurement by X-ray detection, *Nucl. Instrum. Methods* 148 (3) (1978) 561–566.
- [8] K. Shatendra, K.L. Allawadhi, B.S. Sood, Energy dependence of photon-induced L-shell X-ray intensity ratios in some high-Z elements, *J. Phys. B: Atom. Mol. Phys.* 16 (23) (1983) 4313–4322.
- [9] D. Demir, Y. Şahin, Li/L $\alpha$  X-ray intensity ratios for elements in the range  $73 < Z < 92$  excited by 59.54keV photons in an external magnetic field, *Radiat. Phys. Chem.* 77 (2) (2008) 121–124.
- [10] V. Ayilicci, A. Kahoul, N. Kup Ayilicci, E. Tıraşoğlu, İ.H. Karahan, A. Abassi, M. Dogan, Empirical and semi-empirical interpolation of L X-ray fluorescence parameters for elements in the atomic range  $50 \leq Z \leq 92$ , *Radiat. Phys. Chem.* 106 (2015) 99–125.
- [11] A. Hamidani, S. Daoudi, A. Kahoul, J.M. Sampaio, J.P. Marques, F. Parente, S. Croft, A. Favalli, N. Kup Ayilicci, V. Ayilicci, Y. Kasri, K. Meddouh, Updated database, semi-empirical and theoretical calculation of K $\beta$ /K $\alpha$  intensity ratios for elements ranging from 11Na to 96Cm, *At. Data Nucl. Data Tables* 149 (2023) 101549–101558.
- [12] S. Singh, D. Mehta, M.L. Garg, S. Kumar, N. Singh, P.C. Mangal, P.N. Trehan, Measurement of L X-ray fluorescence cross sections and relative intensities for elements  $56 < Z < 66$  in the energy range 11–41keV, *J. Phys. B: Atom. Mol. Phys.* 20 (20) (1987) 5345–5353.
- [13] S. Singh, M.L. Garg, D. Mehta, P.N. Trehan, N. Singh, H.R. Verma, P.C. Mangal, Measurements of photon-induced L X-ray fluorescence cross sections and relative intensities for Ba, Ce and Nd at 15.2, 17.8, 22.6 and 25.8keV, *J. Phys. B: Atom. Mol. Phys.* 20 (5) (1987) 941–947.
- [14] S. Singh, D. Mehta, M.L. Garg, P.N. Trehan, N. Singh, S. Kumar, P.C. Mangal, Measurement of photon-induced L X-ray fluorescence cross sections and relative intensities for Tm, Lu, Th and U in the energy range 15–60keV, *J. Phys. B: Atom. Mol. Phys.* 20 (14) (1987) 3325–3333.
- [15] S. Singh, B. Chand, D. Mehta, S. Kumar, M.L. Garg, N. Singh, P.C. Mangal, P. N. Trehan, L X-ray fluorescence cross section and relative intensity measurements for Hf, Re, Ir, Pt and Pb in the energy range 15–60keV, *J. Phys. B: At. Mol. Opt. Phys.* 22 (8) (1989) 1163–1173.
- [16] K. Al-Saleh, N. Saleh, L X-ray fluorescence cross-sections of heavy elements excited by 16.04, 16.90 and 17.78keV photons, *Radiat. Phys. Chem.* 54 (2) (1999) 117–124.
- [17] M. Saad, L (X-ray) cross sections of heavy elements excited by 15.20keV photons, *Can. J. Phys.* 81 (4) (2003) 691–967.
- [18] E.R. Cengiz, E. Tıraşoğlu, V. Ayilicci, G. Apaydin, The investigations on K and L X-ray fluorescence parameters of gold compounds, *Radiat. Phys. Chem.* 79 (2010) 809–815.
- [19] H. Duggal, A. Kapil, D.M. Kailash, S. Kumar, Influence of chemical effects on the Li ( $i = 1-3$ ) subshell X-ray spectra for  $^{79}\text{Au}$  compounds, *Radiat. Phys. Chem.* 193 (2022) 109885.
- [20] D. Mehta, H. Kaur, M.L. Garg, H.R. Verma, N. Singh, T.S. Cheema, P.N. Trehan, X-ray and gamma ray intensity measurements in  $^{141}\text{Ce}$  and  $^{170}\text{Tm}$  decays, *Nucl. Instrum. Methods Phys. Res. A: Accel. Spectrom. Detect. Assoc. Equip.* 242 (1) (1985) 149–152.
- [21] D. Mehta, M.L. Garg, J. Singh, N. Singh, T.S. Cheema, P.N. Trehan, Precision measurements of X and gamma-ray intensities in  $^{192}\text{Ir}$ ,  $^{160}\text{Tb}$ ,  $^{169}\text{Yb}$  and  $^{152}\text{Eu}$  decays, *Nucl. Instrum. Methods Phys. Res. A: Accel. Spectrom. Detect. Assoc. Equip.* 245 (1986) 447–454.
- [22] D. Mehta, S. Singh, H.R. Verma, N. Singh, P.N. Trehan, X and gamma-ray intensity measurements in  $^{137}\text{Cs}$  and  $^{203}\text{Hg}$  decays, *Nucl. Instrum. Methods Phys. Res. A: Accel. Spectrom. Detect. Assoc. Equip.* 254 (1987) 578–582.
- [23] D. Mehta, B. Chand, S. Singh, M.L. Garg, N. Singh, T.S. Cheema, P.N. Trehan, X-ray and gamma-ray intensity measurements in  $^{210}\text{Pb}$ ,  $^{177}\text{Lu}$ ,  $^{170}\text{Tm}$  and  $^{141}\text{Ce}$  decays, *Nucl. Instrum. Methods Phys. Res. A: Accel. Spectrom. Detect. Assoc. Equip.* 260 (1) (1987) 157–159.
- [24] B. Chand, J. Goswamy, D. Mehta, N. Singh, P.N. Trehan, X-ray and gamma-ray intensity measurements in  $^{131}\text{I}$ ,  $^{166}\text{Ho}$ ,  $^{198}\text{Au}$  and  $^{199}\text{Au}$  decays, *Nucl. Instrum. Methods Phys. Res. A: Accel. Spectrom. Detect. Assoc. Equip.* 284 (1989) 393–398.
- [25] B. Chand, J. Goswamy, D. Mehta, N. Singh, P.N. Trehan, Level structure studies of  $^{182}\text{Ta}$  from the decay of  $^{182}\text{Ta}$ , *Can. J. Phys.* 70 (4) (1992) 242–251.
- [26] B. Chand, J. Goswamy, D. Mehta, N. Singh, P.N. Trehan, Studies on the decays of  $^{153}\text{Sm}$  and  $^{153}\text{Gd}$  to  $^{153}\text{Eu}$ , *Int. J. Radiat. Appl. Instrum. Part A: Appl. Radiat. Isot.* 43 (8) (1992) 997–1004.
- [27] L. Demir, I. Han, M. Şahin, Measurement of L X-ray fluorescence cross sections and relative intensities for some elements in the atomic range  $78 < Z < 92$ , *J. Electron Spectrosc. Relat. Phenom.* 162 (1) (2008) 44–48.
- [28] P.V. Rao, J.M. Palms, R.E. Wood, High-Z L-Subshell X-Ray emission rates, *Phys. Rev. A* 3 (5) (1971) 1568–1575.
- [29] C. Bhan, A. Rani, S.N. Chaturvedi, N. Nath, K and L shell X-ray relative intensity measurements, *J. Anal. At. Spectrom.* 2 (1987) 411–412.
- [30] V. Raghavaiah, N.V. Rao, S.B. Reddy, G. Satyanarayana, D.L. Sastry,  $L\alpha/LI$  X-ray intensity ratios for elements in the region  $55 \leq Z \leq 80$ , *J. Phys. B: At. Mol. Phys.* 20 (1987) 5647–5651.
- [31] M. Tan, Y. Şahin, A. Şaplakoğlu, LIII subshell intensity ratios of Pb, Th and U, *X-Ray Spectrom* 19 (5) (1990) 233235.
- [32] J.B. Darko, G.K. Tetteh, Measurement of relative intensities of L-shell x-rays of some heavy elements using Cd-109 radioisotope source, *X-Ray Spectrom* 21 (3) (1992) 111–114.
- [33] M. Ertuğrul, The vacancy transfer probability dependence on relative L X-ray intensities in the atomic range  $57 \leq Z \leq 92$  at 59.5keV, *Nucl. Instrum. Methods Phys. Res. B: Beam Interact. Mater. At.* 111 (3–4) (1996) 229–233.
- [34] M. Ertuğrul, E. Büyükkasap, H. Erdogan, Angular dependence of L X-ray relative intensities of uranium and thorium at 59.5keV, *Appl. Spectrosc. Rev.* 32 (1–2) (1997) 159–165.
- [35] O. Dogan, Ö. Simsek, Ü. Turgut, M. Ertugrul, L X-ray intensity ratios in heavy elements at 59.5 and 122keV photons, *J. Radioanal. Nucl. Chem.* 232 (1–2) (1998) 143–146.
- [36] A.M. Ismail, N.B. Malhi, L-shell x-ray relative intensities of some heavy elements excited by 20.48keV x-rays, *X-Ray Spectrom* 29 (4) (2000) 317–319.
- [37] Ö. Şimşek, Measurement of relative intensities of L 3-subshell x rays in some high-Z elements, *Phys. Rev. A* 63 (1) (2000) 012515.
- [38] R. Durak, Y. Özdemir, Measurement of  $L\alpha/L\beta$ ,  $L\alpha/L\gamma$  and  $L\alpha/L\gamma$  X-ray intensity ratios for elements in the atomic range  $57 \leq Z \leq 92$  using radioisotope X-ray fluorescence, *Phys. Lett. A* 284 (1) (2001) 43–48.
- [39] E. Tıraşoğlu, U. Çevik, B. Ertuğral, G. Apaydin, M. Ertuğrul, A. Kobya, Chemical effects on  $L\alpha$ ,  $L\beta$ ,  $L\gamma$ ,  $LI$ , and  $LII$  X-ray production cross-sections and  $Li/L\alpha$  X-ray intensity ratios of Hg, Pb and Bi compounds at 59.54keV, *Eur. Phys. J. D* 26 (2003) 231–236.
- [40] A. Küçükönder, B. Durdu, Ö. Söğüt, E. Büyükkasap, L X-ray production cross sections, average L shell fluorescence yield and intensity ratios in heavy elements, *J. Radioanal. Nucl. Chem.* 260 (2004) 89–97.

- [41] E. Öz, E. Baydaş, M. Ertuğrul, Y. Şahin, Measurement of L shell X-ray fluorescence intensity ratios for some elements in the atomic number range of  $66 \leq Z \leq 90$  by photoionization of consecutive L subshells, *J. Radioanal. Nucl. Chem.* 260 (1) (2004) 75–79.
- [42] Ö. Sögüt, E. Büyükkasap, A. Küçükönder, Measurement of  $L\alpha/L\gamma$  X-ray intensity ratios, *Can. J. Phys.* 83 (9) (2005) 951–955.
- [43] A. Karabulut, A. Gürol, Measurements of L XRF fluorescence cross-sections and relative intensity ratios for some elements in the atomic range  $72 \leq Z \leq 92$ , *Nucl. Instrum. Methods Phys. Res. B: Beam Interact. Mater. At.* 244 (2) (2006) 303–306.
- [44] D. Demir, Y. Şahin, Measurement of L X-ray intensity ratios for 92U and 90 Th elements using photoionization in an external magnetic field, *Chin. Phys. Lett.* 24 (3) (2007) 668–671.
- [45] D. Demir, Y. Şahin, The effect of an external magnetic field on L X-ray intensity ratios for elements in the range  $73 \leq Z \leq 92$  at 59.54keV, *J. Phys. Soc. Jpn.* 76 (11) (2007) 114302.
- [46] P. Yalçın, S. Porikli, Y. Kurucu, Y. Şahin, Measurement of relative L X-ray intensity ratio following radioactive decay and photoionization, *Phys. Lett. B* 663 (3) (2008) 186–190.
- [47] M.R. Kaçal, R. Durak, F. Akman, M.F. Turhan, I. Han, Measurement of L subshell fluorescence cross sections and intensity ratios of heavy elements at 22.6keV, *Radiat. Phys. Chem.* 80 (6) (2011) 692–700.
- [48] S. Porikli, Influence of the chemical environment changes on the line shape and intensity ratio values for La, Ce and Pr L lines spectra, *Chem. Phys. Lett.* 508 (1–3) (2011) 165–170.
- [49] S. Porikli, Chemical shift and intensity ratio values of dyspersium, holmium and erbium L X-ray emission lines, *Radiat. Phys. Chem.* 81 (2) (2012) 113–117.
- [50] R. Cesareo, J.T. De Assis, C. Roldán, A.D. Bustamante, A. Brunetti, N. Schiavon, Multilayered samples reconstructed by measuring  $K\alpha/K\beta$  or  $L\alpha/L\beta$  X-ray intensity ratios by EDXRF, *Nucl. Instrum. Methods Phys. Res. B: Beam Interact. Mater. At.* 312 (2013) 15–22.
- [51] S. Durdagi, Effect of applied external magnetic field on the L X-ray emission line structures of the lanthanide elements, *Radiat. Phys. Chem.* 92 (2013) 1–7.
- [52] X. Wang, Z. Xu, L. Zhang, L X-ray intensity ratios for high Z elements induced with X-ray tube, *Radiat. Phys. Chem.* 112 (2015) 121–124.
- [53] S. Krishnananda, M. Santosh, N. Badiger, M. Tiwari, Measurement of the radiative L3 -M vacancy transfer probabilities of some 4f elements and compounds using Indus-2 synchrotron radiation, *Chem. Phys. Lett.* 658 (2016) 192–196.
- [54] H. Bansal, M.K. Tiwari, R. Mittal, L X-ray intensity ratio measurements using selective L sub-shell photo-ionisation on synchrotron, *Radiat. Phys. Chem.* 139 (2017) 22–26.
- [55] G.B. Hiremath, S. Mirji, M.M. Hosamani, N.M. Badiger, M.K. Tiwari, Study the effect of crystal structure on radiative vacancy transfer probabilities from L3 to M<sub>i</sub>, Ni and O<sub>i</sub> subshells, *Chem. Phys. Lett.* 715 (2019) 317–322.
- [56] C.V. Raghavaiah, N.V. Rao, S.B. Reddy, G. Satyanarayana, G.S.K. Murty, M.V.S. C. Rao, D.L. Sastry,  $L\alpha/L\beta$  and  $L\alpha/L\gamma$  X-ray intensity ratios for elements in the range  $Z = 55-80$ , *X-Ray Spectrom* 19 (1) (1990) 23–26.
- [57] S.I. Salem, R.E. Winchell, L x-ray transition probabilities in elements of medium atomic numbers, *Phys. Rev. A* 10 (4) (1974) 1041–1044.
- [58] M.L. Garg, J. Singh, H.R. Verma, N. Singh, P.C. Mangal, P.N. Trehan, Relative intensity measurements of L-shell X-rays for Ta, Au, Pb and Bi in the energy range 17–60keV, *J. Phys. B: Atom. Mol. Phys.* 17 (4) (1984) 577–584.
- [59] H.R. Verma, D. Pal, M.L. Garg, P.N. Trehan, Photon-induced L-shell X-ray intensity ratios for 74W and 80Hg in the energy range  $17 \leq E \leq 47$  keV, *J. Phys. B: Atom. Mol. Phys.* 18 (6) (1985) 1133–1138.
- [60] M.L. Garg, D. Mehta, H.R. Verma, N. Singh, P.C. Mangal, P.N. Trehan, Measurement of L X-ray fluorescence cross sections and relative intensities for Ho, Er and Yb in the energy range 11–41keV, *J. Phys. B: At. Mol. Phys.* 19 (11) (1986) 1615–1622.
- [61] N.S. Saleh, K.A. Al-Saleh, A.J.A. El-Hajja, N.A. Halim, J.M. Khalifeh, Photon-induced L-Shell xRay Intensity Ratio for Elements with  $73 \leq Z \leq 83$  in the Energy Range  $17 \leq E \leq 47$ keV, *Appl. Radiat. Isot.* 39 (1988) 1213–1217.
- [62] D.V. Rao, R. Cesareo, G.E. Gigante, L x-ray fluorescence cross sections and intensity ratios in some high- Z elements excited by 23.62- and 24.68-keV photons, *Phys. Rev. A* 47 (2) (1993) 1087–1092.
- [63] B. Dhal, H. Padhi, Relative L-shell X-ray intensities of Pt, Pb and Bi following ionization by 59.54keV  $\gamma$ -rays, *Nucl. Instrum. Methods Phys. Res. B: Beam Interact. Mater. At.* 94 (4) (1994) 373–376.
- [64] D.V. Rao, R. Cesareo, G.E. Gigante, L X-ray fluorescence cross sections, fluorescence yields and intensity ratios for Au and Pb at excitation energies 21.56, 31.64 and 34.17 keV, *Radiat. Phys. Chem.* 46 (1) (1995) 17–22.
- [65] M. Ertuğrul, Measurement of Li/L $\alpha$  intensity ratios for elements in the region  $57 \leq Z \leq 92$  by a Si(Li) detector, *Spectrochim. Acta Part B: At. Spectrosc.* 52 (2) (1997) 201–204.
- [66] A. Küçükönder, Chemical effects on L X-ray intensity ratios of U and Th, *Can. J. Phys.* 80 (8) (2002) 925–930.
- [67] W. Salah, L x-ray fluorescence cross-sections of heavy elements in the atomic region  $57 \leq Z \leq 71$  excited by 17.78keV photons, *X-Ray Spectrom.* 33 (5) (2004) 372–375.
- [68] U. Turgut, M. Ertuğrul, L X-ray intensity ratios for elements in the range 74Zr2 at 31.635keV, *Nucl. Instrum. Methods Phys. Res. B: Beam Interact. Mater. At.* 222 (3–4) (2004) 432–436.
- [69] W. Salah, J. Al-Jundi, Measurement of L X-ray cross-sections and relative intensities of heavy elements by 15.2keV photons, *J. Quant. Spectrosc. Radiat. Transf.* 94 (3–4) (2005) 325–333.
- [70] Y. Zou, M. Oura, R. Hutton, H. Yamaoka, N. Takeshima, K. Takahiro, K. Kawatsura, T. Mukoyama, Study of vacancy decays in the L-shell photoionization of barium in the excitation energy range of 5.6–30 keV: from L2 edge to energy high above the thresholds of double L-vacancy production", *J. Phys. B: At. Mol. Opt. Phys.* 39 (22) (2006) 4775–4788.
- [71] V.O. Aylıkci, E. Tıraşoğlu, G.Ö. Apaydin, N.E. Kaya, E.R. Cengiz, Chemical effect on the K and L shell intensity ratios of Hf compounds, *Phys. Scr.* 76 (2007) 31–36.
- [72] I. Han, M. Şahin, L. Demir, Angular variations of K and L X-ray fluorescence cross sections for some lanthanides, *Can. J. Phys.* 86 (2) (2008) 361–367.
- [73] E. Cengiz, E. Tıraşoğlu, V. Aylıkci, G. Apaydin, N.K. Aylıkci, Investigation on L-shell X-ray fluorescence parameters for heavy elements and compounds, *Chem. Phys. Lett.* 498 (1–3) (2010) 107–112.
- [74] C. Aksoy, E. Tıraşoğlu, E. Cengiz, G. Apaydin, M. Saydam, V. Aylıkci, N.K. Aylıkci, Chemical effects on the L-shell X-ray fluorescence parameters of Ta and W compounds, *J. Electron Spectrosc. Relat. Phenom.* 184 (11–12) (2012) 556–560.
- [75] A. Kumar, S. Puri, Li( $i=1-3$ ) sub-shell x-ray relative intensities for some compounds of  $^{66}\text{Dy}$  at 22.6 and 59.54keV incident photon energies, *Radiat. Phys. Chem.* 81 (7) (2012) 735–739.
- [76] M.K. Alqadi, Y. Alsenjlawi, F.Y. Alzoubi, Measurement of L X-Ray relative intensities for selected heavy elements, *Radiat. Phys. Chem.* 87 (2013) 31–34.
- [77] M. Doğan, E. Cengiz, A. Nas, E. Tıraşoğlu, H. Kantekin, V. Aylıkci, L shell X-ray fluorescence parameters of Pb in phthalocyanine complexes, *Appl. Radiat. Isot.* 104 (2015) 43–48.
- [78] R. Kaur, A. Kumar, M.K. Tiwari, S. Puri, Measurements of X-ray production cross sections at photon energies across the Li ( $i=1-3$ ) sub-shell absorption edges of 74W and 76Os using synchrotron radiation", *J. Electron Spectrosc. Relat. Phenom.* 213 (2016) 22–31.
- [79] V. Ayri, S. Kaur, A. Kumar, M. Czyzycki, A.G. Karydas, S. Puri, Experimental -L-series x ray production cross sections for Re by tuning synchrotron radiation across its Li ( $i=1-3$ ) sub-shell ionization thresholds", *Radiat. Phys. Chem.* 188 (2021) 109599.
- [80] R. Fernández-Ruiz, Quantitation of the production cross-section and transition probabilities of the L and M X-ray series in the Au(0) and Au(3+) atomic environments using Total-reflection X-ray fluorescence, *Spectrochim. Acta B: At. Spectrosc.* 180 (2021) 106207.
- [81] M. Alqadi, S. Al-Humaidi, H. Alkhateeb, F. Alzoubi, L-shell x-ray fluorescence relative intensities for elements with  $62 \leq Z \leq 83$  at 18keV and 23keV by synchrotron radiation, *Chin. Phys. B* 32 (8) (2023) 083201.
- [82] M.M. Bé, V.P. Chechev, A. Pearce, Uncertainties in nuclear decay data evaluations, *Metrologia* 52 (2015) S66–S72.
- [83] S. Daoudi, A. Kahoul, N.K. Aylıkci, J.M. Sampaio, J.P. Marques, V. Aylıkci, B. Deghfel, Review of experimental photon-induced  $K\beta/K\alpha$  intensity ratios, *At. Data Nucl. Data Tables* 132 (2020) 101308–101340.
- [84] E. Baydaş, Ö. Sögüt, E. Büyükkasap, Y. Şahin, L X-ray intensity ratios of some elements in the region of  $56 \leq Z \leq 83$ , *J. Radioanal. Nucl. Chem.* 247 (3) (2001) 487–489.
- [85] K. Shatendra, K.L. Allawadhi, B.S. Sood, Measurement of Li, L $\alpha$ , L $\beta$ , and L $\gamma$  x-ray-production cross sections in some high- Z elements by 60keV photons, *Phys. Rev. A* 31 (5) (1985) 2918–2921.
- [86] A. Kumar, S. Puri, Chemical effects on the Li( $i=1-3$ ) sub-shell X-ray relative intensities for some compounds of Hg", *Radiat. Phys. Chem.* 80 (11) (2011) 1166–1171.
- [87] B.G. Durdu, A. Kucukonder, Variation of the L X-ray fluorescence cross-sections, intensity ratios and fluorescence yields of Sm and Eu in halogen compounds, *Radiat. Phys. Chem.* 81 (2) (2012) 135–142.
- [88] D.V. Rao, G.E. Gigante, R. Cesareo, L shell x-ray intensity ratios for Au and Pb at excitation energies 36.82, 43.95, 48.60, 50.20 and 53.50keV, *Physica Scripta* 47 (6) (1993) 765–768.
- [89] S. Kumar, R. Mittal, K.L. Allawadhi, B.S. Sood, Measurement of relative intensities of L-shell Xrays in some high-Z elements, *J. Phys. B: Atom. Mol. Phys.* 15 (19) (1982) 3377–3383.
- [90] Ö. Sögüt, E. Büyükkasap, M. Ertugrul, A. Küçükönder, Chemical Effect on L X-ray Intensity Ratios of Mercury, Lead, and Bismuth, *Appl. Spectrosc. Rev.* 32 (1–2) (1997) 167–173.
- [91] S.P. Durdagi, Chemical environment change analysis on L X-ray emission spectra of some lanthanide compounds, *Microchem. J.* 130 (2017) 27–32.
- [92] R. Kaur, A. Kumar, M. Czyzycki, A. Migliori, A.G. Karydas, S. Puri, A study of the influence of chemical environment on the Li ( $i=1-3$ ) subshell X-ray intensity ratios and the L3 absorption-edge energy for some compounds of  $^{66}\text{Dy}$  using synchrotron radiation, *X-Ray Spectrom* 48 (2) (2019) 126–137.